DOCTORAL THESIS

Hypoxia effect on genetic regulation and virulence in *Acinetobacter baumannii* and *Pseudomonas aeruginosa*, *in vitro* and *in vivo*, and on innate immune response in infections caused by both pathogens

María Luisa Gil Marqués

Seville 2018

Director 1: Dr. Jerónimo Pachón Díaz

Director 2: María Eugenia Pachón Ibáñez

Director 3: Michael J. McConnell

Departamento de Medicina

El Dr. Jerónimo Pachón Díaz, Catedrático de Medicina de la Universidad de Sevilla y Jefe de Servicio de Enfermedades Infecciosas del Hospital Universitario Virgen del Rocío, como Director y Tutor de la Tesis Doctoral, la Dra. María Eugenia Pachón Ibáñez, investigadora posdoctoral de la Red Española de Investigación en Patología Infecciosa (REIPI), como Directora de la Tesis Doctoral, y el Dr. Michael J. McConnell, Científico Titular del Centro Nacional de Microbiología (ISCIII), como Director de la Tesis Doctoral,

CERTIFICAN:

Que la Tesis para optar al grado de Doctor por la Universidad de Sevilla que lleva por título "**Hypoxia effect on genetic regulation and virulence in *Acinetobacter baumannii* and *Pseudomonas aeruginosa*, *in vitro* and *in vivo*, and on innate immune response in infections caused by both pathogens**" ha sido realizada por la Licenciada Doña María Luisa Gil Marqués bajo nuestra supervisión, considerando que reúne los requisitos necesarios para su presentación.

Para que conste a los efectos oportunos, expiden la presente certificación en Sevilla, a 17 de septiembre de 2018.

MCCONNELL MICHAEL JAMES - Y01798372 Digitally signed by MCCONNELL MICHAEL JAMES - Y01798372 Date: 2018.09.18 13:00:56 +02'00'

Jerónimo Pachón Díaz	María Eugenia Pachón Ibáñez	Michael J. McConnell
Director y Tutor	Directora	Director

DOCTORAL THESIS FUNDING

This work was supported by the Instituto de Salud Carlos III, Subdirección General de Redes y Centros de Investigación Cooperativa, Ministerio de Economía, Industria y Competitividad (PIE13/0004) and by Plan Nacional de I+D+i 2013-2016 and Instituto de Salud Carlos III, Subdirección General de Redes y Centros de Investigación Cooperativa, Ministerio de Economía, Industria y Competitividad, Spanish Network for Research in Infectious Diseases (REIPI RD12/0015/0001; RD12/0015/0012; RD16/0016/0009) - cofinanced by European Development Regional Fund "A way to achieve Europe", Operative program Intelligent Growth 2014-2020.

M.L.G.M. is supported by the program FPU (Formación de Profesorado Universitario; FPU13/04545), Ministerio de Educación, Cultura y Deporte, Spain. M.E.P.I. has a grant by the Ministerio de Economía y Competitividad, Instituto de Salud Carlos III, cofinanced by the European Development Regional Fund ("A way to achieve Europe"), and by the Spanish Network for Research in Infectious Diseases (grant REIPI RD16/0009). M.J.M. is supported by the Subprograma Miguel Servet (CPII16/00061), Instituto de Salud Carlos III, Ministerio de Economía, Industria y Competitividad.

SCIENTIFIC PRODUCTION RESULTING FROM THE THESIS

Publications

1. **ML Gil-Marqués**, ME Pachón-Ibáñez, J Pachón, Y Smani. Effect of hypoxia on the pathogenesis of *Acinetobacter baumannii* and *Pseudomonas aeruginosa in vitro* and in murine experimental models of infections. Infection and Immunity 2018; Aug 6. pii: IAI.00543-18. doi: 10.1128/IAI.00543-18. [Epub ahead of print]

Congress communications

1. **ML Gil-Marqués**, A Puppo, A Gutiérrez-Pizarraya, A Díaz, Y Smani, M McConnell, J Pachón, J Garnacho, ME Pachón-Ibáñez. Tissue hypoxia, HIF-1α and inflammation biomarkers in patients with septic shock. 26th European Congress of Clinical Microbiology and Infectious Diseases (ECCMID). 9-12 April 2016; Amsterdam, Netherlands.

2. A. Díaz Martín*, **ML Gil-Marqués***, A. Puppo Moreno, A. Gutiérrez Pizarraya, Y. Smani, M. McConnell, I. Palacios García, J. Pachón Díaz, J. Garnacho Montero, ME Pachón Ibáñez. Hipoxia Tisular, HIF-1α y Biomarcadores de Inflamación en Pacientes con Shock Séptico. LI Congreso Nacional de la Sociedad Española de Medicina Intensiva y Unidades Coronarias (SEMICYUC). 19-22 June 2016; Valencia, Spain. *The authors contributed equally.

3. Puppo AM*, **Gil Marqués ML***, Gutierrez Pizarraya A, Diaz A, Pachón Ibañez ME, Pachón J, Escoresca A, Garnacho J. Factor HIF-1α e Hipoxia Tisular en pacientes con Shock Séptico. LI Congreso Nacional de la Sociedad Española de Medicina Intensiva y Unidades Coronarias (SEMICYUC). 19-22 June 2016; Valencia, Spain. *The authors contributed equally.

4. A. Díaz-Martín*, **ML Gil-Marqués***, A. Puppo-Moreno, A. Gutiérrez-Pizarraya, Y. Smani, M. McConnell, I. Palacios-García, J. Pachón-Díaz, J. Garnacho-Montero, ME Pachón-Ibáñez. HIF-1α levels and inflammation biomarkers in hypoxemic septic shock patients. 29th European Society of Intensive Care Medicine (ESICM) Annual Congress. 1-5 October 2016; Milan, Italy. *The authors contributed equally.

5. **ML Gil-Marqués**, A Puppo, Y Smani, A Díaz, J Pachón, J Garnacho, ME Pachón-Ibáñez. Hipoxia tisular, Factor Inducible por Hipoxia 1α (HIF-1α) y biomarcadores de inflamación en pacientes con shock séptico. XVIII Congreso de la Sociedad Andaluza de Enfermedades Infecciosas (SAEI). 24-26 November 2016; Córdoba, Spain.

6. **Gil-Marqués ML**, Pachón-Ibáñez ME, Pachón J, Smani Y. *In vitro* effect of hypoxia on the infections caused by *Acinetobacter baumannii* and *Pseudomonas aeruginosa*. 27th European Congress of Clinical Microbiology and Infectious Diseases (ECCMID). 22-25 April 2017; Vienna, Austria.

7. **ML Gil-Marqués**, Y Smani, J Pachón, ME Pachón-Ibáñez. *In vivo* effect of hypoxia on infections caused by *Acinetobacter baumannii* and *Pseudomonas aeruginosa* in different murine models. 27th European Congress of Clinical Microbiology and Infectious Diseases (ECCMID). 22-25 April 2017; Vienna, Austria.

8. **ML Gil-Marqués**, Y Smani, M McConnell, ME Pachón-Ibáñez, J Pachón. Global transcriptional profiling of *Acinetobacter baumannii* under microaerobiosis and normoxy conditions. 11th International Symposium on the Biology of *Acinetobacter*. 20-22 September 2017; Sevilla, Spain.

OTHER SCIENTIFIC PRODUCTION ASSOCIATED WITH THE RESEARCH LINE

1. MR Pulido, M García-Quintanilla, **ML Gil-Marqués**, MJ McConnell. Identifying targets for antibiotic development using omics technologies. Drug Discovery Today 2016; Mar;21(3):465-72. doi: 10.1016/j.drudis.2015.11.014. Epub 2015 Dec 12.

2. **ML Gil-Marqués**, P Moreno-Martínez, C Costas, J Pachón, J Blázquez, MJ McConnell. Peptidoglycan recycling contributes to intrinsic resistance to fosfomycin in *Acinetobacter baumannii*. Journal of Antimicrobial Chemotherapy 2018; Aug 13. doi: 10.1093/jac/dky289. [Epub ahead of print]

ABBREVIATIONS

ADP: Adenosine diphosphate

ARDS: Adult respiratory distress syndrome

AUC: Area under the curve

BadA: Bartonella adhesin A

CF: Cystic fibrosis

cfu: Colony-forming unit

CI: Confidence interval

CO_2: Carbon dioxide

COPD: Chronic obstructive pulmonary disease

CRP: C-reactive protein

DAP: Diapinopimelic acid

DDD: Defined daily doses

DGE-test: Digital gene expression test

DMEM: Dulbecco's modified Eagle's medium

DMOG: Dimethyloxaloylglycine

DNA: Deoxyribonucleic acid

EARS-Net: European Antimicrobial Resistance Surveillance Network

EDCD: European Center for Disease Prevention and Control

EEA: European Economic Area

ELISA: Enzyme-linked immunosorbent assay

EU: European Union

FIH: Factor inhibiting HIF-1

FIO_2: Fractional inspired oxygen

GNB: Gram-negative bacilli

GO: Gene onthology

HAI: Healthcare-acquired infection

HEPES: 4-(2-hydroxyethyl)-1-piperazineethanesulfonic acid

HIF: Hypoxia inducible factor

HRE: Hypoxia response element

ICU: Intensive care unit

IL: Interleukin

i.p.: Intraperitoneal

IQR: Interquartile range

iTRAQ: Isobaric tags for relative and absolute quantitation

KO: Knockout

LB: Lysogenic Broth

LPC: Lysophosphatidylcholine

LPS: Lipopolysaccharides

MDR: Multi-drug resistant

MHB: Mueller Hinton Broth

MLD: Minimal lethal dose

MOI: Multiplicity of infection

MRSA: Methicillin-resistant *Staphylococcus aureus*

MS/MS: Tandem mass spectrometry

N_2: Nitrogen

NaCl: Sodium chloride

NIRS: Noninvasive near infrared spectroscopy

O_2: Oxygen

OMP: Outer membrane protein

OMV: Outer membrane vesicle

PaO_2: Arterial oxygen partial pressure

PBS: Phosphate-buffered saline

PCR: Polymerase chain reaction

PCT: Procalcitonin

PDR: Pan-drug resistant

PF: Peritoneal fluid

PHD: Proline hydroxylase

PMN: Polymorphonuclear leukocytes

PNAG: Polysaccharide polymer poly-beta-1,6-N-acetylglucosamine

PRIOAM: Programme for the Optimization of Antimicrobial Treatment

qRT-PCR: Quantitative real-time PCR

RNA: Ribonucleic acid

RNA-seq: RNA sequencing

RND: Resistance-nodulation-division

ROC: Receiver operating characteristic

ROI: Reactive oxygen species

ROS: Reactive oxygen species

RPKM: Reads per kilobase of exon model per million mapped reads

rRNA: Ribosomal RNA

$SatO_2$: Oxygen saturation

$SataO_2$: Arterial oxygen saturation

siRNA: Small interfering RNA

sPLA2-IIA: Secretory Phospholipase A2 Group IIA

T2SS, T3SS, T6SS: Type II/III/VI secretion system

Tat: Twin arginine transport

TLR4: Toll-like receptor 4

TNF-α: Tumor necrosis factor alpha

tRNA: Transfer RNA

USA: United States

WHO: World Health Organization

XDR: Extensively-drug resistant

INTRODUCTION

1. Healthcare-acquired infections (HAIs) due to gram-negative bacteria

A HAI, also known as a nosocomial infection, is an infection that is acquired in a hospital or other health care facility. Such infection is manifested after 72 h or more after the admission of the patient in the hospital [1]. HAIs are a considerable challenge to modern medicine. It is estimated that 4.2 million HAIs occurred in the European Union in 2013 [2], resulting in around 175,000 deaths [3]. Similar data have been reported from United States (USA), with a total of 1.7 million of HAIs and almost 99,000 deaths in 2002. [4] This fact makes HAIs the sixth leading cause of death in the USA [5] and the European Union (EU) [3]. The estimated medical costs associated to HAIs were between $9310-21,013 per patient in the USA [6], which corresponds to $5 billion to $10 billion annually [4].

HAIs are associated with invasive medical devices or surgical procedures. The most frequent types of HAIs are lower respiratory tract infections (such as hospital-acquire pneumonia and ventilator-associated pneumonia), surgical site, urinary tract, and bloodstream infections [4, 7, 8]. They constitute one of the most important problems in immunosuppressive patients in intensive care units (ICUs), and lead an increased hospital length of stay, higher mortality rates and higher health costs [6, 9].

Gram-negative bacteria are responsible for more than 30% of HAIs according to recent studies from the U.S. National Healthcare Safety Network. These bacteria predominate in cases of ventilator-associated pneumonia (47%) and urinary tract infections (45%) [10]. In the ICUs in USA, about 70% of these types of infections are caused by gram-negative bacteria, and similar data are reported from other countries [11]. Recent surveillance studies in the USA and Europe showed that the most common gram-

negative pathogens responsible for nosocomial infections are *Pseudomonas aeruginosa*, *Acinetobacter baumannii*, *Escherichia coli*, *Klebsiella pneumoniae*, and *Enterobacter* species [11, 12, 13].

2. Current situation of antimicrobial resistance

Antimicrobial resistance in gram-negative pathogens causing nosocomial infections has been a major concern in recent years due to the emergence of multi-drug resistant (MDR) strains and the lack of active antibiotics against them [14]. The 2014 report by the World Health Organization (WHO) warned about this circumstance, and remarked that a post-antibiotic era is a real possibility for the 21st century [15].

These MDR strains have developed effective resistance mechanisms like antibiotic efflux pumps or modifications of the outer membrane proteins, among others, to survive to the antibiotic treatment [16]. The development of new antibiotic resistance mechanisms has led to the emergence of extensively-drug resistant (XDR) and even pan-drug resistant (PDR) organisms [17]. The European Center for Disease Prevention and Control (ECDC) met in 2008 to establish standard definitions for MDR (resistant to more than 1 agent in 3 or more antimicrobial categories), XDR (non-susceptible to more than 1 agent in all but 2 categories), and PDR (resistant to all categories), as well as to begin to establish consistency in the categorization of susceptible and non-susceptible for different organisms and antimicrobial classes [18]. The objective of developing such definitions was for public health and epidemiology purposes.

Numerous protocols have been taken to contain multi-drug resistant gram-negative bacilli, such as hand hygiene to prevent patient-to-patient transmission of pathogens or contact isolation precautions including wearing gloves and a gown [1, 19]. However,

these infections have still a significant clinical impact. The ECDC reported in 2014 that the percentages of organisms exhibiting antimicrobial resistance, especially resistance to multiple antibiotics, continued to increase in Europe. Data from the European Antimicrobial Resistance Surveillance Network (EARS-Net) shows large variations in percentages of antimicrobial resistance in Europe depending on microorganism, antimicrobial agent and geographical region [2].

The use of antimicrobial drugs has become widespread over several decades, and has been extensively misused in both humans and food-producing animals, where it is not only used for disease treatment, but also for prevention, control, and growth promotion [20]. This has contributed to the selection and spread of resistant bacteria. In 2012, consumption of antibiotics for systemic use in the community ranged from 11.3 to 31.9 defined daily doses (DDD) per 1000 inhabitants and per day. The DDD per 1000 inhabitants and per day was 20.9 in Spain in 2012, while in the European Union/European Economic Area (EU/EEA) population was 21.5 DDD. Among the 29 reporting countries, just one country reported a significant decrease in antibiotic consumption [2]. Therefore, it is necessary to promote prudent use of antimicrobial agents and comprehensive infection control measures to reduce the selection and control the transmission of resistant bacteria. Vasudevan et al. [21] reported a prediction tool for nosocomial multi-drug resistant gram-negative bacilli infections in critically ill patients to help the clinicians to identify critically ill patients who are at risk of antibiotic resistant gram-negative infections. A similar study was reported by Ren et al. [22] and they conclude that the active screening and culture of MDR strains in patients has important value for the controlling and prevention of the infection. This should lead to targeted antibiotic treatment and avoid antibiotic overuse which worsens the vicious cycle of resistance in the ICU. Furthermore, University Hospital Virgen del Rocío

(Seville, Spain) launched the Institutional Programme for the Optimization of Antimicrobial Treatment (PRIOAM) in 2011. This programme is coordinated by a multidisciplinary team chosen by the Committee on Infections and Antimicrobials and its aim is to educate, train and promote the knowledge for the proper use of antimicrobials in order to reduce mortality and morbidity in patients with infections and delay the development of resistance [20].

Unfortunately, the increasing problem of multidrug resistance in gram-negative pathogens was not paralleled by the development of novel antimicrobials, as we can see in the Figure 1, which has led to the persistence and spread of these resistant strains [23]. Due to a diminishing antibiotic pipeline and an alarming rise in MDR gram-negative bacteria, clinicians are reintroducing older antibiotics (eg, aminoglycosides, fosfomycin or colistin) and examining new strategies to optimize the treatment with existing classes of antibiotics, such as combination antibiotic therapy [24]. Moreover, small companies are trying to modify compounds in existing classes used in human or animal health to circumvent emerging resistance mechanisms and to improve pharmacokinetics [25]. Furthermore, there are a few new compounds which are being clinically studied in some trials and might be used in the next future, like plazomicin or cefiderocol [26].

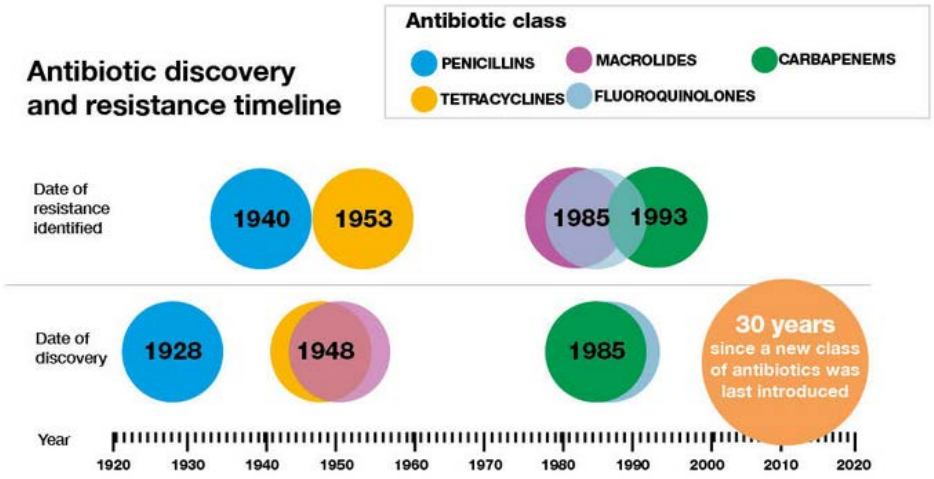

Figure 1. Antibiotic discovery and resistance timeline. (Health matters: antimicrobial resistance-GOV.UK).

As mentioned above, the most common gram-negative pathogens responsible for nosocomial infections are *P. aeruginosa*, *A. baumannii*, *E. coli*, *K. pneumoniae*, and *Enterobacter* species [11, 12, 13]. All of them form the "ESKAPE" group of pathogens, together with *Enterococcus faecium* and *Staphylococcus aureus*, which was defined in 2008 [27] and then embraced by the Infectious Diseases Society of America [28]. These are pathogens that cause the majority of HAIs while effectively "escaping" the effects of available antimicrobials [19].

3. Gram-negative bacilli (GNB): epidemiology, antimicrobial resistance, virulence factors and pathogenesis

The emergence of MDR GNB creates a challenge in the treatment of nosocomial infections. GNB are the most common causes of nosocomial infections, especially in the ICU, including most cases of hospital-acquired pneumonia and urinary tract infections and 25% to 30% of bloodstream and surgical site infections [29]. One of the

most common causes of HAIs are infections caused by the non-lactose fermenting bacteria *A. baumannii* and *P. aeruginosa*. Both bacteria are considered as priority 1 (critical) for research and development of new antibiotics by the WHO in 2017 [30].

3.1. *Acinetobacter baumannii*

3.1.1. Epidemiology and antimicrobial resistance

Acinetobacter spp. are glucose-non-fermentative, non-motile, non-fastidious, oxidative-negative, catalase-positive, aerobic gram-negative coccobacilli with a DNA G+C content of 39% to 47% [31]. Its ability to survive to desiccation and colonize any type of surface has made this pathogen one of the most common species causing nosocomial outbreaks in hospitals [32]. In the ECDC point prevalence survey of HAIs in European acute care hospitals 2011-2012, *Acinetobacter* spp. were the 11th most frequently reported microorganisms (3.6%) in microbiologically documented HAIs [2]. Among *Acinetobacter* species, *Acinetobacter baumannii* is the most important pathogen associated with HAIs [33]. Most *A. baumannii* infections occur in critically ill patients in the ICU and account for up to 20% of infections in ICUs worldwide [34].

A. baumannii is a successful pathogen responsible of opportunistic infections of the lower respiratory tract, skin, bloodstream, urinary tract, and other soft tissues [35, 36]. Crude mortality rates of 30-75% have been reported for nosocomial pneumonia caused by this pathogen, and the mortality attributable to *A. baumannii* infection was found to range from 7.8-43%, with higher levels in patients admitted to ICUs (10-43%) [37].

A. baumannii has a high level of intrinsic resistance to many groups of antimicrobials (e.g. glycopeptides, macrolides, lincosamides, and streptogramins). Moreover, it is able to develop resistance to all classes of antimicrobial agents used in the therapy [38]. For this reason, the resistance of *A. baumannii* has been highly increased in the last decades,

which supposes an important problem for the health system. Some European countries reported that more than half of *Acinetobacter* spp. isolates were resistant to all antimicrobial categories under surveillance (carbapenems, fluoroquinolones and aminoglycosides) [2]. Multicenter surveillance studies have also reported that the proportion of imipenem-resistant *A. baumannii* strains is as high as 85% in bloodstream isolates from ICU patients in Greece, and 48% in clinical isolates from hospitalized patients in Spain and Turkey [39].

The rapid emergence of MDR and PDR strains of *Acinetobacter* highlights the organism's ability to quickly acclimatize to selective changes in environmental pressures [31] and to acquire antimicrobial resistance [35, 40]. A number of *A. baumannii* resistance mechanisms are known, including enzymatic degradation of drugs (β-lactamases…), target modifications (PBP2, ArmA…), multidrug efflux pumps (AdeABC, AdeFGH, CmlA…), and permeability defects (OmpA, CarO…) [33, 35].

Figure 2 shows a summary about virulence factors, pathogenesis, antimicrobial resistance and treatment options of this successful pathogen which is important to develop new strategies for combating MDR *A. baumannii* infections.

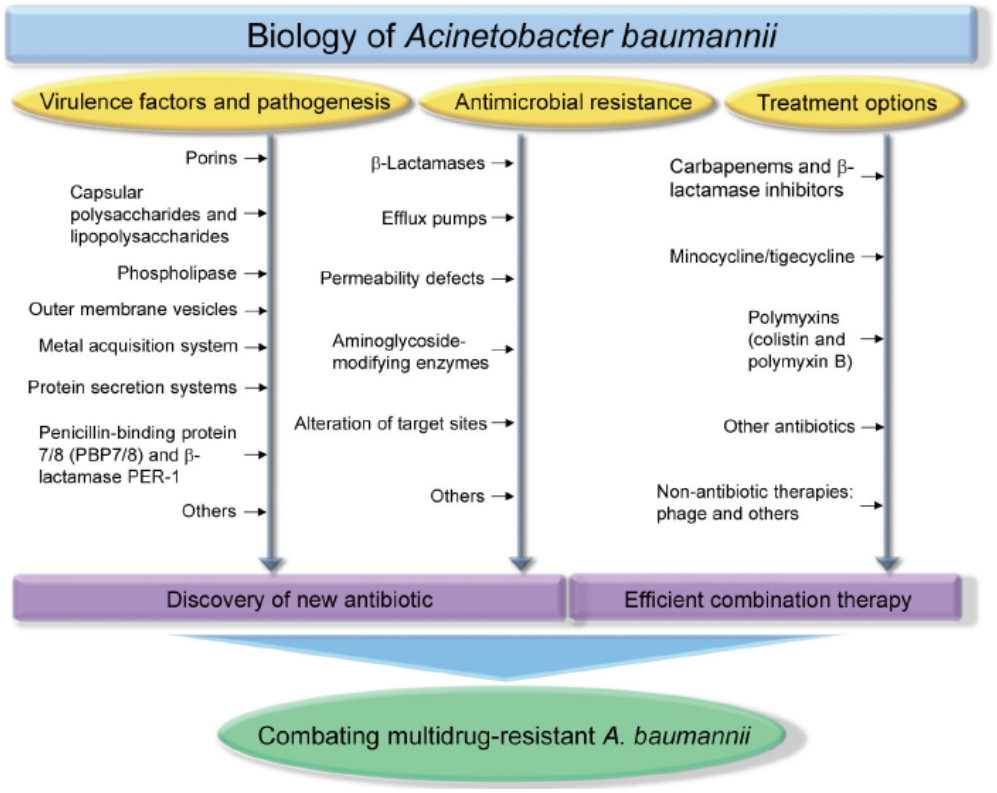

Figure 2. Biology of *Acinetobacter baumannii* [35].

3.1.2. Virulence factors and pathogenesis

A. baumannii use their virulence factors to first colonize and then infect the host. Different genomic, transcriptomic and proteomic analyses have helped to identify several virulence factors that participate in the pathogenesis of *A. baumannii*, including outer membrane porins, proteases, phospholipases, protein secretion systems, lipopolysaccharides (LPS), capsular polysaccharides, and iron-chelating systems [35, 41]. Although recent genomic and phenotypic analyses have identified several virulence factors responsible for its pathogenicity, we still know relatively few virulence factors in *A. baumannii*, compared to other GNB [42]. Due to the increasing antimicrobial resistance rates and the lack of treatments to combat infections, it is important to identify new virulence factors to characterize the pathogenesis and determine new therapeutic targets that allow the control of this kind of infections.

The main identified virulence factors of *A. baumannii* are:

a. Porins:

A. baumannii, as the rest of GNB, has a double membrane (outer and inner membrane) which constitutes the first line of contact between bacteria and its external environment (Fig. 3). These two membranes, which differ substantially in their compositions, are separated by the periplasmic space [43]. This double membrane is a selective barrier which acts as a protection mechanism and it allows the entry of nutrients to promote cell survival.

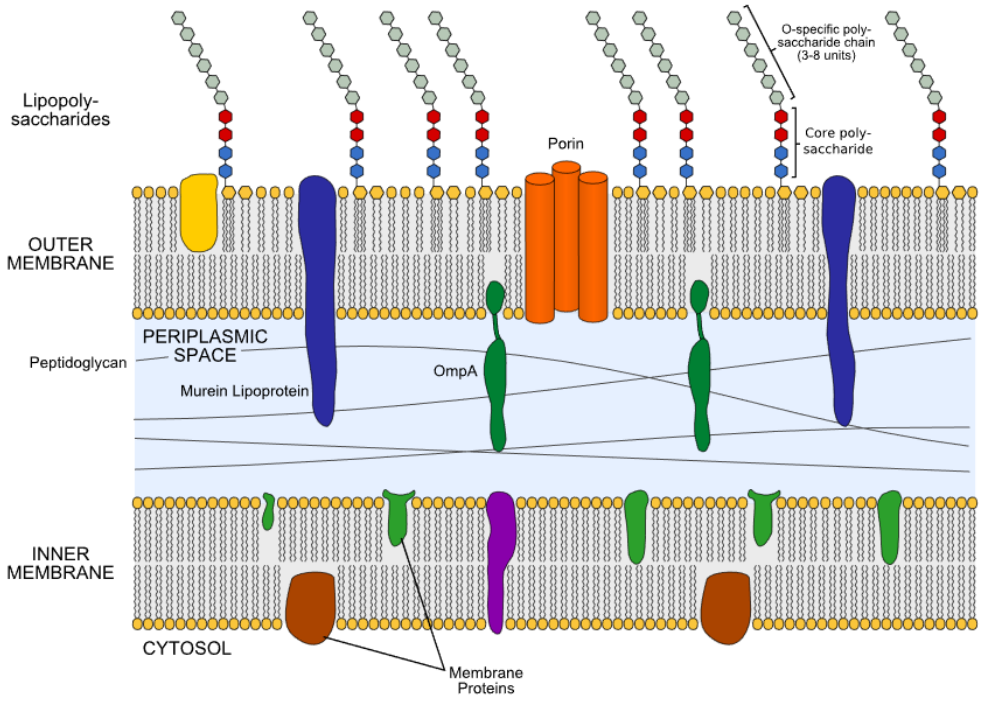

Figure 3. Structure of a GNB double membrane. (https://en.wikipedia.org/wiki/Gram-negative_bacteria)

The outer membrane has a unique composition and asymmetrical distribution of lipids, with the inner leaflet containing phospholipids, whereas the outer leaflet is composed of lipopolysaccharide (LPS), a highly negatively charged molecule [44]. The outer

membrane is mainly composed by proteins, called outer membrane proteins (OMPs) or porins, which are associated with the modulation of cellular permeability [35]. These proteins are involved in nutrient uptake, cell adhesion, cell signaling and waste export [45]. Moreover, for the pathogenic strains, these OMPs also serve as virulence factors for nutrient scavenging and evasion of host defense mechanisms [44].

One of the main OMPs that has been characterized is OmpA. OmpA is a β-barrel porin and one of the most abundant porins in the outer membrane [35]. It plays a considerable role in adherence and invasion of epithelial cells by interacting with fibronectin [46], and binds to factor H in human serum which may allow *A. baumannii* to resist complement-mediated killing [47]. OmpA is also involved in antibiotic resistance of *A. baumannii* [48, 49] and in biofilm formation [50].

Omp33-36 is another OMP associated with *A. baumannii* cytotoxicity [51]. Other porins, such as carbapenem-associated outer membrane protein (CarO) and OprD-like, are also virulence factors associated with attenuated virulence in a mouse model [52].

b. Capsular polysaccharides and lipopolysaccharides (LPS):

Capsular polysaccharides are involved in antimicrobial resistance of *A. baumannii*. It is known that mutants deficient in capsular polysaccharides have lower intrinsic resistance to peptide antibiotics. Moreover, the presence of antibiotics induces hyperproduction of capsular polysaccharides [53]. This increased capsule production depends on the regulation of K locus gene expression by *bfmRS* two-component regulatory system. *bfm*R is important for persistence in the lung in a murine pneumonia model [54] and *bfm*S is involved in biofilm formation, adherence to eukaryotic cells, and resistance to human serum [55]. Capsular polysaccharides also promote survival during periods of desiccation due to their ability to retain water.

LPS is the major component of the outer leaflet of the outer membrane in most GNB and is an immunoreactive molecule that induces release of tumor necrosis factor and IL-8 from macrophages in a Toll-like receptor 4 (TLR4)-dependent manner [35]. LPS is composed of an endotoxic lipid A moiety, an oligosaccharide core, and a repetitive O-antigen and it plays a major role in virulence and survival of *A. baumannii* [56, 57].

c. Phospholipase:

Phospholipase is a lipolytic enzyme essential for phospholipid metabolism and is a virulence factor in *A. baumannii* [58]. There are three classes of phospholipases: phospholipase A (hydrolyzes fatty acids from the glycerol backbone), phospholipase C (cleaves the phosphorylated head group from the phospholipid), and phospholipase D (transphosphatidylase that only cleaves off the head group). Degradation of phospholipids affects the stability of host cell membranes, and the cleaved head group can interfere with cellular signaling, changing the host immune response [58, 59].

d. Outer Membrane Vesicles (OMVs):

OMVs are spherical, 20-200 nm diameter vesicles secreted by various pathogenic GNB. They are composed of LPS, outer membrane and periplasmic proteins, phospholipids, and DNA or RNA, and are recognized as delivery vehicles for bacterial virulence factors to the interior of host cells [60]. These virulence factors include OmpA, proteases and phospholipases [61]. *A. baumannii* OMVs has also been reported to participate in the spread of antibiotic resistance and induce the horizontal transfer of the OXA-24 carbapenemase gene [62].

e. Metal acquisition system:

It is well known that iron is essential for the growth of bacteria. Therefore, pathogens have developed highly efficient iron-acquisition systems to obtain iron from the outside medium. *A. baumannii* produces high-affinity iron chelators known as a siderophores to use the limited environmental iron. One of the best characterized *A. baumannii* siderophores is acinetobactin, which is a virulence factor that allows bacteria to persist within epithelial cells and cause cell damage and animal death [63]. There are another metal acquisition system as NfuA Fe-S scaffold protein [64], the metal-chelating protein calprotectin [65], and the zinc acquisiont system ZnuABC [66] which also are virulence factors and contribute to the pathogenesis of *A. baumannii*.

f. Protein secretion systems:

Several protein secretion systems have been described in *A. baumannii*. Three of them, the type II secretion system (T2SS), the type VI secretion system (T6SS) and the type V system autotransporter Ata, are virulence factors involved in the pathogenesis mechanism [35]. The T2SS is a multi-protein complex that translocates a lot of range of proteins from the periplasmic space to the extracellular medium or the outer membrane surface. First of all, it is necessary that the target protein is transported from the inside of the bacteria to the periplasmic space by the general secretory (Sec) system or the twin arginine transport (Tat) system [67]. *A. baumannii* uses this T2SS to transport LipA, a lipase that breaks down long-chain fatty acids and allow the pathogen to grow in a neutropenic murine model of bacteremia [68]. The T6SS is a multicomponent secretion machine capable of mediating lethal injections of protein toxins into other bacteria in a contact-dependent manner [69]. *A. baumannii* is able to kill *K. pneumoniae* and *P. aeruginosa* using the T6SS, and different strains of *A. baumannii* are also able to kill

each other [70, 71]. Finally, the type V system autotransporter Ata is involved in biofilm formation, adherence to extracellular matrix, and virulence in a murine systemic model of *Acinetobacter* infection [72].

g. Biofilm formation:

The ability of *A. baumannii* to form biofilms allows it to grow persistently in unfavorable conditions and environments [31], reduces the antibiotic penetration [73] and plays an important role in immune evasion [74]. Pili are essential for *A. baumannii* adherence and biofilm formation on abiotic surfaces as well as virulence [75]. The type I chaperone-usher pilus system (Csu pili), regulated by the BfmRS two-component system, are crucial for biofilm formation and maintenance on abiotic surfaces, constituting an *A. baumannii* virulence factor [76]. Furthermore, another virulence factor is the polysaccharide polymer poly-beta-1,6-N-acetylglucosamine (PNAG), one of the most important components of exopolysaccharides constituting biofilm matrix that is crucial for maintaining the integrity of *A. baumannii* biofilm under environmental stresses [77].

3.2. *Pseudomonas aeruginosa*

3.2.1. Epidemiology and antimicrobial resistance

P. aeruginosa is a facultative aerobic, catalase-positive, non-fermentative GNB, which has unipolar motility. It is a ubiquitous bacterium that normally inhabits the soil and surfaces in aqueous environments. It can adapt to different environments and it has a high intrinsic antibiotic resistance which enable it to survive in a wide range of other natural and artificial settings, including surfaces in medical facilities [78]. *P. aeruginosa* is among the most common hospital pathogens in the United States and is the second

most common pathogen isolated from patients with ventilator-associated pneumonia [79]. The ECDC 2011-2012 Point-Prevalence Survey for HAIs found that almost 9% of all infections were caused by *P. aeruginosa*, and that it was the 4th most common pathogen in Europe [2]. This pathogen produces a wide range of infections such as pneumonia, urinary tract infection, skin and soft tissue infections, ocular infection, bacteremia, septicemia and endocarditis [80]. Mortality due to *P. aeruginosa* has been shown to be as high as 70% [81].

P. aeruginosa infections are difficult to treat due to its intrinsic ability to resist many antibiotics as well as its ability to acquire resistance [78]. Intrinsic resistance is due to the low permeability of its outer membrane, the constitutive expression of membrane efflux pumps, and the inducible chromosomal β-lactamase AmpC [82]. The increasing prevalence of MDR strains is a cause of concern and it hinders the selection of appropriate empirical and definitive antimicrobial treatments. This situation is associated with worse outcomes, increased costs, and higher mortality [83]. Data provided in 2012 by the EARS-Net in 2015 showed that high percentages of *P. aeruginosa* isolates were resistant to aminoglycosides and ceftazidime (13%), and fluoroquinolones, piperacillin/tazobactam and carbapenems (20%) [84].

3.2.2. Virulence factors and pathogenesis

P. aeruginosa is an opportunistic pathogen that mainly causes acute or chronic lung infections [78]. Several analyses have reported that its phenotype differs when the pathogen has been isolated from acute infections or from chronic infections [85]. Isolates from acute infections express a different arsenal of virulence factors while those isolated from chronic infections lack some of them, like the flagella and pili, and form more biofilm [86].

The main identified virulence factors of *P. aeruginosa* are:

a. Porins:

P. aeruginosa has large channel porins (formed by OprF, an OmpA homologue protein) and a number of small channel porins (such as OprD and OprB) [78]. Moreover, six resistance-nodulation-division (RND) family efflux pumps have been described [87]. These efflux pumps can eject a wide range of antibiotics making the bacteria resistant and more virulent. Some studies have reported that OprF is involved in *P. aeruginosa* adherence to host cells [88]. Furthermore, *P. aeruginosa* shows increased levels of OprF when they grow under anaerobic conditions in the presence of nitrate, suggesting a possible involvement of OprF in the diffusion of nitrates and nitrites [89]. It is suggested that OprF is also involved in biofilm formation, OMV biogenesis and quorum sensing response [89].

b. Flagella and type 4 pili:

P. aeruginosa possess a single polar flagellum and several type 4 pili localized at a cell pole. These appendages are involved in adherence and motility and they can also start and inflammatory response [90]. Mutants that do not present flagella are defective in models of acute infection [91].

Type 4 pili are important adhesins involved in twitching motility and the formation of biofilms [92] and in swarming motility [93]. Pili allow bacteria to form aggregates on target tissues which protect bacteria from the host immune system and antibiotics [94].

c. Type 3 secretion system (T3SS):

T3SS is a secretion system involved in injecting toxins directly from the cytoplasm into host cells. Its expression is associated to increased mortality in infected patients [86,

95]. *P. aeruginosa* T3SS is encoded by 36 genes on five operons, with six other genes encoding the effector proteins and their chaperones [95]. This system is controlled by the transcriptional activator ExsA [96]. It is still not known the exact role of each of the toxins in pathogenesis, but T3SS may allow *P. aeruginosa* to exploit breaches in the epithelial barrier and to promote cell injury [95].

d. Quorum sensing:

Quorum sensing is a mechanism of bacterial cell-to cell communication that allows bacteria to adapt to the environment through small membrane-diffusible molecules called autoinducers. Autoinducers act as cofactors of transcriptional regulators and they activate the expression of determined genes once a population threshold is reached [97]. *P. aeruginosa* produces three autoinducers. Two of them are acyl homoserine lactones and the third one is the Pseudomonas quinolone signal [97]. These systems control cell survival, biofilm formation, and virulence [86, 92, 98].

e. Biofilm formation:

P. aeruginosa form highly organized biofilms that consist of polysaccharides, nucleic acids, lipids, and proteins. Biofilms protect bacteria from toxic chemicals like antibiotics or host defense molecules [99]. Furthermore, gene expression in *P. aeruginosa* differs depending on bacteria states (planktonic or forming biofilms) [100]. It is known that an upregulation of stress response genes occur during biofilm formation and this may lead to increased antibiotic resistance [101]. The shift between motile and sessile states is triggered by several regulatory systems. For example, the GacA/GacS two-component system, which is implicated in biofilm formation and virulence [102].

f. Proteases:

P. aeruginosa secretes several proteases which are important for degradating immunoglobulins and fibrin and disrupt epithelial tight junctions during infection [92]. Some of the proteases that this pathogen secretes are alkaline protease 1, two elastases (LasA and LasB), and protease IV [78].

g. Capsular polysaccharides and lipopolysaccharides (LPS):

Some strains of *P. aeruginosa* produce a mucoid exopolysaccharide capsule, comprised of alginate, L-guluronic acid, and an acetylated random co-polymer of β 1-4 linked D-mannuronic acid. These mucoid strains usually are isolated from patients with cystic fibrosis (CF) and it plays a role in cell adherence in the CF lung. Furthermore, it is involved in resistance to host defense because it reduces susceptibility to phagocytosis and hinder diffusion of antibiotics [103].

LPS is a complex glycolipid that forms the outer leaflet of the outer membrane and is involved in antigenicity, inflammatory response, exclusion of external molecules, and it mediates interactions with antibiotics. LPS in *P. aeruginosa*, like in *A. baumannii*, consists of a membrane-anchored lipid A, a polysaccharide core region and a variable O-polysaccharide [104].

Lipid A is localized at the end of LPS so it can bind to host cell receptors MD2 and CD14 leading to an activation of the Toll-like-receptor 4 (TLR4) to NFκβ signaling pathway and triggering the production of inflammatory cytokines and endotoxic shock [105]. Modifications to lipid A can alter *P. aeruginosa* susceptibility to polymyxins and cationic antimicrobial peptides [78]. Isolates from chronically infected cystic fibrosis lungs showed hexa- and hepta-acylated species that increase inflammatory response and

the severity of lung disease [106]. Lipid A modifications may be regulated and induced by environmental changes [78].

P. aeruginosa can present simultaneously two types of O-polysaccharide, the A-band and the B-band. A-band elicits a weak antibody response while B-band elicits a strong antibody response [104]. Some strains do not produce any O-polysaccharide and other strains just produce one of them [78]. Many chronic isolates change their proportion of A-band and B-band to evade host adaptive immune response [104].

h. Other virulence factors:

Exotoxin A is an ADP-ribosyltransferase that inhibits host elongation factor EF2, so it inhibits protein synthesis and causes cell death. Moreover, it also represses host immune response [107]. Exotoxin A also induces host cell death by apoptosis [108] and strains that produce it show more virulence in a murine model of infection [109].

Phospholipases are also virulent factors of *P. aeruginosa* because they break down lipids and phospholipids of host cell membranes [92].

Pyocyanin is a blue-green pigment of *P. aeruginosa* that causes oxidative stress to the host, disrupting its catalase and mitochondrial electron transport [110]. Moreover, it is known that pyocyanin *in vitro* induces apoptosis in neutrophils and inhibit the phagocytosis of apoptotic bodies by macrophages [110, 111]. Pyocyanin also retards the growth of some other bacteria and thus facilitates colonization by *P. aeruginosa* [103].

This pathogen also needs iron chelation systems to establish and produce a chronic infection, since host environment has little free iron available. Therefore, *P. aeruginosa* has several siderophores like pyoverdine or pyochelin. Pyoverdine also acts like a

signaling molecule causing the upregulation of exotoxin A, endoprotease and of pyoverdine itself [112].

4. Hypoxia influence on infections and immune response

4.1. Hypoxia regulation: HIF-1α

Hypoxia occurs when cellular oxygen demand exceeds supply. Tissue hypoxia can occur in a wide variety of pathologic conditions including vascular disease, cancer, dermal wounds and respiratory illnesses, and it is common during inflammation associated with acute or chronic bacterial infection [113, 114]. The reasons for the occurrence of hypoxia (or even anoxia) during inflammation is a combination of increased oxygen demand in order to satisfy the requirements of inflamed resident cells, infiltrating inflammatory cells and in some cases multiplying pathogens, along with a decreased perfusion due to vascular dysfunction (during chronic inflammation) [114]. Thus, oxygen levels in the foci of infection are much lower (<1%) than in healthy tissues (2.5-9%) [115].

It is essential that eukaryotic cells, especially immune cells, remain effective under such hypoxic conditions. Therefore, eukaryotic cells have developed the ability to adapt to the hypoxic environment through the transcriptional regulation of multiple genes [116]. One of them is the hypoxia inducible factor 1 (HIF-1), a heterodimeric transcription factor (HIF-1α and HIF-1β) whose expression is regulated at the protein level. Under hypoxia and/or bacterial infection, different oxygen and iron dependent proline hydroxylases (PHDs; PHD1, PHD2 and PHD3) are inhibited, so HIF-1α accumulates and translocates into the nucleus, where it dimerizes with HIF-1β, constitutively expressed [113]. Then, the heterodimeric HIF-1 make a complex with the p300/CBP

transcriptional coactivator protein and this active HIF-1 complex binds to the hypoxic response elements (HREs). These bindings induce the expression of multiple genes involved in angiogenesis, glycolysis and cellular stress, among others, as well as the repression of genes involved in a reduction in energy demanding processes (Fig. 4) [117]. In addition, HIF-1 is also activated under iron deprivation because Fe^{2+} is an essential cofactor of PHDI-3, which promotes HIF-1 degradation [118]. The HIF family also comprises the HIF-2 and HIF-3, but they have been less studied. HIF-2 has similar functions to HIF-1, but HIF-3 seems to inhibit HIF-1 and HIF-2 activities [119].

Under normoxic conditions, oxygen and iron dependent proline hydroxylases are active and hydroxylate the proline residues of HIF-1α. Moreover, the hydroxylation of an asparagine residue by the Factor Inhibiting HIF-1 (FIH) on HIF-1α blocks the interactions between p300/CBP transcriptional coactivator proteins and the α subunit, thereby preventing the transcription of several genes. Finally, the hydroxylated prolines become ubiquitinated by the von Hippel-Lindau tumor suppressor protein and the HIF-1α undergoes proteosomal degradation. Therefore, HIF-1 gets inhibited and degraded in the presence of oxygen (Fig. 4) [120, 118].

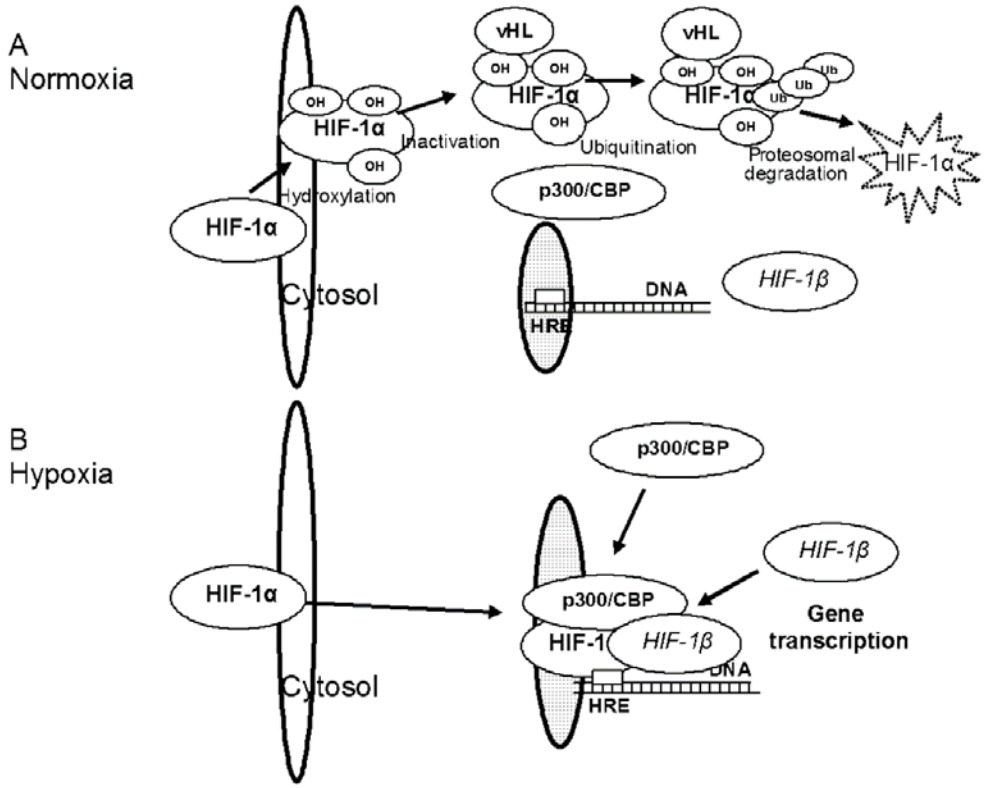

Figure 4. HIF-1α pathway during normoxia and hypoxia [120].

4.2. Functions of HIF-1

a. Recovery after hypoxia/ischemia:

HIF-1 prevent tissue damage induced by ischemia by two fundamental mechanisms: shifting the cellular metabolism to the anaerobic mode, and promoting new vascularization towards the hypoxic areas hence increasing oxygen supply. Several studies show that HIF-1 overexpression induces angiogenesis in hypoxic tissues and it can lead to increased oxygenation of the organ [121].

b. Induction of proinflammatory and antimicrobial responses:

After microbial infection, the immune system activates an immune reaction starting with the innate immune response. A key element is the activation of polymorphonuclear leukocytes (PMN-s) which are parts of the myeloid cell family. PMN-s seek out, migrate, identify, phagocytize and eliminate the invading microbes by releasing reactive oxygen species (ROS). ROS are generated in PMN-s in a process called respiratory burst. Recent studies employing HIF-1α gene knock out mice showed that HIF-1α is a regulator of energy metabolism, aggregation, migration and bactericidal activity of PMN-s [122, 123]. In addition, it is known that HIF-1α expression plays a crucial role in the differentiation of myeloid cells into monocytes and macrophages [123].

c. Shifting metabolism toward anaerobic mode:

The oxidative phosphorylation is the main source of adenosine triphosphate (ATP) in human cells during normoxia. However, the cellular metabolism needs to be shifted toward anaerobic energy production during hypoxia. HIF-1 is one of the principal molecules to regulate this shift. HIF-1 activates glucose transporters, aldolase A, pyruvate kinase M and a number of glycolytic enzymes [124]. In addition, HIF-1 efficiently downregulates mitochondrial oxygen consumption [125]. Therefore, HIF-1 helps cells to produce energy even in environments of low oxygen concentrations.

d. Induction of angiogenesis:

HIF-1 promotes angiogenesis in a number of different tissues. During hypoxia, HIF-1α binds the transcription regulatory region of the VEGF gene and induces its transcription and translation [124]. Then the VEGF induces migration of mature endothelial cells toward the hypoxic tissue. These activated endothelial cells start producing new blood vessels which supply the hypoxic areas with more blood and oxygen [126].

e. Promoting tumor progression:

When a tumor grows, its quickly dividing cells need an enormous amount of energy, and this induces angiogenesis to meet the increasing needs for blood supply providing oxygen, glucose and other essential molecules. In cancerous tissues HIF-1α activates VEGF inducing angiogenesis, as stated above. Moreover, HIF-1 promotes anaerobic metabolic adaptation of hypoxic metastasizing tumors. It has been found that in vHL-lacking renal carcinoma cells, HIF-1 activation decreases oxygen consumption by inhibiting C-MYC, a transcription factor that regulates mitochondrial oxygen consumption. The down-regulation of C-MYC results in increased glycolysis and suppressed mitochondrial respiration [127, 128].

f. Pro-apoptotic effects:

Hypoxia can activate the p53 tumor suppressor via HIF-1, and p53 induces p21 which promotes cell death by apoptosis in embryonic stem cells. A different study in primary alveolar epithelial cells reported that low oxygen levels induce apoptosis via the HIF-1 pathway [129]. The majority of studies describe the HIF-1 as an apoptosis promoting factor, but it has also been reported that in hypoxia-challenged neonatal brain tissues the activation of HIF-1 protected the cells by preventing them from undergoing apoptosis [130].

4.3. Hypoxia and infection

Tissue hypoxia happens *in vivo* during a range of infections (bacterial, viral and fungal infections). For example, hypoxia occurs within the mucus filled airways of cystic fibrosis patients who are often infected with the pathogen *P. aeruginosa* [131]. Furthermore, studies have reported that *Mycobacterium tuberculosis* resides in a hypoxic environment within granulomas in guinea rabbits, pigs, and primates [132].

Pulmonary infection with *Aspergillus fumigatus* in mice also leads to the establishment of a hypoxic microenvironment in the infected tissue [133]. Sendai virus (also known as a murine parainfluenza virus) responsible for respiratory diseases, shows enhanced replication under hypoxia condition [134]. In summary, tissue hypoxia is a common microenvironmental feature in a different number of infections.

HIF-1 is activated during infections of all kind of pathogens, including group A and b *Streptococci*, *Staphylococcus aureus*, *Salmonella typhimurium Escherichia coli*, *Chlamydia pneumoniae* and *P. aeruginosa* [135]. This HIF-1 activation occurs due to the low oxygen level because of the presence of a high amount of bacteria in the foci of infection that are consuming it (Fig. 5). It was first reported in some studies using the pathogen *Bartonella henselae* [136]. In *B. henselae* infections, enhanced oxygen consumption has been associated with the expression of the outer membrane protein Bartonella Adhesin A (BadA), which is a virulence factor involved in adherence (Fig. 5). Cells infected with a *B. henselae* mutant in BadA did not get hypoxic upon infection, and no HIF-1 activation was detected. In addition, HIF-1 activation also occurs due to low iron concentrations. *Klebsiella pneumoniae* siderophores chelate the host cellular iron, causing an inactivation of iron-dependent prolyl hydroxylases and HIF-1α stabilization in lung epithelial cells (Fig. 5). This induces vascular permeability and angiogenesis, so *K. pneumoniae* can disseminate better under hypoxia than normoxy [137]. Recent studies have shown that bacterial lipopolysaccharide (LPS), a component of the gram negative bacteria, also activates HIF-1α in a TLR4 dependent fashion in macrophages and neutrophils under normoxic conditions due to the activation of p44/42 MAPK and NF-κβ pathways, because HIF-1α gene contains binding sites for this factor (Fig. 5) [138].

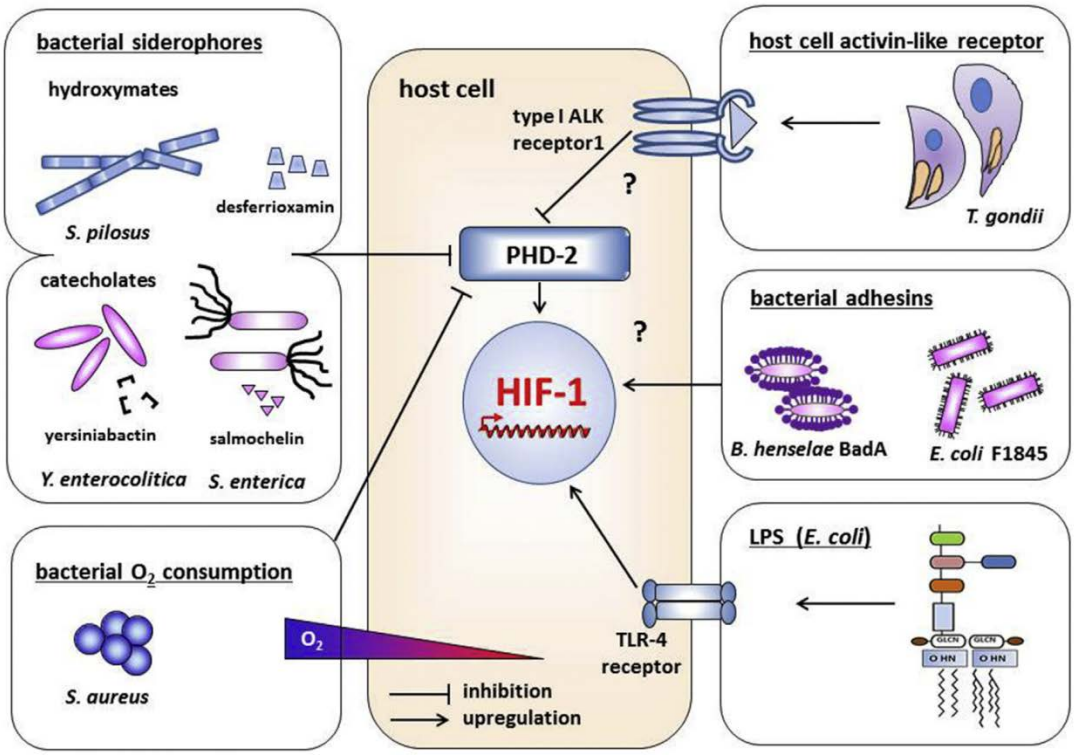

Figure 5. Influence of the interaction pathogen-host cells results in HIF-1 activation [118].

Hypoxia and HIF-1 have a protective role in the defense against pathogens, mainly due to NF-κβ, which promote the bactericidal capacity of phagocytes, monocyte/macrophages, dendritic cells, neutrophils and, even, epithelial cells, through the production of inflammatory cytokines and antimicrobial peptides such as cathelicidins (Fig. 6) [115, 139, 140]. Several mouse models have been used to investigate the role of HIF in infections. For example, knockout (KO) mice in HIF-1 are more susceptible to bacterial infection [141]. Moreover, HIF-1α keratinocytes KO mice have shown to develop larger necrotic lesions and had decreased capacity to clear group A *Streptococcus* because they recruited less neutrophils to the site of infection [142, 143]. Internalization of *P. aeruginosa* into airway epithelial cells is also lower under hypoxia than normoxia [144] and mice infected with *Mycobacterium tuberculosis* under hypoxic conditions shown increased survival time compared with those under normoxia

[113]. HIF-1α KO mice displayed impaired leucocyte invasion and inflammation using ear and skin inflammation models [122] and BALB/c mice, which are resistant to *P. aeruginosa* keratitis, suffer severe infection when HIF-1α is knocked down using siRNA [145]. Moreover, another study showed that IL-6 production was lower under hypoxia than normoxia in a keratinocyte culture, but a treatment using a compound which boosts HIF resulted in an increase in IL-6 levels compared even to normoxia. These treated keratinocytes were more efficient in the clearance of *S. aureus*, *P. aeruginosa* and *A. baumannii*. This result suggests that additional changes during hypoxia, and not HIF levels alone, can alter cytokine production and immune response [142, 146].

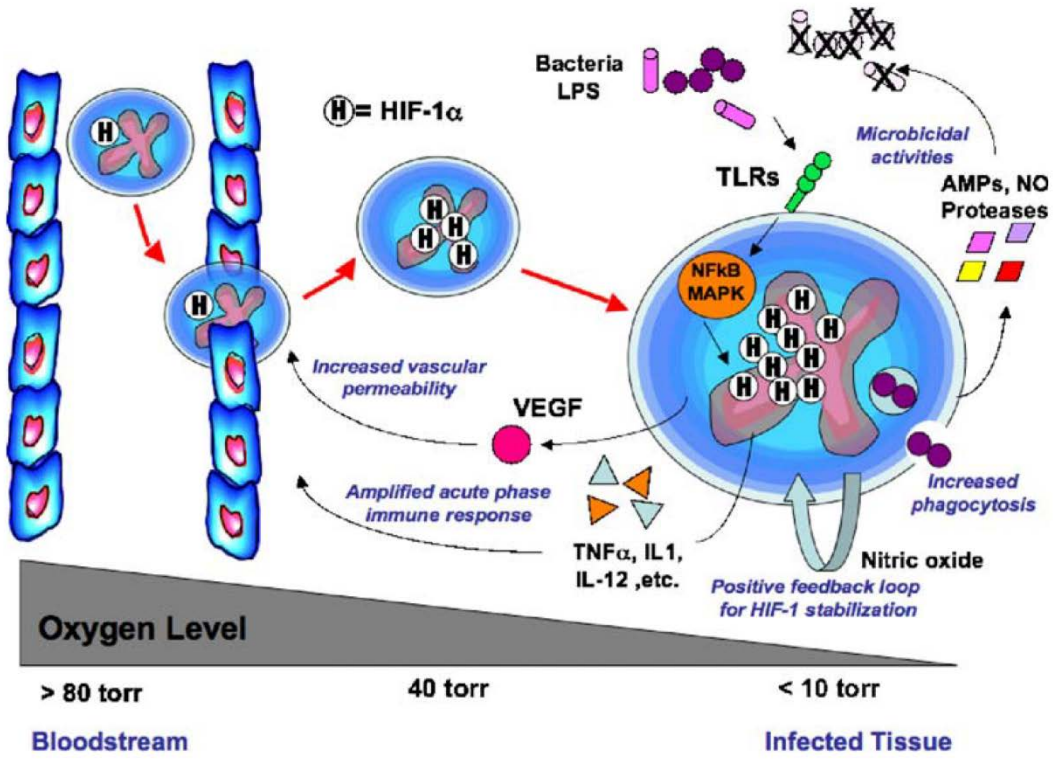

Figure 6. HIF-1α transcriptional regulation of phagocyte innate immune functions [115].

However, HIF-1 can have a negative role in the course of systemic infection, e.g. in sepsis. A KO of HIF-1α in the myeloid cells showed increased survival rates in a murine LPS-induced sepsis model and decreased serum levels of proinflammatory cytokines [147]. VEGF, another HIF-1 regulated cytokine, is elevated in serum of septicemic patients. Methicillin-resistant *S. aureus* (MRSA) and *Streptococcus pneumoniae* infections in meningitis patients induce higher serum VEGF levels [148, 149]. Blocking of VEGF with soluble VEGF receptors increased survival in a murine LPS-sepsis model [150]. This harmful effect of VEGF and HIF-1 might be mediated by enhanced overwhelming immune response and subsequently to vascular leakage, and organ failure, which has already been demonstrated for patients suffering from septic shock (Fig. 7) [151]. HIF-1α is also a determinant of sepsis phenotype through the production of inflammatory cytokines (IL-1, IL-4, IL-6, IL-12 and TNF-α). High cytokines levels may be harmful to the host during early sepsis [152]. Therefore, a potential use of HIF-1 inhibitors in sepsis patients could be an interesting option, especially in times of widespread antibiotic resistances in clinically relevant pathogens, but there is no information from clinical studies available if inhibition of HIF-1 is beneficial for the outcome so far [118].

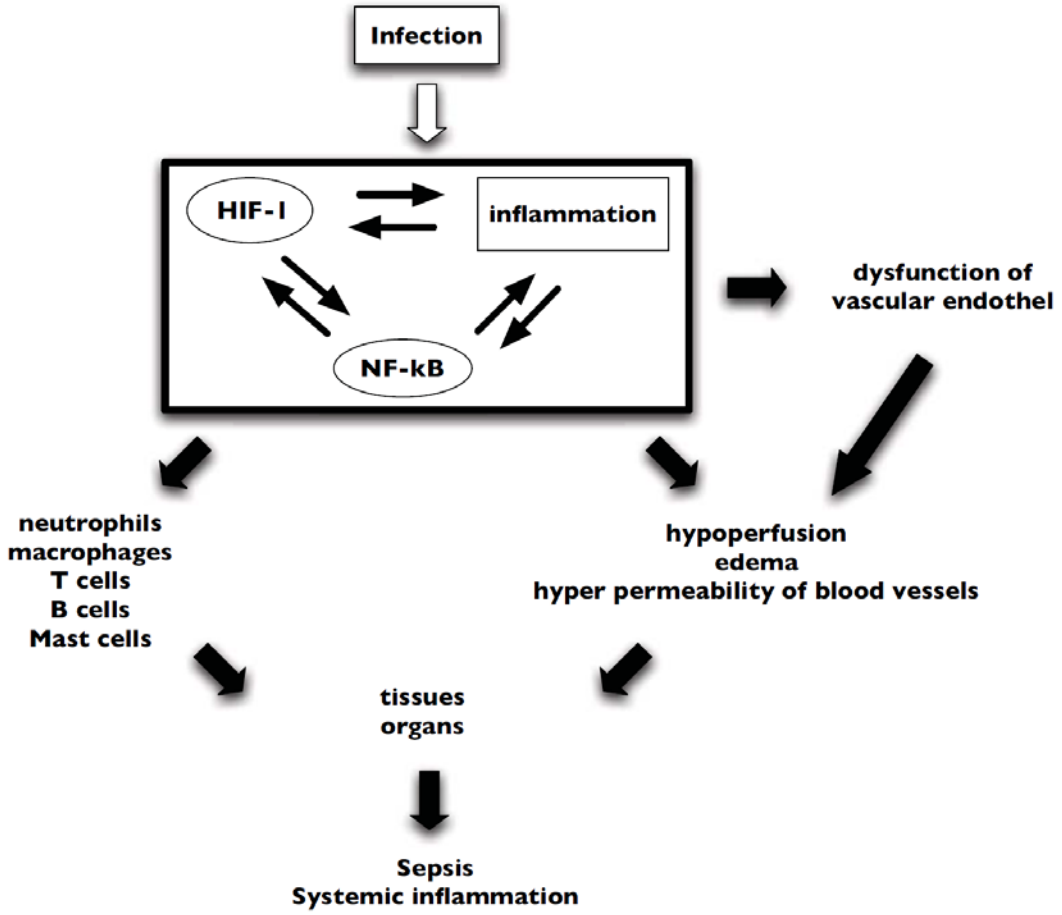

Figure 7. Interdependence of HIF-1and NF-κβ plays an essential role in the progress of sepsis [153].

Hypoxia and HIF-1 activation not only modifies the host cells but also the bacterial metabolism and virulence [118]. Therefore, the microenvironment at the foci of infection plays a crucial role in determining the outcome of an infection. It has been demonstrated that hypoxia reduces the virulence of *P. aeruginosa* because it decreases the expression of multiple virulence factor such as alkaline protease, siderophores and exotoxin A [154]. Exposure to hypoxia also induces antibiotic resistance in *P. aeruginosa* by an alteration of efflux pumps expression [155] and increases the alginate production [156]. In addition, some pathogens required an hypoxic environment to grow in optimal conditions, e.g. *C. pneumoniae* or *Toxoplasma gondii* (Fig. 5). These pathogens show a decreased growth and survival rates in HIF-1α KO cells under

hypoxic conditions [157, 158]. Together, these results demonstrate the complexity of HIF-pathogen interactions.

4.4. HIF-1α as a pharmacological target for infection treatment

Nowadays, antimicrobial resistance is a global public health challenge. Therefore, there is an urgent need to search for alternative strategies to overcome this problem. Although the knowledge of the role of HIF-1 in infections is still unclear and limited, it could be considered as one major target for fighting infections in future.

Modifying the course of infection could diminish the overwhelming inflammatory cascades which cause the high lethality in severe sepsis [118]. It has been reported that a neutralization of VEGF (regulated by HIF-1) is beneficial in a murine sepsis model [150]. Therefore, inhibition of HIF-1 might be beneficial in severe and acute infections. There are several compounds available which inhibit HIF-1, e.g. echinomycin (produced from *Streptomyces lasalienis*) that inhibits HIF-1 transcription; or chetomin (produced from the fungus *Chaetomium* spp.) which prevents the binding of HIF-1a to the coactivator p300 [159]. A study in a *S. aureus* peritonitis model showed that the use of 17-DMAG, an HIF-1 inhibitor targeting HIF-1 protein stability, reduced lethality from 100% down to 70% [135]. On the other hand, activation of HIF-1 might stimulate the immune response to overcome infections which cannot be cleared by the host [118]. Okumura et al. [146] showed that a new pharmacological compound called AKB-4924 increased HIF-1 levels and enhanced the antibacterial activity of phagocytes and keratinocytes against *S. aureus, P. aeruginosa* and *A. baumanii in vitro*.

Therefore, all these data demonstrate why hypoxia is being extensively studied today to try to find out a new way of treatment of MDR bacteria.

FUNDAMENTS

The emergence of MDR GNB infections is a well-recognized global health challenge in urgent need of effective solutions. These pathogens cause infections that are very difficult to treat due to the high rate of resistance strains to a lot or even all antimicrobials used in the clinical practice. Furthermore, these kinds of infections are associated to important mortality rates. Unfortunately, the increasing problem of multidrug resistance is not followed by the development of novel antimicrobials. For this reason, there is an important need to develop new strategies to combat MDR, XDR and PDR GNB.

A new alternative to combat this kind of infections might be blocking specific bacterial virulence factors that bacteria need to infect. It is known that bacteria modulate their gene expression in function of the environment. Therefore, expression of virulence factors can change during the course of infection according to every microenvironment in which bacteria are found. Several studies have reported that hypoxia occurs in a wide range of infection, so it would be interesting to determine the gene profile of these MDR pathogens in order to find out new virulence factors that we could block. Moreover, it is also important to know how hypoxia affects to this kind of infection to know better what is happening *in vitro* and *in vivo*. Because *A. baumannii* and *P. aeruginosa* are two of the most common pathogens that cause HAIs, we have chosen them to study their virulence mechanism under hypoxia in more depth. We have selected the strains *A. baumannii* ATCC 17978 and *P. aeruginosa* PAO1 because they are well-known sequenced strains which allow us to analyze virulence factors in a better way.

On the other hand, septic shock patients present tissue hypoxia that might influence the disease. Moreover, septic shock is the most severe complication of sepsis and most

studies about this syndrome report a high mortality rate. Hence, it would be useful to study the relationship between tissue hypoxia, HIF-1α levels and immune response, and to determine new biomarkers to predict the outcome.

HYPOTHESES

The hypotheses of this Doctoral Thesis are:

Chapter I

1. Environmental oxygen levels modify *A. baumannii* gene expression and regulate its pathogenicity and virulence.

Chapter II

2. Hypoxia affects to the bactericidal activity of eukaryotic cells against *A. baumannii* and *P. aeruginosa*.
3. Hypoxia affects to the bacterial adherence and invasion of both pathogens into eukaryotic cells.
4. Hypoxia modifies innate immune response of eukaryotic cells against both pathogens.

Chapter III

5. Hypoxia modifies innate immune response in septic shock patients.

OBJECTIVES

The general aim of this Doctoral Thesis is to find out the effect of hypoxia on genetic regulation and virulence in *A. baumannii* and *P. aeruginosa*, *in vitro* and *in vivo*, and on innate immune response in infections caused by both pathogens. In addition, we would like to determine new biomarkers to predict the outcome of septic shock patients in the early stages of the disease.

The specific objectives of each chapter are the following:

Objectives of chapter I:

1. To identify the genes of *A. baumannii* whose expression is regulated by environmental oxygen levels.
2. To characterize the role of those genes in infection, *in vitro* and in murine models.

Objectives of chapter II:

1. To evaluate the effect of hypoxia on the bactericidal activity of cell lines *A. baumannii* and *P. aeruginosa*.
2. To evaluate the effect of hypoxia on the bacterial adherence and invasion of *A. baumannii* and *P. aeruginosa* into cell lines.
3. To characterize the effect of hypoxia on the expression of virulence factors of *A. baumannii* during the infection.
4. To characterize the *in vitro* innate immune response in infections of *A. baumannii* and *P. aeruginosa* under hypoxic conditions.

5. To study the effect of hypoxia on the innate immune response and prognosis in lethal murine models of sepsis by *A. baumannii* and pneumonia by *P. aeruginosa*.

Objectives of chapter III:

1. To investigate the relationship between tissue hypoxia, HIF-1α levels and immune response in patients with septic shock (20).
2. To determine new biomarkers to predict the outcome of septic shock patients.

METHODS AND RESULTS

Chapter I. Article I. Comparative gene expression profile of *Acinetobacter baumannii* growing under microaerobiosis and normoxia.

It will be submitted to The Journal of Infectious Diseases.

Chapter II. Article II. Effect of hypoxia on the pathogenesis of *Acinetobacter baumannii* and *Pseudomonas aeruginosa in vitro* and in murine experimental models of infections.

Published in Infection and Immunity 2018.

Chapter III. Article III. Predictive value of APACHE II, and serum lactate, pyruvate, IL-10 and lysophosphatidylcholine levels on survival in patients with septic shock.

It will be submitted to Critical Care Medicine.

CHAPTER I. ARTICLE I.

COMPARATIVE GENE EXPRESSION PROFILE OF *ACINETOBACTER BAUMANNII* GROWING UNDER MICROAEROBIOSIS AND NORMOXIA.

Acinetobacter baumannii is an aerobic Gram-negative pathogen responsible for healthcare-associated infections of the respiratory tract, skin, bacteremia, urinary tract, and other soft tissues [1]. During the process of infection, bacteria adapt to different environments modifying their gene expression [2]. It is known that tissue hypoxia occurs in the course of inflammation, due to a higher rate of oxygen consumption by immune cells and pathogens together with a reduction of the perfusion caused by vascular dysfunction [3]. This means that oxygen levels in the foci of infection are much lower (<1%) than in healthy tissues [4]. Moreover, there are different common medical conditions that produce hypoxemia and peripheral tissue hypoxia and they are often associated with infection and inflammation [5]. Therefore, bacteria must adapt to a hypoxic environment during infection, which modifies the expression of genes involved in metabolism and virulence [6]. Several virulence factors of *A. baumannii* have been identified through genomic and phenotypic analyses [7]. However, we still have not a whole picture of its pathogenic mechanisms. Nowadays, techniques that utilize next-generation sequencing, such as RNA-seq, have been used for characterization of bacterial genomes under different conditions [8, 9]. Some analyses of the *A. baumannii* transcriptome have provided important information regarding *A. baumannii* biological characteristics. RNA-seq has been used to characterize and compare gene expression in *A. baumannii* under biofilm and planktonic growth conditions [10, 11], to analyze *A. baumannii* response and resistance mechanisms to different antibiotics and antibacterial agents [12-16], and to examine genetic changes that happen during host infection,

bacteremia and treatment [17, 18]. However, no study has investigated the influence of hypoxia/microaerobiosis in *A. baumannii* growth, which is an important condition that bacteria have to adapt to during infection. The objective of this study was to identify genes of *A. baumannii* whose expression is regulated by environmental oxygen levels to identify virulence factors. Thus, we compare the transcriptional response in *A. baumannii* ATCC 17978 under microaerobiosis (0.1-0.3% of oxygen) and normoxia (21% of oxygen) growth conditions. We identified several up and down-regulated genes under microaerobiosis. One of the upregulated genes was *A1S_2448* (*pstS*), which is part of the pst operon (*pstA*, *pstB*, *pstC*, *pstS* and *phoU*) encoding a high-affinity phosphate transport system that is activated under low phosphate conditions. This transport system together with the low-affinity transporter Pit are the main phosphate uptake systems of *A. baumannii* [19].

Materials and Methods

Bacterial Strain and Growth curve analysis

A. baumannii ATCC 17978 was used in this study. Independent growth in MHB, M9 minimal medium and phosphate-limiting M9 minimal medium was evaluated over time for wild-type strain ATCC 17978 and the *pstS* mutant. Strains were grown overnight in 20 ml of Mueller-Hinton broth (MHB, Sigma) in static, and then, a 1:10000 dilution was performed to obtain 10^5 cfu/ml in a 40 ml culture of MHB or minimal medium M9. Minimal medium M9 was supplemented with 0.4% glucose, 2 mM magnesium sulfate and 0.1 mM calcium chloride. The growth under microaerobiosis (0.1-0.3% O_2), hypoxia (1% O_2), and normoxia (21% O_2) were monitored during 24 h at 37 ºC and 160 rpm. We used a hypoxia chamber (Coy Laboratories, Grass Lake, MI, USA) to culture

the bacteria under microaerobiosis and hypoxia conditions. After 4 h of growth in MHB, 6 samples (3 of microaerobiosis and 3 of normoxia condition) of bacterial cultures ($8 \cdot 10^8$ cells each) were taken to perform RNA extraction.

Bacterial RNA extraction, sequencing and analysis

Bacterial RNA was purified from the cultures using the RNeasy Mini Kit (Qiagen). Quality control of the RNA samples (integrity number and concentration) was analyzed prior sequencing. The enrichment of mRNA was carried out by depletion of rRNA with Ribo-Zero rRNA Removal Kit (Illumina). The mRNA enriched fraction was used for library construction of cDNA molecules and the sequencing was performed on Illumina Hiseq2500 platform using 100bp paired-end sequencing reads. Then, the analysis of the generated sequence raw data was performed using CLC Genomics Workbench 8.5.1 (Qiagen) (http://www.clcsupport.com/clcgenomicsworkbench/802/index.php?manual). The bioinformatics analysis started with trimming of raw sequences to generate high quality data. This high-quality sequencing reads were mapped against the *A. baumannii* ATCC 17978 genome (accession No. NC_009085). The result of mapping against this genome served to determine the gene expression levels based on the Reads per Kilobase of exon model per Million mapped reads (RPKM) method [20]. Finally, a gene differential expression analysis between normoxia and microaerobiosis groups was carried out through an Empirical Analysis of Digital Gene Expression test (DGE-test) [21]. The differentially expressed genes were filtered using standard conditions: False Discovery Rate P-value ≤ 0.05 and Fold change > 2 or < -2 [22, 23]. Genes considered as differentially expressed were used in an enrichment analysis. The R package clusterProfiler, included in Bioconductor [24], was selected with *A. baumannii* ATCC 17978 (acb) as the organism, and KEGG as the annotation source. All KEGG pathways with a p-value cut-off equal to 1 was taken into account. In addition, genes belonging to

the Sulfur metabolism pathway, together with their fold-change values were analyzed with the Pathview web tool to show these genes in their corresponding KEGG pathway graph [25]. Finally, the raw expression for the differentially expressed genes belonging to a KEGG pathway were taken and a heatmap with the 6 different experiments (3 for normoxia, and 3 for microaerobiosis) was built, using the heatmap.2 method from the R gplot package.

Quantitative Real-Time PCR (qRT-PCR) verification

The RNA was isolated as described in the previous section and using the same conditions. Then, rests of DNA were removed from the RNA samples using the TURBO DNA-free Kit (Invitrogen). The reverse transcription step was carried out using the Thermo-Script RT-PCR kit (Invitrogen), according to the manufacturer's instructions. The primer3 v.0.4.0 software (http://bioinfo.ut.ee/primer3-0.4.0/) was used to select primers that would amplify a product of approximately 120 bp. We selected two subexpressed genes under microaerobiosis: Glyoxalase/bleomycin resistance protein/dioxygenase *A1S_3416* (F: GACCCAAATGGACATCGTTT; R: ATGGAGTAAAACCAAACGCG) and Maleylacetoacetate isomerase *A1S_3415* (F: TAGTGGACGGCGATTTAACC; R: AGAAAGAGCCAAAATCCGTG); two overexpressed genes under microaerobiosis: taurine ATP-binding transport system component *A1S_1443* (F: GGGTTGTGGCAAAACAACTT; R: TCACGCCTTACTTCCTTGGT) and sulfate transport protein *A1S_2531* (F: GCCAGGCGTGGAAATTATTA; R: GGTAACGATGCAAAAGCACA); and two housekeeping genes: gyrB *A1S_0004* (F: CAGCTTTGGGAAACCACAAT; R: CGATGATGTTGAACCACGTC) and rpoD *A1S_2706* (F: CATGCGTGAAATGGGTACAG; R: TTACTGGCCAAATGCTGTTG). The quantitative real-time PCR assay was performed with SYBR Premix Ex Taq (Takara) in

a MxPro 3005p system (Stratagene). Three technical replicates for each sample were included. The amplification conditions were: 95 °C, 30 s, followed by 35 cycles of 95 °C 10 s, 56 °C 25 s, and 72 °C 25 s. The specificity of the reaction was confirmed by a melting curve assay from 95 to 55 °C. Relative quantification of gene expression was analyzed following the Comparative CT Method (Applied Biosystems Guide).

Construction of mutant and complemented strains

A stable, in-frame deletion mutant strain was constructed in the *A. baumannii* ATCC 17978 strain by homologous recombination using a described protocol [26]. For construction of the *A1S_2448* deletion mutant (ATCC 17978 Δ*A1S_2448*::Kan), the 500 bp immediately upstream of the genes open reading frame, and the 500 bp immediately downstream were amplified using the primers *A1S_2448* Up Forward (CTTGCGGTTTTAGCGATTATG), *A1S_2448* Up Reverse (GCCCCAGCTGGCAATTCCGGTCTGTTCTCTCTCATTAATG), *A1S_2448* Down Forward (CTAAGGAGGATATTCATATGGTTGGTTTGAATAGGGGCTG) and *A1S_2448* Down Reverse (GCGGCACAGACAACAACAGC). The kanamycin resistance gene from the plasmid pKD4 was amplified using the primers Kanamycin Up Forward (CCGGAATTGCCAGCTGGGGC) and Kanamycin Down Reverse (CATATGAATATCCTCCTTAG), resulting in a PCR product with sequences overlapping the PCR fragments containing the sequences upstream and downstream of the genes. The three PCR products were mix in a stitching PCR reaction, and 5 µg of the resulting construct were transformed into the ATCC 17978 strain by electroporation before selection on LB agar plates with 10 mg/L kanamycin. All deletion mutants were confirmed by sequencing and maintained in 30 mg/L kanamycin.

In order to complement the obtained mutant, the gene reading frame and 200-400 bp upstream and downstream were amplified using the primers EcoRI *A1S_2448* prom. Forward (ACAGAATTCGTGATATTGCGGTTATCTGAC) and XbaI *A1S_2448* reg. Reverse (ACATCTAGATATTCTCCACTGTTTTCTCAATTG). This fragment was cloned into the pUCp24 and introduced into the mutant strains by electroporation before selection on LB agar plates containing 10 mg/L of gentamicin to create the complemented strain (ATCC 17978 Δ*A1S_2448*::Kan/pUCp24-2448). Primers Seq.insert.pUCp24.Forward (TCCCAGTCACGACGTTGTAAAACG) and Seq.insert.pUCp24.Reverse (AATTTCACACAGGAAACAGCTATG) were used to check and sequence the cloned gene. The deletion mutant was also transformed with the empty pUCp24 plasmid for use as controls (ATCC 17978 Δ*A1S_2448*::Kan/pUCp24).

A549 culture and infection

Human lungs epithelial cell line A549 was grown in DMEM containing 10% Fetal Bovine Serum (Gibco), 1% HEPES 1M, vancomycin (50 mg/ml), gentamicin (20 mg/ml) and amphotericin B (0.25 mg/ml; Gibco), as previously described [27]. In the case of hypoxia condition studies (1% O2), cells were transferred to a hypoxia chamber with a humidified atmosphere of 1% O_2, 5% CO_2 and the balance N_2 at 37 °C for 6 h prior infection. Cells were seeded (10^5 cells/well in a 24-well plate) for 30 h in 24-well plates before infection with *A. baumannii* ATCC 17978 and mutant strains at a multiplicity of infection (MOI) of 500. Immediately before the infection, A549 cells were washed thrice with PBS and incubated in supplemented DMEM.

Bactericidal activity, bacterial adherence and bacterial invasion in cell cultures

After A549 cells infections with *A. baumannii* ATCC 17978 and mutant strains under hypoxia and normoxia conditions, extracellular medium was removed and serially diluted to determine bacterial concentration at 2 and 24 h post-infection [27].

Adherence and invasion assays were carried out as previously described [27]. To measure the adherent bacteria number, cells were infected as mentioned before, and, after washing with PBS, 200µl of trypsin-EDTA (Gibco) was added for 5 min at 37 °C. Then, 200 µl of 0.5% Triton X-100 (Sigma) was added for 3 min. The invasion protocol also includes a treatment with tetracycline 256 µg/ml (Sigma) before the addition of trypsin-EDTA. Diluted lysates were counted to determine the attached and internalized bacteria. All assays were performed in triplicate.

Biofilm assay

Biofilm production was measured based on a previously described method [28]. Strains were cultured in 10 ml MHB overnight at 37 °C, and subsequently diluted to 10^5 cfu/ml in MHB. Two-hundred µl of the cell suspension were added to each well of a round-bottom 96-well plate and growth overnight at 37 ºC. We washed twice every well to remove non-adherent bacteria and added two-hundred µl of 0.4% crystal violet dye (Sigma). After 10 min incubation, we washed twice and added two-hundred µl of 96% ethanol. After 15 min incubation, biofilm formation was quantified measuring the O.D. at 580 nm (Asys UVM 340 Microplate Reader). All assays were performed in triplicate.

Surface motility assay

Surface motility was measured based on a previously described method [29]. Overnight cultures of each strain were adjusted to an O.D. at 600 nm of 0.6 in PBS (Lonza). Three

µl of the bacterial suspension were placed in the center of a LB plate containing 0.3% agarose. Plates were incubated at 37 ºC with 80% of humidity and the radius of surface extension was measured at 24 hours of incubation. All assays were performed in triplicate.

Statistical analysis

Differences in bactericidal activity, bacterial adherence and invasion were determined using the multiple t-test one per row (GraphPad 6). Differences in biofilm formation and motility were determined using an unpaired t test (GraphPad 6). A *P* value < 0.05 was considered significant.

Results

A. baumannii gene expression profile under microaerobiosis

To identify genes associated with an inducible virulence response in *A. baumannii*, we searched for genes that were differentially expressed between microaerobiosis and normoxia conditions. A total of 203 genes were identified as differentially expressed by ≥ 2-fold (106 genes were subexpressed and 97 were overexpressed under microaerobiosis) (Table 1, Fig. 1A). This accounts for 5% of the *A. baumannii* ATCC 17978 genome. The RNA-seq results were validated by qRT-PCR analysis on a subset of differentially expressed genes (Table 2). Data from the qRT-PCR and RNA-seq showed the same trends, although the qRT-PCR expression data generally showed higher fold changes than the RNA-seq data.

Analysis of the differentially expressed genes by Gene Onthology (GO) enrichment showed that genes that were overexpressed under microaerobiosis were mainly involved

in sulfur metabolism (sulfate transport protein, taurine transport system and alkanesulfonate transport system), phenylalanine metabolism, and ABC transporters (Fig. 1B). Another set of genes that were overexpressed under microaerobiosis were a group of genes involved in lactate metabolism, TatABC transporters, phosphate transport system, positive pho regulon response regulator and some hypothetical proteins with unknown function (Fig. 1A). In contrast, genes that were subexpressed under microaerobiosis were involved in valine, leucine and isoleucine metabolism, aminoacyl-tRNA biosynthesis and urea metabolism (Fig. 1A and 1B).

Fig. 2A shows all the genes that were overexpressed and subexpressed under microaerobiosis compared to normoxia with a P <0.05. We identified 17 genes that were involved in sulfur metabolism, and all of them were overexpressed under microaerobiosis besides *A1S_1709*. These genes codify proteins involved in the extracellular uptake of sulfate (*A1S_2531-2536*), taurine (*A1S_1442-1445*) and alkanesulfonate (*A1S_0028-0030*) to obtain sulfate and sulfite inside the cells; and genes involved in sulfate (*A1S_ 1000-1001*) and sulfite (*A1S_2846*) metabolism to obtain energy (Fig. 2B). However, *A1S_1709* codifies a quinone reductase involved in sulfide metabolism, a parallel pathway inside sulfur metabolism. These data suggest that *A. baumannii* changes its metabolism from an aerobic metabolism to a growth based on sulfur (non aerobic metabolism pathway) as main source of energy. Moreover, it seems that bacterial protein synthesis is decreased under microaerobiosis due to the subexpression of genes involved in aminoacid metabolism and aminoacyl-tRNA biosynthesis. This could explain the lower bacterial growth rate under microaerobiosis compare to normoxia (see below).

A. baumannii virulence factors under hypoxia

We selected five different genes that were overexpressed under microaerobiosis to determine if they are involved in *A. baumannii* pathogenesis. The genes *A1S_0030* (alkanesulfonate transport protein) and *A1S_2532* (sulfate transport protein) are involved in two of the pathways that bacteria use to obtain sulfate and sulfite inside the cell and use it as a source of energy under microaerobiosis. The gene *A1S_2448* (putative phosphate transporter PstS) is involved in the transport of phosphate, a very important mechanism that bacteria need during infection process. The gene *A1S_0464* (Sec-independent protein translocase protein TatC) is part of a 3 protein-complex (TatABC) that is involved in transport. And the gene *A1S_0172* is a hypothetical protein highly expressed under microaerobiosis. Finally, the mutant in the gene *A1S_2448* was the most promising, so we continue with it for the analysis.

Growth curves analysis

Growth curves in MHB under normoxia (21% O_2), hypoxia (1% O_2), and microaerobiosis (0.1-0.3% O_2) were performed to find out if ATCC 17978 wild-type strain and the mutant Δ*A1S_2448*::Kan had different growth rates. We showed that both strains growths´s during 2 and 24 h were indistinguishable under normoxia and hypoxia (Fig. 3A). However, strains showed less growth under microaerobiosis at 24 h, proving the results we showed in the RNA-seq experiment (less growth rate). Nevertheless, there were no significant differences between the wild-type and the mutant strain growth, although the mutant strain grew slightly less than the wild-type under normoxia. Complemented strain and strains harboring the empty pUCp24 had the same growth than the respectives strains (ATCC 17978 Δ*A1S_2448*::Kan) and under all the conditions.

Growth curves in minimal medium M9 under hypoxia were the same for the ATCC 17978 and the mutant Δ*A1S_2448*::Kan (Fig. 3B) because the limitation in carbohydrate availability is not key in the hypoxic growth due to the bacterial metabolic shift to an anaerobic metabolism based on sulfur. However, the mutant Δ*A1S_2448*::Kan showed less growth than the ATCC 17978 in minimal medium M9 under normoxia (Fig. 3C).

Bactericidal activity, bacterial adherence and bacterial invasion in cell cultures

We determined if hypoxia affects the bactericidal activity of epithelial cells against the mutant strains more than against the wild-type strain. Bacterial counts of ATCC 17978, ATCC 17978/pUCp24, Δ*A1S_2448*::Kan, Δ*A1S_2448*::Kan/pUCp24-2448, and Δ*A1S_2448*::Kan/pUCp24 strains decreased in the extracellular medium of A549 cell line under hypoxia (1% O2) condition, after 2 and 24 h, compared to normoxia (data not shown). This decrease was higher in the case of the mutant strain after 2 and 24 h infection, compared to the wild-type (P <0.01 and P <0.001 at 2 and 24 h after infection, respectively) (Fig. 4A). These data support an increase in the bactericidal activity of epithelial cells line after 2 and 24 h under hypoxia against the mutant strain. Complementation of Δ*A1S_2448*::Kan restored the wild-type count levels.

The bacterial adherence of the wild-type and the mutant strain to A549 cell line was significantly lower at 2 and 24 h post-infection under hypoxia compared to normoxia. This decrease was higher in the case of the mutant compared to the wild-type (P<0.05 and P<0.01 at 2 and 24 h after infection, respectively) (Fig. 4B). Complementation of Δ*A1S_2448*::Kan restored the wild-type adherence levels.

Bacterial counts of the mutant strain inside epithelial cells showed a higher decrease than the wild-type strain at 24 h post-infection under hypoxia compared to normoxia (P<0.001) (Fig. 4C). Complementation of Δ*A1S_2448*::Kan restored almost the wild-type invasion levels. These data indicate that hypoxia affects the adherence and invasion

of mutant strains more than the wild-type, being *A1S_2448* an important gene under hypoxia.

Biofilm formation analysis

Biofilm assays were performed to analyze the biofilm-forming potential of the mutant strain compared to the wild-type strain. *A. baumannii* ATCC 17978 produced thick biofilm (Fig. 5A). The mutant Δ*A1S_2448*::Kan demonstrated significantly lower biofilm formation (35.47%) compared to the wild-type strain (100%), as well as the Δ*A1S_2448*::Kan/pUCp24 strain (25.19%) (P<0.001 and P<0.05, respectively). Complementation of Δ*A1S_2448*::Kan restored biofilm production to wild-type levels (104.58%).

Motility assay

Surface motility of the ATCC 17978 strain and the mutant Δ*A1S_2448*::Kan was assessed. As shown in Fig. 5B-F, Δ*A1S_2448*::Kan showed reduced surface motility (19.5 mm) compared to ATCC 17978 (42 mm) (P<0.001). The strain ATCC 17978/pUCp24 showed reduced surface motility (10 mm) compared to ATCC 17978 due to the introduction of the plasmid pUCp24 in the wild-type strain. The complemented strain Δ*A1S_2448*::Kan/pUCp24-2448 showed the same motility than ATCC 17978/pUCp24. Results were confirmed with the strain Δ*A1S_2448*::Kan/pUCp24, which showed reduced surface motility (6 mm) than ATCC 17978/pUCp24 (P<0.01).

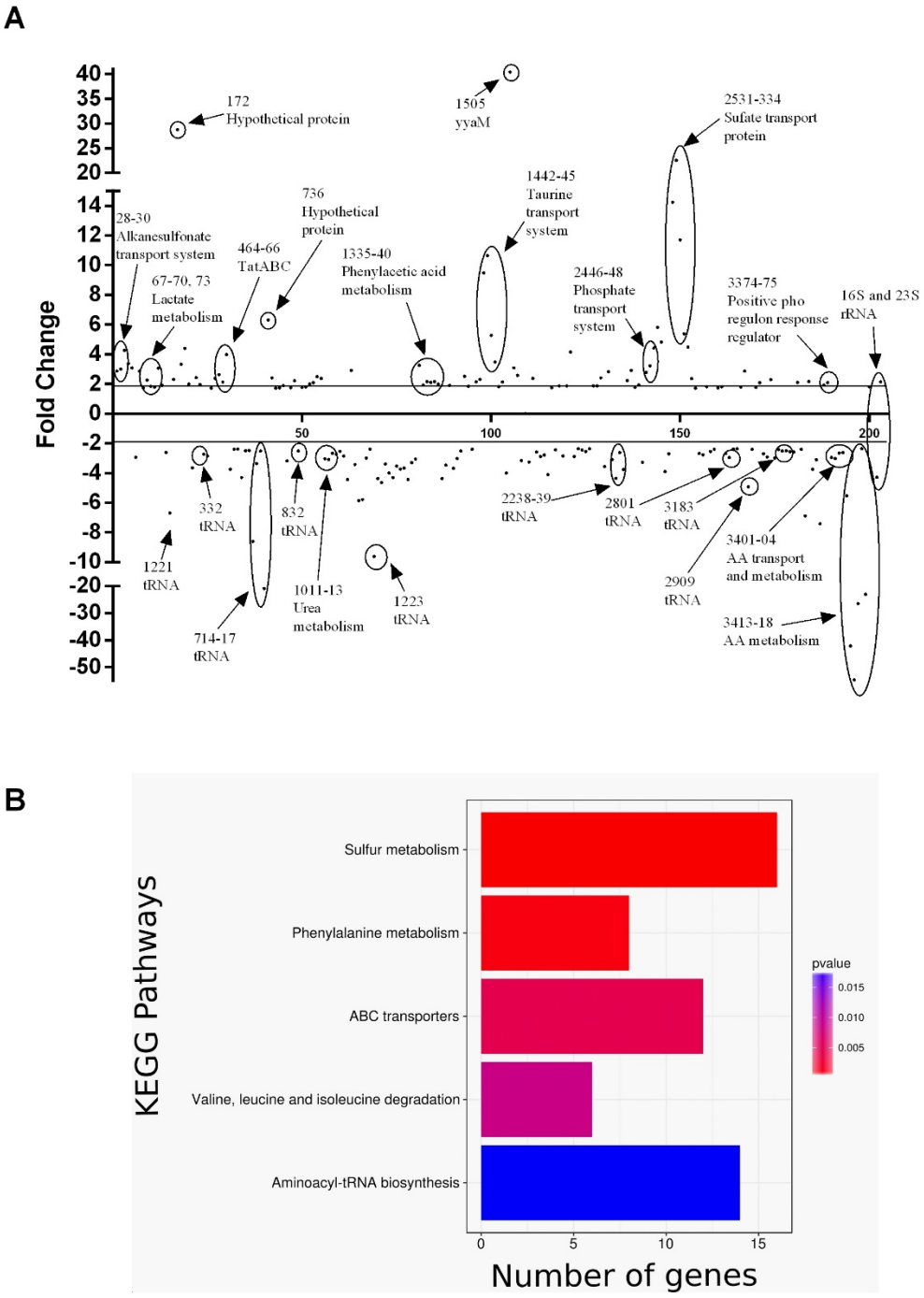

Figure 1. A) Plot of differential gene expression under microaerobiosis compared with normoxia with respect to gene locus tag number. The fold change in expression for each gene meeting the study threshold (False Discovery Rate ≤ 0.05; 2-Fold change) was plotted against the gene locus tag number. Genes of interest are highlighted. **B)** KEGG pathways enriched in the differentially expressed genes. It shows the number of genes involved in each pathway and the statistical significance of the pathway (P-value). Note that Sulfur metabolism is both the pathway more significant and with a higher number of genes.

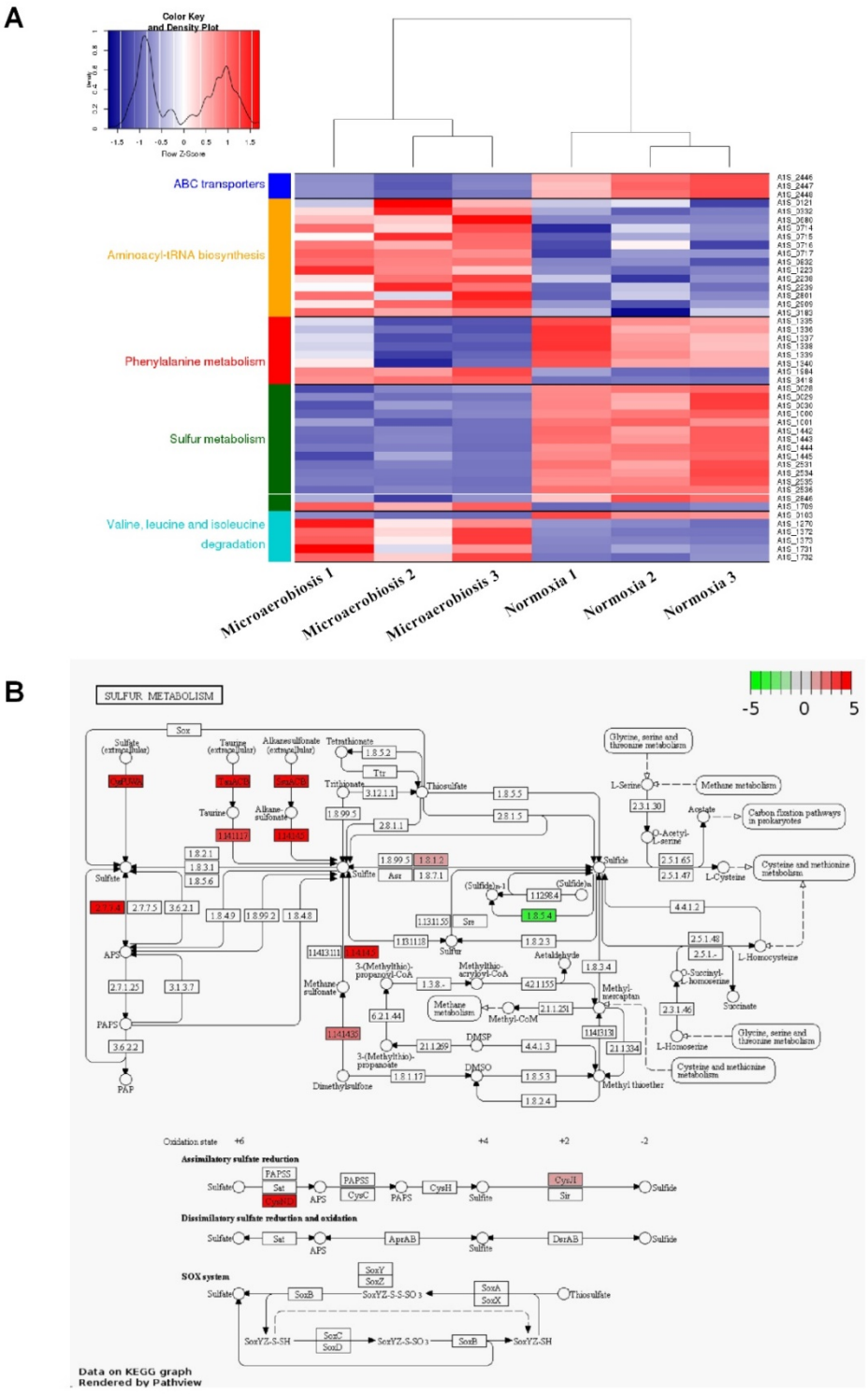

Figure 2. A) Clustering of differentially expressed genes assigned to a pathway. All of the genes were grouped by pathways and the expression values were converted to Z-Score for normalization. Note that the same gene can sometimes belong to other of the pathways, but here it is only shown in one of them. **B)** KEGG pathway for Sulfur metabolism highlighting the differentially expressed genes. In red and green color are highlighted the upregulated and downregulated genes, respectively.

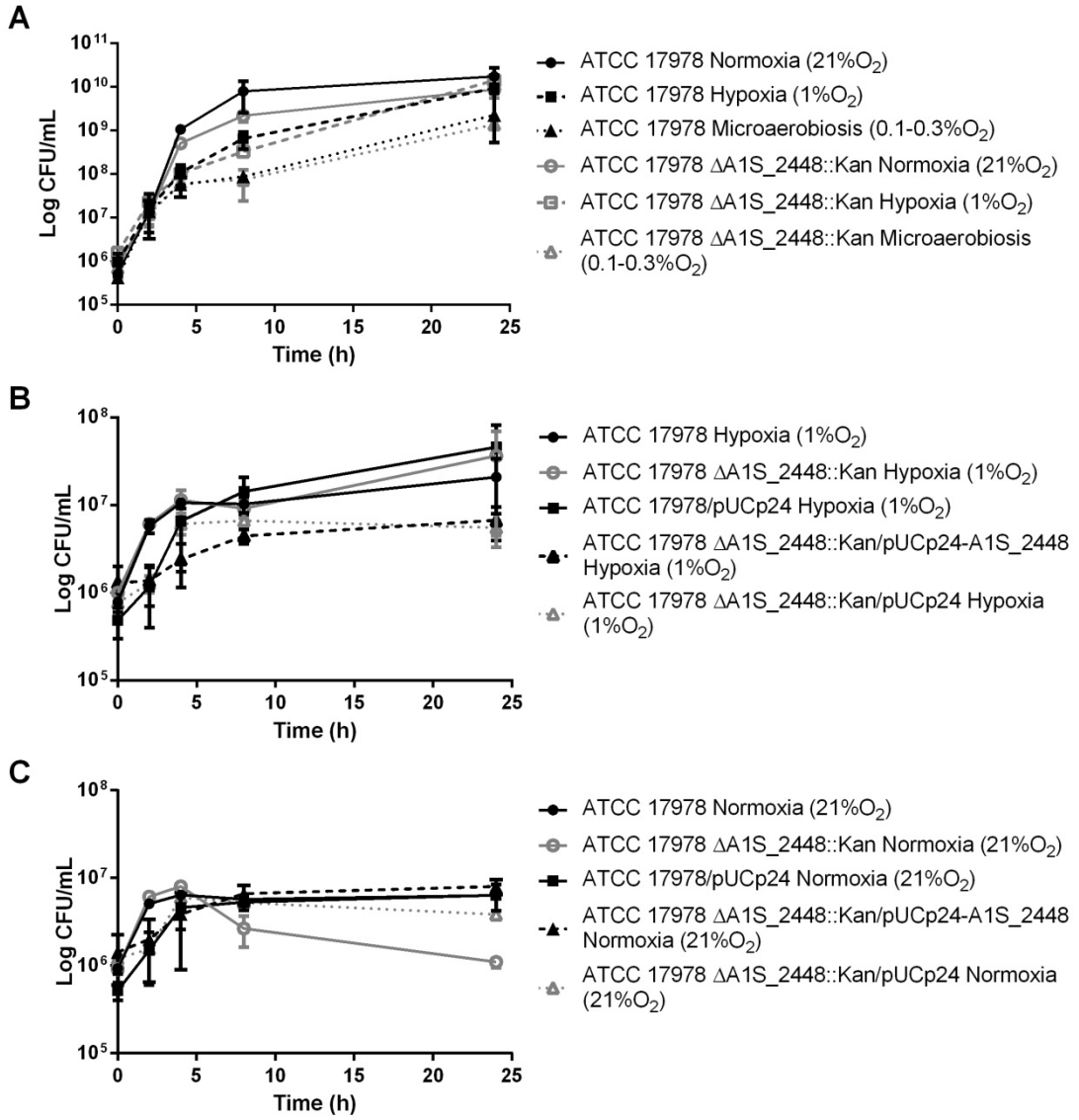

Figure 3. A) Growth curves of *A. baumannii* ATCC 17978 and Δ*A1S_2448*::Kan in MHB under normoxia, hypoxia and microaerobiosis (21%, 1% and 0.1-0.3% O_2, respectively). **B)** Growth curves of *A. baumannii* ATCC 17978, Δ*A1S_2448*::Kan, ATCC 17978/pUCp24, Δ*A1S_2448*::Kan/pUCp24-2448, and Δ*A1S_2448*::Kan/pUCp24 in minimal medium M9 (supplemented) under hypoxia. **C)** Growth curves of *A. baumannii* ATCC 17978, Δ*A1S_2448*::Kan, ATCC 17978/pUCp24, Δ*A1S_2448*::Kan/pUCp24-2448, and Δ*A1S_2448*::Kan/pUCp24 in minimal medium M9 (supplemented) under normoxia.

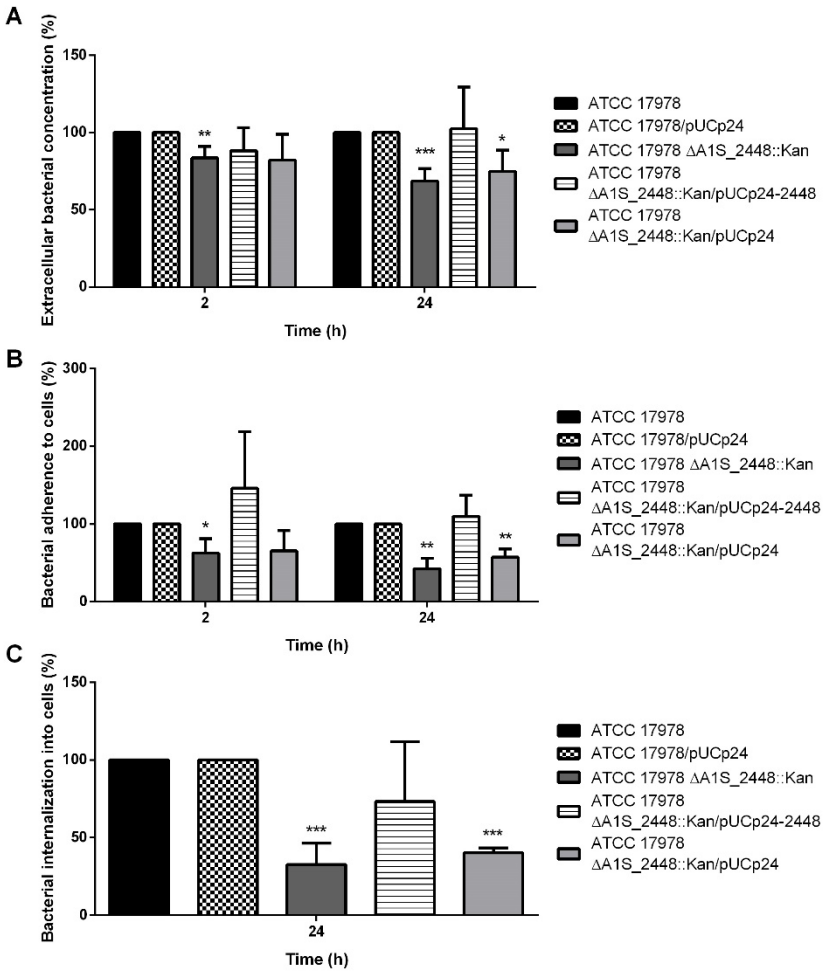

Figure 4. A) Measurement of bacterial concentration (%) in the extracellular medium after 2 and 24 h of A549 infection by *A. baumannii* ATCC 17978, Δ*A1S_2448*::Kan, ATCC 17978/pUCp24, Δ*A1S_2448*::Kan/pUCp24-2448, and Δ*A1S_2448*::Kan/pUCp24 under normoxia and hypoxia (1% O_2). Bars represent the reduction of bacterial concentration under hypoxia compared to normoxia, being the reduction obtained in the wild-type equal to 100%. ***: *P*<0.001 Mutant *vs.* wild-type at 2 or 24 h; **: *P*<0.01 Mutant *vs.* wild-type at 2 or 24 h; *: *P*<0.05 Mutant *vs.* wild-type at 2 or 24 h. **B)** Measurement of bacterial adherence (%) after 2 and 24 h of A549 infection by *A. baumannii* ATCC 17978, Δ*A1S_2448*::Kan, ATCC 17978/pUCp24, Δ*A1S_2448*::Kan/pUCp24-2448, and Δ*A1S_2448*::Kan/pUCp24 under normoxia and hypoxia (1% O_2). Bars represent the reduction of bacterial adherence under hypoxia compared to normoxia, being the reduction obtained in the wild-type equal to 100%. **: *P*<0.01 Mutant *vs.* wild-type at 2 or 24 h; *: *P*<0.05 Mutant *vs.* wild-type at 2 or 24 h. **C)** Measurement of bacterial internalization (%) after 2 and 24 h of A549 infection by *A. baumannii* ATCC 17978, Δ*A1S_2448*::Kan, ATCC 17978/pUCp24, Δ*A1S_2448*::Kan/pUCp24-2448, and Δ*A1S_2448*::Kan/pUCp24 under normoxia and hypoxia (1% O_2). Bars represent the reduction of bacterial internalization under hypoxia compared to normoxia, being the reduction obtained in the wild-type equal to 100%. ***: *P* <0.001 Mutant *vs.* wild-type at 2 or 24 h.

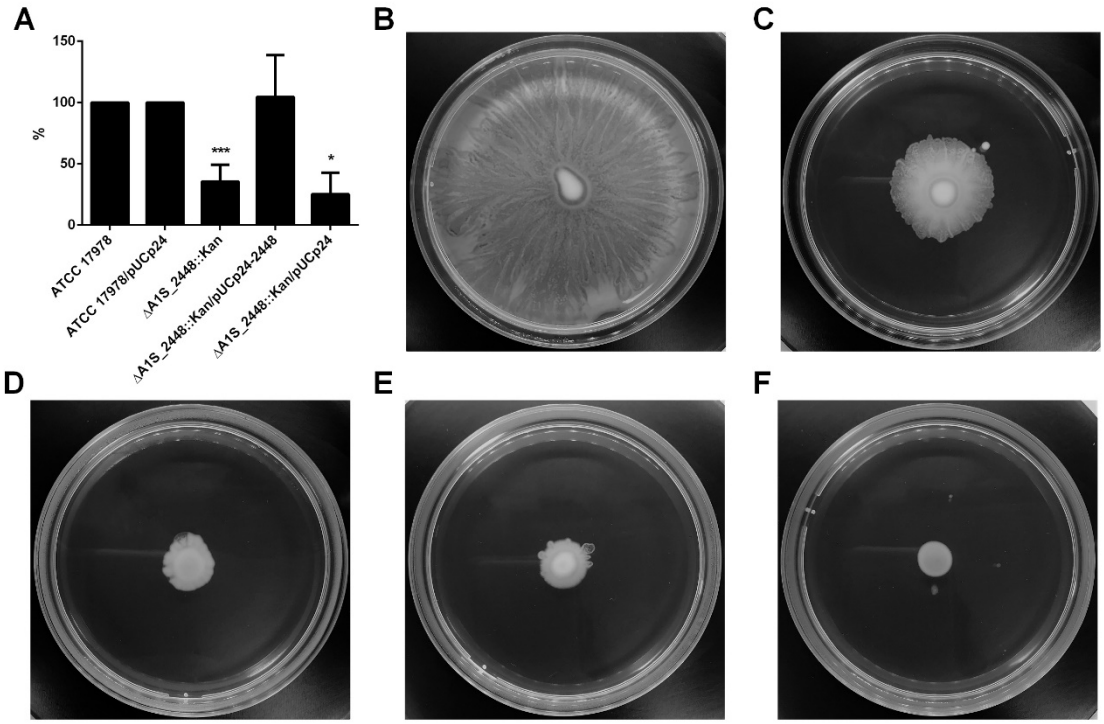

Figure 5. A) Effect of PstS loss on biofilm production. Biofilm production was determined for ATCC 17978, Δ*A1S_2448*::Kan, ATCC 17978/pUCp24, Δ*A1S_2448*::Kan/pUCp24-2448, and Δ*A1S_2448*::Kan/pUCp24. Bars represent the average of three separate assays, with error bars representing the SEM. ***: $P<0.001$ Mutant *vs.* wild-type; *: $P<0.05$ Mutant *vs.* wild-type. **B-F)** Efect of PstS loss on surface motility (B: ATCC 17978; C: Δ*A1S_2448*::Kan; D: ATCC 17978/pUCp24; E: Δ*A1S_2448*::Kan/pUCp24-2448; F:Δ*A1S_2448*::Kan/pUCp24).

Table 1. Genes up-regulated and down-regulated in *A. baumannii* ATCC 17978 under microaerobiosis (0.1-0.3% O_2).

Gene ID	Protein description	Fold Change
A1S_0028	FMNH(2)-dependent alkanesulfonate monooxygenase	2,867637691
A1S_0029	ABC-type nitrate/sulfonate/bicarbonate transport system	2,990097961
A1S_0030	Alkanesulfonate transport protein	4,262666192
A1S_0040	Putative oxidoreductase	3,36292177
A1S_0041	Putative linoleoyl-CoA desaturase	3,074780083
A1S_0059	Putative glycosyltransferase	-2,934814162
A1S_0067	L-lactate permease	2,867983694
A1S_0068	L-lactate utilization transcriptional repressor (GntR family)	1,740266254
A1S_0069	L-lactate dehydrogenase FMN linked	2,261836192
A1S_0070	D-lactate dehydrogenase NADH independent, FAD-binding domain	1,839352742
A1S_0073	2-methylisocitrate lyase	1,779592074
A1S_0101	Pseudo	3,071015888
A1S_0103	3-hydroxyisobutyrate dehydrogenase	1,909511059
A1S_0119	Phosphopantethiene-protein transferase	-2,615172123
A1S_0121	tRNA	-6,677734407
A1S_0170	Putative outer membrane copper receptor (OprC)	2,302305958
A1S_0172	Hypothetical protein A1S_0172	28,76221182
A1S_0179	NADPH-dependent FMN reductase	3,316713266
A1S_0180	Putative membrane protein	4,4043089
A1S_0224	Hypothetical protein A1S_0224	1,993084202
A1S_0233	Type 4 fimbriae expression regulatory protein	-3,648849006
A1S_0251	Thiamine hydroxymethylpyrimidine moiety synthesis	2,431468999
A1S_0256	High affinity phosphate uptake transcriptional repressor	1,965328674
A1S_0332	tRNA	-2,734469972
A1S_0408	Putative glutathione S-transferase	-2,848996933
A1S_0427	Aspartate-semialdehyde dehydrogenase NAD(P)-binding	1,723788434
A1S_0463	Putative alkaline phosphatase	2,37093695
A1S_0464	Sec-independent protein translocase protein (TatC)	2,626200932
A1S_0465	Sec-independent protein translocase protein TatB	2,119553888
A1S_0466	Sec-independent protein translocase protein TatA	3,974749135
A1S_0550	Putative VGR-related protein	-3,748574485
A1S_0566	Pyridine nucleotide transhydrogenase (proton pump) alpha subunit (part1)	-2,398701486
A1S_0567	Pyridine nucleotide transhydrogenase (proton pump) alpha subunit (part2)	-2,378531377
A1S_0595	Putative membrane protein	-4,298445076
A1S_0617	Hypothetical protein A1S_0617	-2,501352623
A1S_0644	Hypothetical protein A1S_0644	-2,476797404
A1S_0714	tRNA	-8,603938479
A1S_0715	tRNA	-3,367487475
A1S_0716	tRNA	-2,520040074

A1S_0717	tRNA	-20,90999886
A1S_0736	Hypothetical protein A1S_0736	6,307013814
A1S_0737	5-methyltetrahydropteroyltriglutamate-homocysteine methyltransferase	2,406360233
A1S_0738	Putative flavoprotein oxidoreductase	1,708012196
A1S_0746	Ribonucleoside-diphosphate reductase beta subunit	1,725080265
A1S_0747	Ribonucleoside diphosphate reductase alpha subunit	1,876363877
A1S_0800	Bacterioferritin	-3,193016034
A1S_0801	Putative transport protein (permease)	1,753161686
A1S_0804	Trehalose-6-phosphate phophatase	2,213668666
A1S_0832	tRNA	-2,513627493
A1S_0908	RND family multidrug resistance secretion protein	1,771695997
A1S_0909	Putative MFS family drug transporter	1,797570144
A1S_0922	Putative homocysteine S-methyltransferase family protein	2,001867888
A1S_0923	Malate dehydrogenase FAD/NAD(P)-binding domain / Malate dehydrogenase [quinone]	2,08194988
A1S_1000	Sulfate adenylyltransferase subunit 2	2,496503751
A1S_1001	ATP-sulfurylase subunit 1	2,373560166
A1S_1011	Urease accessory protein UreD	-3,038251236
A1S_1012	EsvC / Urea amidohydrolase subunit gamma	-3,096672296
A1S_1013	Urea amidohydrolase subunit beta	-2,661961516
A1S_1049	Hypothetical protein A1S_1049	-2,741753861
A1S_1085	Amino acid transporter	-2,539007574
A1S_1088	Hypothetical protein A1S_1088	-2,860965483
A1S_1089	Hypothetical protein A1S_1089	-4,443066817
A1S_1090	Putative transcription regulator (AsnC family)	2,92148878
A1S_1091	Succinylornithine transaminase (carbon starvation protein C)	-3,43656727
A1S_1092	Succinylornithine transaminase (carbon starvation protein C)	-5,862639426
A1S_1093	Arginine/ornithine N-succinyltransferase beta subunit	-5,786008422
A1S_1094	D-serine/D-alanine/glycine transporter	-2,998003217
A1S_1216	LysR regulator	-2,393257685
A1S_1223	tRNA	-9,61263552
A1S_1224	Transposase	-4,374194522
A1S_1228	Cold shock protein	-4,65134289
A1S_1229	Pyrroline-5-carboxylate reductase	-3,387635633
A1S_1255	Lipid A biosynthesis lauroyl acyltransferase	-3,996642143
A1S_1266	Putative membrane protein	-4,307066915
A1S_1267	Putative lactam utilization protein	-3,526606631
A1S_1268	Hypothetical protein A1S_1268	-3,735897828
A1S_1269	Putative allophanate hydrolase subunit 1 and 2	-3,658727334
A1S_1270	Hypothetical protein A1S_1270	-4,433917777
A1S_1288	Putative VGR-related protein	-3,288256628
A1S_1320	Transcriptional regulator SoxR	-3,066609102
A1S_1335	Phenylacetic acid degradation protein paaN	3,244622056
A1S_1336	Phenylacetate-CoA oxygenase subunit PaaA	1,925774812
A1S_1337	Phenylacetate-CoA oxygenase subunit PaaB	2,151943853
A1S_1338	Hypothetical protein A1S_1338	2,095589207

A1S_1339	Phenylacetate-CoA oxygenase PaaJ subunit	2,158694898
A1S_1340	Phenylacetate-CoA oxygenase/reductase PaaK subunit	1,988164111
A1S_1354	(Acyl-carrier protein) phosphodiesterase	-4,371305981
A1S_1355	p-hydroxybenzoate hydroxylase transcriptional activator	-3,458178368
A1S_1356	p-hydroxybenzoate hydroxylase transcriptional activator	1,909067312
A1S_1372	Hypothetical protein A1S_1372	-3,685048519
A1S_1373	Putative acyl-CoA carboxylase alpha chain protein	-3,020431978
A1S_1374	3-methylglutaconyl-CoA hydratase	-2,521101799
A1S_1396	ABC-type amino acid transport system	2,514269767
A1S_1398	GlnQ protein	1,839868743
A1S_1435	Hypothetical protein A1S_1435	-2,395374661
A1S_1436	Putative acyl-CoA dehydrogenase	2,136771227
A1S_1437	Putative acyl-CoA dehydrogenase	2,303810193
A1S_1442	Taurine ABC transporter periplasmic taurine-binding protein	9,469009538
A1S_1443	Taurine ATP-binding transport system component	10,64067184
A1S_1444	ABC taurine transporter permease subunit	5,268788099
A1S_1445	Taurine dioxygenase	3,468959789
A1S_1487	Putative Acyl-CoA dehydrogenase	1,812699687
A1S_1488	Putative Acyl-CoA dehydrogenase	2,132746095
A1S_1498	Putative transcriptional regulator (TetR family)	-4,003875641
A1S_1505	yyaM	40,4300082
A1S_1665	Putative membrane protein	3,073765337
A1S_1677	Putative porin precursor	2,57721949
A1S_1708	Beta-lactamase-like protein	-3,161623735
A1S_1709	Hypothetical protein A1S_1709	0,254873163
A1S_1710	Putative membrane protein	-3,257280351
A1S_1726	Aspartate ammonia-lyase (aspartase)	2,378126552
A1S_1731	Acetoacetyl-CoA transferase beta subunit	-2,579954492
A1S_1732	Acetoacetyl-CoA transferase alpha subunit	-2,890598255
A1S_1735	Hypothetical protein A1S_1735	-2,791113316
A1S_1760	Hypothetical protein A1S_1760	-4,097559303
A1S_1762	Hypothetical protein A1S_1762	1,742620352
A1S_1811	Hypothetical protein A1S_1811	-2,426624706
A1S_1821	Short-chain dehydrogenase/reductase SDR	1,86515805
A1S_1841	Hypothetical protein A1S_1841	-2,862129625
A1S_1926	Putative membrane protein	1,873695091
A1S_1928	Putative signal peptide	4,142089126
A1S_1943	Putative membrane protein	-2,884976522
A1S_1984	D-amino acid dehydrogenase small subunit	-2,364748955
A1S_2057	Methyl viologen resistance protein (MFS superfamily)	-2,451248433
A1S_2090	Hypothetical protein A1S_2090	-2,551398493
A1S_2091	Putative exported protein	-2,365873959
A1S_2093	Hypothetical protein A1S_2093	1,859723965
A1S_2122	Transcriptional regulator	1,875285287
A1S_2202	Aspartate racemase	2,402465914
A1S_2218	CsuA/B	-3,557110164

A1S_2224	Threonine efflux protein	2,836132945
A1S_2230	Hypothetical protein A1S_2230	-3,089609662
A1S_2238	tRNA	-4,361194157
A1S_2239	tRNA	-2,617275074
A1S_2289	Putative signal peptide	-3,75877858
A1S_2296	Putative protease	2,224288367
A1S_2319	Putative membrane protein	2,908415896
A1S_2320	Transcriptional regulator AraC family	1,763689515
A1S_2334	S-adenosyl-L-homocysteine hydrolase	1,931879168
A1S_2347	Hypothetical protein A1S_2347	-3,280881456
A1S_2446	High-affinity phosphate transport protein	2,779460265
A1S_2447	EsvD	3,211746538
A1S_2448	Putative phosphate transporter	4,415621921
A1S_2458	Putative fatty acid desaturase	5,815884329
A1S_2459	Putative oxidoreductase	4,811424151
A1S_2490	UDP-N-acetyl glucosamine-2-epimerase	-3,89628889
A1S_2512	Hypothetical protein A1S_2512	-2,702934785
A1S_2531	Sulfate transport protein	14,23755414
A1S_2532	Sulfate transport protein	22,54708807
A1S_2533	Putative esterase	11,70258487
A1S_2534	Sulfate transport protein	5,367772795
A1S_2535	Putative sulfate permease	4,474063585
A1S_2536	Putative ATPase	2,363384072
A1S_2537	Putative LysR-type transcriptional regulator	1,717536577
A1S_2555	Transposition site target selection protein D	-2,684175378
A1S_2648	Hypothetical protein A1S_2648	-2,76460688
A1S_2654	Putative periplasmic binding protein of transport/transglycosylase	1,812087761
A1S_2694	Mur ligase middle region	-2,5493552
A1S_2695	Hypothetical protein A1S_2695	-2,397710105
A1S_2699	Putative transcriptional regulator	1,732122956
A1S_2710	Hypothetical protein A1S_2710	1,820533836
A1S_2748	Putative ammonium transporter	-2,695259213
A1S_2801	tRNA	-2,965003472
A1S_2841	Putative type 4 fimbrial biogenesis protein FimT	-2,383966682
A1S_2844	Quaternary ammonium compound-resistance protein	-2,373154232
A1S_2846	CysI-like sulfite reductase protein	1,795908099
A1S_2863	Putative antioxidant protein	2,866965402
A1S_2909	tRNA	-4,931625423
A1S_2911	Uncharacterized membrane protein LemA family	-2,40884189
A1S_3010	Hypothetical protein A1S_3010	1,768451868
A1S_3035	Xanthine phosphoribosyltransferase	2,081840296
A1S_3043	Hypothetical protein A1S_3043	-2,706572314
A1S_3044	Hypothetical protein A1S_3044	-2,922101167
A1S_3085	Putative flavohemoprotein	2,283046794
A1S_3135	Putative APC family S-methylmethionine transporter (MmuP)	-2,995657413

A1S_3166	Pilin like competence factor	-2,418282511
A1S_3183	tRNA	-2,516094839
A1S_3212	Hypothetical protein A1S_3212	-2,508738565
A1S_3224	Acyl coenzyme A reductase	-2,570691211
A1S_3225	Putative sulfate permease	-2,594439793
A1S_3231	Putative acetyl-CoA hydrolase/transferase	2,09959443
A1S_3237	Exonuclease putative	-2,392405255
A1S_3251	Transporter LysE family	-6,89413316
A1S_3305	NADH-dependent FMN reductase	2,176815627
A1S_3350	Hypothetical protein A1S_3350	-3,744907286
A1S_3363	Membrane metalloendopeptidase protein	-3,116653492
A1S_3364	Putative VGR-related protein	-7,40947075
A1S_3374	Positive pho regulon response regulator	1,92233217
A1S_3375	Positive pho regulon response regulator	2,089499576
A1S_3401	Hypothetical protein A1S_3401	-2,955676254
A1S_3402	Arginase/agmatinase/formimionoglutamate hydrolase	-3,028239302
A1S_3403	Imidazolonepropionase	-2,661908071
A1S_3404	Proline transport protein (APC family)	-2,627117238
A1S_3413	APC family aromatic amino acid transporter	-5,539609242
A1S_3414	Fumarylacetoacetase	-42,06992163
A1S_3415	Maleylacetoacetate isomerase	-54,71945548
A1S_3416	Glyoxalase/bleomycin resistance protein/dioxygenase	-26,46556666
A1S_3417	Regulatory proteins IclR	-2,362911036
A1S_3418	4-hydroxyphenylpyruvate dioxygenase	-23,0065767
A1S_3436	Putative alcohol dehydrogenase	1,794177485
A1S_r01	16S ribosomal RNA	-4,406220125
A1S_r08	23S ribosomal RNA	-4,297087141
A1S_r12	16S ribosomal RNA	2,13706962

Table 2. qRT-PCR data to validate RNA-seq results.

Sample	Fold difference A1S_3416 relative to microaerobiosis	Fold difference A1S_3414 relative to microaerobiosis	Fold difference A1S_1443 relative to normoxia	Fold difference A1S_2531 relative to normoxia
Normoxia	51.15 (36.89 ± 70.93)	166.96 (113.08 ± 246.51)	1 (0.39 ± 2.57)	1 (0.16 ± 6.38)
Microaerobiosis	1 (0.38 ± 2.72)	1 (0.43 ± 2.35)	5.38 (3.06 ± 9.46)	15.45 (2.86 ± 83.42)

Discussion

RNA-seq is a useful tool that allows a high-throughput sequencing of RNA to study transcription on a genome-wide scale [30]. RNA-seq measures RNA abundance, which is a product of gene transcription as well as RNA stability. This method has been applied to find out new virulence factors in different microorganisms. In this study we showed that the gene *A1S_2448*, which codifies for the PstS protein, is overexpressed in *A. baumannii* under microaerobiosis.

The gene *pstS* is located in an operon and the operon genes have different functions. *pstA*, *pstB* and *pstC* encode an ABC phosphate transporter, while *pstS* encodes a periplasmic phosphate-binding protein which senses phosphate levels and transfers the phosphate to the bacterial cytoplasm through the transporter [31]. Transcription of the system genes is regulated by PhoB/R, a two-component system activated by phosphate depletion. When phosphate levels in the bacteria are low, PhoR phosphorylates PhoB, which binds to a consensus Pho Box and activates genes expression, such as the *pst* operon. Conversely, when phosphate levels are high, the Pho regulon is not induced because PhoU interacts with Pst and PhoR constituting a complex that prevents PhoB phosphorylation [32].

Pathogenic bacteria, like *A. baumannii*, must withstand diverse host environments during infection. Environmental signals, such as pH, temperature or oxygen levels, not only trigger adaptive responses to these stress conditions but also induce the expression of virulence genes [33]. Microaerobiosis is a stress condition that bacteria face during the course of infection. In this study, we showed that genes from the sulfate assimilation pathway are up-regulated in *A. baumannii* under microaerobiosis, to facilitate bacterial adaptation to oxygen-limiting conditions. This metabolism yields less energy than the aerobic one, supporting the fact that *A. baumannii* growth rate is lower under

microaerobiosis condition. In this condition we also observed an increased expression of phosphate uptake system, which is very important to colonize during the infection due to the phosphate-limiting conditions that are found inside the host [34]. It seems that this stressful condition exacerbates the virulence of *A. baumannii* taking advantage of the induction of phosphate uptake mechanism. Camarena et al. [35] showed a strong induction of genes involved in phosphate transport when *A. baumannii* was grown in ethanol, indicating that this pathogen makes a better use of the phosphate resources under that stressful condition. There is also evidence of a higher PstS secretion associated with nutritional stress in other bacteria [36]. Therefore, the slightly less growth of the mutant Δ*A1S_2448*::Kan compared to the ATCC 17978 in minimal medium M9 (carbohydrates limitation) under normoxia might be due to a hyperproduction of PstS in the ATCC 17978 that emphasize the differences between the mutant and the wild-type strains.

The *pst* and *pho* regulon is highly conserved in Gram-negative and Gram-positive bacteria and controls the expression of multiple genes, regulating bacterial virulence. It has been shown that the activation of the regulon PhoB in *Vibrio cholerae* results in a decreased expression of toxin-co-regulated pilus and the ADP ribosylating cholera toxin which impairs bacterial colonization [37]. Moreover, the deletion of the *pst* operon decreases the expression of the main adhesins in *Escherichia coli* (BFP and intimin) and reduces bacterial adherence to Hep-2 cells [38]. Esparza et al. [39] showed that PstS is indeed an adhesin which can bind the macrophage mannose receptor and promote phagocytosis in *Mycobacterium tuberculosis*. We showed that *pstS* deletion reduces bacterial adherence in *A. baumannii*, confirming the influence of PstS in *A. baumannii* adherence like in other microorganisms. Other studies have proposed that the Pst system is involved in intracellular invasion. For example, the *pstS* deletion in *Salmonella*

enterica serotype Typhimurium reduces hilA and invasion gene expression [40]. We also found that *pstS* deletion mutant in *A. baumannii* is less invasive than the wild-type strain. Therefore, *pstS* deletion reduces adherence as well as invasion, supporting the idea of PstS as an *A. baumannii* virulence factor.

Biofilms play many important roles in pathogenesis, making bacteria more resistant to environmental stresses such as exposure to biocides and antimicrobial agents [41]. PhoB induces expression of *acgAB*, an operon which encodes c-di-GMP metabolic enzymes resulting in an increased motility and less biofilm formation in *V. cholera* [42]. Moreover, Pho modulation of the c-di-GMP cellular level was shown to be linked to LapA adhesin-decreased secretion, which is required for biofilm formation, in *Pseudomonas fluorescens* [43]. Previous studies have also linked the Pst system with the regulation of biofilm formation by *Proteus mirabilis* and *Pseudomonas aeruginosa*, having the mutants in the *pst* system less biofilm-forming ability [44, 45]. PhoB also controls swarming motility in *P. aeruginosa*, having a hyper swarming phenotype when PhoB is active [46]. However, in our study, we showed that a deletion in *pstS* in *A. baumannii*, and therefore, a constitutive activation of the PhoB regulon, produced a decrease in both motility and biofilm formation, evidencing the existence of a different regulatory mechanism in this pathogen. Motility and biofilm formation are usually part of bacterial virulence factors that allow a more effective infectious process. Therefore, impairing the *pstS* gene might reduce *A. baumannii* virulence.

Zaborina et al. [47] showed that MDR clinical isolates of *P. aeruginosa* produced PstS-rich appendages during phosphate limitation condition and they were involved in adherence and disruption of intestinal epithelial cells. Moreover, an increased expression of PstS in *P. aeruginosa* produced higher mortality rates in a mouse model of gut-derived sepsis model. In this regard, another environmental cue that could shift

the virulence of *A. baumannii* to a more virulent phenotype may be low extracellular phosphate. Hypophosphatemia is present in a variety of physiologic stress states such as the use of intravenous nutrition [48], and during sepsis [49, 50], remarking the importance of this study.

In summary, we have identified multiple genes that are differentially expressed under the stressful condition of microaerobiosis, such as *pstS*. This virulence factor confers a highly adhesive and virulent phenotype to *A. baumannii* and seems to have a broader regulatory impact beyond its role in phosphate metabolism. However, a better understanding of the molecular regulation is needed to completely define its role in the virulence of *A. baumannii*.

References

1. Lee CR, Lee JH, Park M, Park KS, Bae IK, Kim YB, Cha CJ, Jeong BC, Lee SH. Biology of *Acinetobacter baumannii*: Pathogenesis, antibiotic resistance mechanisms, and prospective treatment options. Front Cell Infect Microbiol 2017; 7:1-35.

2. Cullen L, McClean S. Bacterial Adaptation during Chronic Respiratory Infections. Pathogens. 2015; 4:66-89.

3. Cummins EP, Keogh CE, Crean D, Taylor CT. The role of HIF in immunity and inflammation. Mol Aspects Med 2016; 47-48:24-34.

4. Zinkernagel AS, Johnson RS, Nizet V. Hypoxia inducible factor (HIF) function in innate immunity and infection. J Mol Med 2007; 85:1339-46.

5. Bosseto MC, Palma PV, Covas DT, Giorgio S. Hypoxia modulates phenotype, inflammatory response, and leishmanial infection of human dendritic cells. APMIS 2010; 118:108-14.

6. Schaible B, Schaffer K, Taylor CT. Hypoxia, innate immunity and infection in the lung. Respir Physiol Neurobiol 2010; 174:235-43.

7. McConnell MJ, Actis L, Pachón J. Acinetobacter baumannii: human infections, factors contributing to pathogenesis and animal models. FEMS Microbiol Rev 2013; 37:130-55.

8. Pulido MR, García-Quintanilla M, Gil-Marqués ML, McConnell MJ. Identifying targets for antibiotic development using omics technologies. Drug Discov Today 2016; 21:465-72.

9. Croucher NJ, Thomson NR. Studying bacterial transcriptomes using RNA-seq. Curr Opin Microbiol 2010; 13:619-24.

10. Li S, Li H, Qi T, Yan X, Wang B, Guan J, Li Y. Comparative transcriptomics analyses of the different growth states of multidrug-resistant *Acinetobacter baumannii*. Biomed Pharmacother. 2017; 85:564-74.

11. Rumbo-Feal S, Gómez MJ, Gayoso C, Álvarez-Fraga L, Cabral MP, Aransay AM, Rodríguez-Ezpeleta N, Fullaondo A, Valle J, Tomás M, Bou G, Poza M. Whole transcriptome analysis of *Acinetobacter baumannii* assessed by RNA-sequencing reveals different mRNA expression profiles in biofilm compared to planktonic cells. PLoS One. 2013; 8:e72968.

12. Hua X, Chen Q, Li X, Yu Y. Global transcriptional response of *Acinetobacter baumannii* to a subinhibitory concentration of tigecycline. Int J Antimicrob Agents 2014; 44:337-44.

13. Fernando DM, Chong P, Singh M, Spicer V, Unger M, Loewen PC, Westmacott G, Kumar A. Multi-omics approach to study global changes in a triclosan-resistant mutant strain of *Acinetobacter baumannii* ATCC 17978. Int J Antimicrob Agents 2017; 49:74-80.

14. Qin H, Lo NW, Loo JF, Lin X, Yim AK, Tsui SK, Lau TC, Ip M, Chan TF. Comparative transcriptomics of multidrug-resistant *Acinetobacter baumannii* in response to antibiotic treatments. Sci Rep 2018; 8:3515.

15. Henry R, Crane B, Powell D, Deveson Lucas D, Li Z, Aranda J, Harrison P, Nation RL, Adler B, Harper M, Boyce JD, Li J. The transcriptomic response of *Acinetobacter baumannii* to colistina and doripenem alone and in combination in an in vitro pharmacokinetics/pharmacodynamics model. J Antimicrob Chemother 2015; 70:1303-13.

16. Camarena L, Bruno V, Euskirchen G, Poggio S, Snyder M. Molecular mechanisms of ethanol-induced pathogenesis revealed by RNA-sequencing. PLoS Pathog 2010; 6:e1000834.

17. Wright MS, Jacobs MR, Bonomo RA, Adams MD. Transcriptome remodeling of *Acinetobacter baumannii* during infection and treatment. MBio 2017; 8. pii: e02193-16.

18. Murray GL, Tsyganov K, Kostoulias XP, Bulach DM, Powell D, Creek DJ, Boyce JD, Paulsen IT, Peleg AY. Global Gene Expression Profile of Acinetobacter baumannii During Bacteremia. J Infect Dis 2017; 215(suppl_1):S52-S57.

19. Rosenberg H, Gerdes RG, Chegwidden K. Two systems for the uptake of phosphate in *Escherichia coli*. J Bacteriol 1977; 131:505-11.

20. Mortazavi A, Williams BA, McCue K, Schaeffer L, Wold B. Mapping and quantifying mammalian transcriptomes by rna-seq. Nat Methods 2008; 5:621-8.

21. Robinson MD, Smyth GK. Small-sample estimation of negative binomial dispersion, with applications to sage data. Biostatistics 2008; 9:321-32.

22. Raza K, Mishra A. A Novel Anticlustering Filtering Algorithm for the Prediction of Genes as a Drug Target. American Journal of Biomedical Engineering 2012; 2:206-11.

23. Van Iterson M, Boer JM, Menezes RX. Filtering, FDR and power. BMC Bioinformatics 2010; 11:450.

24. Yu G, Wang LG, Han Y, He QY. clusterProfiler: an R package for comparing biological themes among gene clusters. OMICS 2012; 16:284-7.

25. Luo W, Pant G, Bhavnasi YK, Blanchard SG Jr, Brouwer C. Pathview Web: user friendly pathway visualization and data integration. Nucleic Acids Res 2017; 45:W501-8.

26. Aranda J, Poza M, Pardo BG, Rumbo S, Rumbo C, Parreira JR, Rodríguez-Velo P, Bou G. A rapid and simple method for constructing stable mutants of Acinetobacter baumannii. BMC Microbiology 2010; 10: 279.

27. Gil-Marqués ML, Pachón-Ibáñez ME, Pachón J, Smani Y. Effect of hypoxia on the pathogenesis of *Acinetobacter baumannii* and *Pseudomonas aeruginosa* in vitro and in murine experimental models of infections. Infect Immun 2018; pii: IAI.00543-18.

28. O'Toole GA, Pratt LA, Watnick PI, Newman DK, Weaver VB, Kolter R. Genetic approaches to study of biofilms. Methods Enzymol. 1999; 310:91-109.

29. Carretero-Ledesma M, García-Quintanilla M, Martín-Peña R, Pulido MR, Pachón J, McConnell MJ. Phenotypic changes associated with Colistin resistance due to Lipopolysaccharide loss in *Acinetobacter baumannii*. Virulence 2018; 9:930-42.

30. Wang Z, Gerstein M and Snyder M. RNA-Seq: a revolutionary tool for transcriptomics. Nat. Rev. Genet 2009; 10:57-63.

31. Hsieh YJ, Wanner BL. Global regulation by the seven-component Pi signaling system. Curr Opin Microbiol 2010; 13:198-203.

32. Chekabab SM, Harel J, Dozois CM. Interplay between genetic regulation of phosphate homeostasis and bacterial virulence. Virulence 2014; 5:786-93.

33. Fang FC, Frawley ER, Tapscott T, Vázquez-Torres A. Bacterial stress responses during host infection. Cell Host Microbe 2016; 20:133-43.

34. Lamarche MG, Wanner BL, Crépin S, Harel J. The phosphate regulon and bacterial virulence: a regulatory network connecting phosphate homeostasis and pathogenesis. FEMS Microbiol Rev 2008; 32:461-73.

35. Camarena L, Bruno V, Euskirchen G, Poggio S, Snyder M. Molecular mechanisms of ethanol-induced pathogenesis revealed by RNA-sequencing. PLoS Pathog 2010; 6:e1000834.

36. Neznansky A, Blus-Kadosh I, Yerushalmi G, Banin E, Opatowsky Y. The *Pseudomonas aeruginosa* phosphate transport protein PstS plays a phosphate-independent role in biofilm formation. FASEB J 2014; 28:5223-33.

37. Pratt JT, Ismail AM, Camilli A. PhoB regulates both environmental and virulence gene expression in *Vibrio cholerae*. Mol Microbiol 2010; 77:1595-605.

38. Ferreira GM, Spira B. The pst operon of enteropathogenic *Escherichia coli* enhances bacterial adherence to epithelial cells. Microbiology. 2008; 154:2025-36.

39. Esparza M, Palomares B, García T, Espinosa P, Zenteno E, Mancilla R. PstS-1, the 38-kDa *Mycobacterium tuberculosis* glycoprotein, is an adhesin, which binds the macrophage mannose receptor and promotes phagocytosis. Scand J Immunol 2015; 81:46-55.

40. Lucas RL, Lostroh CP, DiRusso CC, Spector MP, Wanner BL, Lee CA. Multiple factors independently regulate hilA and invasion gene expression in Salmonella enterica serovar Typhimurium. J Bacteriol 2000; 182:1872-82.

41. Davey ME, O'Toole GA. Microbial biofilms: from ecology to molecular genetics. Microbiol Mol Biol Rev 2000; 64:847-67.

42. Pratt JT, McDonough E, Camilli A. PhoB regulates motility, biofilms, and cyclic di-GMP in Vibrio cholerae. J Bacteriol 2009; 191:6632-42.

43. Monds RD, Newell PD, Gross RH, O'Toole GA. Phosphate-dependent modulation of c-di-GMP levels regulates *Pseudomonas fluorescens* Pf0-1 biofilm formation by controlling secretion of the adhesin LapA. Mol Microbiol. 2007; 63:656-79.

44. O'May G, Jacobsen SM, Longwell M, Stoodley P, Mobley HL, Shirtliff ME. The high-affinity phosphate transporter Pst in *Proteus mirabilis* HI4320 and its importance in biofilm formation. Microbiology 2009; 155:1523-35.

45. Monds RD, Silby MW, Mahanty KH. Expression of the Pho regulon negatively regulates biofilm formation by *Pseudomonas aureofaciens* PA147-2. Mol Microbiol 2001; 42:415-26.

46. Blus-Kadosh I, Zilka A, Yerushalmi G, Banin E. The effect of pstS and phoB on quorum sensing and swarming motility in *Pseudomonas aeruginosa*. PLoS One 2013; 8:e74444.

47. Zaborina O, Holbrook C, Chen Y, Long J, Zaborin A, Morozova I, Fernandez H, Wang Y, Turner JR, Alverdy JC. Structure-function aspects of PstS in multi-drug-resistant Pseudomonas aeruginosa. PLoS Pathog 2008; 4:e43.

48. Llop Talaverón JM, Comas Sugrañes D, Badía Tahull MB, Sáez Fernández A, Jódar Masanés R, Gómez Sáez JM. Hypophosphatemia in parenteral nutrition: Prevention and associated risks factors]. Nutr Hosp 2004; 19:362-6.

49. Barak V, Schwartz A, Kalickman I, Nisman B, Gurman G, Shoenfeld Y. Prevalence of hypophosphatemia in sepsis and infection: the role of cytokines. Am J Med 1998; 104:40-7.

50. Shor R, Halabe A, Rishver S, Tilis Y, Matas Z, Fux A, Boaz M, Weinstein J. Severe hypophosphatemia in sepsis as a mortality predictor. Ann Clin Lab Sci 2006; 36:67-72.

ADDITIONAL DATA

We selected five different genes that were overexpressed under microaerobiosis to determine if they were involved in *A. baumannii* pathogenesis. The genes were *A1S_0030, A1S_2532, A1S_0464, A1S_0172* and *A1S_2448*. We have analyzed the last one in this chapter I.

Stable, in-frame deletion mutants were constructed in the *A. baumannii* ATCC 17978 strain by homologous recombination using the described protocol. For construction of the *A1S_0030* and *A1S_2532* deletion mutant (ATCC 17978 Δ*A1S_0030*::Kan, and ATCC 17978 Δ*A1S_2532*::Kan, respectively), the 500 bp immediately upstream of the genes open reading frame, and the 500 bp immediately downstream were amplified using the primers indicated in Table A1.

A more efficient technique was used to construct in-frame deletion mutants of the *A1S_0464* and *A1S_0172* genes. Gene deletions were performed with an allelic exchange plasmid called pMJG42, which harbors the *sacB* gene for counterselection via growth on medium containing sucrose as previously described [1]. For construction of the deletion mutants ATCC 17978 Δ*A1S_0464* and ATCC 17978 Δ*A1S_0172* the 2000 bp immediately upstream of the genes open reading frame, and the 2000 bp immediately downstream were amplified using the primers indicated in Table A1. The plasmid pMJG42 was digested with SpeI and NotI (New England Biolabs). The Up insert was digested with SpeI and XhoI/ BamHI, and the Down insert was digested with XhoI/ BamHI and NotI (XhoI or BamHI depending on the mutant). The plasmid and both inserts were ligated, and the resulting construction was transformed into the *Escherichia coli* DH5α λpir by electroporation before selection on LB agar plates with Tetracycline 5 mg/L (Sigma). The construction was then transformed into *E. coli* MFD

[2], a Diaminopimelic acid (DAP) auxotrophic strain. MFD donor strain harboring the respective pMJG42-gene(Up/Down) construct and the ATCC 17978 recipient strain were cultured overnight at 37°C in LB (supplemented with tetracycline 5 mg/L and DAP 200 mg/L for the donor strain). Aliquots of 1 mL of the donor strain and 0.5 mL of the recipient strain were washed twice and mix together. The cells were suspended in 30 µl of LB and added on to a sterile 0.45 µm cellulose nitrate filter paper (Millipore) on LB agar plates and incubated for 4 h at 37°C. The cells were washed off from the filter by adding 1 ml of LB and they were plated onto LB agar plates containing tetracycline 5 mg/L. The obtained colonies were grown in LB, plated onto 10% Sucrose plates and incubated overnight at room temperature. All deletion mutants were confirmed by PCR and sequencing.

In order to complement the obtained mutants, the genes reading frames and 200-400 bp upstream and downstream were amplified using the primers indicated in Table A1. These fragments were cloned into the pUCp24 and introduced into the mutant strains by electroporation before selection on LB agar plates containing 10 mg/L of gentamicin to create the complemented strains (ATCC 17978 Δ*A1S_0030*::Kan/pUCp24-0030, ATCC 17978 Δ*A1S_2532*::Kan/pUCp24-2532, ATCC 17978 Δ*A1S_0464*/pUCp24-0464, ATCC 17978 Δ*A1S_0172*/pUCp24-0172). Deletion mutants were also transformed with the empty pUCp24 plasmid for use as controls (ATCC 17978 Δ*A1S_0030*::Kan/pUCp24, ATCC 17978 Δ*A1S_2532*::Kan/pUCp24, ATCC 17978 Δ*A1S_0464*/pUCp24, ATCC 17978 Δ*A1S_0172*/pUCp24).

Growth curves analysis

Growth curves in MHB under normoxia (21% O_2), hypoxia (1% O_2), and microaerobiosis (0.1-0.3% O_2) were performed to find out if ATCC 17978 wild-type strain and the mutant strains had a different growth rate (Fig. A1). We showed that there

were no significant differences between the wild-type and the mutant strains growth. Complemented strain and strains harboring the empty pUCp24 had the same growth than the other strains under all the conditions (data not shown).

Bactericidal activity, bacterial adherence and bacterial invasion in cell cultures

We determined if hypoxia affects the bactericidal activity of epithelial cells against the mutant strains more than against the wild-type strain. Bacterial counts of ATCC 17978, Δ*A1S_0030*::Kan, Δ*A1S_2532*::Kan, Δ*A1S_0464*, and Δ*A1S_0172* strains found in the extracellular medium of A549 cell line under hypoxia (1% O2) showed a decrease of bacterial concentrations after 2 and 24 h compared to normoxia (data not shown). No significant reductions were found between the mutant strains and the wild-type (Fig. A2). Moreover, bacterial concentration was higher in the case of the mutants Δ*A1S_0464* and Δ*A1S_0172* at 24 h post-infection.

The bacterial adherence of all the mutant strains to A549 cell line was significantly lower at 2 and 24 h post-infection under hypoxia compared to normoxia (data not shown). This decrease was higher in the case of the mutants Δ*A1S_0030*::Kan, Δ*A1S_2532*::Kan, Δ*A1S_0464*, and Δ*A1S_0172* at 2 h and Δ*A1S_0030*::Kan, Δ*A1S_2532*::Kan, and Δ*A1S_0464* at 24 h post-infection compared to the wild-type (Fig. A3). Bacterial counts of the mutant strains Δ*A1S_0030*::Kan and Δ*A1S_2532*::Kan, inside epithelial cells showed a higher decrease than the wild-type strain at 24 h post-infection under hypoxia compared to normoxia (Fig. A4). These data indicate that hypoxia affects the adherence and invasion of these mutant strains more than the wild-type. No significant differences were found in the case of the mutants Δ*A1S_0464* and Δ*A1S_0172*.

According to these results we chose the mutant strain *A1S_2448* to continue with the analysis.

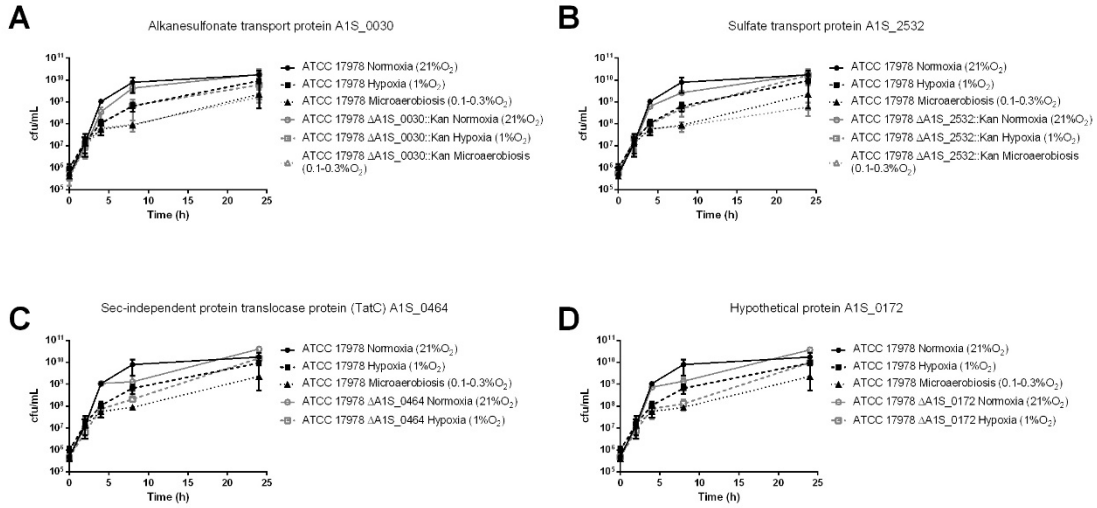

Figure A1. A) Growth curves of *A. baumannii* ATCC 17978 and Δ*A1S_0030*::Kan in MHB under normoxia, hypoxia and microaerobiosis (21%, 1% and 0.1-0.3% O_2, respectively). **B)** Growth curves of *A. baumannii* ATCC 17978 and Δ*A1S_2532*::Kan in MHB under normoxia, hypoxia and microaerobiosis (21, 1 and 0.1-0.3% O_2, respectively). **C)** Growth curves of *A. baumannii* ATCC 17978 and Δ*A1S_0464* in MHB under normoxia and hypoxia (21% and 1% O_2, respectively). **D)** Growth curves of *A. baumannii* ATCC 17978 and Δ*A1S_0172* in MHB under normoxia and hypoxia (21% and 1% O_2, respectively).

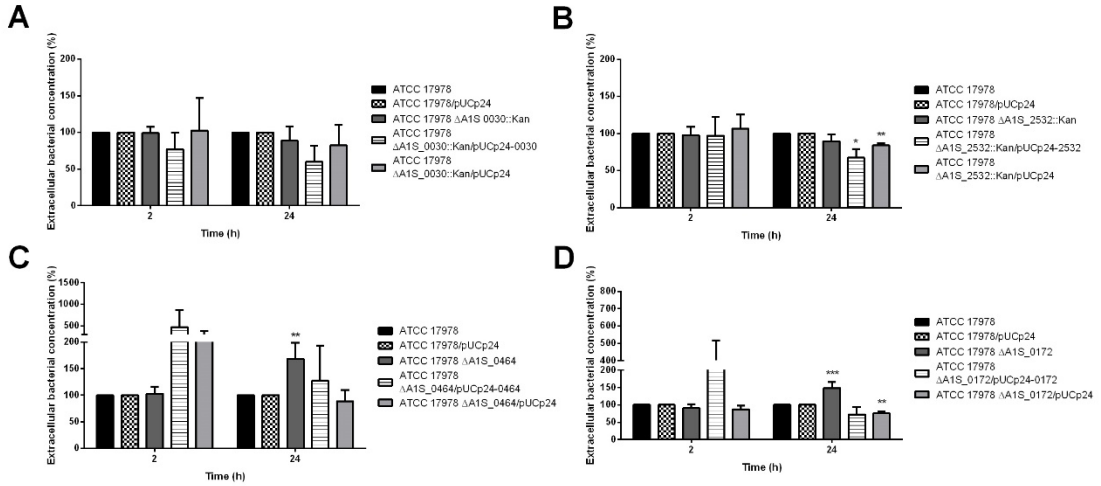

Figure A2. A-D) Measurement of bacterial concentration (%) in the extracellular medium after 2 and 24 h of A549 infection by *A. baumannii* ATCC 17978, ATCC 17978/pUCp24, Δ*A1S_0030*::Kan, Δ*A1S_2532*::Kan, Δ*A1S_0464*, Δ*A1S_0172*, and the respective complemented strains and the mutant strains harboring the empty pUCp24 under normoxia and hypoxia (1% O_2). Bars represent the reduction of bacterial concentration under hypoxia compared to normoxia, being the reduction obtained in the wild-type equal to 100%. ***: P<0.001 Mutant *vs.* wild-type at 2 or 24 h; **: P<0.01 Mutant *vs.* wild-type at 2 or 24 h; *: P<0.05 Mutant *vs.* wild-type at 2 or 24 h.

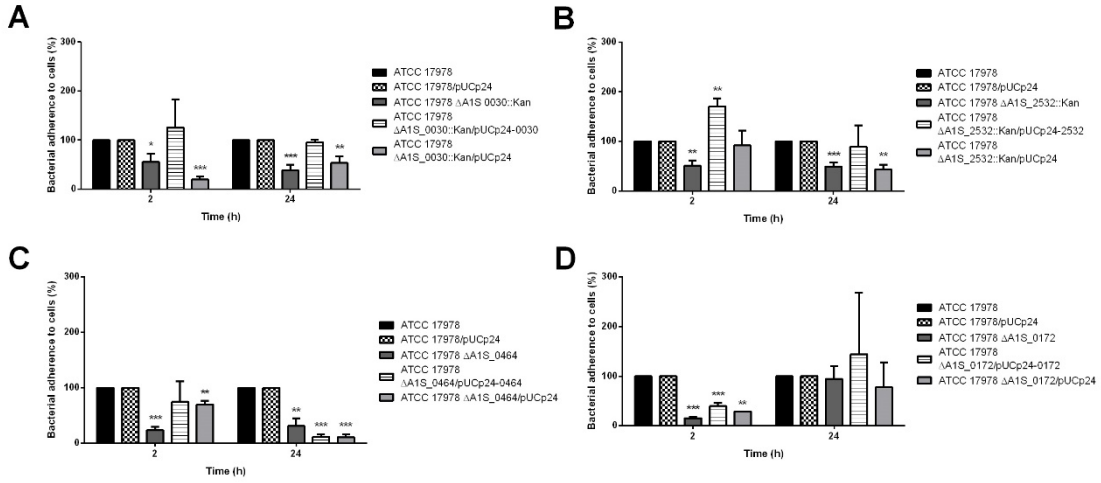

Figure A3. A-D) Measurement of bacterial adherence (%) after 2 and 24 h of A549 infection by *A. baumannii* ATCC 17978, ATCC 17978/pUCp24, Δ*A1S_0030*::Kan, Δ*A1S_2532*::Kan, Δ*A1S_0464*, Δ*A1S_0172*, and the respective complemented strains and the mutant strains harboring the empty pUCp24 under normoxia and hypoxia (1% O_2). Bars represent the reduction of bacterial concentration under hypoxia compared to normoxia, being the reduction obtained in the wild-type equal to 100%. ***: $P<0.001$ Mutant *vs.* wild-type at 2 or 24 h; **: $P<0.01$ Mutant *vs.* wild-type at 2 or 24 h; *: $P<0.05$ Mutant *vs.* wild-type at 2 or 24 h.

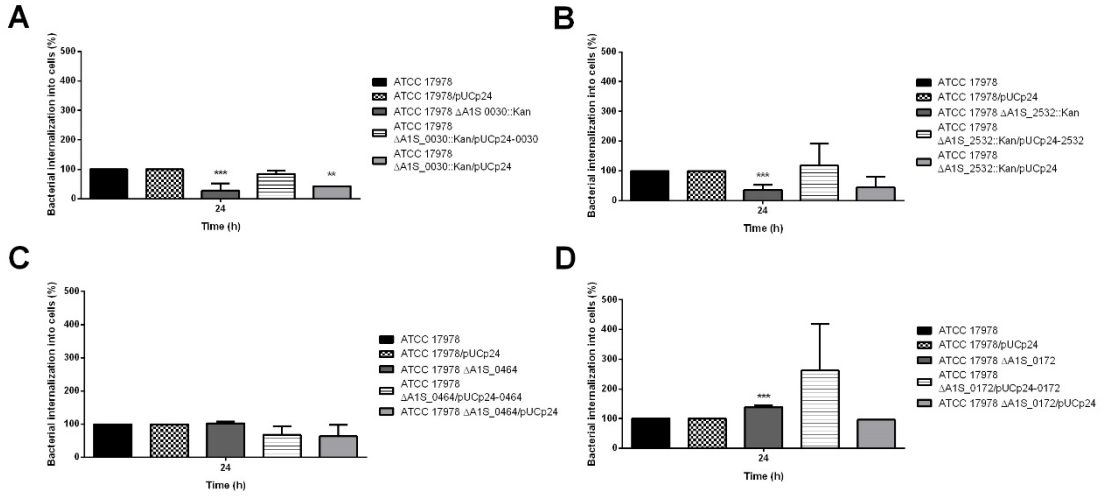

Figure A4. A-D) Measurement of bacterial internalization (%) after 2 and 24 h of A549 infection by *A. baumannii* ATCC 17978, ATCC 17978/pUCp24, Δ*A1S_0030*::Kan, Δ*A1S_2532*::Kan, Δ*A1S_0464*, Δ*A1S_0172*, and the respective complemented strains and the mutant strains harboring the empty pUCp24 under normoxia and hypoxia (1% O_2). Bars represent the reduction of bacterial concentration under hypoxia compared to normoxia, being the reduction obtained in the wild-type equal to 100%. ***: $P<0.001$ Mutant *vs.* wild-type at 2 or 24 h; **: $P<0.01$ Mutant *vs.* wild-type at 2 or 24 h.

Table A1. Primers used in this study.

Name	Sequence	Observations
A1S_0030 Up Forward	AACAAGGTATTCGTCAATTG	Amplification of *A1S_0030* upstream region
A1S_0030 Up Reverse	GCCCCAGCTGGCAATTCCGG GTGGTTTCGTGCTCCCCGA	Amplification of *A1S_0030* upstream region
A1S_0030 Down Forward	CTAAGGAGGATATTCATATG ACCCAGCTTGGGCACAGCT	Amplification of *A1S_0030* downstream region
A1S_0030 Down Reverse	GCTAGAACCTTTCTGTAGCG	Amplification of *A1S_0030* downstream region
EcoRI *A1S_0030* prom. Forward	ACAGAATTCACTATGCATTT TTTAAGATATTC	Amplification of the wild-type *A1S_0030* gene to complement
XbaI *A1S_0030* reg. Reverse	ACATCTAGAATTGATATCCT TGTTCCC	Amplification of the wild-type *A1S_0030* gene to complement
A1S_2532 Up Forward	CAAATTAAAGATTGGGGTG	Amplification of *A1S_2532* upstream region
A1S_2532 Up Reverse	GCCCCAGCTGGCAATTCCGG TGGCTTAAATACATTGCTA	Amplification of *A1S_2532* upstream region
A1S_2532 Down Forward	CTAAGGAGGATATTCATATG TTCTTTGTTCTAACGATAAG	Amplification of *A1S_2532* downstream region
A1S_2532 Down Reverse	GACCGACTTGTCCAAGGTT	Amplification of *A1S_2532* downstream region
EcoRI *A1S_2532* prom. Forward	ACAGAATTCGCCACCAGTTG CAATTGTTG	Amplification of the wild-type *A1S_2532* gene to complement
XbaI *A1S_2532* reg. Reverse	ACATCTAGATCTGTTCTCCTT ATCGTTAG	Amplification of the wild-type *A1S_2532* gene to complement
A1S_0464 pMJG42 SpeI Up F	GGGCCCACTAGTCCATATAG CCTTTGAATACCACG	Amplification of *A1S_0464* upstream region
A1S_0464 pMJG42 XhoI Up R	GGGCCCCTCGAGTTGGTTCA TACGGCAATCTTCAAT	Amplification of *A1S_0464* upstream region
A1S_0464 pMJG42 XhoI Down F	GGGCCCCTCGAGGCTGAATA AAAATAATATAAAAAAGCC TG	Amplification of *A1S_0464* downstream region
A1S_0464 pMJG42 NotI Down R	GGGCCCGCGGCCGCGCGAA GTTTTTCTGAGAACTTCA	Amplification of *A1S_0464* downstream region
EcoRI *A1S_0464* prom. Forward	ACAGAATTCGCTCTCTCCTC TCGCTCG	Amplification of the wild-type *A1S_0464* gene to complement
XbaI *A1S_0464* reg. Reverse	ACATCTAGAAATAAATCCGT AACTTTTGTGTGTATAT	Amplification of the wild-type *A1S_0464* gene to complement
Seq. Deletion	TCACAATCGGAATCAGGAG	To sequence and confirm the

A1S_0464 Up F		deletion
Seq. Deletion *A1S_0464* Down R	GCTTTGTAACGCGACCAGTA	To sequence and confirm the deletion
A1S_0172 pMJG42 SpeI Up F	GGGCCCACTAGTTAGTAGAC ATCGTTTACGGCATG	Amplification of *A1S_0172* upstream region
A1S_0172 pMJG42 BamHI Up R	GGGCCCGGATCCCATTTGCA TATCGTTACTTACTTATTG	Amplification of *A1S_0172* upstream region
A1S_0172 pMJG42 BamHI Down F	GGGCCCGGATCCCATCAATA ATTCTGGAATCTAAAAAAG	Amplification of *A1S_0172* downstream region
A1S_0172 pMJG42 NotI Down R	GGGCCCGCGGCCGCTATGAC CGGATTTCTGTGATTAAG	Amplification of *A1S_0172* downstream region
EcoRI *A1S_0172* prom. Forward	ACAGAATTCCGTTTTTTATTC GTTAAATGCGAATTG	Amplification of the wild-type *A1S_0172* gene to complement
XbaI *A1S_0172* reg. Reverse	ACATCTAGACAGCTCAATAA GGTTCTTAATAGTTG	Amplification of the wild-type *A1S_0172* gene to complement
Seq. Deletion *A1S_0172* Up F	TCCACACAAGTTGTTCTTC	To sequence and confirm the deletion
Seq. Deletion *A1S_0172* Down R	CAGAAACTTTACCTAGTGGT	To sequence and confirm the deletion

References

1. Jacobs AC, Thompson MG, Gebhardt M, Corey BW, Yildirim S, Shuman HA, Zurawski DV. Genetic manipulation of *Acinetobacter baumannii*. Curr Protoc Microbiol 2014 ; 35:6G.2.1–6G.2.11.

2. Ferrières L, Hémery G, Nham T, Guérout AM, Mazel D, Beloin C, Ghigo JM. Silent mischief: bacteriophage Mu insertions contaminate products of *Escherichia coli* random mutagenesis performed using suicidal transposon delivery plasmids mobilized by broad-host-range RP4 conjugative machinery. J Bacteriol 2010 ; 192:6418-27.

CHAPTER II. ARTICLE II.

EFFECT OF HYPOXIA ON THE PATHOGENESIS OF *ACINETOBACTER BAUMANNII* AND *PSEUDOMONAS AERUGINOSA IN VITRO* AND IN MURINE EXPERIMENTAL MODELS OF INFECTIONS.

Several pathogens, including *Escherichia coli*, *Pseudomonas aeruginosa*, *Salmonella typhimurium*, group A and B *Streptococci*, *Staphylococcus aureus*, and *Chlamydia pneumoniae* have been shown to regulate hypoxia inducible factor 1 alpha (HIF-1α) [1-6]. The bacterial lipopolysaccharide has been reported to activate HIF-1α through toll-like receptor 4 in macrophages and neutrophils under normoxia [2, 7-10].

It is known that hypoxia seems to have protective role against bacterial infections. In this way, HIF-1α-deficient macrophages and PMN affect *in vitro* the intracellular killing of group B *Streptococcus* and *P. aeruginosa*, respectively [1,9]. In mice, the HIF-1α-knockout (KO) keratinocytes induced the development of larger necrotic lesions and decreased the mice capacity to clear group A *Streptococcus* by reducing the recruitment of neutrophils to the site of infection [11, 12]; and the HIF-1α knockdown by siRNA reduced the mice resistance to *P. aeruginosa* keratitis [9]. Likewise, the use of mimosine, a HIF-1α agonist, can boost the ability of phagocytes and whole blood to kill *S. aureus* and reduce the lesion size in a murine model of skin infection [13].

However, hypoxia influence on Gram-negative bacterial infection remains to be understood. We know that hypoxia impairs innate immune functions of the airway epithelial cells during *P. aeruginosa* infection, and reducing the HIF-1α expression by siRNA in the bronchial epithelial cells enhances the immune response [14]. More specifically, hypoxia reduced the IL-6 production by keratinocytes when compared to

normoxia [11]. Consecutively, the HIF-1α deletion, but not HIF-1α isoform I.1, in T lymphocytes prevents the antibacterial effect of these cells [15, 16].

During infection, bacteria must adapt to heterogeneous environments [17-19]. The oxygen levels in the foci of infection are much lower (<1%) than in healthy tissues (2.5-9%) [20] due to a combination of increased oxygen consumption by immune cells and pathogens, along with a decreased perfusion due to vascular dysfunction [21-23]. Therefore, the microenvironment at the area of infection plays a crucial role in determining the outcome of an infection. Hypoxia not only modifies the host cells but also the bacterial metabolism and virulence [5]. In *P. aeruginosa* and *Mycobacterium tuberculosis* the expression of virulence factors such as alkaline protease, siderophores and exotoxin A are reduced by hypoxia [24, 25]. However, hypoxia can also increase the production of alginate and the expression of the PA-I lectin/adhesin by *P. aeruginosa* causing a disruption in intestinal barrier and allowing exotoxin A to cross the epithelium [26, 27]. Exposure to hypoxia also induces antibiotic resistance in *P. aeruginosa* by an alteration of efflux pumps expression [28]. Together, these studies demonstrate the complexity of HIF-pathogen interactions.

The aim of this study was to evaluate the effect of hypoxia on *A. baumannii* and *P. aeruginosa* pathogenesis, *in vitro*, regarding to bactericidal activity and adherence/invasion, and in murine models of infection, regarding to survival, and bacterial load; and the innate immune response in vitro and in vivo.

Materials and Methods

Bacterial strains and growth condition

The wild-type strains *A. baumannii* ATCC 17978 and *P. aeruginosa* PAO1 were used. They were cultured at 37ºC overnight (160 rpm) in Mueller Hinton Broth (MHB) (Sigma, Spain). Cultured strains were washed with phosphate-buffered saline (PBS) and suspended in Dulbecco's modified Eagle's medium (DMEM) before their use in eukaryotic cell culture experiments (human lungs epithelial cell line A549 and murine macrophage cell line RAW 264.7).

Growth curves analysis

The growth of *A. baumannii* ATCC 17978 and *P. aeruginosa* PAO1 strains under hypoxia (1% and 10% O_2) and normoxia (21% O_2) in static were monitored during 24 h. Both strains were grown overnight in 20 ml of MHB, and a 1:10000 dilution was performed to obtain, approximately, 10^5 cfu/ml in a 40 ml culture of MHB (10% and 21% O_2) or DMEM (1% and 21% O_2). Three replicates were performed in different days.

A549 and RAW 264.7 culture and infection

Human lungs epithelial cell line A549 and murine macrophage cell line RAW 264.7 were grown in DMEM containing 10% Fetal Bovine Serum (Gibco, Spain), 1% HEPES 1M, vancomycin (50 mg/ml), gentamicin (20 mg/ml) and amphotericin B (0.25 mg/ml; Gibco), as previously described [43]. In the case of hypoxia condition studies, cells were transferred to a hypoxia chamber (Coy Laboratories, USA) with a humidified atmosphere of 1% O_2, 5% CO_2 and the balance N_2 at 37°C. Cells were seeded (10^5 cells/well in a 24-well plate) for 30 h in 24-well plates before infection with *A.*

baumannii ATCC 17978 or *P. aeruginosa* PAO1 at a multiplicity of infection (MOI) of 500. To mimic hypoxia condition we treated the cells with 0.1 mM Dimethyloxaloylglycine (DMOG) (Sigma, Spain), an inhibitor of prolyl hydroxylases [44], 6 h prior bacterial infection and during infection. Immediately before the infection, A549 cells were washed thrice with PBS and incubated in supplemented DMEM.

HIF-1α measurement in cell cultures

A549 and RAW 264.7 cells were seeded for 24 h in 6-well plates (10^6 cells/well). After 6 and 24 h in hypoxia (1% O_2) or normoxia condition, cells were washed thrice with PBS, harvested using cell scraper and homogenized in RIPA buffer supplemented with 1 mM phenylmethylsulfonyl fluoride and 10% cocktail of protease inhibitors (Sigma, Spain), and centrifuged at 13000*g* 4°C for 20 min. The supernatant was removed and the amount of proteins was determined using BCA assay (Promega, Spain). The samples were stored at -80°C. Forty µg of proteins of each sample was used to measure HIF-1α levels with an enzyme-linked immunosorbent assay (ELISA) kit (Thermo Fisher Scientific, Spain).

Bactericidal activity, bacterial adherence and bacterial invasion in cell cultures

After A549 and RAW 264.7 cells infections with *A. baumannii* ATCC 17978 and *P. aeruginosa* PAO1 strains under hypoxia and normoxia conditions, extracellular medium was removed and serially diluted to determine bacterial concentration as previously described [45].

Adherence and invasion assays were performed as previously described [45]. To measure the number of adherent bacteria, cells were infected as mentioned before, and, after washing thrice with PBS, 200 µl of trypsin-EDTA (Gibco, Spain) was added for 5 min at 37°C. Then, 200 µl of 0.5% Triton X-100 (Sigma, Spain) was added for 3 min.

The invasion protocol included a treatment with gentamicin 256 µg/ml (Gibco, Spain) before the addition of trypsin-EDTA. Diluted lysates were counted to determine the attached and internalized bacteria by A549 and RAW 264.7 cells.

Every assay was performed three times in different days. In the case of invasion assay, four replicates were performed in different days.

Cytokine Assay

Extracellular medium of infected A549 and RAW 264.7 cells with *A. baumannii* ATCC 17978 and *P. aeruginosa* PAO1 strains under hypoxia and normoxia conditions were collected and centrifuged at 5000*g* for 15 min at 4ºC. The supernatant was stored at -80ºC until analysis. TNF-α, IL-6 and IL-10 levels were measured in using an ELISA kit (Affymetrix eBioscience, USA), in accordance with the manufacturer's instructions. Levels of pro- and anti-inflammatory cytokines (IL-6, IL-10 and TNF-α) in mice serum were measured by ELISA assays (Affymetrix eBioscience, USA).

iTRAQ assay

We analyzed the differential protein expression profile between normoxia and hypoxia conditions in A549 cell infected by *A. baumannii* ATCC 17978. After 2 h infection, we collected the cells in a lysis buffer composed by 1 M Triethylammonium bicarbonate buffer (Sigma, Spain), 0.05% SDS, 1:100 phosphatase inhibitor cocktail (PhosSTOP EASYpack, Roche, Spain), 1:100 protease inhibitor cocktail (Complete Mini EDTA-free, Roche, Spain), and 0.002% benzonase (Novagen, USA). Pellet was separated from the supernatant and protein concentration was quantified by fluorimetry (Qubit life technology, USA). Samples were treated with 50 mM TCEP (AB Sciex, Spain) to reduce disulfide bonds and 200 mM MMTS (AB Sciex, Spain), and then they were digested with trypsin (Promega, Spain) at a 10:1 substrate:enzyme ratio at 37°

overnight. We used an isobaric tag iTRAQ 4 plex (reporters at 114 to 117, AB Sciex, Spain). Samples were analyzed by nano-liquid chromatography (nano LC 100, Thermo Fisher Scientific, USA) and tandem mass spectrometry (Q Exactive Plus Orbitrap, Thermo Electron, USA). Protein identification was performed using Proteome Discoverer 1.4 (Thermo Fisher Scientific, USA). MS/MS fragmentation patterns were mapped against Uniprot database. We considered quantifiable proteins those that were identified through more than 2 peptides with a confidence level ≥ 95%, a *P*-value ≤ 0.05, and an error factor < 2 with every reference tag.

Animals

Immunocompetent C57BL/6 male mice, weighing approximately 20 g (Production and Experimentation Animal Center, University of Seville, Seville, Spain) were used; they had a sanitary status of murine pathogen free and were assessed for genetic authenticity. Mice were housed in an individually ventilated cage system under specific pathogen-free conditions, and water and food supplied *ad libitum*. This study was carried out following the recommendations in the Guide for the Care and Use of Laboratory Animals [46]. This study was carried out in strict accordance with Directive 2010/63/EU on the protection of animals used for scientific purposes. Experiments were approved by the Committee on the Ethics of Animal Experiments of the University Hospital of Virgen del Rocío of Seville, Spain (20-05-14-84). All procedures were performed under sodium thiopental (B. Braun Medical S.A., Spain) anesthesia, and all efforts were made to minimize suffering.

Experimental models

Both models of infection were carried out under the following conditions: i) hypoxia (10% O_2), ii) normoxia and iii) six hours under hypoxia followed by normoxia. The

minimum lethal doses (MLD) were calculated for *A. baumannii* and *P. aeruginosa* under hypoxia and normoxia conditions. Briefly, groups of 6 mice were inoculated intraperitoneally (ip.) for *A. baumannii* and intratracheally for *P. aeruginosa* with increasing concentrations until reaching 100% mortality, of each pathogen and the survival rate was monitored for 7 days. For the hypoxia condition studies, mice were maintained in a hypoxic chamber (Coy Laboratories, USA) with a humidified atmosphere of 10% O_2 (standard hypoxic condition) 6 h prior the infection and until the animal death or the end of the experiment. In the experiments in which mice were 6 h under hypoxia followed by normoxia, the animals were maintained in a hypoxic chamber during 6 h prior the infection, and placed outside normoxia until the end of the experiment or the animal death. The same conditions were used with control mice (not infected).

To evaluate pneumonia, after 4 h of infection and at the time of death, lungs were aseptically extracted, fixed in 10% formalin and embedded in paraffin wax. Serial sections (3 μm) were cut onto glass slides and stained with hematoxylin and eosin.

A N of no more than 5 mice per condition was performed in different weeks to reproduce the experimental models results.

(i) Experimental murine model of peritoneal sepsis. A previously characterized murine peritoneal sepsis model by *A. baumannii* was used [36]. Briefly, animals were inoculated i.p. with 0.5 ml of $MLD_{100,}$ mixed 1:1 with a saline solution containing 10% (wt/vol) mucin from porcine stomach Type II (Sigma, Spain).

After 4 h of infection, a group of 34 mice (17 under hypoxia and 17 under normoxia) were sacrificed by i.p. injection of sodium thiopental (200 μl; Braun Medical, USA) and analyzed, and 48 mice (21 under normoxia, 22 under hypoxia and 5 under 6h hypoxia + normoxia) were analyzed at the time of death. Survival rates were recorded under

hypoxia and normoxia conditions. Bacteremia was evaluated, both qualitatively and quantitatively after the animal's death. For qualitative analysis, the blood was inoculated into sterile tubes with 1 ml of MHB and incubated for 24 h at 37ºC, and then 10 µl was plated on sheep blood agar. To evaluate quantitatively the bacteremia (log_{10} cfu/ml), blood was serially diluted and plated on sheep blood agar. Finally, bacterial load was quantified in spleen and lungs. Briefly, organs were aseptically removed and homogenized (Stomacher 80; Tekmar Co.) in 2 ml of sterile 0.9% NaCl solution. Serial dilutions of the homogenized organs were plated on sheep blood agar for quantitative cultures (log_{10} cfu/g). Finally, bacterial concentration in peritoneal fluid was also determined by injecting 2 mL of sterile 0.9% NaCl solution i.p. and, after a brief massage on the abdomen, peritoneal lavage was collected and plated on sheep blood agar (log_{10} cfu/mL). HIF-1α levels in mice serum were measured by ELISA assays (MyBioSource, USA).

(ii) Pneumonia model. A previously characterized pneumonia model by *P. aeruginosa* [47] was used as follows: anesthetized mice (thiopental at 5% [wt/vol], i.p.) were infected by intratracheal instillation, using 50µL of the MLD_{100} calculated previously. Mice remained in a vertical position for 3 min and then resting at 30º positions until they awakened. After 4 h of infection, 36 mice (18 under normoxia and 18 under hypoxia) were sacrificed (sodium thiopental, Braun Medical, USA) to be analyzed and 46 mice (20 under normoxia, 18 under hypoxia and 8 under 6 h hypoxia + normoxia) were analyzed at the time of death. Survival rates were analyzed for the different conditions. Bacteremia, bacterial load in blood and tissue (spleen and lungs) were performed as described above. HIF-1α levels in mice serum were measured by ELISA assays (MyBioSource, USA).

Statistical analysis

Statistical analyses were performed using the IBM SPSS Statistics 22 software program. Tests used included ANOVA (bacterial counts in tissues and fluids and mortality time), Chi-square test (bacteremia), and when required Dunnett's and Tukey post-hoc tests and Student's t-test (bacterial counts *in vitro*, cytokines and HIF-1α levels). A *P*-value <0.05 was considered significant.

Results

Hypoxia increases HIF-1α levels in epithelial and macrophages cells

HIF-1α levels in cell lines after 6 and 24 h under hypoxia (1% O2) and normoxy (21% O2) were measured. In epithelial cells, HIF-1α levels were 2.69 times higher after 6 h in hypoxia than in normoxy (2296.98 ± 157.74 pg/mL *vs*. 853.63 ± 95.47 pg/mL, *P*<0.001) and were higher than after 24 h (1107.70 ± 96.08 pg/mL *vs.* 592.27 ± 48.86 pg/mL, *P*<0.01). In macrophages cells, HIF-1α levels were 1.50 times higher after 6 h in hypoxia than in normoxia (331.64 ± 52.93 pg/mL *vs*. 220.67 ± 11.87 pg/mL) and were higher than after 24 h under hypoxia (223.59 ± 7.05 pg/mL *vs.* 235.27 ± 9.31 pg/mL; hypoxia 6 h *vs.* hypoxia 24 h). No significant differences in HIF-1α levels were observed in normoxia between the different times points analysed.

The marked increase of HIF-1α levels after 6 h under hypoxia (1% O_2) defined the time of hypoxia condition prior the infection for the in vitro and in vivo experiments.

Hypoxia increases bactericidal activity of epithelial and macrophages cells against A. baumannii and P. aeruginosa

First, we observed that ATCC 17978 and PAO1 strains growth during 2 and 24 h was indistinguishable between hypoxia (1% O_2) and normoxia (Fig. 1A). Next, we determined if hypoxia affects the bactericidal activity of epithelial and macrophages cells. Bacterial counts of ATCC 17978 and PAO1 strains found in the extracellular medium of both cell lines under hypoxia (1% O_2) showed a decrease of bacterial concentrations after 2 and 24 h compared to normoxia, (Fig. 1B and 1C). These data support an increase in the bactericidal activity of these cell lines under hypoxia.

HIF-1α overexpression increases bactericidal activity of epithelial and macrophages cells against A. baumannii and P. aeruginosa

Bacterial counts of ATCC 17978 and PAO1 strains found in the extracellular medium of both cell lines under a 0.1 mM DMOG treatment showed a decrease of bacterial concentrations after 24 h compared to normoxia, (Fig. 1B and 1C). These data support an increase in the bactericidal activity of these cell lines when HIF-1α is overexpressed due to the treatment with DMOG.

Hypoxia decreases bacterial adherence and invasion to epithelial and macrophages cells

The bacterial adherence of ATCC 17978 and PAO1 strains to both cell lines was significantly lower under hypoxia (1% O2), except in the case of 2 h post-infection by ATCC 17978 strain in the RAW 264.7 cells in which it presented higher bacterial adherence (182.67 ± 11% *vs*. 100% ± 0%, $P<0.001$) (Fig. 2A and 2B).

Bacterial counts of ATCC 17978 strain inside epithelial and macrophages cells under hypoxia (1% O_2) showed an increase of bacterial concentrations 2 h post-infection (150 ± 0% for epithelial cells, and 146.73 ± 5.01% for macrophages cells, $P<0.001$), and a decrease at 24 h post-infection compared to normoxia (48.55 ± 34.80% for epithelial

cells, P<0.001 and 8.69 ± 6.85% for macrophages cells, P<0.001) (Fig. 2C). On the other hand, PAO1 strain counts inside both cell lines under hypoxia (1% O_2) showed a decrease of bacterial concentrations after 2 h (P<0.001 for macrophages cells) and 24 h (P<0.001) compared to normoxia (Fig. 2D). These data indicated that hypoxia affects the adherence and invasion of *A. baumannii* and *P. aeruginosa* 24 h after bacterial infection.

Hypoxia reduces the expression of proteins involved in cell adherence

iTRAQ results show that there are 51 down-expressed proteins under hypoxia (Fold Change < 0.6) present in the extracellular medium of a 2 h infection of A549 cells by *A. baumannii* ATCC 17978 strain (Table S1). Forty-five % are localized in the cytoplasm, 16% are secreted, 19% are in the inner membrane, 10% in the outer membrane, 6% in the periplasm and 4% in the mitochondrion (Fig. S1). The proteins localized in the outer membrane and could be involved in cell adhesion are OmpW, putative ferric siderophore receptor protein *A1S_3339*, putative ferric siderophore receptor protein *A1S_0474*, ferric enterobactin receptor *A1S_0981*, and ferrichrome-iron receptor *A1S_1921*. Moreover, the secreted uncharacterized protein *A1S_3900*, which is a protein that presents SH3-like domains, could also be involved in cell adhesion.

Hypoxia reduces bacterial load in tissues and fluids in a peritonitis sepsis model by A. baumannii

The MLD needed to achieve 100% mortality for ATCC 17978 strain was lower in hypoxia (10% O_2) than in normoxia (2.08 *vs*. 3.20 $\log_{10}$ cfu/mL). For the rest of experiments, we used the MLD calculated in normoxia. The survival time was higher in mice infected under normoxia than hypoxia (10%O_2) (36.42 *vs.* 23.92 h, P<0.001) (Fig. 3A).

In the sepsis model by *A. baumannii*, regardless the studied condition, all mice presented bacteremia after 4 h infection. No differences were found in the bacterial load in tissues (spleen, and lungs) and fluids (PF and blood) between hypoxia and normoxia after 4 h infection (Table 1). However, at the time of death, significant differences between hypoxia and normoxia were found in the bacterial loads in lungs, PF, and blood (Table 1). Moreover, significant differences between animals under normoxia and under hypoxia (6 h) followed by normoxia were found in the bacterial loads at the time of death in spleen, lungs and PF (Table 1). Bacterial loads in spleen, lungs, PF and blood were lower under hypoxia (hypoxia 6 h prior infection, or during the whole experiment) compared to normoxia.

HIF-1α levels showed no differences between hypoxia and normoxia in controls animals (not infected). Contradictorily, infected mice under the different studied conditions presented higher HIF-1α levels than controls mice under normoxia at the time of death (Fig. 3B).

Hypoxia reduces bacterial load in tissues and blood in a pneumonia model by P. aeruginosa

The MLD calculated for PAO1 strain was the same for both conditions (8.54 $\log_{10}$ cfu/mL). Survival time was significantly higher under normoxia than under hypoxia (10% O_2) (P<0.01) or six hours' hypoxia followed by normoxia (P<0.05) (Fig. 3A). Pathological studies confirmed pneumonia 4 h after infection in all the conditions analyzed, but the symptoms were higher under normoxia (data not shown).

After 4 h of infection, no significant differences were found in the bacterial loads in tissues and blood between both conditions (Table 2). Nevertheless, at the mice time of death, significant differences were found in spleen, lungs and blood (between hypoxia

and normoxia (Table 2). Similarly, significant differences at the time of death were found in the bacterial loads in blood between mice under 6 h hypoxia prior the infection followed by normoxia and the animals infected in normoxia (Table 2). Bacterial loads in tissues and blood were lower under both hypoxemic conditions than under normoxia. HIF-1α levels were not significant among the studied conditions. Opposing to what happened in the peritoneal sepsis model by *A. baumannii*; infected mice under the different conditions studied presented lower HIF-1α levels than non-infected mice at the time of death (Fig. 3B).

In vitro and in vivo cytokines production under hypoxia and normoxia

The infection of epithelial cells by ATCC 17978 and PAO1 strains showed that IL-6, TNF-α and IL-10 levels were similar for both conditions at 2 and 24 h post-infection (Fig. 4A). When infecting the RAW 264.7 cells by ATCC 17978 and PAO1 strains, IL-6 and TNF-α levels at 24 h and 2 h post-infection were significantly higher in hypoxia (P<0.05), respectively (Fig. 4B).

In the sepsis model by ATCC 17978 strain, only IL-10 levels were significantly higher after 4 h infection in hypoxia (P<0.05). No differences were found in IL-6 or TNF-α levels, although they were slightly higher under hypoxia. No differences in cytokines levels were found at the animal time of death (Fig. 4C). In the pneumonia model by PAO1 strain, IL-6 levels were significantly higher in hypoxia (P<0.05) after 4 h infection. Again, no differences were found for IL-10 and TNF-α levels although they were rather higher under hypoxia (Fig. 4C). Contradictory to what we observed in the sepsis model, at the mice time of death, we observed lower IL-10 levels under hypoxia (P<0.05). Again, no differences were found in IL-6 or TNF-α levels, although they were slightly lower under hypoxia (Fig. 4C).

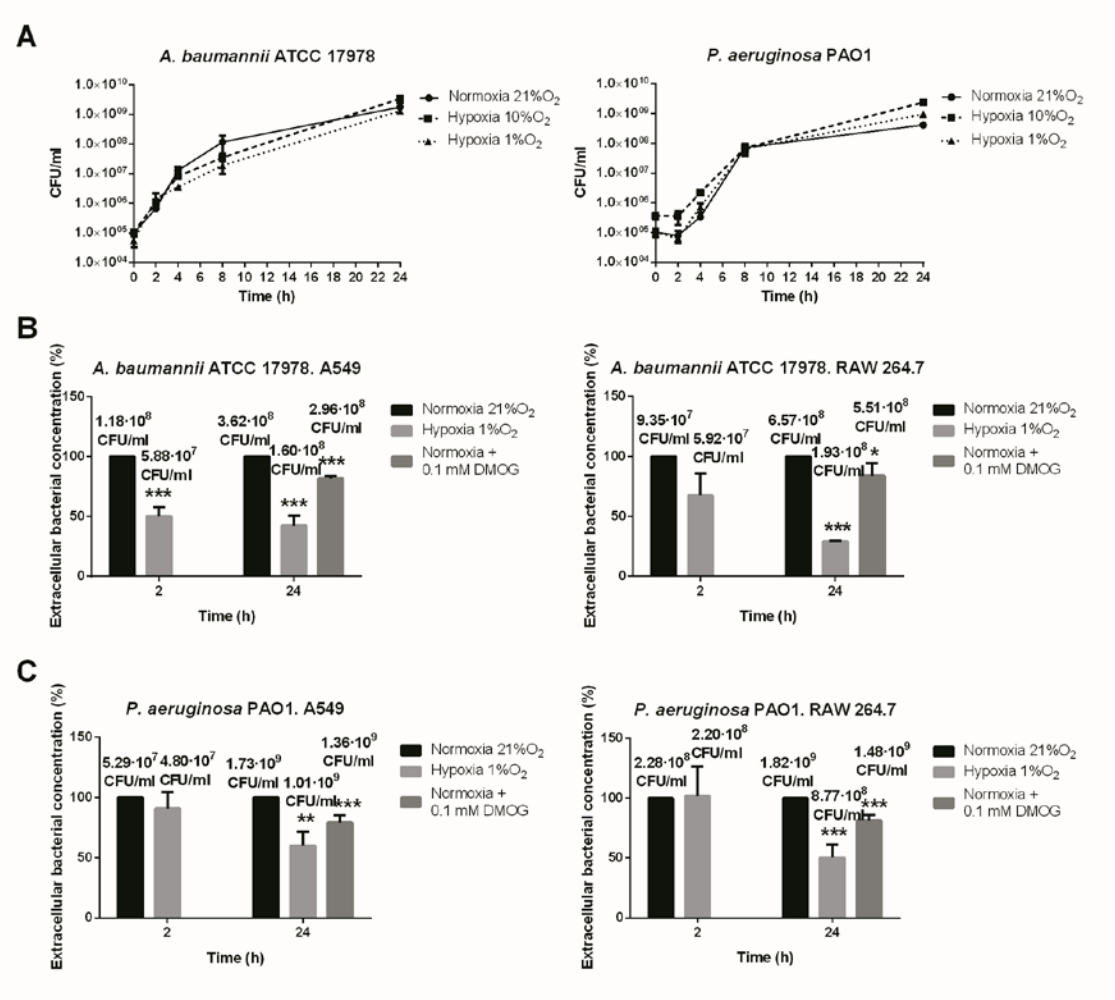

Figure 1. **A**) Growth curves of *A. baumannii* ATCC 17978 and *P. aeruginosa* PAO1 strains under normoxia and hypoxia (10% and 1% O_2). N=3 **B**) Measurement of bacterial concentration (%) in the extracellular medium after 2 and 24 h of A549 and RAW 264.7 infection by *A. baumannii* ATCC 17978 strain under normoxia, hypoxia (1% O_2) and treated with 0.1 mM DMOG. N=3 ***: P<0.001; *: P<0.05 Hypoxia vs. Normoxia at 2 or 24 h and Normoxia + DMOG vs. Normoxia at 24 h. Normoxia + DMOG vs. Normoxia at 24 h. **C**) Measurement of bacterial concentration (%) in the extracellular medium after 2 and 24 h of A549 and RAW 264.7 infection by *P. aeruginosa* PAO1 strain under normoxia, hypoxia (1% O_2) and treated with 0.1 mM DMOG. N=3 **: P<0.01; ***: P<0.001 Hypoxia *vs*. Normoxia at 2 or 24 h and Normoxia + DMOG vs.

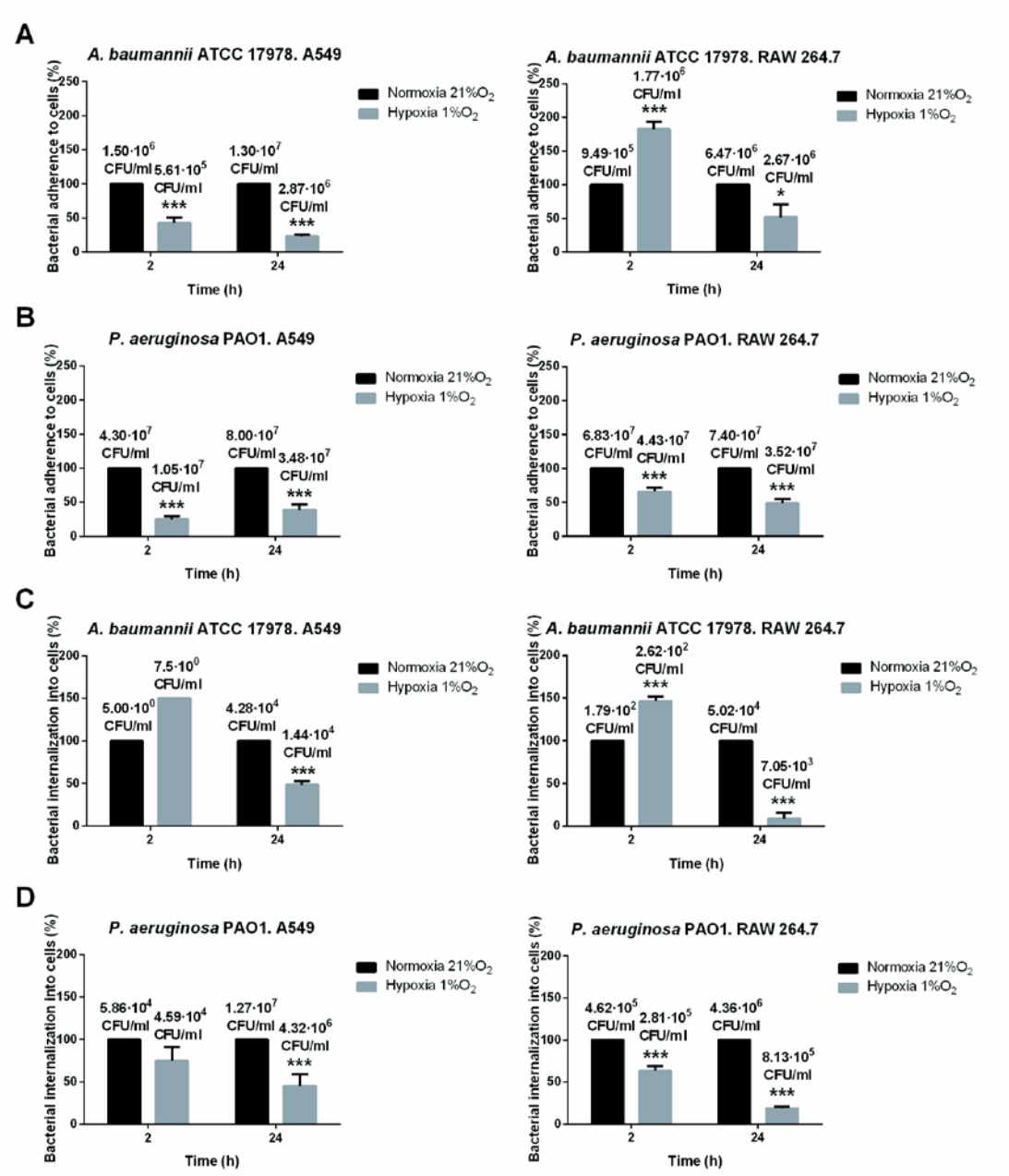

Figure 2. **A**) Measurement of bacterial adherence (%) after 2 and 24 h of A549 and RAW 264.7 infection by *A. baumannii* ATCC 17978 strain under normoxia and hypoxia (1% O_2). N=3 *: P<0.05 and ***: P<0.001 Hypoxia *vs*. Normoxia at 2 or 24 h. **B**) Measurement of bacterial adherence (%) after 2 and 24 h of A549 and RAW 264.7 infection by *P. aeruginosa* PAO1 under normoxia and hypoxia (1% O_2). N=3 ***: P<0.001 Hypoxia *vs*. Normoxia at 2 or 24 h. **C**) Measurement of bacterial internalization (%) after 2 and 24 h of A549 RAW 264.7 infection by *A. baumannii* ATCC 17978 strain under normoxia and hypoxia (1% O_2). N=4 ***: P<0.001 Hypoxia *vs*. Normoxia at 2 h or 24 h. **D)** Measurement of bacterial internalization (%) after 2 and 24 h of A549 RAW 264.7 infection by *P. aeruginosa* PAO1 strain under normoxia and hypoxia (1% O_2). ***: P<0.001 Hypoxia *vs*. Normoxia at 2 h or 24 h. N=4.

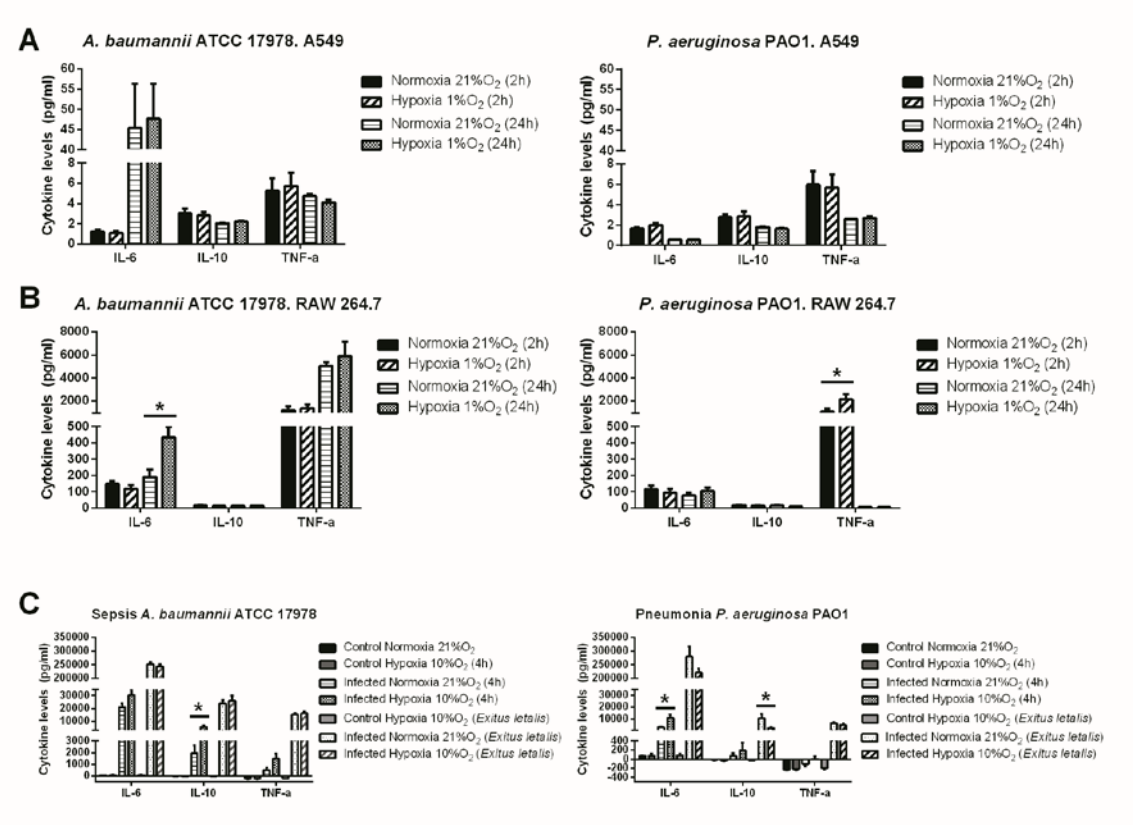

Figure 3. **A**) Analysis of survival time in the sepsis model by *A. baumannii* ATCC 17978 strain (P<0.001 Hypoxia *vs.* Normoxia) and in the pneumonia model by *P. aeruginosa* PAO1 strain under normoxia, hypoxia (10% O_2), and 6 h of hypoxia (10% O_2) + normoxia (P<0.01 Hypoxia *vs.* Normoxia; P<0.05 6 h Hypoxia + Normoxia *vs.* Normoxia). **B**) HIF-1α levels (pg/mL) in mice serum in the sepsis model by *A. baumannii* ATCC 17978 strain and in the pneumonia model by *P. aeruginosa* PAO1 strain at 4 h after infection and at the time of death under normoxia and hypoxia (10% O_2).

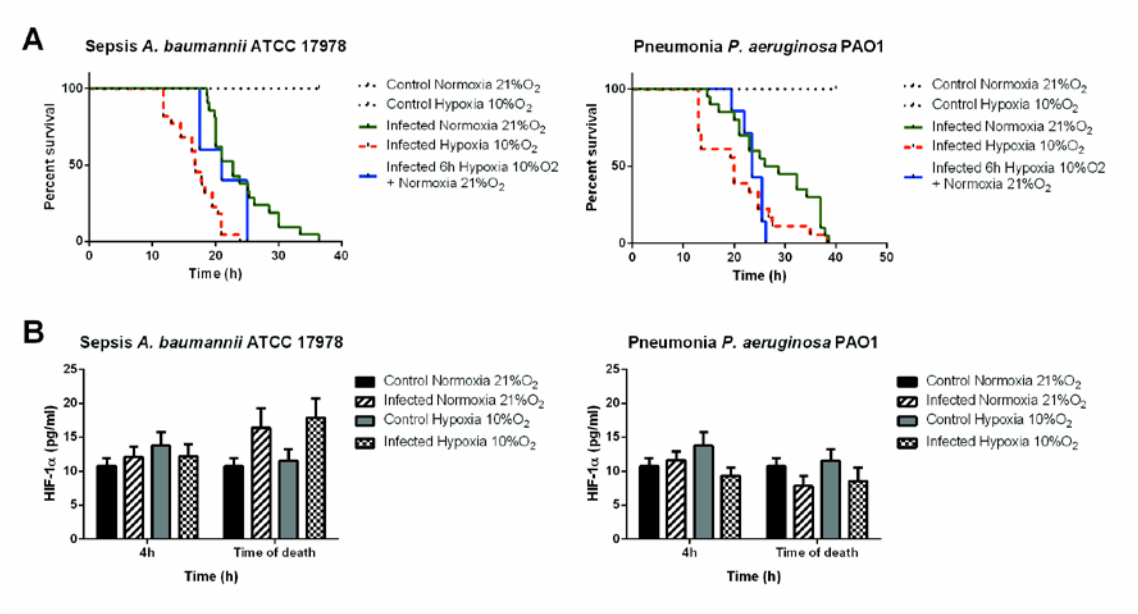

Figure 4. **A**) Cytokines levels (pg/mL) in the extracellular medium of A549 infections by *A. baumannii* ATCC 17978 and *P. aeruginosa* PAO1 strains after 2 and 24 h under normoxia and hypoxia (1% O_2). **B**) Cytokines levels (pg/mL) in the extracellular medium of RAW 264.7 infections by *A. baumannii* ATCC 17978 and *P. aeruginosa* PAO1 strains after 2 and 24 h under normoxia and hypoxia (1% O_2). **C**) Cytokines levels (pg/mL) in mice serum in the sepsis model by *A. baumannii* ATCC 17978 strain and in the pneumonia model by *P. aeruginosa* PAO1 strain. *: $P<0.05$.

Table 1. Bacterial load in fluids and tissues in the sepsis model by *A. baumannii* ATCC 17978 strain.

Time and condition[a]	Bacterial load (log_{10} CFU per g of tissue or per ml of fluid) in:				Bacteremia (%)
	Spleen	Lungs	PF[b]	Blood	
4 h					
N	3.98 ± 0.30	4.07 ± 0.53	4.06 ± 1.29	3.19 ± 0.42	100
H	3.88 ± 0.23	4.07 ± 0.70	3.72 ± 1.15	3.18 ± 0.28	100
Time of death					
N	8.79 ± 0.56	9.36 ± 0.35	9.31 ± 0.33	8.40 ± 0.56	100
H	8.32 ± 0.71	8.25 ± 0.54[e]	8.88 ± 0.53[c]	7.73 ± 0.20[d]	100
H (6 h) + N	7.90 ± 0.30[f]	8.32 ± 0.46[f]	8.75 ± 0.33[f]	7.85 ± 0.32	100

[a]N, normoxia; H, hypoxia.
[b]PF, peritoneal fluid.
[c]$P \leq 0.05$ (H versus N at the time of death).
[d]$P \leq 0.01$ (H versus N at the time of death).
[e]$P \leq 0.001$ (H versus N at the time of death).
[f]$P \leq 0.05$ [H (6 h) + N versus N at the time of death].

Table 2. Bacterial loads in fluids and tissues in the pneumonia model with *P. aeruginosa* strain PAO1

Time and condition[a]	Bacterial load (log_{10} CFU per g of tissue or per ml of fluid) in:			Bacteremia (%)
	Spleen	Lungs	Blood	
4 h				
N	2.64 ± 0.69	7.77 ± 0.61	0.26 ± 0.36	44.44
H	3.10 ± 0.80	7.79 ± 0.42	0.99 ± 0.84	61.11
Time of death				
N	6.96 ± 0.57	9.81 ± 0.45	7.90 ± 0.67	100
H	5.27 ± 0.60[c]	9.04 ± 0.58[c]	5.66 ± 0.78[b]	100
H (6 h) + N	6.60 ± 0.34	9.79 ± 0.27	6.30 ± 0.46[d]	100

[a]N, normoxia; H, hypoxia.
[b]$P \leq 0.01$ (H versus N at the time of death).
[c]$P \leq 0.001$ (H versus N at the time of death).
[d]$P \leq 0.05$ [H (6 h) + N versus N at the time of death].

Discussion

To our knowledge, this is the first study that analyses *in vitro* and *in vivo* the effect of hypoxia during infection by *A. baumannii* and *P. aeruginosa*. We observed that hypoxia *in vitro* increases bactericidal activity of host cells, and reduce bacterial adherence and invasion. We also found that hypoxia *in vivo* diminish bacterial load in fluids and tissues, but mice survival time was shorter under hypoxia.

We showed that hypoxia doesn't affect the *in vitro* growth of *A. baumannii* and *P. aeruginosa*. However, it increases the bactericidal activity in epithelial and macrophage cells. The study of Peyssonnaux *et al*. showed that hypoxia modifies gene regulation in host cells and it increases the LL-37 cathelicidin levels, an antimicrobial peptide involved in the clearance of pathogens [12]. Moreover, we see that hypoxia decreases the bacterial adherence to host cells. This effect might be due to the modification of cell or bacterial membrane under this condition. iTRAQ results confirmed that hypoxia downregulates 51 proteins in *A. baumannii* ATCC 17978, five of them are localized in the outer membrane which could be involved in cell adherence due to the previous reports of their involvement in the bacterial adherence [29-33].

Regarding to bacterial invasion, we observed differences in behavior between *A. baumannii* and *P. aeruginosa* under hypoxia. Our data showed a reduction in the *P. aeruginosa* internalization into epithelial and macrophages cells, confirming the results obtained in a previous study in which it is demonstrated that hypoxia decreases the *P. aeruginosa* internalization into A549 cells [34]. However, *A. baumannii* internalization in both host cells is higher after 2 h under hypoxia, but it is reduced after 24 h. Consequently, hypoxia cannot stop the *A. baumannii* invasion during the first few hours of infection but it is finally hindered after 24 h. Therefore, we believe that hypoxia

confers higher resistance against bacterial invasion to host cells in order to avoid an intracellular replication and the infection evolution.

In the *in vivo* experiments, we observe that a lower bacterial inoculum is needed to cause 100% of mice mortality under hypoxia in the peritoneal sepsis model by *A. baumannii*. All infected mice presented bacteremia 4 h post-infection for the studied conditions. Moreover, we observe lower bacterial load in blood, PF lungs and spleen under hypoxia. We also show that maintaining animals 6 h under hypoxia before the infection is enough to reduce bacterial load at the time of death. These results are in accordance with a previous study in which the use of the compound AKB-4924, that increases HIF-1α levels, reduced bacterial loads recovered in a *S. aureus* skin infection model [35]. Moreover, these results are in accordance with the *in vitro* adherence assays data. The increase of host cells bactericidal activity under hypoxia as well as a reduction of bacterial adherence could allow the immune system to eliminate the infection better.

In the pneumonia model of infection by *P. aeruginosa*, we observed no differences in the inoculum needed to cause 100% of mortality between the studied conditions. Bacteremia observed in mice 4 h post-infection was 44.44% and 61.11% for normoxia and hypoxia, respectively. The difference found in the bacteremia levels between both animal models is because the severity of the sepsis model [36, 37]. As in the sepsis model by *A. baumannii*, we observed lower bacterial load in fluids and tissues under hypoxia, and under hypoxia followed by normoxia, are in accordance with the *in vitro* results of adherence and invasion. Again, as in the sepsis animal model, survival time was longer under normoxia.

In both animal models, HIF-1α levels were higher after 4 h under hypoxia, being the levels similar at the animal time of death regardless the studied conditions. These results are in accordance with the *in vitro* studies in which HIF-1α levels increased over time

under hypoxia and then decreased 24 h after. We observed that *A. baumannii* causes an increase of HIF-1α levels compared to the control as what reported in another study in which infection with *A. baumannii* produced HIF-1α levels increase [4]. In contrast, *P. aeruginosa* produces HIF-1α levels reduction under hypoxia compared to the control. This result could be explained because 2-alkyl-4-quinolone and Pseudomonas Quinolone Signal triggers the HIF-1α degradation through the 26S-proteasome proteolytic pathway, blocking the HIF-1α effect [38, 39].

As it is well defined in the literature, hypoxia regulates the immune response [20]. In the *A. baumannii* sepsis model, we observed under hypoxia high IL-10 levels after 4 h infection. Meng *et al*. indicated that HIF-1α is involved in IL-10 production by B cells [40], and IL-10 is an anti-inflammatory cytokine that suppresses macrophage and dendritic cells function [41]. In the *P. aeruginosa* pneumonia model, we detected high IL-6 levels 4 h post-infection under hypoxia. It has been showed that HIF-1α increase TNF-α and IL-6 levels [20, 42]. Moreover, IL-10 levels decreased under hypoxia in the pneumonia model by *P. aeruginosa* at the time of death. However, we did not find differences in cytokines levels between hypoxia and normoxy neither *in vitro* nor *in vivo*. Therefore, we found that hypoxia has not a strong impact on cytokine production [20], being more important on the bactericidal activity of host cells and on the reduction of infection in animals.

However, this study has some limitations. HIF-1α is a factor involved in multiple cellular pathways and its expression is also regulated by different proteins. Therefore, finding a clear correlation between hypoxia, HIF-1α expression, inflammatory responses and infection is complex, and multiple cellular processes have to be taken into consideration.

In conclusion, hypoxia increases the bactericidal activity of host cells. In contrast, mortality in animals under hypoxia is faster even with a lower bacterial load in tissues and fluids. Moreover, we find that hypoxia has not a strong impact on cytokine production by both pathogens. Finally, despite both studied microorganism are close phylogenetically, they present slightly different behavior under hypoxia.

References

1. Cramer T, Yamanishi Y, Clausen BE, Förster I, Pawlinski R, Mackman N, Haase VH, Jaenisch R, Corr M, Nizet V, Firestein GS, Gerber HP, Ferrara N, Johnson RS. 2003. HIF-1α is essential for myeloid cell mediated inflammation. Cell 112:645-657.
2. Peyssonnaux C, Cejudo-Martin P, Doedens A, Zinkernagel AS, Johnson RS, Nizet V. 2007. Cutting edge: essential role of hypoxia inducible factor-1α in development of lipopolysaccharide-induced sepsis. J Immunol 178:7516-7519.
3. Bayele HK, Peyssonnaux C, Giatromanolaki A, Arrais-Silva WW, Mohamed HS, Collins H, Giorgio S, Koukourakis M, Johnson RS, Blackwell JM, Nizet V, Srai SK. 2007. HIF-1 regulates heritable variation and allele expression phenotypes of the macrophage immune response gene SLC11A1 from a Z-DNA forming microsatellite. Blood 110:3039-3048.
4. Werth N, Beerlage C, Rosenberger C, Yazdi AS, Edelmann M, Amr A, Bernhardt W, von Eiff C, Becker K, Schäfer A, Peschel A, Kempf VA. 2010. Activation of hypoxia inducible factor 1 is a general phenomenon in infections with human pathogens. PLoS One 5:e11576.
5. Schaible B, Schaffer K, Taylor CT. 2010. Hypoxia, innate immunity and infection in the lung. Respir Physiol Neurobiol 174:235-243.
6. Rupp J, Gieffers J, Klinger M, van Zandbergen G, Wrase R, Maass M, Solbach W, Deiwick J, Hellwig-Burgel T. 2007. *Chlamydia pneumoniae* directly interferes with HIF-1a stabilization in human host cells. Cell Microbiol 9:2181-2191.
7. Devraj G, Beerlage C, Brüne B, Kempf VA. 2017. Hypoxia and HIF-1 activation in bacterial infections. Microbes Infect 19:144-156.

8. Peyssonnaux C, Datta V, Cramer T, Doedens A, Theodorakis EA, Gallo RL, Hurtado-Ziola N, Nizet V, Johnson RS. 2005. HIF-1α expression regulates the bactericidal capacity of phagocytes. J Clin Invest 115:1806-1815.
9. Berger EA, McClellan SA, Vistisen KS, Hazlett LD. 2013. HIF-1α is essential for effective PMN bacterial killing, antimicrobial peptide production and apoptosis in *Pseudomonas aeruginosa* keratitis. PLoS Pathog 9:e1003457.
10. Frede S, Stockmann C, Freitag P, Fandrey J. 2006. Bacterial lipopolysaccharide induces HIF-1 activation in human monocytes via p44/42 MAPK and NF-κB. Biochem J 396:517-527.
11. Leire E, Olson J, Isaacs H, Nizet V, Hollands A. 2013. Role of hypoxia inducible factor-1 in keratinocyte inflammatory response and neutrophil recruitment. J Inflamm 10:28.
12. Peyssonnaux C, Boutin AT, Zinkernagel AS, Datta V, Nizet V, Johnson RS. 2008. Critical role of HIF-1 α in keratinocyte defense against bacterial infection. J Invest Dermatol 128:1964-1968.
13. Zinkernagel AS, Peyssonnaux C, Johnson RS, Nizet V. 2008. Pharmacologic augmentation of hypoxia-inducible factor–1α with mimosine boosts the bactericidal capacity of phagocytes. J Infect Dis 197:214-217.
14. Polke M, Seiler F, Lepper PM, Kamyschnikow A, Langer F, Monz D, Herr C, Bals R, Beisswenger C. 2017. Hypoxia and the hypoxia-regulated transcription factor HIF-1a suppress the host defence of airway epithelial cells. Innate Immun 23:373-380.
15. Thiel M, Caldwell CC, Kreth S, Kuboki S, Chen P, Smith P, Ohta A, Lentsch AB, Lukashev D, Sitkovsky MV. 2007. Targeted deletion of HIF-1alpha gene in T cells

prevents their inhibition in hypoxic inflamed tissues and improves septic mice survival. PLoS One 2:e853.

16. Georgiev P, Belikoff BG, Hatfield S, Ohta A, Sitkovsky MV, Lukashev D. 2013. Genetic deletion of the alternative isoform I.1 of HIF-1α in T cells enhances anti-bacterial immune response and improves survival in the model of bacterial peritonitis in mice. Eur J Immunol 43:655-666.
17. Eichner A, Günther N, Arnold M, Schobert M, Heesemann J, Hogardt M. 2014. Marker genes for the metabolic adaptation of *Pseudomonas aeruginosa* to the hypoxic cystic fibrosis lung environment. Int J Med Microbiol 304:1050-1061.
18. Legendre C, Mooij MJ, Adams C, O'Gara F. 2011. Impaired expression of hypoxia-inducible factor-1α in cystic fibrosis airway epithelial cells – a role for HIF-1 in the pathophysiology of CF. J Cyst Fibros 10:286-290.
19. Cullen L, McClean S. 2015. Bacterial adaptation during chronic respiratory infections. Pathogens 4:66-89.
20. Nizet V, Johnson RS. 2009. Interdependence of hypoxic and innate immune responses. Nat Rev Immunol 9:609-617.
21. Cummins EP, Keogh CE, Crean D, Taylor CT. 2016. The role of HIF in immunity and inflammation. Mol Aspects Med 47-48:24-34.
22. Eltzschig HK, Carmeliet P. 2011. Hypoxia and inflammation. N Engl J Med 364:656-665.
23. Campbell EL, Colgan SP. 2015. Neutrophils and inflammatory metabolism in antimicrobial functions of the mucosa. J Leukoc Biol 98:517-522.
24. Schaible B, Rodriguez J, Garcia A, von Kriegsheim A, McClean S, Hickey C, Keogh CE, Brown E, Schaffer K, Broquet A, Taylor CT. 2017. Hypoxia reduces

the pathogenicity of *Pseudomonas aeruginosa* by decreasing the expression of multiple virulence factors. J Infect Dis 215:1459-1467.

25. Sever JL, Youmans GP. 1957. The relation of oxygen tension to virulence of tubercle bacilli and to acquired resistance in tuberculosis. J Infect Dis 101:193-202.
26. Worlitzsch D, Tarran R, Ulrich M, Schwab U, Cekici A, Meyer KC, Birrer P, Bellon G, Berger J, Weiss T, Botzenhart K, Yankaskas JR, Randell S, Boucher RC, Döring G. 2002. Effects of reduced mucus oxygen concentration in airway *Pseudomonas* infections of cystic fibrosis patients. J Clin Invest 109:317-325.
27. Patel NJ, Zaborina O, Wu L, Wang Y, Wolfgeher DJ, Valuckaite V, Ciancio MJ, Kohler JE, Shevchenko O, Colgan SP, Chang EB, Turner JR, Alverdy JC. 2007. Recognition of intestinal epithelial HIF-1α activation by *Pseudomonas aeruginosa*. Am J Physiol Gastrointest Liver Physiol 92:G134-142.
28. Schaible B, Taylor CT, Schaffer K. 2012. Hypoxia increases antibiotic resistance in *Pseudomonas aeruginosa* through altering the composition of multidrug efflux pumps. Antimicrob Agents Chemother 56:2114-2118.
29. McClean S, Healy ME, Collins C, Carberry S, O'Shaughnessy L, Dennehy R, Adams Á, Kennelly H, Corbett JM, Carty F, Cahill LA, Callaghan M, English K, Mahon BP, Doyle S, Shinoy M. 2016. Linocin and OmpW are involved in attachment of the cystic fibrosis-associated pathogen *Burkholderia cepacia* complex to lung epithelial cells and protect mice against infection. Infect Immun 84:1424-1437.
30. Kurochkina N. 2015. SH Domains. Springer International Publishing. {Structure-Function Relationship of Bacterial SH3 Domains}. 71-89.
31. Carnielli CM, Artier J, de Oliveira JC, Novo-Mansur MT. 2017. *Xanthomonas citri* subsp. citri surface proteome by 2D-DIGE: Ferric enterobactin receptor and other

outer membrane proteins potentially involved in citric host interaction. J Proteomics 151:251-263.

32. Russo TA, McFadden CD, Carlino-MacDonald UB, Beanan JM, Barnard TJ, Johnson JR. 2002. IroN functions as a siderophore receptor and is a urovirulence factor in an extraintestinal pathogenic isolate of *Escherichia coli*. Infect Immun 70:7156-7160.
33. Feldmann F, Sorsa LJ, Hildinger K, Schubert S. 2007. The salmochelin siderophore receptor IroN contributes to invasion of urothelial cells by extraintestinal pathogenic *Escherichia coli in vitro*. Infect Immun. 75:3183-3187.
34. Schaible B, McClean S, Selfridge A, Broquet A, Asehnoune K, Taylor CT, Schaffer K. 2013. Hypoxia modulates infection of epithelial cells by *Pseudomonas aeruginosa*. PLoS One 8:e56491.
35. Okumura CY, Hollands A, Tran DN, Olson J, Dahesh S, von Köckritz-Blickwede M, Thienphrapa W, Corle C, Jeung SN, Kotsakis A, Shalwitz RA, Johnson RS, Nizet V. 2012. A new pharmacological agent (AKB-4924) stabilizes hypoxia inducible factor-1 (HIF-1) and increases skin innate defenses against bacterial infection. J Mol Med 90:1079-1089.
36. Smani Y, Domínguez-Herrera J, Ibáñez-Martínez J, Pachón J. 2015. Therapeutic efficacy of lysophosphatidylcholine in severe infections caused by *Acinetobacter baumannii*. Antimicrob Agents Chemother 59:3920-3924.
37. Vila-Farrés X, Parra-Millán R, Sánchez-Encinales V, Varese M, Ayerbe-Algaba R, Bayó N, Guardiola S, Pachón-Ibáñez ME, Kotev M, García J, Teixidó M, Vila J, Pachón J, Giralt E, Smani Y. 2017. Combating virulence of Gram-negative bacilli by OmpA inhibition. Sci Rep 7:14683.

38. Legendre C, Reen FJ, Mooij MJ, McGlacken GP, Adams C, O'Gara F. 2012. *Pseudomonas aeruginosa* alkyl quinolones repress Hypoxia-Inducible Factor 1 (HIF-1) signaling through HIF-1α degradation. Infect Immun 80:3985-3992.
39. Legendre C, Reen FJ, Woods DF, Mooij MJ, Adams C, O'Gara F. 2014. Bile acids repress hypoxia-inducible factor 1 signaling and modulate the airway immune response. Infect Immun 82:3531-3541.
40. Meng X, Grötsch B, Luo Y, Knaup KX, Wiesener MS, Chen XX, Jantsch J, Fillatreau S, Schett G, Bozec A. 2018. Hypoxia-inducible factor-1α is a critical transcription factor for IL-10-producing B cells in autoimmune disease. Nat Commun 9:251.
41. Couper KN, Blount DG, Riley EM. 2008. IL-10: the master regulator of immunity to infection. J Immunol 180:5771-5777.
42. Harris AJ, Thompson AR, Whyte MK, Walmsley SR. 2014. HIF-mediated innate immune responses: cell signaling and therapeutic implications. Hypoxia (Auckl) 2:47-58.
43. Smani Y, Dominguez-Herrera J, Pachón J. 2013. Association of the outer membrane protein Omp33 with fitness and virulence of *Acinetobacter baumannii*. J Infect Dis 208:1561-1570.
44. Asikainen TM, Schneider BK, Waleh NS, Clyman RI, Ho WB, Flippin LA, Günzler V, White CW. 2005. Activation of hypoxia-inducible factors in hyperoxia through prolyl 4-hydroxylase blockade in cells and explants of primate lung. Proc Natl Acad Sci U S A 102:10212-7.
45. Smani Y, Docobo-Pérez F, López-Rojas R, Domínguez-Herrera J, Ibáñez-Martínez J, Pachón J. 2012. Platelet-activating factor receptor initiates contact of

Acinetobacter baumannii expressing phosphorylcholine with host cells. J Biol Chem 287:26901-26910.

46. National Research Council. 2011. Guide for the care and use of laboratory animals, 8th ed. National Academies Press, Washington, DC.
47. Rumbo C, Vallejo JA, Cabral MP, Martínez-Guitián M, Pérez A, Beceiro A, Bou G. 2016. Assessment of antivirulence activity of several d-amino acids against *Acinetobacter baumannii* and *Pseudomonas aeruginosa*. J Antimicrob Chemother. 71:3473-81.

SUPPLEMENTAL DATA

Table S1. Identification of the *A. baumannii* ATCC 17978 subexpressed proteins under hypoxia condition (1%O_2).

Accession	Description	Fold Change	Location
A3M753	Putative outer membrane protein OmpW OS=Acinetobacter baumannii (strain ATCC 17978 / CIP 53.77 / LMG 1025 / NCDC KC755 / 5377) GN=A1S_2325 PE=4 SV=2 - [A3M753_ACIBT]	0,38	Outer membrane
A3M6R9	DNA-binding protein OS=Acinetobacter baumannii (strain ATCC 17978 / CIP 53.77 / LMG 1025 / NCDC KC755 / 5377) GN=A1S_2186 PE=4 SV=1 - [A3M6R9_ACIBT]	0,39	Cytoplasm
A3M6Q5	30S ribosomal protein S18 OS=Acinetobacter baumannii (strain ATCC 17978 / CIP 53.77 / LMG 1025 / NCDC KC755 / 5377) GN=rpsR PE=3 SV=1 - [RS18_ACIBT]	0,44	Cytoplasm
A3M178	Uncharacterized protein OS=Acinetobacter baumannii (strain ATCC 17978 / CIP 53.77 / LMG 1025 / NCDC KC755 / 5377) GN=A1S_0191 PE=4 SV=2 - [A3M178_ACIBT]	0,45	Secreted
A7FBY7	Uncharacterized protein OS=Acinetobacter baumannii (strain ATCC 17978 / CIP 53.77 / LMG 1025 / NCDC KC755 / 5377) GN=A1S_3900 PE=4 SV=2 - [A7FBY7_ACIBT]	0,45	Secreted
A3M3Z7	Benzoate transporter OS=Acinetobacter baumannii (strain ATCC 17978 / CIP 53.77 / LMG 1025 / NCDC KC755 / 5377) GN=A1S_1211 PE=4 SV=2 - [A3M3Z7_ACIBT]	0,45	Inner membrane
A3M4R4	Putative membrane protein OS=Acinetobacter baumannii (strain ATCC 17978 / CIP 53.77 / LMG 1025 / NCDC KC755 / 5377) GN=A1S_1480 PE=4 SV=2 - [A3M4R4_ACIBT]	0,46	Inner membrane
A3M9Y4	Putative ferric siderophore receptor protein OS=Acinetobacter baumannii (strain ATCC 17978 / CIP 53.77 / LMG 1025 / NCDC KC755 / 5377) GN=A1S_3339 PE=3 SV=2 - [A3M9Y4_ACIBT]	0,46	Outer membrane
A3M6W6	Uncharacterized protein OS=Acinetobacter baumannii (strain ATCC 17978 / CIP 53.77 / LMG 1025 / NCDC KC755 / 5377) GN=A1S_2233 PE=4 SV=1 - [A3M6W6_ACIBT]	0,46	Cytoplasm
A7FBL2	Uncharacterized protein OS=Acinetobacter baumannii (strain ATCC 17978 / CIP 53.77 / LMG 1025 / NCDC KC755 / 5377) GN=A1S_3775 PE=4 SV=2 - [A7FBL2_ACIBT]	0,47	Cytoplasm
A3M745	Putative lipoprotein (RlpA-like) OS=Acinetobacter baumannii (strain ATCC 17978 / CIP 53.77 / LMG 1025 / NCDC KC755 / 5377) GN=A1S_2317 PE=3 SV=2 - [A3M745_ACIBT]	0,47	Secreted
A7FBU1	Uncharacterized protein OS=Acinetobacter baumannii (strain ATCC 17978 / CIP 53.77 / LMG 1025 / NCDC KC755 / 5377) GN=A1S_3854 PE=4 SV=2 - [A7FBU1_ACIBT]	0,49	Inner membrane
A7FAY0	Uncharacterized protein OS=Acinetobacter baumannii (strain ATCC 17978 / CIP 53.77 / LMG 1025 / NCDC KC755 / 5377) GN=A1S_3543 PE=4 SV=2 - [A7FAY0_ACIBT]	0,49	Inner membrane
A3M9A7	Putative ATP-dependent RNA helicase OS=Acinetobacter	0,49	Cytoplasm

	baumannii (strain ATCC 17978 / CIP 53.77 / LMG 1025 / NCDC KC755 / 5377) GN=A1S_3104 PE=3 SV=1 - [A3M9A7_ACIBT]		
A3M4B3	FAD-dependent pyridine nucleotide-disulphide oxidoreductase OS=Acinetobacter baumannii (strain ATCC 17978 / CIP 53.77 / LMG 1025 / NCDC KC755 / 5377) GN=A1S_1329 PE=4 SV=1 - [A3M4B3_ACIBT]	0,49	Cytoplasm
A7FAV9	Uncharacterized protein OS=Acinetobacter baumannii (strain ATCC 17978 / CIP 53.77 / LMG 1025 / NCDC KC755 / 5377) GN=A1S_3522 PE=4 SV=2 - [A7FAV9_ACIBT]	0,49	Secreted
A3M2E7	Uncharacterized protein OS=Acinetobacter baumannii (strain ATCC 17978 / CIP 53.77 / LMG 1025 / NCDC KC755 / 5377) GN=A1S_0642 PE=4 SV=2 - [A3M2E7_ACIBT]	0,49	Cytoplasm
A3M9R3	Uncharacterized protein OS=Acinetobacter baumannii (strain ATCC 17978 / CIP 53.77 / LMG 1025 / NCDC KC755 / 5377) GN=A1S_3268 PE=4 SV=2 - [A3M9R3_ACIBT]	0,50	Secreted
A3M5K5	Putative MFS family drug transporter OS=Acinetobacter baumannii (strain ATCC 17978 / CIP 53.77 / LMG 1025 / NCDC KC755 / 5377) GN=A1S_1772 PE=4 SV=2 - [A3M5K5_ACIBT]	0,51	Inner membrane
A3M4T1	Putative acyltransferase OS=Acinetobacter baumannii (strain ATCC 17978 / CIP 53.77 / LMG 1025 / NCDC KC755 / 5377) GN=A1S_1497 PE=4 SV=2 - [A3M4T1_ACIBT]	0,51	Cytoplasm
A3M5H9	Putative transcriptional regulator OS=Acinetobacter baumannii (strain ATCC 17978 / CIP 53.77 / LMG 1025 / NCDC KC755 / 5377) GN=A1S_1746 PE=4 SV=2 - [A3M5H9_ACIBT]	0,51	Cytoplasm
A3M2X6	Putative signal peptide OS=Acinetobacter baumannii (strain ATCC 17978 / CIP 53.77 / LMG 1025 / NCDC KC755 / 5377) GN=A1S_0836 PE=4 SV=1 - [A3M2X6_ACIBT]	0,51	Cytoplasm
A3M268	Putative NAD(P)-binding enzyme OS=Acinetobacter baumannii (strain ATCC 17978 / CIP 53.77 / LMG 1025 / NCDC KC755 / 5377) GN=A1S_0559 PE=4 SV=2 - [A3M268_ACIBT]	0,52	Inner membrane
A3M1Y5	Putative ferric siderophore receptor protein OS=Acinetobacter baumannii (strain ATCC 17978 / CIP 53.77 / LMG 1025 / NCDC KC755 / 5377) GN=A1S_0474 PE=3 SV=1 - [A3M1Y5_ACIBT]	0,52	Outer membrane
A3M2F0	Uncharacterized protein OS=Acinetobacter baumannii (strain ATCC 17978 / CIP 53.77 / LMG 1025 / NCDC KC755 / 5377) GN=A1S_0645 PE=4 SV=2 - [A3M2F0_ACIBT]	0,52	Secreted
A3M140	ATP synthase subunit b OS=Acinetobacter baumannii (strain ATCC 17978 / CIP 53.77 / LMG 1025 / NCDC KC755 / 5377) GN=atpF PE=3 SV=2 - [ATPF_ACIBT]	0,52	Inner membrane
A3M3P2	Uncharacterized protein OS=Acinetobacter baumannii (strain ATCC 17978 / CIP 53.77 / LMG 1025 / NCDC KC755 / 5377) GN=A1S_1106 PE=4 SV=1 - [A3M3P2_ACIBT]	0,52	Secreted
A3M3U3	Uncharacterized protein OS=Acinetobacter baumannii (strain ATCC 17978 / CIP 53.77 / LMG 1025 / NCDC KC755 / 5377) GN=A1S_1157 PE=4 SV=2 - [A3M3U3_ACIBT]	0,52	Cytoplasm
A3M3E9	Urease accessory protein UreD OS=Acinetobacter baumannii (strain ATCC 17978 / CIP 53.77 / LMG 1025 /	0,52	Cytoplasm

	NCDC KC755 / 5377) GN=ureD PE=3 SV=2 - [URED_ACIBT]		
A3M146	Uncharacterized protein OS=Acinetobacter baumannii (strain ATCC 17978 / CIP 53.77 / LMG 1025 / NCDC KC755 / 5377) GN=A1S_0157 PE=4 SV=2 - [A3M146_ACIBT]	0,52	Periplasm
A3M5D5	Dihydrolipoamide dehydrogenase OS=Acinetobacter baumannii (strain ATCC 17978 / CIP 53.77 / LMG 1025 / NCDC KC755 / 5377) GN=A1S_1702 PE=4 SV=1 - [A3M5D5_ACIBT]	0,54	Cytoplasm
A3M976	50S ribosomal protein L29 OS=Acinetobacter baumannii (strain ATCC 17978 / CIP 53.77 / LMG 1025 / NCDC KC755 / 5377) GN=rpmC PE=3 SV=1 - [RL29_ACIBT]	0,54	Cytoplasm
A3M615	Uncharacterized protein OS=Acinetobacter baumannii (strain ATCC 17978 / CIP 53.77 / LMG 1025 / NCDC KC755 / 5377) GN=A1S_1932 PE=4 SV=1 - [A3M615_ACIBT]	0,54	Inner membrane
A3M4U6	Putative membrane protein OS=Acinetobacter baumannii (strain ATCC 17978 / CIP 53.77 / LMG 1025 / NCDC KC755 / 5377) GN=A1S_1513 PE=3 SV=2 - [A3M4U6_ACIBT]	0,55	Cytoplasm
A3M1W4	Putative biopolymer transport protein (ExbB) OS=Acinetobacter baumannii (strain ATCC 17978 / CIP 53.77 / LMG 1025 / NCDC KC755 / 5377) GN=A1S_0453 PE=3 SV=2 - [A3M1W4_ACIBT]	0,56	Inner membrane
A3M2C9	Putative lipoprotein OS=Acinetobacter baumannii (strain ATCC 17978 / CIP 53.77 / LMG 1025 / NCDC KC755 / 5377) GN=A1S_0624 PE=3 SV=2 - [A3M2C9_ACIBT]	0,56	Periplasm
A3M3B9	Ferric enterobactin receptor OS=Acinetobacter baumannii (strain ATCC 17978 / CIP 53.77 / LMG 1025 / NCDC KC755 / 5377) GN=A1S_0981 PE=3 SV=1 - [A3M3B9_ACIBT]	0,57	Outer membrane
A3M7D6	Oxidoreductase short-chain dehydrogenase/reductase family OS=Acinetobacter baumannii (strain ATCC 17978 / CIP 53.77 / LMG 1025 / NCDC KC755 / 5377) GN=A1S_2411 PE=4 SV=2 - [A3M7D6_ACIBT]	0,57	Cytoplasm
A3M472	Putative VGR-related protein OS=Acinetobacter baumannii (strain ATCC 17978 / CIP 53.77 / LMG 1025 / NCDC KC755 / 5377) GN=A1S_1288 PE=4 SV=1 - [A3M472_ACIBT]	0,58	Cytoplasm
A3M604	Ferrichrome-iron receptor OS=Acinetobacter baumannii (strain ATCC 17978 / CIP 53.77 / LMG 1025 / NCDC KC755 / 5377) GN=A1S_1921 PE=3 SV=2 - [A3M604_ACIBT]	0,58	Outer membrane
A3M3V8	Putative transposase OS=Acinetobacter baumannii (strain ATCC 17978 / CIP 53.77 / LMG 1025 / NCDC KC755 / 5377) GN=A1S_1172 PE=4 SV=2 - [A3M3V8_ACIBT]	0,58	Cytoplasm
A3M9R8	Putative peptide signal OS=Acinetobacter baumannii (strain ATCC 17978 / CIP 53.77 / LMG 1025 / NCDC KC755 / 5377) GN=A1S_3273 PE=4 SV=1 - [A3M9R8_ACIBT]	0,58	Secreted
A3M3R8	Oxidoreductase short chain dehydrogenase/reductase family OS=Acinetobacter baumannii (strain ATCC 17978 / CIP 53.77 / LMG 1025 / NCDC KC755 / 5377) GN=A1S_1132 PE=3 SV=2 - [A3M3R8_ACIBT]	0,59	Cytoplasm
A3M2V3	ATP-dependent dethiobiotin synthetase BioD OS=Acinetobacter baumannii (strain ATCC 17978 / CIP 53.77 / LMG 1025 / NCDC KC755 / 5377) GN=bioD PE=3 SV=2 - [A3M2V3_ACIBT]	0,59	Cytoplasm
A7FAX8	Uncharacterized protein OS=Acinetobacter baumannii	0,59	Cytoplasm

	(strain ATCC 17978 / CIP 53.77 / LMG 1025 / NCDC KC755 / 5377) GN=A1S_3541 PE=4 SV=2 - [A7FAX8_ACIBT]		
A3M5R8	Aldehyde dehydrogenase OS=Acinetobacter baumannii (strain ATCC 17978 / CIP 53.77 / LMG 1025 / NCDC KC755 / 5377) GN=A1S_1835 PE=4 SV=2 - [A3M5R8_ACIBT]	0,60	Cytoplasm
A3M2E9	Uncharacterized protein OS=Acinetobacter baumannii (strain ATCC 17978 / CIP 53.77 / LMG 1025 / NCDC KC755 / 5377) GN=A1S_0644 PE=4 SV=2 - [A3M2E9_ACIBT]	0,60	Mitochondrion
A3M1E1	Alginate biosynthesis protein OS=Acinetobacter baumannii (strain ATCC 17978 / CIP 53.77 / LMG 1025 / NCDC KC755 / 5377) GN=A1S_0260 PE=4 SV=2 - [A3M1E1_ACIBT]	0,60	Inner membrane
A7FAX2	Uncharacterized protein OS=Acinetobacter baumannii (strain ATCC 17978 / CIP 53.77 / LMG 1025 / NCDC KC755 / 5377) GN=A1S_3535 PE=4 SV=2 - [A7FAX2_ACIBT]	0,60	Periplasm
A3M6C3	Putative phage integrase OS=Acinetobacter baumannii (strain ATCC 17978 / CIP 53.77 / LMG 1025 / NCDC KC755 / 5377) GN=A1S_2040 PE=4 SV=2 - [A3M6C3_ACIBT]	0,60	Mitochondrion
A7FB06	Uncharacterized protein OS=Acinetobacter baumannii (strain ATCC 17978 / CIP 53.77 / LMG 1025 / NCDC KC755 / 5377) GN=A1S_3569 PE=4 SV=2 - [A7FB06_ACIBT]	0,60	Cytoplasm

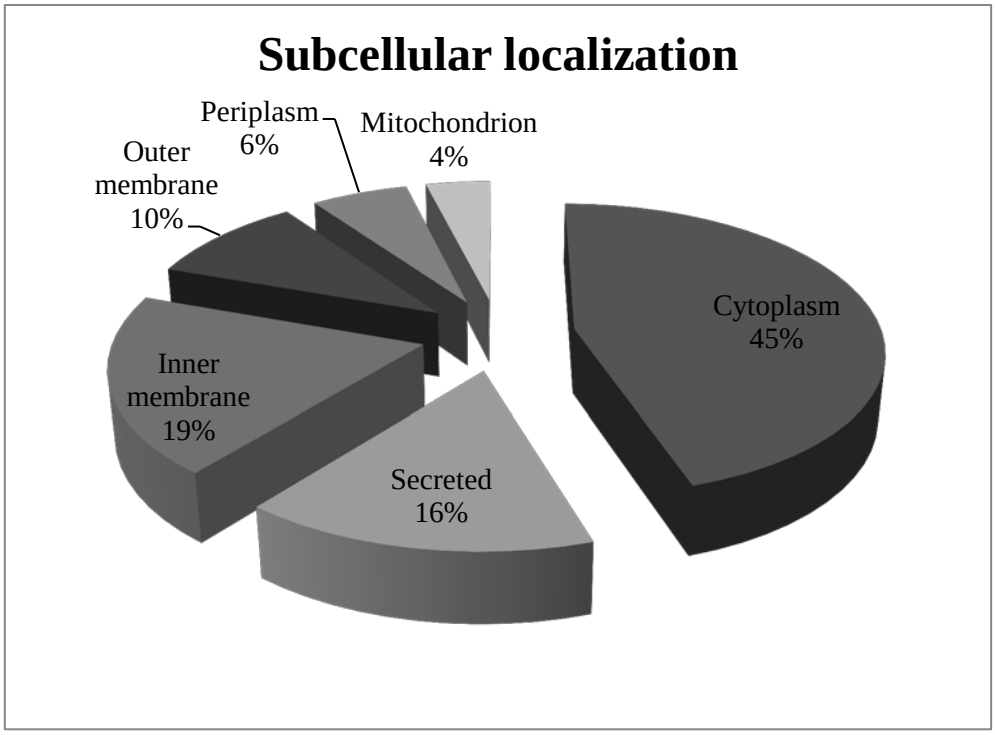

Figure S1. Subcellular localization of subexpressed proteins under hypoxia (1%O_2).

ADDITIONAL DATA

Table A1. Identification of the *A. baumannii* ATCC 17978 overexpressed proteins under hypoxia condition (1%O_2).

Accession	Description	Fold Change
A3M7U7	23-dihydroxybenzoate-AMP ligase OS=Acinetobacter baumannii (strain ATCC 17978 / CIP 53.77 / LMG 1025 / NCDC KC755 / 5377) GN=A1S_2574 PE=4 SV=2 - [A3M7U7_ACIBT]	1,49
A3M1P4	Uncharacterized protein OS=Acinetobacter baumannii (strain ATCC 17978 / CIP 53.77 / LMG 1025 / NCDC KC755 / 5377) GN=A1S_0379 PE=4 SV=2 - [A3M1P4_ACIBT]	1,49
A3M6H4	Putative exported protein OS=Acinetobacter baumannii (strain ATCC 17978 / CIP 53.77 / LMG 1025 / NCDC KC755 / 5377) GN=A1S_2091 PE=4 SV=2 - [A3M6H4_ACIBT]	1,49
A3M4I6	Putative amino acid efflux transmembrane protein OS=Acinetobacter baumannii (strain ATCC 17978 / CIP 53.77 / LMG 1025 / NCDC KC755 / 5377) GN=A1S_1402 PE=4 SV=2 - [A3M4I6_ACIBT]	1,49
A3M4F4	Oxidoreductase OS=Acinetobacter baumannii (strain ATCC 17978 / CIP 53.77 / LMG 1025 / NCDC KC755 / 5377) GN=A1S_1370 PE=4 SV=1 - [A3M4F4_ACIBT]	1,49
A3M7E7	50S ribosomal protein L31 OS=Acinetobacter baumannii (strain ATCC 17978 / CIP 53.77 / LMG 1025 / NCDC KC755 / 5377) GN=rpmE PE=3 SV=1 - [RL31_ACIBT]	1,49
A3M5N6	Uncharacterized protein OS=Acinetobacter baumannii (strain ATCC 17978 / CIP 53.77 / LMG 1025 / NCDC KC755 / 5377) GN=A1S_1803 PE=4 SV=2 - [A3M5N6_ACIBT]	1,49
A3M194	Uncharacterized protein OS=Acinetobacter baumannii (strain ATCC 17978 / CIP 53.77 / LMG 1025 / NCDC KC755 / 5377) GN=A1S_0212 PE=4 SV=2 - [A3M194_ACIBT]	1,50
A3M6J0	Putative glutamine amidotransferase OS=Acinetobacter baumannii (strain ATCC 17978 / CIP 53.77 / LMG 1025 / NCDC KC755 / 5377) GN=A1S_2107 PE=4 SV=2 - [A3M6J0_ACIBT]	1,50
A3M700	RNA-splicing ligase RtcB OS=Acinetobacter baumannii (strain ATCC 17978 / CIP 53.77 / LMG 1025 / NCDC KC755 / 5377) GN=rtcB PE=3 SV=2 - [A3M700_ACIBT]	1,50
A3M6X5	Uncharacterized protein OS=Acinetobacter baumannii (strain ATCC 17978 / CIP 53.77 / LMG 1025 / NCDC KC755 / 5377) GN=A1S_2246 PE=4 SV=2 - [A3M6X5_ACIBT]	1,50
A3M343	Putative D-amino acid oxidase OS=Acinetobacter baumannii (strain ATCC 17978 / CIP 53.77 / LMG 1025 / NCDC KC755 / 5377) GN=A1S_0905 PE=4 SV=2 - [A3M343_ACIBT]	1,51
A3M6Q0	Cytochrome o ubiquinol oxidase subunit I OS=Acinetobacter baumannii (strain ATCC 17978 / CIP 53.77 / LMG 1025 / NCDC KC755 / 5377) GN=A1S_2167 PE=3 SV=2 - [A3M6Q0_ACIBT]	1,51
A3M5Z0	Putative peroxidase OS=Acinetobacter baumannii (strain ATCC 17978 / CIP 53.77 / LMG 1025 / NCDC KC755 / 5377) GN=A1S_1907 PE=4 SV=2 - [A3M5Z0_ACIBT]	1,51
A3M4R7	Methionine import ATP-binding protein MetN OS=Acinetobacter baumannii (strain ATCC 17978 / CIP 53.77 / LMG 1025 / NCDC KC755 / 5377) GN=metN PE=3 SV=2 - [A3M4R7_ACIBT]	1,51
A3M9I0	Fimbrial protein OS=Acinetobacter baumannii (strain ATCC 17978 / CIP 53.77 / LMG 1025 / NCDC KC755 / 5377) GN=A1S_3177 PE=3 SV=1 - [A3M9I0_ACIBT]	1,52
A3M185	Putative signal peptide OS=Acinetobacter baumannii (strain ATCC 17978 / CIP 53.77 / LMG 1025 / NCDC KC755 / 5377) GN=A1S_0202 PE=4 SV=2	1,52

	- [A3M185_ACIBT]	
A3M7C9	Uncharacterized protein OS=Acinetobacter baumannii (strain ATCC 17978 / CIP 53.77 / LMG 1025 / NCDC KC755 / 5377) GN=A1S_2404 PE=4 SV=2 - [A3M7C9_ACIBT]	1,53
A3M8V7	Uncharacterized protein OS=Acinetobacter baumannii (strain ATCC 17978 / CIP 53.77 / LMG 1025 / NCDC KC755 / 5377) GN=A1S_2946 PE=4 SV=2 - [A3M8V7_ACIBT]	1,54
A3M7Y3	Competence factor involved in DNA uptake OS=Acinetobacter baumannii (strain ATCC 17978 / CIP 53.77 / LMG 1025 / NCDC KC755 / 5377) GN=A1S_2610 PE=4 SV=2 - [A3M7Y3_ACIBT]	1,54
A7FBB0	Uncharacterized protein OS=Acinetobacter baumannii (strain ATCC 17978 / CIP 53.77 / LMG 1025 / NCDC KC755 / 5377) GN=A1S_3673 PE=4 SV=1 - [A7FBB0_ACIBT]	1,54
A3M308	Putative metal-dependent hydrolase OS=Acinetobacter baumannii (strain ATCC 17978 / CIP 53.77 / LMG 1025 / NCDC KC755 / 5377) GN=A1S_0870 PE=4 SV=2 - [A3M308_ACIBT]	1,54
A3M4Z2	Type 4 fimbrial biogenesis protein OS=Acinetobacter baumannii (strain ATCC 17978 / CIP 53.77 / LMG 1025 / NCDC KC755 / 5377) GN=A1S_1559 PE=4 SV=2 - [A3M4Z2_ACIBT]	1,54
A3M2S3	Putative threonine efflux protein (RhtC) OS=Acinetobacter baumannii (strain ATCC 17978 / CIP 53.77 / LMG 1025 / NCDC KC755 / 5377) GN=A1S_0777 PE=4 SV=2 - [A3M2S3_ACIBT]	1,54
A3M1A1	Transcriptional repressor NrdR OS=Acinetobacter baumannii (strain ATCC 17978 / CIP 53.77 / LMG 1025 / NCDC KC755 / 5377) GN=nrdR PE=3 SV=2 - [NRDR_ACIBT]	1,55
A3M5P7	Putative transporter OS=Acinetobacter baumannii (strain ATCC 17978 / CIP 53.77 / LMG 1025 / NCDC KC755 / 5377) GN=A1S_1814 PE=4 SV=2 - [A3M5P7_ACIBT]	1,55
A3M731	ABC Lysine-arginine-ornithine transporter periplasmic ligand binding protein OS=Acinetobacter baumannii (strain ATCC 17978 / CIP 53.77 / LMG 1025 / NCDC KC755 / 5377) GN=A1S_2302 PE=3 SV=2 - [A3M731_ACIBT]	1,55
A3M1E7	Putative membrane protein OS=Acinetobacter baumannii (strain ATCC 17978 / CIP 53.77 / LMG 1025 / NCDC KC755 / 5377) GN=A1S_0266 PE=4 SV=2 - [A3M1E7_ACIBT]	1,55
A3M3A6	Putative phthalate transporter OS=Acinetobacter baumannii (strain ATCC 17978 / CIP 53.77 / LMG 1025 / NCDC KC755 / 5377) GN=A1S_0968 PE=4 SV=2 - [A3M3A6_ACIBT]	1,56
A3M175	Putative transport protein (MFS superfamily) OS=Acinetobacter baumannii (strain ATCC 17978 / CIP 53.77 / LMG 1025 / NCDC KC755 / 5377) GN=A1S_0188 PE=4 SV=2 - [A3M175_ACIBT]	1,56
A3M426	Putative ABC family drug transporter OS=Acinetobacter baumannii (strain ATCC 17978 / CIP 53.77 / LMG 1025 / NCDC KC755 / 5377) GN=A1S_1242 PE=4 SV=2 - [A3M426_ACIBT]	1,56
A3M1I3	Putative acyl-CoA thioesterase II OS=Acinetobacter baumannii (strain ATCC 17978 / CIP 53.77 / LMG 1025 / NCDC KC755 / 5377) GN=A1S_0311 PE=4 SV=2 - [A3M1I3_ACIBT]	1,57
A3M3E0	Uncharacterized protein OS=Acinetobacter baumannii (strain ATCC 17978 / CIP 53.77 / LMG 1025 / NCDC KC755 / 5377) GN=A1S_1002 PE=4 SV=1 - [A3M3E0_ACIBT]	1,57
A3M2Y3	Putative flavodoxin or tryptophan repressor binding protein OS=Acinetobacter baumannii (strain ATCC 17978 / CIP 53.77 / LMG 1025 / NCDC KC755 / 5377) GN=A1S_0843 PE=4 SV=2 - [A3M2Y3_ACIBT]	1,57
A3M1X9	Non-canonical purine NTP pyrophosphatase OS=Acinetobacter baumannii (strain ATCC 17978 / CIP 53.77 / LMG 1025 / NCDC KC755 / 5377) GN=A1S_0468 PE=3 SV=2 - [NTPA_ACIBT]	1,57
A3M2V2	Malonyl-[acyl-carrier protein] O-methyltransferase OS=Acinetobacter baumannii (strain ATCC 17978 / CIP 53.77 / LMG 1025 / NCDC KC755 / 5377) GN=bioC PE=3 SV=2 - [A3M2V2_ACIBT]	1,57
A3M3N7	Probable 5-dehydro-4-deoxyglucarate dehydratase OS=Acinetobacter	1,58

	baumannii (strain ATCC 17978 / CIP 53.77 / LMG 1025 / NCDC KC755 / 5377) GN=A1S_1101 PE=3 SV=2 - [KDGD_ACIBT]	
A3M9S0	Putative methyltransferase OS=Acinetobacter baumannii (strain ATCC 17978 / CIP 53.77 / LMG 1025 / NCDC KC755 / 5377) GN=A1S_3275 PE=4 SV=2 - [A3M9S0_ACIBT]	1,58
A3M169	Uncharacterized protein OS=Acinetobacter baumannii (strain ATCC 17978 / CIP 53.77 / LMG 1025 / NCDC KC755 / 5377) GN=A1S_0182 PE=4 SV=2 - [A3M169_ACIBT]	1,59
A3M4R9	D-methionine transport protein OS=Acinetobacter baumannii (strain ATCC 17978 / CIP 53.77 / LMG 1025 / NCDC KC755 / 5377) GN=A1S_1485 PE=4 SV=2 - [A3M4R9_ACIBT]	1,59
A3M590	Putative siderophore biosynthesis protein putative acetyltransferase OS=Acinetobacter baumannii (strain ATCC 17978 / CIP 53.77 / LMG 1025 / NCDC KC755 / 5377) GN=A1S_1657 PE=4 SV=2 - [A3M590_ACIBT]	1,60
A3M4M0	Putative acyl-CoA dehydrogenase OS=Acinetobacter baumannii (strain ATCC 17978 / CIP 53.77 / LMG 1025 / NCDC KC755 / 5377) GN=A1S_1436 PE=4 SV=1 - [A3M4M0_ACIBT]	1,60
A3M998	ATP-dependent DNA helicase RecG OS=Acinetobacter baumannii (strain ATCC 17978 / CIP 53.77 / LMG 1025 / NCDC KC755 / 5377) GN=recG PE=3 SV=2 - [A3M998_ACIBT]	1,61
A3M5R5	Oxidoreductase FMN-binding OS=Acinetobacter baumannii (strain ATCC 17978 / CIP 53.77 / LMG 1025 / NCDC KC755 / 5377) GN=A1S_1832 PE=4 SV=2 - [A3M5R5_ACIBT]	1,61
A3M8U2	Uncharacterized protein OS=Acinetobacter baumannii (strain ATCC 17978 / CIP 53.77 / LMG 1025 / NCDC KC755 / 5377) GN=A1S_2931 PE=4 SV=2 - [A3M8U2_ACIBT]	1,61
A3M3L8	Uncharacterized protein OS=Acinetobacter baumannii (strain ATCC 17978 / CIP 53.77 / LMG 1025 / NCDC KC755 / 5377) GN=A1S_1082 PE=4 SV=1 - [A3M3L8_ACIBT]	1,62
A3M684	Molybdenum cofactor guanylyltransferase OS=Acinetobacter baumannii (strain ATCC 17978 / CIP 53.77 / LMG 1025 / NCDC KC755 / 5377) GN=mobA PE=3 SV=2 - [MOBA_ACIBT]	1,62
A3M445	Putative 3-hydroxyacyl-CoA dehydrogenase OS=Acinetobacter baumannii (strain ATCC 17978 / CIP 53.77 / LMG 1025 / NCDC KC755 / 5377) GN=A1S_1261 PE=4 SV=2 - [A3M445_ACIBT]	1,63
A3M5D4	Dihydrolipoamide acetyltransferase OS=Acinetobacter baumannii (strain ATCC 17978 / CIP 53.77 / LMG 1025 / NCDC KC755 / 5377) GN=A1S_1701 PE=3 SV=1 - [A3M5D4_ACIBT]	1,63
A3M5K3	Uncharacterized protein OS=Acinetobacter baumannii (strain ATCC 17978 / CIP 53.77 / LMG 1025 / NCDC KC755 / 5377) GN=A1S_1770 PE=4 SV=2 - [A3M5K3_ACIBT]	1,63
A3M3E7	Putative lipoprotein OS=Acinetobacter baumannii (strain ATCC 17978 / CIP 53.77 / LMG 1025 / NCDC KC755 / 5377) GN=A1S_1009 PE=4 SV=2 - [A3M3E7_ACIBT]	1,64
A3M5M6	Transcriptional regulator LysR family OS=Acinetobacter baumannii (strain ATCC 17978 / CIP 53.77 / LMG 1025 / NCDC KC755 / 5377) GN=A1S_1793 PE=4 SV=2 - [A3M5M6_ACIBT]	1,64
A3M2N6	Putative phage related protein OS=Acinetobacter baumannii (strain ATCC 17978 / CIP 53.77 / LMG 1025 / NCDC KC755 / 5377) GN=A1S_0740 PE=4 SV=2 - [A3M2N6_ACIBT]	1,64
A3M255	Putative membrane protein OS=Acinetobacter baumannii (strain ATCC 17978 / CIP 53.77 / LMG 1025 / NCDC KC755 / 5377) GN=A1S_0546 PE=4 SV=2 - [A3M255_ACIBT]	1,64
A3M2G3	Transposase OS=Acinetobacter baumannii (strain ATCC 17978 / CIP 53.77 / LMG 1025 / NCDC KC755 / 5377) GN=A1S_0658 PE=4 SV=2 - [A3M2G3_ACIBT]	1,64
A7FBX4	Uncharacterized protein OS=Acinetobacter baumannii (strain ATCC 17978 / CIP 53.77 / LMG 1025 / NCDC KC755 / 5377) GN=A1S_3887 PE=4 SV=1 - [A7FBX4_ACIBT]	1,65
A3M9L6	Putative RND family drug transporter OS=Acinetobacter baumannii (strain	1,66

	ATCC 17978 / CIP 53.77 / LMG 1025 / NCDC KC755 / 5377) GN=A1S_3219 PE=4 SV=2 - [A3M9L6_ACIBT]	
A3M5U7	Acyl-CoA dehydrogenase-like protein OS=Acinetobacter baumannii (strain ATCC 17978 / CIP 53.77 / LMG 1025 / NCDC KC755 / 5377) GN=A1S_1864 PE=4 SV=2 - [A3M5U7_ACIBT]	1,66
A3M5A0	Putative ferric hydroxamate siderophore receptor OS=Acinetobacter baumannii (strain ATCC 17978 / CIP 53.77 / LMG 1025 / NCDC KC755 / 5377) GN=A1S_1667 PE=3 SV=2 - [A3M5A0_ACIBT]	1,68
A3M6X9	Putative membrane protein OS=Acinetobacter baumannii (strain ATCC 17978 / CIP 53.77 / LMG 1025 / NCDC KC755 / 5377) GN=A1S_2250 PE=4 SV=2 - [A3M6X9_ACIBT]	1,69
A3M8R5	Uncharacterized protein OS=Acinetobacter baumannii (strain ATCC 17978 / CIP 53.77 / LMG 1025 / NCDC KC755 / 5377) GN=A1S_2903 PE=4 SV=2 - [A3M8R5_ACIBT]	1,69
A3M8Y0	Putative vanillate O-demethylase oxygenase subunit OS=Acinetobacter baumannii (strain ATCC 17978 / CIP 53.77 / LMG 1025 / NCDC KC755 / 5377) GN=A1S_2971 PE=4 SV=2 - [A3M8Y0_ACIBT]	1,70
A3M5F8	Putative ferric siderophore receptor protein OS=Acinetobacter baumannii (strain ATCC 17978 / CIP 53.77 / LMG 1025 / NCDC KC755 / 5377) GN=A1S_1725 PE=3 SV=2 - [A3M5F8_ACIBT]	1,70
A3M2R7	Putative membrane protein OS=Acinetobacter baumannii (strain ATCC 17978 / CIP 53.77 / LMG 1025 / NCDC KC755 / 5377) GN=A1S_0771 PE=4 SV=2 - [A3M2R7_ACIBT]	1,70
A3M944	Putative membrane protein OS=Acinetobacter baumannii (strain ATCC 17978 / CIP 53.77 / LMG 1025 / NCDC KC755 / 5377) GN=A1S_3041 PE=4 SV=2 - [A3M944_ACIBT]	1,71
A3M3M5	Uncharacterized protein OS=Acinetobacter baumannii (strain ATCC 17978 / CIP 53.77 / LMG 1025 / NCDC KC755 / 5377) GN=A1S_1089 PE=3 SV=2 - [A3M3M5_ACIBT]	1,72
A3M5Y0	Uncharacterized protein OS=Acinetobacter baumannii (strain ATCC 17978 / CIP 53.77 / LMG 1025 / NCDC KC755 / 5377) GN=A1S_1897 PE=4 SV=2 - [A3M5Y0_ACIBT]	1,72
A3M4F1	Uncharacterized protein OS=Acinetobacter baumannii (strain ATCC 17978 / CIP 53.77 / LMG 1025 / NCDC KC755 / 5377) GN=A1S_1367 PE=4 SV=2 - [A3M4F1_ACIBT]	1,73
A3M9G3	Lipase OS=Acinetobacter baumannii (strain ATCC 17978 / CIP 53.77 / LMG 1025 / NCDC KC755 / 5377) GN=A1S_3160 PE=4 SV=2 - [A3M9G3_ACIBT]	1,74
A3M5N0	Aldehyde dehydrogenase OS=Acinetobacter baumannii (strain ATCC 17978 / CIP 53.77 / LMG 1025 / NCDC KC755 / 5377) GN=A1S_1797 PE=4 SV=1 - [A3M5N0_ACIBT]	1,74
A3M236	Putative holo-(Acyl carrier protein) synthase 2 OS=Acinetobacter baumannii (strain ATCC 17978 / CIP 53.77 / LMG 1025 / NCDC KC755 / 5377) GN=A1S_0527 PE=4 SV=2 - [A3M236_ACIBT]	1,74
A3MA44	VirP protein OS=Acinetobacter baumannii (strain ATCC 17978 / CIP 53.77 / LMG 1025 / NCDC KC755 / 5377) GN=A1S_3399 PE=4 SV=2 - [A3MA44_ACIBT]	1,75
A3M1N5	General secretion pathway protein F OS=Acinetobacter baumannii (strain ATCC 17978 / CIP 53.77 / LMG 1025 / NCDC KC755 / 5377) GN=A1S_0369 PE=3 SV=2 - [A3M1N5_ACIBT]	1,75
A7FB98	Uncharacterized protein OS=Acinetobacter baumannii (strain ATCC 17978 / CIP 53.77 / LMG 1025 / NCDC KC755 / 5377) GN=A1S_3661 PE=4 SV=1 - [A7FB98_ACIBT]	1,77
A3M3L5	Dichlorophenol hydroxylase OS=Acinetobacter baumannii (strain ATCC 17978 / CIP 53.77 / LMG 1025 / NCDC KC755 / 5377) GN=A1S_1079 PE=4 SV=2 - [A3M3L5_ACIBT]	1,77
A3M0R6	Anhydro-N-acetylmuramic acid kinase OS=Acinetobacter baumannii (strain ATCC 17978 / CIP 53.77 / LMG 1025 / NCDC KC755 / 5377) GN=anmK PE=3 SV=2 - [A3M0R6_ACIBT]	1,78
A7FBY9	Uncharacterized protein OS=Acinetobacter baumannii (strain ATCC 17978 /	1,81

	CIP 53.77 / LMG 1025 / NCDC KC755 / 5377) GN=A1S_3902 PE=4 SV=2 - [A7FBY9_ACIBT]	
A3M6J9	Uncharacterized protein OS=Acinetobacter baumannii (strain ATCC 17978 / CIP 53.77 / LMG 1025 / NCDC KC755 / 5377) GN=A1S_2116 PE=4 SV=1 - [A3M6J9_ACIBT]	1,82
A3M5B9	Ribonuclease D OS=Acinetobacter baumannii (strain ATCC 17978 / CIP 53.77 / LMG 1025 / NCDC KC755 / 5377) GN=A1S_1686 PE=4 SV=2 - [A3M5B9_ACIBT]	1,83
A3M0Z5	Putative transcriptional regulator (LysR family) OS=Acinetobacter baumannii (strain ATCC 17978 / CIP 53.77 / LMG 1025 / NCDC KC755 / 5377) GN=A1S_0100 PE=4 SV=1 - [A3M0Z5_ACIBT]	1,83
A3M754	Putative nitrate transporter transmembrane protein (MFS superfamily) OS=Acinetobacter baumannii (strain ATCC 17978 / CIP 53.77 / LMG 1025 / NCDC KC755 / 5377) GN=A1S_2326 PE=4 SV=2 - [A3M754_ACIBT]	1,83
A3M7B7	Putative acinetobactin utilization protein OS=Acinetobacter baumannii (strain ATCC 17978 / CIP 53.77 / LMG 1025 / NCDC KC755 / 5377) GN=A1S_2392 PE=4 SV=2 - [A3M7B7_ACIBT]	1,84
A3M6K4	UPF0756 membrane protein A1S_2121 OS=Acinetobacter baumannii (strain ATCC 17978 / CIP 53.77 / LMG 1025 / NCDC KC755 / 5377) GN=A1S_2121 PE=3 SV=2 - [Y2121_ACIBT]	1,86
A3M910	Stringent starvation protein B OS=Acinetobacter baumannii (strain ATCC 17978 / CIP 53.77 / LMG 1025 / NCDC KC755 / 5377) GN=A1S_3003 PE=4 SV=2 - [A3M910_ACIBT]	1,86
A3M7V7	MFS family drug transporter OS=Acinetobacter baumannii (strain ATCC 17978 / CIP 53.77 / LMG 1025 / NCDC KC755 / 5377) GN=A1S_2584 PE=4 SV=2 - [A3M7V7_ACIBT]	1,86
A3M3A1	Putative transcriptional regulator (AraC family) OS=Acinetobacter baumannii (strain ATCC 17978 / CIP 53.77 / LMG 1025 / NCDC KC755 / 5377) GN=A1S_0963 PE=4 SV=2 - [A3M3A1_ACIBT]	1,86
A3M539	Uncharacterized protein OS=Acinetobacter baumannii (strain ATCC 17978 / CIP 53.77 / LMG 1025 / NCDC KC755 / 5377) GN=A1S_1606 PE=4 SV=1 - [A3M539_ACIBT]	1,89
A3M833	Glycerophosphoryl diester phosphodiesterase OS=Acinetobacter baumannii (strain ATCC 17978 / CIP 53.77 / LMG 1025 / NCDC KC755 / 5377) GN=A1S_2661 PE=4 SV=2 - [A3M833_ACIBT]	1,89
A3M7T9	Putative ferric siderophore receptor protein OS=Acinetobacter baumannii (strain ATCC 17978 / CIP 53.77 / LMG 1025 / NCDC KC755 / 5377) GN=A1S_2566 PE=3 SV=2 - [A3M7T9_ACIBT]	1,92
A7FBD9	Uncharacterized protein OS=Acinetobacter baumannii (strain ATCC 17978 / CIP 53.77 / LMG 1025 / NCDC KC755 / 5377) GN=A1S_3702 PE=4 SV=2 - [A7FBD9_ACIBT]	1,92
A3M5T4	Penicillin G amidase OS=Acinetobacter baumannii (strain ATCC 17978 / CIP 53.77 / LMG 1025 / NCDC KC755 / 5377) GN=A1S_1851 PE=4 SV=2 - [A3M5T4_ACIBT]	1,93
A3M9V2	Putative transcriptional regulator (Lrp-like) OS=Acinetobacter baumannii (strain ATCC 17978 / CIP 53.77 / LMG 1025 / NCDC KC755 / 5377) GN=A1S_3307 PE=4 SV=2 - [A3M9V2_ACIBT]	1,94
A3M4S8	Uncharacterized protein OS=Acinetobacter baumannii (strain ATCC 17978 / CIP 53.77 / LMG 1025 / NCDC KC755 / 5377) GN=A1S_1494 PE=4 SV=2 - [A3M4S8_ACIBT]	1,97
A3M4G2	Putative long chain fatty-acid CoA ligase OS=Acinetobacter baumannii (strain ATCC 17978 / CIP 53.77 / LMG 1025 / NCDC KC755 / 5377) GN=A1S_1378 PE=4 SV=2 - [A3M4G2_ACIBT]	2,02
A3M1P9	DNA gyrase inhibitor YacG OS=Acinetobacter baumannii (strain ATCC 17978 / CIP 53.77 / LMG 1025 / NCDC KC755 / 5377) GN=yacG PE=3 SV=1 - [A3M1P9_ACIBT]	2,02
A3M3W0	DNA polymerase V component OS=Acinetobacter baumannii (strain ATCC 17978 / CIP 53.77 / LMG 1025 / NCDC KC755 / 5377) GN=A1S_1174 PE=4 SV=1 - [A3M3W0_ACIBT]	2,06
A3M7R9	Secreted trypsin-like serine protease OS=Acinetobacter baumannii (strain	2,07

	ATCC 17978 / CIP 53.77 / LMG 1025 / NCDC KC755 / 5377) GN=A1S_2546 PE=4 SV=2 - [A3M7R9_ACIBT]	
A3M6Y3	Uncharacterized protein OS=Acinetobacter baumannii (strain ATCC 17978 / CIP 53.77 / LMG 1025 / NCDC KC755 / 5377) GN=A1S_2254 PE=4 SV=2 - [A3M6Y3_ACIBT]	2,08
A3M3Y0	Uncharacterized protein OS=Acinetobacter baumannii (strain ATCC 17978 / CIP 53.77 / LMG 1025 / NCDC KC755 / 5377) GN=A1S_1194 PE=4 SV=2 - [A3M3Y0_ACIBT]	2,09
A3M6A5	Putative tail fiber OS=Acinetobacter baumannii (strain ATCC 17978 / CIP 53.77 / LMG 1025 / NCDC KC755 / 5377) GN=A1S_2022 PE=4 SV=2 - [A3M6A5_ACIBT]	2,10
A3M598	Putative membrane protein OS=Acinetobacter baumannii (strain ATCC 17978 / CIP 53.77 / LMG 1025 / NCDC KC755 / 5377) GN=A1S_1665 PE=3 SV=2 - [A3M598_ACIBT]	2,12
A3M2F8	Ferrous iron transport protein B OS=Acinetobacter baumannii (strain ATCC 17978 / CIP 53.77 / LMG 1025 / NCDC KC755 / 5377) GN=A1S_0653 PE=3 SV=1 - [A3M2F8_ACIBT]	2,16
A3M5P4	Uncharacterized protein OS=Acinetobacter baumannii (strain ATCC 17978 / CIP 53.77 / LMG 1025 / NCDC KC755 / 5377) GN=A1S_1811 PE=4 SV=2 - [A3M5P4_ACIBT]	2,17
A3M5L0	Methylenetetrahydrofolate reductase OS=Acinetobacter baumannii (strain ATCC 17978 / CIP 53.77 / LMG 1025 / NCDC KC755 / 5377) GN=A1S_1777 PE=3 SV=1 - [A3M5L0_ACIBT]	2,17
A3M1I7	Putative fusaric acid resistance protein OS=Acinetobacter baumannii (strain ATCC 17978 / CIP 53.77 / LMG 1025 / NCDC KC755 / 5377) GN=A1S_0317 PE=4 SV=2 - [A3M1I7_ACIBT]	2,25
A3M6H7	Uncharacterized protein OS=Acinetobacter baumannii (strain ATCC 17978 / CIP 53.77 / LMG 1025 / NCDC KC755 / 5377) GN=A1S_2094 PE=4 SV=2 - [A3M6H7_ACIBT]	2,28
A7FBR2	Uncharacterized protein OS=Acinetobacter baumannii (strain ATCC 17978 / CIP 53.77 / LMG 1025 / NCDC KC755 / 5377) GN=A1S_3825 PE=4 SV=2 - [A7FBR2_ACIBT]	2,30
A3M0Y1	Uncharacterized protein OS=Acinetobacter baumannii (strain ATCC 17978 / CIP 53.77 / LMG 1025 / NCDC KC755 / 5377) GN=A1S_0086 PE=4 SV=2 - [A3M0Y1_ACIBT]	2,32
A3M594	Fructose-26-bisphosphatase OS=Acinetobacter baumannii (strain ATCC 17978 / CIP 53.77 / LMG 1025 / NCDC KC755 / 5377) GN=A1S_1661 PE=4 SV=2 - [A3M594_ACIBT]	2,32
A3M166	NADPH-dependent FMN reductase OS=Acinetobacter baumannii (strain ATCC 17978 / CIP 53.77 / LMG 1025 / NCDC KC755 / 5377) GN=A1S_0179 PE=4 SV=2 - [A3M166_ACIBT]	2,37
A3M6U3	Uncharacterized protein OS=Acinetobacter baumannii (strain ATCC 17978 / CIP 53.77 / LMG 1025 / NCDC KC755 / 5377) GN=A1S_2210 PE=4 SV=2 - [A3M6U3_ACIBT]	2,38
A3M525	Putative Phage head-tail adaptor OS=Acinetobacter baumannii (strain ATCC 17978 / CIP 53.77 / LMG 1025 / NCDC KC755 / 5377) GN=A1S_1592 PE=4 SV=1 - [A3M525_ACIBT]	2,40
A3M6S8	Uncharacterized protein OS=Acinetobacter baumannii (strain ATCC 17978 / CIP 53.77 / LMG 1025 / NCDC KC755 / 5377) GN=A1S_2195 PE=4 SV=1 - [A3M6S8_ACIBT]	2,43
A7FBB9	Uncharacterized protein OS=Acinetobacter baumannii (strain ATCC 17978 / CIP 53.77 / LMG 1025 / NCDC KC755 / 5377) GN=A1S_3682 PE=4 SV=1 - [A7FBB9_ACIBT]	2,44
A3M5Q5	Putative transcription regulator protein OS=Acinetobacter baumannii (strain ATCC 17978 / CIP 53.77 / LMG 1025 / NCDC KC755 / 5377) GN=A1S_1822 PE=4 SV=2 - [A3M5Q5_ACIBT]	2,48
A3MA53	Uncharacterized protein OS=Acinetobacter baumannii (strain ATCC 17978 / CIP 53.77 / LMG 1025 / NCDC KC755 / 5377) GN=A1S_3408 PE=4 SV=2 - [A3MA53_ACIBT]	2,62
A3M7D5	Fatty acid desaturase OS=Acinetobacter baumannii (strain ATCC 17978 /	2,75

	CIP 53.77 / LMG 1025 / NCDC KC755 / 5377) GN=A1S_2410 PE=4 SV=2 - [A3M7D5_ACIBT]	
A7FBC0	Uncharacterized protein OS=Acinetobacter baumannii (strain ATCC 17978 / CIP 53.77 / LMG 1025 / NCDC KC755 / 5377) GN=A1S_3683 PE=4 SV=2 - [A7FBC0_ACIBT]	2,88
A7FAV6	Uncharacterized protein OS=Acinetobacter baumannii (strain ATCC 17978 / CIP 53.77 / LMG 1025 / NCDC KC755 / 5377) GN=A1S_3519 PE=4 SV=2 - [A7FAV6_ACIBT]	2,95
A3M1D5	Permease (DMT) superfamily OS=Acinetobacter baumannii (strain ATCC 17978 / CIP 53.77 / LMG 1025 / NCDC KC755 / 5377) GN=A1S_0254 PE=4 SV=2 - [A3M1D5_ACIBT]	3,01
A3M8U0	Putative cation efflux system protein OS=Acinetobacter baumannii (strain ATCC 17978 / CIP 53.77 / LMG 1025 / NCDC KC755 / 5377) GN=A1S_2929 PE=4 SV=2 - [A3M8U0_ACIBT]	3,70
A3M4M1	Putative acyl-CoA dehydrogenase OS=Acinetobacter baumannii (strain ATCC 17978 / CIP 53.77 / LMG 1025 / NCDC KC755 / 5377) GN=A1S_1437 PE=4 SV=1 - [A3M4M1_ACIBT]	4,30
A3M8N5	Uncharacterized protein OS=Acinetobacter baumannii (strain ATCC 17978 / CIP 53.77 / LMG 1025 / NCDC KC755 / 5377) GN=A1S_2873 PE=4 SV=1 - [A3M8N5_ACIBT]	5,01
A3M2Q8	NADH dehydrogenase I chain L OS=Acinetobacter baumannii (strain ATCC 17978 / CIP 53.77 / LMG 1025 / NCDC KC755 / 5377) GN=A1S_0762 PE=4 SV=2 - [A3M2Q8_ACIBT]	5,37

Table A2. Identification of the A549 subexpressed proteins under hypoxia condition ($1\%O_2$).

Accession	Description	Fold Change
Q05823	2-5A-dependent ribonuclease OS=Homo sapiens GN=RNASEL PE=1 SV=2 - [RN5A_HUMAN]	0,25
Q9UJT2	Testis-specific serine kinase substrate OS=Homo sapiens GN=TSKS PE=1 SV=3 - [TSKS_HUMAN]	0,36
B7ZVZ4	KIAA1211 protein OS=Homo sapiens GN=KIAA1211 PE=2 SV=1 - [B7ZVZ4_HUMAN]	0,36
Q9Y4A8	Nuclear factor erythroid 2-related factor 3 OS=Homo sapiens GN=NFE2L3 PE=1 SV=1 - [NF2L3_HUMAN]	0,40
B9EIP2	Olfactory receptor, family 51, subfamily A, member 4 OS=Homo sapiens GN=OR51A4 PE=2 SV=1 - [B9EIP2_HUMAN]	0,48
Q99501	GAS2-like protein 1 OS=Homo sapiens GN=GAS2L1 PE=1 SV=2 - [GA2L1_HUMAN]	0,51
P05543	Thyroxine-binding globulin OS=Homo sapiens GN=SERPINA7 PE=1 SV=2 - [THBG_HUMAN]	0,51
Q8N4C6-10	Isoform 3 of Ninein OS=Homo sapiens GN=NIN - [NIN_HUMAN]	0,55
E9PPJ0	Uncharacterized protein OS=Homo sapiens GN=SF3B2 PE=4 SV=1 - [E9PPJ0_HUMAN]	0,55
Q96JB1	Dynein heavy chain 8, axonemal OS=Homo sapiens GN=DNAH8 PE=1 SV=2 - [DYH8_HUMAN]	0,56
Q96LI6	Heat shock transcription factor, Y-linked OS=Homo sapiens GN=HSFY1 PE=1 SV=1 - [HSFY1_HUMAN]	0,56
Q15058	Kinesin-like protein KIF14 OS=Homo sapiens GN=KIF14 PE=1 SV=1 - [KIF14_HUMAN]	0,57
Q9BWV3	Cytidine and dCMP deaminase domain-containing protein 1 OS=Homo sapiens GN=CDADC1 PE=2 SV=1 - [CDAC1_HUMAN]	0,57
O00420	F19541_1 OS=Homo sapiens GN=PRODH2 PE=2 SV=1 - [O00420_HUMAN]	0,57
Q5U086	Serine/threonine-protein phosphatase OS=Homo sapiens PE=2 SV=1 - [Q5U086_HUMAN]	0,57
Q70EL1	Inactive ubiquitin carboxyl-terminal hydrolase 54 OS=Homo sapiens GN=USP54 PE=1 SV=4 - [UBP54_HUMAN]	0,57
Q9Y678	Coatomer subunit gamma OS=Homo sapiens GN=COPG PE=1 SV=1 - [COPG_HUMAN]	0,59
B4E1D5	cDNA FLJ54400, highly similar to Eukaryotic translation initiation factor 3 subunit 8 OS=Homo sapiens PE=2 SV=1 - [B4E1D5_HUMAN]	0,59
B4DMB1	cDNA FLJ53358, highly similar to Heterogeneous nuclear ribonucleoprotein R OS=Homo sapiens PE=2 SV=1 - [B4DMB1_HUMAN]	0,59
P25705	ATP synthase subunit alpha, mitochondrial OS=Homo sapiens GN=ATP5A1 PE=1 SV=1 - [ATPA_HUMAN]	0,59
B7ZM61	PLCE1 protein OS=Homo sapiens GN=PLCE1 PE=2 SV=1 - [B7ZM61_HUMAN]	0,60
F8W6H6	Uncharacterized protein OS=Homo sapiens GN=MYO5A PE=4 SV=1 - [F8W6H6_HUMAN]	0,60
Q8TER5-3	Isoform 3 of Rho guanine nucleotide exchange factor 40 OS=Homo sapiens GN=ARHGEF40 - [ARH40_HUMAN]	0,60
Q562R1	Beta-actin-like protein 2 OS=Homo sapiens GN=ACTBL2 PE=1 SV=2 - [ACTBL_HUMAN]	0,61
Q9P2F8	Signal-induced proliferation-associated 1-like protein 2 OS=Homo sapiens GN=SIPA1L2 PE=1 SV=2 - [SI1L2_HUMAN]	0,61
F5GYZ0	Uncharacterized protein OS=Homo sapiens GN=KLRC1 PE=4 SV=1 - [F5GYZ0_HUMAN]	0,61
B4DWZ4	cDNA FLJ51365, highly similar to Flap endonuclease 1 (EC 3.1.-.-)	0,61

	OS=Homo sapiens PE=2 SV=1 - [B4DWZ4_HUMAN]	
B4DNW7	Adenylyl cyclase-associated protein OS=Homo sapiens PE=2 SV=1 - [B4DNW7_HUMAN]	0,61
P08582	Melanotransferrin OS=Homo sapiens GN=MFI2 PE=1 SV=2 - [TRFM_HUMAN]	0,62
Q9UHD8	Septin-9 OS=Homo sapiens GN=SEPT9 PE=1 SV=2 - [SEPT9_HUMAN]	0,63
B4DL95	cDNA FLJ54330, highly similar to Usher syndrome type-1G protein OS=Homo sapiens PE=2 SV=1 - [B4DL95_HUMAN]	0,63
B4DG54	cDNA FLJ56635 OS=Homo sapiens PE=2 SV=1 - [B4DG54_HUMAN]	0,63
Q5T215	Trafficking protein particle complex subunit 3-like protein OS=Homo sapiens GN=BET3L PE=1 SV=1 - [TPC3L_HUMAN]	0,64

Table A3. Identification of the A549 overexpressed proteins under hypoxia condition ($1\%O_2$).

Accession	Description	Fold Change
Q8TD06	Anterior gradient protein 3 homolog OS=Homo sapiens GN=AGR3 PE=1 SV=1 - [AGR3_HUMAN]	1,41
O14737	Programmed cell death protein 5 OS=Homo sapiens GN=PDCD5 PE=1 SV=3 - [PDCD5_HUMAN]	1,41
P09936	Ubiquitin carboxyl-terminal hydrolase isozyme L1 OS=Homo sapiens GN=UCHL1 PE=1 SV=2 - [UCHL1_HUMAN]	1,41
P05198	Eukaryotic translation initiation factor 2 subunit 1 OS=Homo sapiens GN=EIF2S1 PE=1 SV=3 - [IF2A_HUMAN]	1,42
P06753-2	Isoform 2 of Tropomyosin alpha-3 chain OS=Homo sapiens GN=TPM3 - [TPM3_HUMAN]	1,42
P56545-2	Isoform 2 of C-terminal-binding protein 2 OS=Homo sapiens GN=CTBP2 - [CTBP2_HUMAN]	1,42
P04080	Cystatin-B OS=Homo sapiens GN=CSTB PE=1 SV=2 - [CYTB_HUMAN]	1,43
B7Z6N2	cDNA FLJ56154, highly similar to Gelsolin OS=Homo sapiens PE=2 SV=1 - [B7Z6N2_HUMAN]	1,43
P13796	Plastin-2 OS=Homo sapiens GN=LCP1 PE=1 SV=6 - [PLSL_HUMAN]	1,43
P26639	Threonyl-tRNA synthetase, cytoplasmic OS=Homo sapiens GN=TARS PE=1 SV=3 - [SYTC_HUMAN]	1,44
B3KVF9	cDNA FLJ16507 fis, clone HCHON2000364, highly similar to Insulin-like growth factor-binding protein 3 OS=Homo sapiens PE=2 SV=1 - [B3KVF9_HUMAN]	1,45
P50238	Cysteine-rich protein 1 OS=Homo sapiens GN=CRIP1 PE=1 SV=3 - [CRIP1_HUMAN]	1,46
B7Z722	Tropomyosin 1 (Alpha), isoform CRA_i OS=Homo sapiens GN=TPM1 PE=2 SV=1 - [B7Z722_HUMAN]	1,46
F5GWF6	Uncharacterized protein OS=Homo sapiens GN=CCT2 PE=3 SV=2 - [F5GWF6_HUMAN]	1,48
P62736	Actin, aortic smooth muscle OS=Homo sapiens GN=ACTA2 PE=1 SV=1 - [ACTA_HUMAN]	1,48
Q9UQ80	Proliferation-associated protein 2G4 OS=Homo sapiens GN=PA2G4 PE=1 SV=3 - [PA2G4_HUMAN]	1,51
Q96HN2-2	Isoform 2 of Putative adenosylhomocysteinase 3 OS=Homo sapiens GN=AHCYL2 - [SAHH3_HUMAN]	1,51
B4DUX5	Methionine aminopeptidase OS=Homo sapiens GN=METAP2 PE=2 SV=1 - [B4DUX5_HUMAN]	1,52
P13196	5-aminolevulinate synthase, nonspecific, mitochondrial OS=Homo sapiens GN=ALAS1 PE=1 SV=2 - [HEM1_HUMAN]	1,58
P67809	Nuclease-sensitive element-binding protein 1 OS=Homo sapiens GN=YBX1 PE=1 SV=3 - [YBOX1_HUMAN]	1,58
A8K3C3	T-complex protein 1 subunit delta OS=Homo sapiens PE=2 SV=1 - [A8K3C3_HUMAN]	1,58
B4DPZ3	cDNA FLJ53290, highly similar to Cytoplasmic dynein 1 intermediate chain 2 OS=Homo sapiens PE=2 SV=1 - [B4DPZ3_HUMAN]	1,58
O43423	Acidic leucine-rich nuclear phosphoprotein 32 family member C OS=Homo sapiens GN=ANP32C PE=2 SV=1 - [AN32C_HUMAN]	1,59
B4DJ30	cDNA FLJ61290, highly similar to Neutral alpha-glucosidase AB OS=Homo sapiens PE=2 SV=1 - [B4DJ30_HUMAN]	1,62
B9A018	Uncharacterized protein OS=Homo sapiens GN=USP39 PE=4 SV=1 - [B9A018_HUMAN]	1,67
Q59G24	Activated RNA polymerase II transcription cofactor 4 variant (Fragment) OS=Homo sapiens PE=2 SV=1 - [Q59G24_HUMAN]	1,68
Q86VN1-2	Isoform 2 of Vacuolar protein-sorting-associated protein 36 OS=Homo	1,68

	sapiens GN=VPS36 - [VPS36_HUMAN]	
P05091	Aldehyde dehydrogenase, mitochondrial OS=Homo sapiens GN=ALDH2 PE=1 SV=2 - [ALDH2_HUMAN]	1,69
P07951-2	Isoform 2 of Tropomyosin beta chain OS=Homo sapiens GN=TPM2 - [TPM2_HUMAN]	1,71
Q9BYV8	Centrosomal protein of 41 kDa OS=Homo sapiens GN=TSGA14 PE=1 SV=1 - [CEP41_HUMAN]	1,73
P62269	40S ribosomal protein S18 OS=Homo sapiens GN=RPS18 PE=1 SV=3 - [RS18_HUMAN]	1,80
Q9UF56	F-box/LRR-repeat protein 17 OS=Homo sapiens GN=FBXL17 PE=2 SV=3 - [FXL17_HUMAN]	1,81
F8VVL1	Uncharacterized protein OS=Homo sapiens GN=DENR PE=4 SV=1 - [F8VVL1_HUMAN]	1,88
P30041	Peroxiredoxin-6 OS=Homo sapiens GN=PRDX6 PE=1 SV=3 - [PRDX6_HUMAN]	1,94
P47813	Eukaryotic translation initiation factor 1A, X-chromosomal OS=Homo sapiens GN=EIF1AX PE=1 SV=2 - [IF1AX_HUMAN]	1,96
P63241-2	Isoform 2 of Eukaryotic translation initiation factor 5A-1 OS=Homo sapiens GN=EIF5A - [IF5A1_HUMAN]	1,98
Q6UY18	Leucine-rich repeat and immunoglobulin-like domain-containing nogo receptor-interacting protein 4 OS=Homo sapiens GN=LINGO4 PE=2 SV=1 - [LIGO4_HUMAN]	2,04
Q6NW36	Proteasome (Prosome, macropain) 26S subunit, ATPase, 1 OS=Homo sapiens GN=PSMC1 PE=2 SV=1 - [Q6NW36_HUMAN]	2,17
O60673	DNA polymerase zeta catalytic subunit OS=Homo sapiens GN=REV3L PE=1 SV=2 - [DPOLZ_HUMAN]	2,22
Q53G85	Elongation factor 1-alpha (Fragment) OS=Homo sapiens PE=2 SV=1 - [Q53G85_HUMAN]	2,58
Q13442	28 kDa heat- and acid-stable phosphoprotein OS=Homo sapiens GN=PDAP1 PE=1 SV=1 - [HAP28_HUMAN]	4,40

1 **Title. Effect of hypoxia on the pathogenesis of *Acinetobacter baumannii* and**

2 ***Pseudomonas aeruginosa in vitro* and in murine experimental models of infections.**

3 **Authors.** María Luisa Gil-Marqués, María Eugenía Pachón-Ibáñez*, Jerónimo Pachón,

4 Younes Smani.

5

6 **Affiliations.** Clinic Unit of Infectious Diseases, Microbiology and Preventive Medicine,

7 Institute of Biomedicine of Seville, IBiS, University Hospital Virgen del

8 Rocío/CSIC/University of Seville, Spain.

9

10 **Running Title.** Hypoxia effect on bacterial pathogenesis

11

12 **Keywords.** Hypoxia, animal models, *Acinetobacter baumannii*, *Pseudomonas*

13 *aeruginosa*, infection.

14

15 **Corresponding author.** #María Eugenia Pachón Ibáñez, Clinic Unit of Infectious

16 Diseases, Microbiology and Preventive Medicine, Institute of Biomedicine of Seville

17 (IBiS), University Hospital Virgen del Rocío, Av. Manuel Siurot s/n, 41013, Seville,

18 Spain. Tel: +34-955923100, E-mail: mpachon-ibis@us.es.

19

ABSTRACT

Hypoxia modulates bacterial virulence and inflammation response through the hypoxia-inducible factor-1α (HIF-1α). Here, we study the influence of hypoxia on *Acinetobacter baumannii* and *Pseudomonas aeruginosa* infections. *In vitro* hypoxia increases bactericidal activity of epithelial cells against *A. baumannii* reducing extracellular bacterial concentration (50.5 ± 7.5%) and against *P. aeruginosa* (90.8 ± 13.9%) 2h post-infection. The same happens in macrophages cells (67.6 ± 18.2% at 2h, and 50.3 ± 10.9% at 24 h, respectively). Hypoxia decreases *A. baumannii* adherence to epithelial (42.87 ± 8.16% at 2 h) and macrophages cells (52.0 ± 18.7% at 24 h). The same happens in *P. aeruginosa* (24.9 ± 4.5% and 65.7 ± 5.5% at 2 h, respectively). Moreover, hypoxia decreases *A. baumannii* invasion 24h post-infection in epithelial (48.6 ± 3.8%) and macrophages cells (8.7 ± 6.9%), and *P. aeruginosa* (75.0 ± 16.3% and 63.4 ± 5.4% at 2 h, respectively). *In vivo* hypoxia diminishes bacterial load in fluids and tissues in animal models of infection by both pathogens. Contradictory, mice survival time was smaller under hypoxia (23.92 *vs.* 36.42 h, for *A. baumannii*). No differences were found *in vitro* and *in vivo* in cytokines and HIF-1α production between hypoxia and normoxia. We conclude that hypoxia increases the bactericidal activity of host cells against both pathogens and reduces their interaction. Moreover, hypoxia accelerates the rate at which animals die despite their lower bacterial concentration *in vivo*.

INTRODUCTION

Several pathogens, including *Escherichia coli*, *Pseudomonas aeruginosa*, *Salmonella typhimurium*, group A and B *Streptococci*, *Staphylococcus aureus*, and *Chlamydia pneumoniae* have been shown to regulate hypoxia inducible factor 1 alpha (HIF-1α) (1-6). The bacterial lipopolysaccharide has been reported to activate HIF-1α through toll-like receptor 4 in macrophages and neutrophils under normoxia (2,7-10).

It is known that hypoxia seems to have protective role against bacterial infections. In this way, HIF-1α-deficient macrophages and PMN affect *in vitro* the intracellularkilling of group B *Streptococcus* and *P. aeruginosa*, respectively (1,9). In mice, the HIF-1α-knockout (KO) keratinocytes induced the development of larger necrotic lesions and decreased the mice capacity to clear group A *Streptococcus* by reducing the recruitment of neutrophils to the site of infection (11,12); and the HIF-1α knockdown by siRNA reduced the mice resistance to *P. aeruginosa* keratitis (9). Likewise, the use of mimosine, a HIF-1α agonist, can boost the ability of phagocytes and whole blood to kill *S. aureus* and reduce the lesion size in a murine model of skin infection (13).

However, hypoxia influence on Gram-negative bacterial infection remains to be understood. We know that hypoxia impairs innate immune functions of the airway epithelial cells during *P. aeruginosa* infection, and reducing the HIF-1α expression by siRNA in the bronchial epithelial cells enhances the immune response (14). More specifically, hypoxia reduced the IL-6 production by keratinocytes when compared to normoxia (11). Consecutively, the HIF-1α deletion, but not HIF-1α isoform I.1, in T lymphocytes prevents the antibacterial effect of these cells (15,16).

During infection, bacteria must adapt to heterogeneous environments (17-19). The oxygen levels in the foci of infection are much lower (<1%) than in healthy tissues (2.5-9%) (20) due to a combination of increased oxygen consumption by immune cells and

pathogens, along with a decreased perfusion due to vascular dysfunction (21-23). Therefore, the microenvironment at the area of infection plays a crucial role in determining the outcome of an infection. Hypoxia not only modifies the host cells but also the bacterial metabolism and virulence (5). In *P. aeruginosa* and *Mycobacterium tuberculosis* the expression of virulence factors such as alkaline protease, siderophores and exotoxin A are reduced by hypoxia (24,25). However, hypoxia can also increase the production of alginate and the expression of the PA-I lectin/adhesin by *P. aeruginosa* causing a disruption in intestinal barrier and allowing exotoxin A to cross the epithelium (26,27). Exposure to hypoxia also induces antibiotic resistance in *P. aeruginosa* by an alteration of efflux pumps expression (28). Together, these studies demonstrate the complexity of HIF-pathogen interactions.

The aim of this study was to evaluate the effect of hypoxia on *A. baumannii* and *P. aeruginosa* pathogenesis, *in vitro*, regarding to bactericidal activity and adherence/invasion, and in murine models of infection, regarding to survival, and bacterial load; and the innate immune response *in vitro* and *in vivo*.

RESULTS

Hypoxia increases HIF-1α levels in epithelial and macrophages cells

HIF-1α levels in cell lines after 6 and 24 h under hypoxia (1% O_2) and normoxy (21% O_2) were measured. In epithelial cells, HIF-1α levels were 2.69 times higher after 6 h in hypoxia than in normoxy (2296.98 ± 157.74 pg/mL *vs*. 853.63 ± 95.47 pg/mL, $P<0.001$) and were higher than after 24 h (1107.70 ± 96.08 pg/mL *vs*. 592.27 ± 48.86 pg/mL, $P<0.01$). In macrophages cells, HIF-1α levels were 1.50 times higher after 6 h in hypoxia than in normoxia (331.64 ± 52.93 pg/mL *vs*. 220.67 ± 11.87 pg/mL) and were higher than after 24 h under hypoxia (223.59 ± 7.05 pg/mL *vs*. 235.27 ± 9.31

pg/mL; hypoxia 6 h *vs.* hypoxia 24 h). No significant differences in HIF-1α levels were observed in normoxia between the different times points analysed.

The marked increase of HIF-1α levels after 6 h under hypoxia (1% O_2) defined the time of hypoxia condition prior the infection for the *in vitro* and *in vivo* experiments.

Hypoxia increases bactericidal activity of epithelial and macrophages cells against *A. baumannii* and *P. aeruginosa*

First, we observed that ATCC 17978 and PAO1 strains growth during 2 and 24 h was indistinguishable between hypoxia (1% O_2) and normoxia (Fig. 1A). Next, we determined if hypoxia affects the bactericidal activity of epithelial and macrophages cells. Bacterial counts of ATCC 17978 and PAO1 strains found in the extracellular medium of both cell lines under hypoxia (1% O_2) showed a decrease of bacterial concentrations after 2 and 24 h compared to normoxia, (Fig. 1B and 1C). These data support an increase in the bactericidal activity of these cell lines under hypoxia.

HIF-1α overexpression increases bactericidal activity of epithelial and macrophages cells against *A. baumannii* and *P. aeruginosa*

Bacterial counts of ATCC 17978 and PAO1 strains found in the extracellular medium of both cell lines under a 0.1 mM DMOG treatment showed a decrease of bacterial concentrations after 24 h compared to normoxia, (Fig. 1B and 1C). These data support an increase in the bactericidal activity of these cell lines when HIF-1α is overexpressed due to the treatment with DMOG.

Hypoxia decreases bacterial adherence and invasion to epithelial and macrophages cells

The bacterial adherence of ATCC 17978 and PAO1 strains to both cell lines was significantly lower under hypoxia (1% O2), except in the case of 2 h post-infection by ATCC 17978 strain in the RAW 264.7 cells in which it presented higher bacterial adherence (182.67 ± 11% *vs*. 100% ± 0%, $P<0.001$) (Fig. 2A and 2B).

Bacterial counts of ATCC 17978 strain inside epithelial and macrophages cells under hypoxia (1% O_2) showed an increase of bacterial concentrations 2 h post-infection (150 ± 0% for epithelial cells, and 146.73 ± 5.01% for macrophages cells, $P<0.001$), and a decrease at 24 h post-infection compared to normoxia (48.55 ± 34.80% for epithelial cells, $P<0.001$ and 8.69 ± 6.85% for macrophages cells, $P<0.001$) (Fig. 2C). On the other hand, PAO1 strain counts inside both cell lines under hypoxia (1% O_2) showed a decrease of bacterial concentrations after 2 h ($P<0.001$ for macrophages cells) and 24 h ($P<0.001$) compared to normoxia (Fig. 2D). These data indicated that hypoxia affects the adherence and invasion of *A. baumannii* and *P. aeruginosa* 24 h after bacterial infection.

Hypoxia reduces the expression of proteins involved in cell adherence

iTRAQ results show that there are 51 down-expressed proteins under hypoxia (Fold Change < 0.6) present in the extracellular medium of a 2 h infection of A549 cells by *A. baumannii* ATCC 17978 strain (Table S1). Forty-five % are localized in the cytoplasm, 16% are secreted, 19% are in the inner membrane, 10% in the outer membrane, 6% in the periplasm and 4% in the mitochondrion (Fig. S1). The proteins localized in the outer membrane and could be involved in cell adhesion are OmpW, putative ferric siderophore receptor protein A1S_3339, putative ferric siderophore receptor protein A1S_0474, ferric enterobactin receptor A1S_0981, and ferrichrome-iron receptor

A1S_1921. Moreover, the secreted uncharacterized protein A1S_3900, which is a protein that presents SH3-like domains, could also be involved in cell adhesion.

Hypoxia reduces bacterial load in tissues and fluids in a peritonitis sepsis model by *A. baumannii*

The MLD needed to achieve 100% mortality for ATCC 17978 strain was lower in hypoxia (10% O_2) than in normoxia (2.08 *vs.* 3.20 $\log_{10}$ cfu/mL). For the rest of experiments, we used the MLD calculated in normoxia. The survival time was higher in mice infected under normoxia than hypoxia (10%O_2) (36.42 *vs.* 23.92 h, $P<0.001$) (Fig. 3A).

In the sepsis model by *A. baumannii*, regardless the studied condition, all mice presented bacteremia after 4 h infection. No differences were found in the bacterial load in tissues (spleen, and lungs) and fluids (PF and blood) between hypoxia and normoxia after 4 h infection (Table 1). However, at the time of death, significant differences between hypoxia and normoxia were found in the bacterial loads in lungs, PF, and blood (Table 1). Moreover, significant differences between animals under normoxia and under hypoxia (6 h) followed by normoxia were found in the bacterial loads at the time of death in spleen, lungs and PF (Table 1). Bacterial loads in spleen, lungs, PF and blood were lower under hypoxia (hypoxia 6 h prior infection, or during the whole experiment) compared to normoxia.

HIF-1α levels showed no differences between hypoxia and normoxia in controls animals (not infected). Contradictorily, infected mice under the different studied conditions presented higher HIF-1α levels than controls mice under normoxia at the time of death (Fig. 3B).

Hypoxia reduces bacterial load in tissues and blood in a pneumonia model by *P. aeruginosa*

The MLD calculated for PAO1 strain was the same for both conditions (8.54 $\log_{10}$ cfu/mL). Survival time was significantly higher under normoxia than under hypoxia (10% O_2) (P<0.01) or six hours' hypoxia followed by normoxia (P<0.05) (Fig. 3A). Pathological studies confirmed pneumonia 4 h after infection in all the conditions analyzed, but the symptoms were higher under normoxia (data not shown).

After 4 h of infection, no significant differences were found in the bacterial loads in tissues and blood between both conditions (Table 2). Nevertheless, at the mice time of death, significant differences were found in spleen, lungs and blood (between hypoxia and normoxia (Table 2). Similarly, significant differences at the time of death were found in the bacterial loads in blood between mice under 6 h hypoxia prior the infection followed by normoxia and the animals infected in normoxia (Table 2). Bacterial loads in tissues and blood were lower under both hypoxemic conditions than under normoxia. HIF-1α levels were not significant among the studied conditions. Opposing to what happened in the peritoneal sepsis model by *A. baumannii*; infected mice under the different conditions studied presented lower HIF-1α levels than non-infected mice at the time of death (Fig. 3B).

In vitro and _in vivo_ cytokines production under hypoxia and normoxia

The infection of epithelial cells by ATCC 17978 and PAO1 strains showed that IL-6, TNF-α and IL-10 levels were similar for both conditions at 2 and 24 h post-infection (Fig. 4A). When infecting the RAW 264.7 cells by ATCC 17978 and PAO1 strains, IL-6 and TNF-α levels at 24 h and 2 h post-infection were significantly higher in hypoxia (P<0.05), respectively (Fig. 4B).

In the sepsis model by ATCC 17978 strain, only IL-10 levels were significantly higher after 4 h infection in hypoxia ($P<0.05$). No differences were found in IL-6 or TNF-α levels, although they were slightly higher under hypoxia. No differences in cytokines levels were found at the animal time of death (Fig. 4C). In the pneumonia model by PAO1 strain, IL-6 levels were significantly higher in hypoxia ($P<0.05$) after 4 h infection. Again, no differences were found for IL-10 and TNF-α levels although they were rather higher under hypoxia (Fig. 4C). Contradictory to what we observed in the sepsis model, at the mice time of death, we observed lower IL-10 levels under hypoxia ($P<0.05$). Again, no differences were found in IL-6 or TNF-α levels, although they were slightly lower under hypoxia (Fig. 4C).

DISCUSSION

To our knowledge, this is the first study that analyses *in vitro* and *in vivo* the effect of hypoxia during infection by *A. baumannii* and *P. aeruginosa*. We observed that hypoxia *in vitro* increases bactericidal activity of host cells, and reduce bacterial adherence and invasion. We also found that hypoxia *in vivo* diminish bacterial load in fluids and tissues, but mice survival time was shorter under hypoxia.

We showed that hypoxia doesn't affect the *in vitro* growth of *A. baumannii* and *P. aeruginosa*. However, it increases the bactericidal activity in epithelial and macrophage cells. The study of Peyssonnaux *et al*. showed that hypoxia modifies gene regulation in host cells and it increases the LL-37 cathelicidin levels, an antimicrobial peptide involved in the clearance of pathogens (12). Moreover, we see that hypoxia decreases the bacterial adherence to host cells. This effect might be due to the modification of cell or bacterial membrane under this condition. iTRAQ results confirmed that hypoxia downregulates 51 proteins in *A. baumannii* ATCC 17978, five of them are localized in

the outer membrane which could be involved in cell adherence due to the previous reports of their involvement in the bacterial adherence (29-33)

Regarding to bacterial invasion, we observed differences in behavior between *A. baumannii* and *P. aeruginosa* under hypoxia. Our data showed a reduction in the *P. aeruginosa* internalization into epithelial and macrophages cells, confirming the results obtained in a previous study in which it is demonstrated that hypoxia decreases the *P. aeruginosa* internalization into A549 cells (34). However, *A. baumannii* internalization in both host cells is higher after 2 h under hypoxia, but it is reduced after 24 h. Consequently, hypoxia cannot stop the *A. baumannii* invasion during the first few hours of infection but it is finally hindered after 24 h. Therefore, we believe that hypoxia confers higher resistance against bacterial invasion to host cells in order to avoid an intracellular replication and the infection evolution.

In the *in vivo* experiments, we observe that a lower bacterial inoculum is needed to cause 100% of mice mortality under hypoxia in the peritoneal sepsis model by *A. baumannii*. All infected mice presented bacteremia 4 h post-infection for the studied conditions. Moreover, we observe lower bacterial load in blood, PF lungs and spleen under hypoxia. We also show that maintaining animals 6 h under hypoxia before the infection is enough to reduce bacterial load at the time of death. These results are in accordance with a previous study in which the use of the compound AKB-4924, that increases HIF-1α levels, reduced bacterial loads recovered in a *S. aureus* skin infection model (35). Moreover, these results are in accordance with the *in vitro* adherence assays data. The increase of host cells bactericidal activity under hypoxia as well as a reduction of bacterial adherence could allow the immune system to eliminate the infection better.

In the pneumonia model of infection by *P. aeruginosa*, we observed no differences in the inoculum needed to cause 100% of mortality between the studied conditions.

Bacteremia observed in mice 4 h post-infection was 44.44% and 61.11% for normoxia and hypoxia, respectively. The difference found in the bacteremia levels between both animal models is because the severity of the sepsis model (36,37). As in the sepsis model by *A. baumannii*, we observed lower bacterial load in fluids and tissues under hypoxia, and under hypoxia followed by normoxia, are in accordance with the *in vitro* results of adherence and invasion. Again, as in the sepsis animal model, survival time was longer under normoxia.

In both animal models, HIF-1α levels were higher after 4 h under hypoxia, being the levels similar at the animal time of death regardless the studied conditions. These results are in accordance with the *in vitro* studies in which HIF-1α levels increased over time under hypoxia and then decreased 24 h after. We observed that *A. baumannii* causes an increase of HIF-1α levels compared to the control as what reported in another study in which infection with *A. baumannii* produced HIF-1α levels increase (4). In contrast, *P. aeruginosa* produces HIF-1α levels reduction under hypoxia compared to the control. This result could be explained because 2-alkyl-4-quinolone and Pseudomonas Quinolone Signal triggers the HIF-1α degradation through the 26S-proteasome proteolytic pathway, blocking the HIF-1α effect (38,39).

As it is well defined in the literature, hypoxia regulates the immune response (20). In the *A. baumannii* sepsis model, we observed under hypoxia high IL-10 levels after 4 h infection. Meng *et al*. indicated that HIF-1α is involved in IL-10 production by B cells (40), and IL-10 is an anti-inflammatory cytokine that suppresses macrophage and dendritic cells function (41). In the *P. aeruginosa* pneumonia model, we detected high IL-6 levels 4 h post-infection under hypoxia. It has been showed that HIF-1α increase TNF-α and IL-6 levels (20,42). Moreover, IL-10 levels decreased under hypoxia in the pneumonia model by *P. aeruginosa* at the time of death. However, we did not find

differences in cytokines levels between hypoxia and normoxy neither *in vitro* nor *in vivo*. Therefore, we found that hypoxia has not a strong impact on cytokine production (20), being more important on the bactericidal activity of host cells and on the reduction of infection in animals.

However, this study has some limitations. HIF-1α is a factor involved in multiple cellular pathways and its expression is also regulated by different proteins. Therefore, finding a clear correlation between hypoxia, HIF-1α expression, inflammatory responses and infection is complex, and multiple cellular processes have to be taken into consideration.

In conclusion, hypoxia increases the bactericidal activity of host cells. In contrast, mortality in animals under hypoxia is faster even with a lower bacterial load in tissues and fluids. Moreover, we find that hypoxia has not a strong impact on cytokine production by both pathogens. Finally, despite both studied microorganism are close phylogenetically, they present slightly different behavior under hypoxia.

MATERIALS AND METHODS

Bacterial strains and growth condition

The wild-type strains *A. baumannii* ATCC 17978 and *P. aeruginosa* PAO1 were used. They were cultured at 37ºC overnight (160 rpm) in Mueller Hinton Broth (MHB) (Sigma, Spain). Cultured strains were washed with phosphate-buffered saline (PBS) and suspended in Dulbecco's modified Eagle's medium (DMEM) before their use in eukaryotic cell culture experiments (human lungs epithelial cell line A549 and murine macrophage cell line RAW 264.7).

Growth curves analysis

The growth of *A. baumannii* ATCC 17978 and *P. aeruginosa* PAO1 strains under hypoxia (1% and 10% O_2) and normoxia (21% O_2) in static were monitored during 24 h. Both strains were grown overnight in 20 ml of MHB, and a 1:10000 dilution was performed to obtain, approximately, 10^5 cfu/ml in a 40 ml culture of MHB (10% and 21% O_2) or DMEM (1% and 21% O_2). Three replicates were performed in different days.

A549 and RAW 264.7 culture and infection

Human lungs epithelial cell line A549 and murine macrophage cell line RAW 264.7 were grown in DMEM containing 10% Fetal Bovine Serum (Gibco, Spain), 1% HEPES 1M, vancomycin (50 mg/ml), gentamicin (20 mg/ml) and amphotericin B (0.25 mg/ml; Gibco), as previously described (43). In the case of hypoxia condition studies, cells were transferred to a hypoxia chamber (Coy Laboratories, USA) with a humidified atmosphere of 1% O_2, 5% CO_2 and the balance N_2 at 37°C. Cells were seeded (10^5 cells/well in a 24-well plate) for 30 h in 24-well plates before infection with *A. baumannii* ATCC 17978 or *P. aeruginosa* PAO1 at a multiplicity of infection (MOI) of 500. To mimic hypoxia condition we treated the cells with 0.1 mM Dimethyloxaloylglycine (DMOG) (Sigma, Spain), an inhibitor of prolyl hydroxylases (44), 6 h prior bacterial infection and during infection. Immediately before the infection, A549 cells were washed thrice with PBS and incubated in supplemented DMEM.

HIF-1α measurement in cell cultures

A549 and RAW 264.7 cells were seeded for 24 h in 6-well plates (10^6 cells/well). After 6 and 24 h in hypoxia (1% O_2) or normoxia condition, cells were washed thrice with PBS, harvested using cell scraper and homogenized in RIPA buffer supplemented with

1 mM phenylmethylsulfonyl fluoride and 10% cocktail of protease inhibitors (Sigma, Spain), and centrifuged at 13000*g* 4°C for 20 min. The supernatant was removed and the amount of proteins was determined using BCA assay (Promega, Spain). The samples were stored at -80°C. Forty µg of proteins of each sample was used to measure HIF-1α levels with an enzyme-linked immunosorbent assay (ELISA) kit (Thermo Fisher Scientific, Spain).

Bactericidal activity, bacterial adherence and bacterial invasion in cell cultures

After A549 and RAW 264.7 cells infections with *A. baumannii* ATCC 17978 and *P. aeruginosa* PAO1 strains under hypoxia and normoxia conditions, extracellular medium was removed and serially diluted to determine bacterial concentration as previously described (45).

Adherence and invasion assays were performed as previously described (45). To measure the number of adherent bacteria, cells were infected as mentioned before, and, after washing thrice with PBS, 200 µl of trypsin-EDTA (Gibco, Spain) was added for 5 min at 37°C. Then, 200 µl of 0.5% Triton X-100 (Sigma, Spain) was added for 3 min. The invasion protocol included a treatment with gentamicin 256 µg/ml (Gibco, Spain) before the addition of trypsin-EDTA. Diluted lysates were counted to determine the attached and internalized bacteria by A549 and RAW 264.7 cells.

Every assay was performed three times in different days. In the case of invasion assay, four replicates were performed in different days.

Cytokine Assay

Extracellular medium of infected A549 and RAW 264.7 cells with *A. baumannii* ATCC 17978 and *P. aeruginosa* PAO1 strains under hypoxia and normoxia conditions were

collected and centrifuged at 5000*g* for 15 min at 4ºC. The supernatant was stored at -80ºC until analysis. TNF-α, IL-6 and IL-10 levels were measured in using an ELISA kit (Affymetrix eBioscience, USA), in accordance with the manufacturer's instructions. Levels of pro- and anti-inflammatory cytokines (IL-6, IL-10 and TNF-α) in mice serum were measured by ELISA assays (Affymetrix eBioscience, USA).

iTRAQ assay

We analyzed the differential protein expression profile between normoxia and hypoxia conditions in A549 cell infected by *A. baumannii* ATCC 17978. After 2 h infection, we collected the cells in a lysis buffer composed by 1 M Triethylammonium bicarbonate buffer (Sigma, Spain), 0.05% SDS, 1:100 phosphatase inhibitor cocktail (PhosSTOP EASYpack, Roche, Spain), 1:100 protease inhibitor cocktail (Complete Mini EDTA-free, Roche, Spain), and 0.002% benzonase (Novagen, USA). Pellet was separated from the supernatant and protein concentration was quantified by fluorimetry (Qubit life technology, USA). Samples were treated with 50 mM TCEP (AB Sciex, Spain) to reduce disulfide bonds and 200 mM MTTS (AB Sciex, Spain), and then they were digested with trypsin (Promega, Spain) at a 10:1 substrate:enzyme ratio at 37° overnight. We used an isobaric tag iTRAQ 8 plex (reporters at 113–119 and 121, AB Sciex, Spain). Samples were analyzed by nano-liquid chromatography (nano LC 100, Thermo Fisher Scientific, USA) and tandem mass spectrometry (Q Exactive Plus Orbitrap, Thermo Electron, USA). Protein identification was performed using Proteome Discoverer 1.4 (Thermo Fisher Scientific, USA). MS/MS fragmentation patterns were mapped against Uniprot database. We considered quantifiable proteins those that were identified through more than 2 peptides with a confidence level ≥ 95%, a *P*-value ≤ 0.05, and an error factor < 2 with every reference tag.

368

369 Animals

370 Immunocompetent C57BL/6 male mice, weighing approximately 20 g (Production and
371 Experimentation Animal Center, University of Seville, Seville, Spain) were used; they
372 had a sanitary status of murine pathogen free and were assessed for genetic authenticity.
373 Mice were housed in an individually ventilated cage system under specific pathogen-
374 free conditions, and water and food supplied *ad libitum*. This study was carried out
375 following the recommendations in the Guide for the Care and Use of Laboratory
376 Animals. This study was carried out in strict accordance with Directive 2010/63/EU on
377 the protection of animals used for scientific purposes. Experiments were approved by
378 the Committee on the Ethics of Animal Experiments of the University Hospital of
379 Virgen del Rocío of Seville, Spain (20-05-14-84). All procedures were performed under
380 sodium thiopental (B. Braun Medical S.A., Spain) anesthesia, and all efforts were made
381 to minimize suffering.

382

383 Experimental models.

384 Both models of infection were carried out under the following conditions: i) hypoxia
385 (10% O_2), ii) normoxia and iii) six hours under hypoxia followed by normoxia. The
386 minimum lethal doses (MLD) were calculated for *A. baumannii* and *P. aeruginosa*
387 under hypoxia and normoxia conditions. Briefly, groups of 6 mice were inoculated
388 intraperitoneally (ip.) for *A. baumannii* and intratracheally for *P. aeruginosa* with
389 increasing concentrations until reaching 100% mortality, of each pathogen and the
390 survival rate was monitored for 7 days. For the hypoxia condition studies, mice were
391 maintained in a hypoxic chamber (Coy Laboratories, USA) with a humidified
392 atmosphere of 10% O_2 (standard hypoxic condition) 6 h prior the infection and until the

animal death or the end of the experiment. In the experiments in which mice were 6 h under hypoxia followed by normoxia, the animals were maintained in a hypoxic chamber during 6 h prior the infection, and placed outside normoxia until the end of the experiment or the animal death. The same conditions were used with control mice (not infected).

To evaluate pneumonia, after 4 h of infection and at the time of death, lungs were aseptically extracted, fixed in 10% formalin and embedded in paraffin wax. Serial sections (3 µm) were cut onto glass slides and stained with hematoxylin and eosin.

A N of no more than 5 mice per condition was performed in different weeks to reproduce the experimental models results.

(i) Experimental murine model of peritoneal sepsis. A previously characterized murine peritoneal sepsis model by *A. baumannii* was used (36). Briefly, animals were inoculated i.p. with 0.5 ml of $MLD_{100,}$ mixed 1:1 with a saline solution containing 10% (wt/vol) mucin from porcine stomach Type II (Sigma, Spain).

After 4 h of infection, a group of 34 mice (17 under hypoxia and 17 under normoxia) were sacrificed by i.p. injection of sodium thiopental (200 µl; Braun Medical, USA) and analyzed, and 48 mice (21 under normoxia, 22 under hypoxia and 5 under 6h hypoxia + normoxia) were analyzed at the time of death. Survival rates were recorded under hypoxia and normoxia conditions. Bacteremia was evaluated, both qualitatively and quantitatively after the animal's death. For qualitative analysis, the blood was inoculated into sterile tubes with 1 ml of MHB and incubated for 24 h at 37ºC, and then 10 µl was plated on sheep blood agar. To evaluate quantitatively the bacteremia (log_{10} cfu/ml), blood was serially diluted and plated on sheep blood agar. Finally, bacterial load was quantified in spleen and lungs. Briefly, organs were aseptically removed and homogenized (Stomacher 80; Tekmar Co.) in 2 ml of sterile 0.9% NaCl solution. Serial

418 dilutions of the homogenized organs were plated on sheep blood agar for quantitative
419 cultures (log_{10} cfu/g). Finally, bacterial concentration in peritoneal fluid was also
420 determined by injecting 2 mL of sterile 0.9% NaCl solution i.p. and, after a brief
421 massage on the abdomen, peritoneal lavage was collected and plated on sheep blood
422 agar (log_{10} cfu/mL). HIF-1α levels in mice serum were measured by ELISA assays
423 (MyBioSource, USA).
424
425 **(ii) Pneumonia model.** A previously characterized pneumonia model by *P. aeruginosa*
426 (46) was used as follows: anesthetized mice (thiopental at 5% [wt/vol], i.p.) were
427 infected by intratracheal instillation, using 50µL of the MLD_{100} calculated previously.
428 Mice remained in a vertical position for 3 min and then resting at 30º positions until
429 they awakened. After 4 h of infection, 36 mice (18 under normoxia and 18 under
430 hypoxia) were sacrificed (sodium thiopental, Braun Medical, USA) to be analyzed and
431 46 mice (20 under normoxia, 18 under hypoxia and 8 under 6 h hypoxia + normoxia)
432 were analyzed at the time of death. Survival rates were analyzed for the different
433 conditions. Bacteremia, bacterial load in blood and tissue (spleen and lungs) were
434 performed as described above. HIF-1α levels in mice serum were measured by ELISA
435 assays (MyBioSource, USA).
436
437 **Statistical analysis**
438 Statistical analyses were performed using the IBM SPSS Statistics 22 softwareprogram.
439 Tests used included ANOVA (bacterial counts in tissues and fluids and mortality time),
440 Chi-square test (bacteremia), and when required Dunnett's and Tukey post-hoc tests and
441 Student's t-test (bacterial counts *in vitro*, cytokines and HIF-1α levels). A *P*-value <0.05
442 was considered significant.

ACKNOWLEDGMENTS

Funding information. This study was supported by the Instituto de Salud Carlos III, Subdirección General de Redes y Centros de Investigación Cooperativa, Ministerio de Economía, Industria y Competitividad (PIE13/0004) and by Plan Nacional de I+D+i 2013-2016 and Instituto de Salud Carlos III, Subdirección General de Redes y Centros de Investigación Cooperativa, Ministerio de Economía, Industria y Competitividad, Spanish Network for Research in Infectious Diseases (REIPI RD12/0015/0001; RD12/0015/0012; RD16/0016/0009) - cofinanced by European Development Regional Fund "A way to achieve Europe", Operative program Intelligent Growth 2014-2020. M.L.G.M. is supported by the program FPU (Formación de Profesorado Universitario; FPU13/04545), Ministerio de Educación, Cultura y Deporte, Spain. M.E.P.I. has a grant by the Ministerio de Economía y Competitividad, Instituto de Salud Carlos III, cofinanced by the European Development Regional Fund ("A way to achieve Europe"), and by the Spanish Network for Research in Infectious Diseases (grant REIPI RD16/0009). Y.S. is supported by the Subprograma Miguel Servet Tipo I, Instituto de Salud Carlos III, Subdirección General de Redes y Centros de Investigación Cooperativa, Ministerio de Economía y Competitividad, Spain (CP15/00132).

REFERENCES

1. Cramer T, Yamanishi Y, Clausen BE, Förster I, Pawlinski R, Mackman N, Haase VH, Jaenisch R, Corr M, Nizet V, Firestein GS, Gerber HP, Ferrara N, Johnson RS. 2003. HIF-1α is essential for myeloid cell mediated inflammation. Cell 112:645-657.
2. Peyssonnaux C, Cejudo-Martin P, Doedens A, Zinkernagel AS, Johnson RS, Nizet V. 2007. Cutting edge: essential role of hypoxia inducible factor-1α in development of lipopolysaccharide-induced sepsis. J Immunol 178:7516-7519.
3. Bayele HK, Peyssonnaux C, Giatromanolaki A, Arrais-Silva WW, Mohamed HS, Collins H, Giorgio S, Koukourakis M, Johnson RS, Blackwell JM, Nizet V, Srai SK. 2007. HIF-1 regulates heritable variation and allele expression phenotypes of the macrophage immune response gene SLC11A1 from a Z-DNA forming microsatellite. Blood 110:3039-3048.
4. Werth N, Beerlage C, Rosenberger C, Yazdi AS, Edelmann M, Amr A, Bernhardt W, von Eiff C, Becker K, Schäfer A, Peschel A, Kempf VA. 2010. Activation of hypoxia inducible factor 1 is a general phenomenon in infections with human pathogens. PLoS One 5:e11576.
5. Schaible B, Schaffer K, Taylor CT. 2010. Hypoxia, innate immunity and infection in the lung. Respir Physiol Neurobiol 174:235-243.
6. Rupp J, Gieffers J, Klinger M, van Zandbergen G, Wrase R, Maass M, Solbach W, Deiwick J, Hellwig-Burgel T. 2007. *Chlamydia pneumoniae* directly interferes with HIF-1a stabilization in human host cells. Cell Microbiol 9:2181-2191.
7. Devraj G, Beerlage C, Brüne B, Kempf VA. 2017. Hypoxia and HIF-1 activation in bacterial infections. Microbes Infect 19:144-156.

8. Peyssonnaux C, Datta V, Cramer T, Doedens A, Theodorakis EA, Gallo RL, Hurtado-Ziola N, Nizet V, Johnson RS. 2005. HIF-1α expression regulates the bactericidal capacity of phagocytes. J Clin Invest 115:1806-1815.
9. Berger EA, McClellan SA, Vistisen KS, Hazlett LD. 2013. HIF-1α is essential for effective PMN bacterial killing, antimicrobial peptide production and apoptosis in *Pseudomonas aeruginosa* keratitis. PLoS Pathog 9:e1003457.
10. Frede S, Stockmann C, Freitag P, Fandrey J. 2006. Bacterial lipopolysaccharide induces HIF-1 activation in human monocytes via p44/42 MAPK and NF-κB. Biochem J 396:517-527.
11. Leire E, Olson J, Isaacs H, Nizet V, Hollands A. 2013. Role of hypoxia inducible factor-1 in keratinocyte inflammatory response and neutrophil recruitment. J Inflamm 10:28.
12. Peyssonnaux C, Boutin AT, Zinkernagel AS, Datta V, Nizet V, Johnson RS. 2008. Critical role of HIF-1 α in keratinocyte defense against bacterial infection. J Invest Dermatol 128:1964-1968.
13. Zinkernagel AS, Peyssonnaux C, Johnson RS, Nizet V. 2008. Pharmacologic augmentation of hypoxia-inducible factor–1α with mimosine boosts the bactericidal capacity of phagocytes. J Infect Dis 197:214-217.
14. Polke M, Seiler F, Lepper PM, Kamyschnikow A, Langer F, Monz D, Herr C, Bals R, Beisswenger C. 2017. Hypoxia and the hypoxia-regulated transcription factor HIF-1a suppress the host defence of airway epithelial cells. Innate Immun 23:373-380.
15. Thiel M, Caldwell CC, Kreth S, Kuboki S, Chen P, Smith P, Ohta A, Lentsch AB, Lukashev D, Sitkovsky MV. 2007. Targeted deletion of HIF-1alpha gene in T cells

prevents their inhibition in hypoxic inflamed tissues and improves septic mice survival. PLoS One 2:e853.

16. Georgiev P, Belikoff BG, Hatfield S, Ohta A, Sitkovsky MV, Lukashev D. 2013. Genetic deletion of the alternative isoform I.1 of HIF-1α in T cells enhances anti-bacterial immune response and improves survival in the model of bacterial peritonitis in mice. Eur J Immunol 43:655-666.

17. Eichner A, Günther N, Arnold M, Schobert M, Heesemann J, Hogardt M. 2014. Marker genes for the metabolic adaptation of *Pseudomonas aeruginosa* to the hypoxic cystic fibrosis lung environment. Int J Med Microbiol 304:1050-1061.

18. Legendre C, Mooij MJ, Adams C, O'Gara F. 2011. Impaired expression of hypoxia-inducible factor-1α in cystic fibrosis airway epithelial cells – a role for HIF-1 in the pathophysiology of CF. J Cyst Fibros 10:286-290.

19. Cullen L, McClean S. 2015. Bacterial adaptation during chronic respiratory infections. Pathogens 4:66-89.

20. Nizet V, Johnson RS. 2009. Interdependence of hypoxic and innate immune responses. Nat Rev Immunol 9:609-617.

21. Cummins EP, Keogh CE, Crean D, Taylor CT. 2016. The role of HIF in immunity and inflammation. Mol Aspects Med 47-48:24-34.

22. Eltzschig HK, Carmeliet P. 2011. Hypoxia and inflammation. N Engl J Med 364:656-665.

23. Campbell EL, Colgan SP. 2015. Neutrophils and inflammatory metabolism in antimicrobial functions of the mucosa. J Leukoc Biol 98:517-522.

24. Schaible B, Rodriguez J, Garcia A, von Kriegsheim A, McClean S, Hickey C, Keogh CE, Brown E, Schaffer K, Broquet A, Taylor CT. 2017. Hypoxia reduces

533 the pathogenicity of *Pseudomonas aeruginosa* by decreasing the expression of
534 multiple virulence factors. J Infect Dis 215:1459-1467.
535 25. Sever JL, Youmans GP. 1957. The relation of oxygen tension to virulence of
536 tubercle bacilli and to acquired resistance in tuberculosis. J Infect Dis 101:193-202.
537 26. Worlitzsch D, Tarran R, Ulrich M, Schwab U, Cekici A, Meyer KC, Birrer P,
538 Bellon G, Berger J, Weiss T, Botzenhart K, Yankaskas JR, Randell S, Boucher RC,
539 Döring G. 2002. Effects of reduced mucus oxygen concentration in airway
540 *Pseudomonas* infections of cystic fibrosis patients. J Clin Invest 109:317-325.
541 27. Patel NJ, Zaborina O, Wu L, Wang Y, Wolfgeher DJ, Valuckaite V, Ciancio MJ,
542 Kohler JE, Shevchenko O, Colgan SP, Chang EB, Turner JR, Alverdy JC. 2007.
543 Recognition of intestinal epithelial HIF-1α activation by *Pseudomonas aeruginosa*.
544 Am J Physiol Gastrointest Liver Physiol 92:G134-142.
545 28. Schaible B, Taylor CT, Schaffer K. 2012. Hypoxia increases antibiotic resistance in
546 *Pseudomonas aeruginosa* through altering the composition of multidrug efflux
547 pumps. Antimicrob Agents Chemother 56:2114-2118.
548 29. McClean S, Healy ME, Collins C, Carberry S, O'Shaughnessy L, Dennehy R,
549 Adams Á, Kennelly H, Corbett JM, Carty F, Cahill LA, Callaghan M, English K,
550 Mahon BP, Doyle S, Shinoy M. 2016. Linocin and OmpW are involved in
551 attachment of the cystic fibrosis-associated pathogen *Burkholderia cepacia*
552 complex to lung epithelial cells and protect mice against infection. Infect Immun
553 84:1424-1437.
554 30. Kurochkina N. 2015. SH Domains. Springer International Publishing. {Structure-
555 Function Relationship of Bacterial SH3 Domains}. 71-89.
556 31. Carnielli CM, Artier J, de Oliveira JC, Novo-Mansur MT. 2017. *Xanthomonas citri*
557 subsp. citri surface proteome by 2D-DIGE: Ferric enterobactin receptor and other

558 outer membrane proteins potentially involved in citric host interaction. J
559 Proteomics 151:251-263.
560 32. Russo TA, McFadden CD, Carlino-MacDonald UB, Beanan JM, Barnard TJ,
561 Johnson JR. 2002. IroN functions as a siderophore receptor and is a urovirulence
562 factor in an extraintestinal pathogenic isolate of *Escherichia coli*. Infect Immun
563 70:7156-7160.
564 33. Feldmann F, Sorsa LJ, Hildinger K, Schubert S. 2007. The salmochelin siderophore
565 receptor IroN contributes to invasion of urothelial cells by extraintestinal
566 pathogenic *Escherichia coli in vitro*. Infect Immun. 75:3183-3187.
567 34. Schaible B, McClean S, Selfridge A, Broquet A, Asehnoune K, Taylor CT,
568 Schaffer K. 2013. Hypoxia modulates infection of epithelial cells by *Pseudomonas*
569 *aeruginosa*. PLoS One 8:e56491.
570 35. Okumura CY, Hollands A, Tran DN, Olson J, Dahesh S, von Köckritz-Blickwede
571 M, Thienphrapa W, Corle C, Jeung SN, Kotsakis A, Shalwitz RA, Johnson RS,
572 Nizet V. 2012. A new pharmacological agent (AKB-4924) stabilizes hypoxia
573 inducible factor-1 (HIF-1) and increases skin innate defenses against bacterial
574 infection. J Mol Med 90:1079-1089.
575 36. Smani Y, Domínguez-Herrera J, Ibáñez-Martínez J, Pachón J. 2015. Therapeutic
576 efficacy of lysophosphatidylcholine in severe infections caused by *Acinetobacter*
577 *baumannii*. Antimicrob Agents Chemother 59:3920-3924.
578 37. Vila-Farrés X, Parra-Millán R, Sánchez-Encinales V, Varese M, Ayerbe-Algaba R,
579 Bayó N, Guardiola S, Pachón-Ibáñez ME, Kotev M, García J, Teixidó M, Vila J,
580 Pachón J, Giralt E, Smani Y. 2017. Combating virulence of Gram-negative bacilli
581 by OmpA inhibition. Sci Rep 7:14683.

582 38. Legendre C, Reen FJ, Mooij MJ, McGlacken GP, Adams C, O'Gara F. 2012.
583 *Pseudomonas aeruginosa* alkyl quinolones repress Hypoxia-Inducible Factor 1
584 (HIF-1) signaling through HIF-1α degradation. Infect Immun 80:3985-3992.
585 39. Legendre C, Reen FJ, Woods DF, Mooij MJ, Adams C, O'Gara F. 2014. Bile acids
586 repress hypoxia-inducible factor 1 signaling and modulate the airway immune
587 response. Infect Immun 82:3531-3541.
588 40. Meng X, Grötsch B, Luo Y, Knaup KX, Wiesener MS, Chen XX, Jantsch J,
589 Fillatreau S, Schett G, Bozec A. 2018. Hypoxia-inducible factor-1α is a critical
590 transcription factor for IL-10-producing B cells in autoimmune disease. Nat
591 Commun 9:251.
592 41. Couper KN, Blount DG, Riley EM. 2008. IL-10: the master regulator of immunity
593 to infection. J Immunol 180:5771-5777.
594 42. Harris AJ, Thompson AR, Whyte MK, Walmsley SR. 2014. HIF-mediated innate
595 immune responses: cell signaling and therapeutic implications. Hypoxia (Auckl)
596 2:47-58.
597 43. Smani Y, Dominguez-Herrera J, Pachón J. 2013. Association of the outer
598 membrane protein Omp33 with fitness and virulence of *Acinetobacter baumannii*. J
599 Infect Dis 208:1561-1570.
600 44. Asikainen TM, Schneider BK, Waleh NS, Clyman RI, Ho WB, Flippin LA,
601 Günzler V, White CW. 2005. Activation of hypoxia-inducible factors in hyperoxia
602 through prolyl 4-hydroxylase blockade in cells and explants of primate lung. Proc
603 Natl Acad Sci U S A 102:10212-7.
604 45. Smani Y, Docobo-Pérez F, López-Rojas R, Domínguez-Herrera J, Ibáñez-Martínez
605 J, Pachón J. 2012. Platelet-activating factor receptor initiates contact of

606 *Acinetobacter baumannii* expressing phosphorylcholine with host cells. J Biol
607 Chem 287:26901-26910.
608 46. Rumbo C, Vallejo JA, Cabral MP, Martínez-Guitián M, Pérez A, Beceiro A, Bou
609 G. 2016. Assessment of antivirulence activity of several d-amino acids against
610 *Acinetobacter baumannii* and *Pseudomonas aeruginosa*. J Antimicrob Chemother.
611 71:3473-81.

612

613 **Figure 1**. **A**) Growth curves of *A. baumannii* ATCC 17978 and *P. aeruginosa* PAO1
614 strains under normoxia and hypoxia (10% and 1% O_2). N=3 **B**) Measurement of
615 bacterial concentration (%) in the extracellular medium after 2 and 24 h of A549 and
616 RAW 264.7 infection by *A. baumannii* ATCC 17978 strain under normoxia, hypoxia
617 (1% O_2) and treated with 0.1 mM DMOG. N=3 ***: $P<0.001$; *: $P<0.05$ Hypoxia vs.
618 Normoxia at 2 or 24 h and Normoxia + DMOG vs. Normoxia at 24 h. Normoxia +
619 DMOG vs. Normoxia at 24 h. **C**) Measurement of bacterial concentration (%) in the
620 extracellular medium after 2 and 24 h of A549 and RAW 264.7 infection by *P.*
621 *aeruginosa* PAO1 strain under normoxia, hypoxia (1% O_2) and treated with 0.1 mM
622 DMOG. N=3 **: $P<0.01$; ***: $P<0.001$ Hypoxia *vs*. Normoxia at 2 or 24 h and
623 Normoxia + DMOG vs. Normoxia at 24 h.

624

625 **Figure 2**. **A**) Measurement of bacterial adherence (%) after 2 and 24 h of A549 and
626 RAW 264.7 infection by *A. baumannii* ATCC 17978 strain under normoxia and
627 hypoxia (1% O_2). N=3 *: $P<0.05$ and ***: $P<0.001$ Hypoxia *vs*. Normoxia at 2 or 24 h.
628 **B**) Measurement of bacterial adherence (%) after 2 and 24 h of A549 and RAW 264.7
629 infection by *P. aeruginosa* PAO1 under normoxia and hypoxia (1% O_2). N=3 ***:
630 $P<0.001$ Hypoxia *vs*. Normoxia at 2 or 24 h. **C**) Measurement of bacterial
631 internalization (%) after 2 and 24 h of A549 RAW 264.7 infection by *A. baumannii*
632 ATCC 17978 strain under normoxia and hypoxia (1% O_2). N=4 ***: $P<0.001$ Hypoxia
633 *vs*. Normoxia at 2 h or 24 h. **D)** Measurement of bacterial internalization (%) after 2 and
634 24 h of A549 RAW 264.7 infection by *P. aeruginosa* PAO1 strain under normoxia and
635 hypoxia (1% O_2). ***: $P<0.001$ Hypoxia *vs*. Normoxia at 2 h or 24 h. N=4

636 **Figure 3**. **A**) Analysis of survival time in the sepsis model by *A. baumannii* ATCC
637 17978 strain (*P*<0.001 Hypoxia *vs.* Normoxia) and in the pneumonia model by *P.*
638 *aeruginosa* PAO1 strain under normoxia, hypoxia (10% O_2), and 6 h of hypoxia (10%
639 O_2) + normoxia (*P*<0.01 Hypoxia *vs.* Normoxia; *P*<0.05 6 h Hypoxia + Normoxia *vs.*
640 Normoxia). **B**) HIF-1α levels (pg/mL) in mice serum in the sepsis model by *A.*
641 *baumannii* ATCC 17978 strain and in the pneumonia model by *P. aeruginosa* PAO1
642 strain at 4 h after infection and at the time of death under normoxia and hypoxia (10%
643 O_2).

644

645 **Figure 4**. **A**) Cytokines levels (pg/mL) in the extracellular medium of A549 infections
646 by *A. baumannii* ATCC 17978 and *P. aeruginosa* PAO1 strains after 2 and 24 h under
647 normoxia and hypoxia (1% O_2). **B**) Cytokines levels (pg/mL) in the extracellular
648 medium of RAW 264.7 infections by *A. baumannii* ATCC 17978 and *P. aeruginosa*
649 PAO1 strains after 2 and 24 h under normoxia and hypoxia (1% O_2). **C**) Cytokines
650 levels (pg/mL) in mice serum in the sepsis model by *A. baumannii* ATCC 17978 strain
651 and in the pneumonia model by *P. aeruginosa* PAO1 strain. *: *P*<0.05.

652

653

654 **Table 1**. Bacterial load in fluids and tissues in the sepsis model by *A. baumannii* ATCC 17978 strain.

	4h		Time of death		
Bacterial load	**N**	**H**	**N**	**H**	**H (6 h) + N**
Log_{10} cfu/g spleen	3.98 ± 0.30	3.88 ± 0.23	8.79 ± 0.56	8.32 ± 0.71	7.90 ± 0.30 [d]
Log_{10} cfu/g lungs	4.07 ± 0.53	4.07 ± 0.70	9.36 ± 0.35	8.25 ± 0.54 [b]	8.32 ± 0.46 [d]
Log_{10} cfu/mL PF	4.06 ± 1.29	3.72 ± 1.15	9.31 ± 0.33	8.88 ± 0.53 [a]	8.75 ± 0.33 [d]
Log_{10} cfu/mL blood	3.19 ± 0.42	3.18 ± 0.28	8.40 ± 0.56	7.73 ± 0.20 [c]	7.85 ± 0.32
Bacteriemia, %	100	100	100	100	100

655 N: Normoxia; H: Hypoxia; PF: peritoneal fluid

656 [a] $P<0.05$, H *vs.* N at the time of death

657 [b] $P<0.001$, H *vs.* N at the time of death

658 [c] $P<0.01$, H *vs.* N at the time of death

659 [d] $P<0.05$, H (6 h) + N *vs.* N at the time of death

660 **Table 2**. Bacterial load in fluids and tissues in the pneumonia model by *P. aeruginosa* PAO1.

	4h		Time of death		
Bacterial load	**N**	**H**	**N**	**H**	**H (6 h) + N**
Log_{10} cfu/g spleen	2.64 ± 0.69	3.10 ± 0.80	6.96 ± 0.57	5.27 ± 0.60 [a]	6.60 ± 0.34
Log_{10} cfu/g lungs	7.77 ± 0.61	7.79 ± 0.42	9.81 ± 0.45	9.04 ± 0.58 [a]	9.79 ± 0.27
Log_{10} cfu/ml blood	0.26 ± 0.36	0.99 ± 0.84	7.90 ± 0.67	5.66 ± 0.78 [b]	6.30 ± 0.46 [c]
Bacteriemia, %	44.44	61.11	100	100	100

661 N: Normoxia; H: Hypoxia

662 [a] $P<0.001$, H *vs.* N at the time of death

663 [b] $P<0.01$, H *vs.* N at the time of death

664 [c] $P<0.05$, H (6 h) + N *vs.* N at the time of death

665

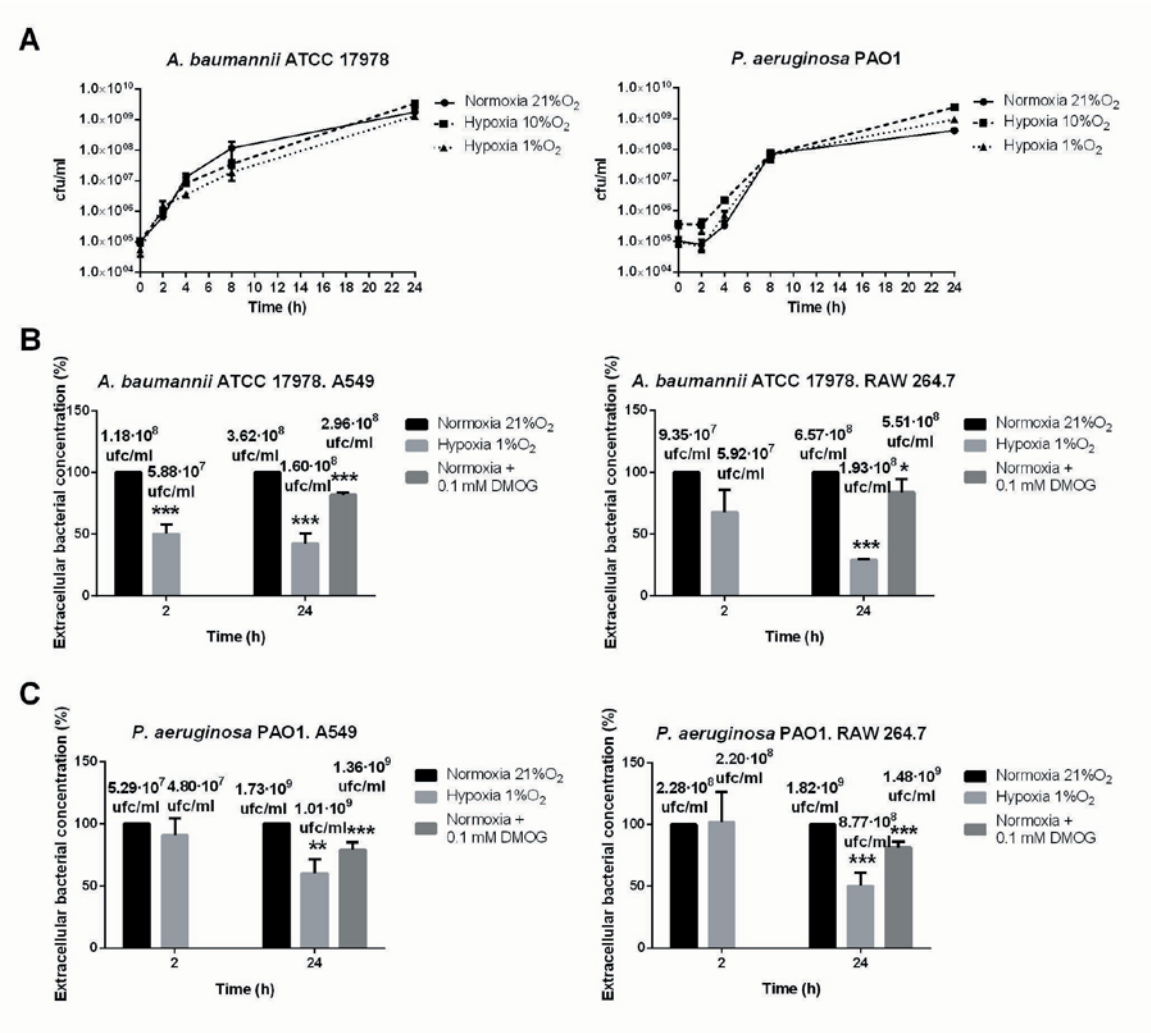

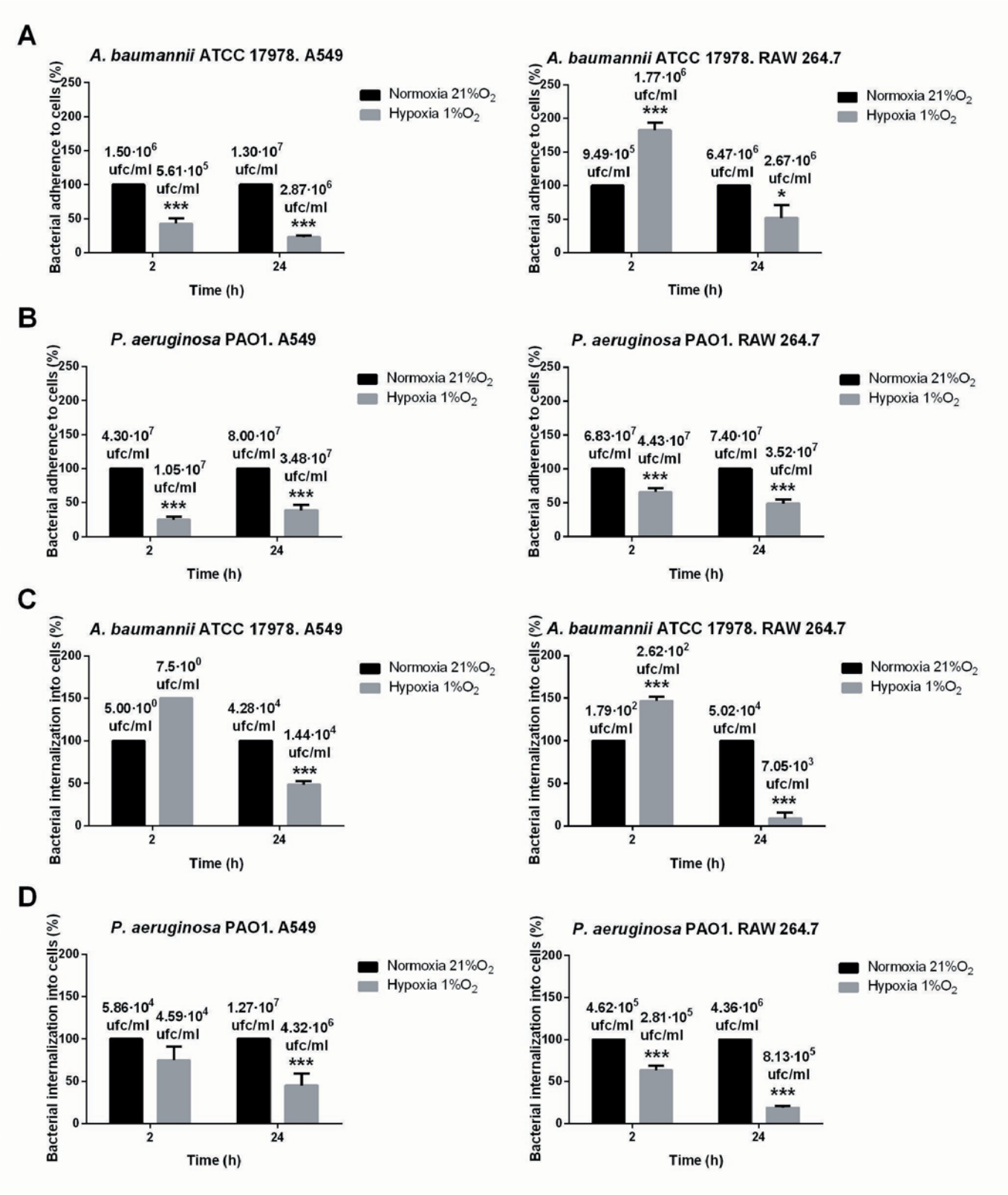

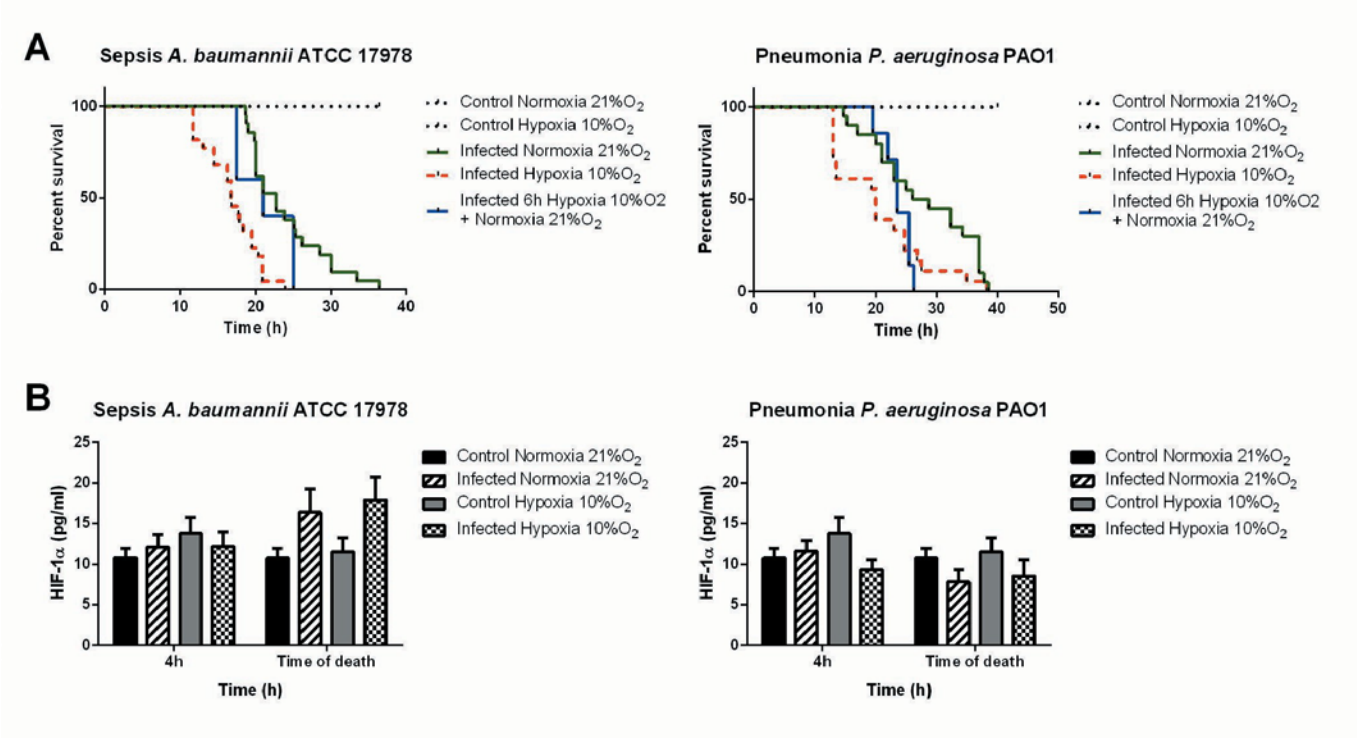

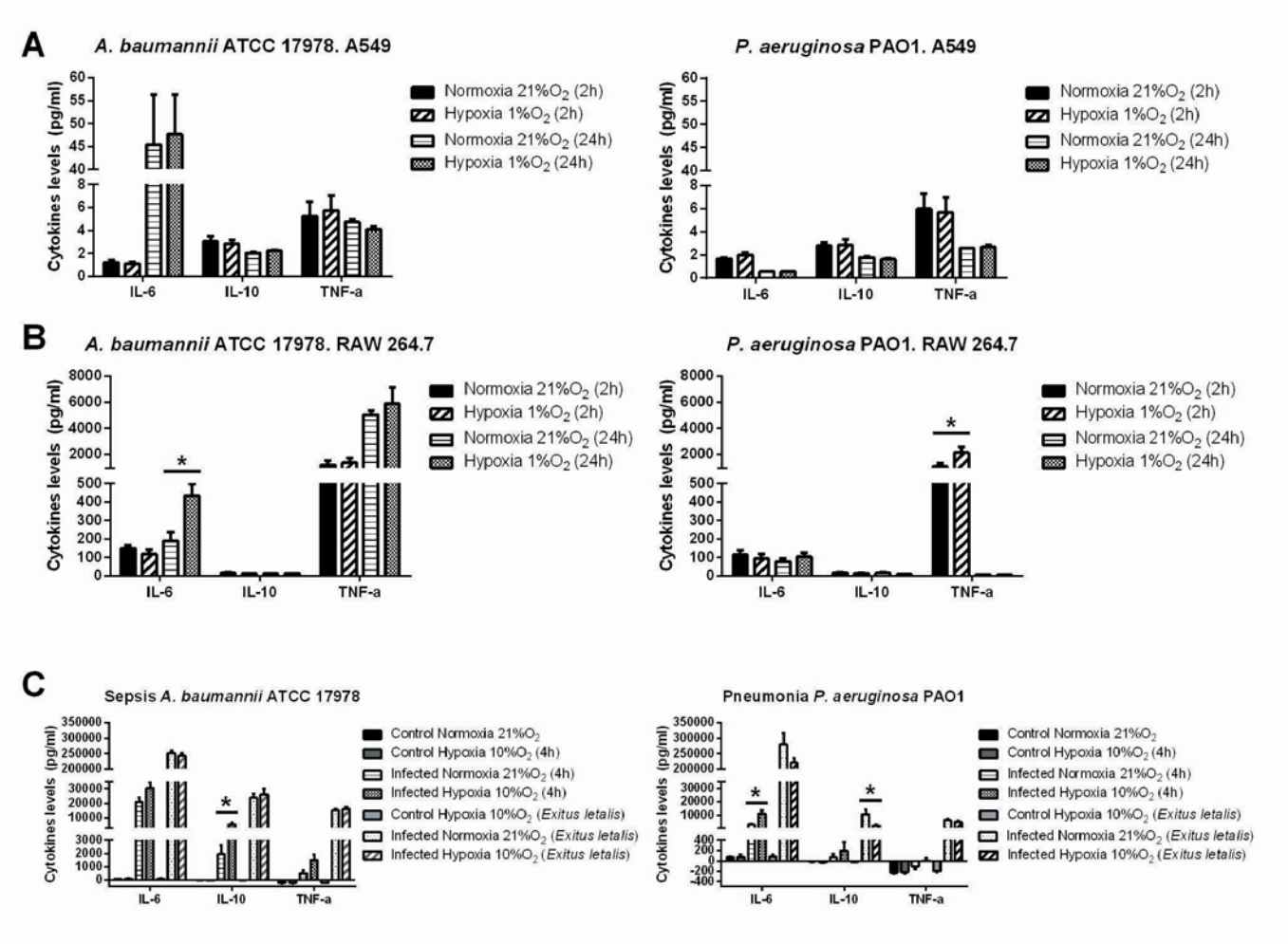

CHAPTER III. ARTICLE III.

PREDICTIVE VALUE OF APACHE II, AND SERUM LACTATE, PYRUVATE, IL-10 AND LYSOPHOSPHATIDYLCHOLINE LEVELS ON SURVIVAL IN PATIENTS WITH SEPTIC SHOCK.

Sepsis is a heterogeneous life-threatening condition caused by an exacerbated systemic inflammatory response [1]. The immune system arises a local inflammatory process in response to infection, but when the auto-regulation fails and systemic inflammation occurs, the infection converted to sepsis or septic shock [2]. Septic shock is a common condition in patients with other underlying diseases [3]. It is a clinical syndrome in which patients present a sepsis with hypotension that persists after resuscitation with intravenous fluid [2], an inadequate tissue perfusion [4] and profound hemodynamic alterations such as hypovolemia, decrease in vascular tone and myocardial depression [5]. Hypovolemia and hypoperfusion lead to an imbalance between the delivery and demand for oxygen and other substrates, inducing a tissue hypoxia and a cellular and organ injury. The cellular injury induces an increased activation of the innate immune response and a release of inflammatory mediators that further compromise perfusion through changes in the microvasculature. All these alterations finally cause a multiorgan failure that lead to death [4]. Thereby, severity of these alterations is associated with increased mortality [5].

In the United States in 2003, sepsis incidence was 50-95 cases per 100000 every year [6] and, in 2015, the incidence had reached 535 cases per 100000 every year, and it is still increasing [7]. In 9% of patients, sepsis progress to severe sepsis, and 3% of those ends up with septic shock [8]. The mortality rate in patients with septic shock decreased from 62% in the early 1990s to 56% in 2000 [9] and it varies from 35-70% depending on different factors (age, sex, underlying disorders, among others) [2, 10].

It was concluded in a study in 2000 that goal-directed therapy at the earliest stages of septic shock has significant benefits [11]. Nowadays, the laboratory parameters used are often late signs associated with organ dysfunction and a higher mortality rate [12]. Thereby, there is a demand for better biomarkers to improve the diagnosis and evolution of septic shock, to determine the severity of the disease and to know the patient prognosis, which will allow applying a more accurate treatment.

Multiple studies have investigated about potentially useful sepsis markers such as IL-6, IL-8, procalcitonin (PCT) [13], lysophosphatidylcholine (LPC) [14], sTREM-1, CD64 expression on polymorpfonuclear leukocytes (PMNs) [15], and lactate [16]. All this biomarkers have shown a modest discriminative value, but CD64 expression on PMNs [15] and lactate [16], and there are contradictory results on the diagnostic accuracy of PCT [13, 17, 18]. Lactate concentration is a marker of tissue hypoperfusion and hypoxia, but it can be a consequence of other alterations. Hence, several studies propose to measure lactate clearance [19] or the lactate/pyruvate ratio to discriminate hypoxic from non-hypoxic lactate [20, 21]. A study showed that persistent hyperlactatemia together with an augmented Pv-aCO_2/Ca-vO_2 ratio was associated with poor outcomes during the initial phases of septic shock [22].

Septic shock patients present a severe tissue hypoxia [23], which seems to modulate bacterial virulence through the hypoxia-inducible factor-1 (HIF-1). HIF-1 is a heterodimeric molecular key regulator (HIF-1α and HIF-1β) which activates gene expression in response to hypoxemic or inflammatory conditions allowing immune cells to function under low oxygen concentration [24, 25]. Thereby, HIF-1α might be a good marker to determine patient´s outcome in septic shock.

The aim of the present study was to prospectively evaluate the association of regional oxygen saturation index, acid-base balance, HIF-1, inflammatory biomarkers - including cytokines,

procalcitonin and lysophosphatidylcholine blood levels, and HLA-DR expression in circulating monocytes with the survival in adult patients with septic shock.

Materials and Methods

Study Population

Clinical prospective and observational study in 20 adult patients (≥ 18 years old) with septic shock [31], who were hospitalized in the Intensive Care Unit (ICU) of the University Hospital of Virgen del Rocio, Seville, Spain, from September 2014 to May 2016. Patients with advanced chronic diseases (heart failure, chronic obstructive pulmonary disease, liver cirrhosis), neutropenia (< 500 cells/µl), advanced, metastatic or disseminated solid neoplasms, chronic immunosuppression, pregnancy, or requiring red blood cells transfusion by the underlying disease at the time of inclusion were excluded. A group of ten healthy adult volunteers was included in the study as control group. The study was approved by the Ethics Committee, and patients and control individuals signed an informed consent before inclusion.

Data collection

Patients were followed up for 7 days since inclusion. Arterial and venous blood samples were drawn every 12 hours the first day and daily until day 3rd to immediately determine the pH, base deficit, oxygen saturation, and lactate concentration (ABL80 Basic FLEX, Radiometer, Copenhagen, Denmark). Tissue hypoxia (regional oxygen saturation index) was monitored by noninvasive near infrared spectroscopy (NIRS) at the same time-points (Somanetics Corporation, Troy, Michigan) in the thenar eminence. At inclusion, 3rd and 7th days, venous blood samples were obtained to determine pyruvate, IL-6, IL-10, TNF-α, HIF-1α, PCT, LPC and HLA-DR in circulating monocytes.

Patient charts were review to collect demographics data and chronic underlying diseases (Charlson Comorbidity Index) [26], acute severity scores (SOFA and APACHE II) [27, 28], source of infection, etiology, presence of bacteremia, C-reactive protein (CRP) levels, total leukocytes and neutrophils counts, and antimicrobial and support treatments. Survival or death were recorded during 30 days after inclusion. Death was as related to septic shock if occurred before its resolution; otherwise, was considered unrelated.

Measurements of variables levels

Venous blood samples were obtained (EDTA tube and serum-separating tube) at inclusion, 3rd and 7th days, and centrifuged at 4 °C; serum was aliquoted and stored at 80 °C until the day of assays. IL-6, IL-10, TNF-α, HIF-1α, PCT and LPC serum levels were determined using commercial assays. IL-6, IL-10 and TNF-α levels were measured using enzyme-linked immunosorbent assay (ELISA) test (eBioscience, Vienna, Austria). HIF-1α levels were determined by Sandwich-ELISA Kit (MyBioSource, San Diego, CA, USA). LPC was measured by Azwell LPC Assay Kit (Alfresa Pharma Corporation, Osaka, Japan). LPC was hydrolyzed with lysophospholipase, followed by glycerophosphorylcholine phosphodiesterase and choline oxidase, and hydrogen peroxides were colorimetrically measured in the presence of peroxidase. Serum PCT concentrations were measured in duplicates in accordance with the manufacturer's instructions (Roche Diagnostic, Basel, Switzerland).

Pyruvate levels and HLA-DR in circulating monocytes were determined in whole blood. Pyruvate levels were determined using commercial Pyruvate Assay Kit (Cayman Chemical Company, Ann Arbor, Michigan). HLA-DR expression in circulating monocytes was measured by flow cytometric assay [29]. The used surface markers were FITC anti-Human HLA-DR, APC anti-Human CD56 and PerCP anti-Human CD14 (BioLegend, San Diego, California).

Statistical Analyses

Values were expressed as % or as the median and interquartile range in the continuous variables, and the 95% confidence interval [95% CI] when required. Comparison of patient and control groups medians differences was done by nonparametric Mann-Whitney U Test. Comparison of variables medians in different days in patients was done by nonparametric Wilcoxon signed-rank test. Sensitivity, specificity, and positive and negative predictive values (PPV and NPV) of each parameter were calculated according to standard methods [30]. Binary logistic regression analysis was applied to obtain a model equation that includes the chosen clinical parameters. This logistic regression analysis was used after to obtain a Receiver Operating Characteristic (ROC) curve with a combination of variables. IBM SPSS Statistics 22 statistical software program was used for data processing and analyses. Statistical significance was set at a p-value < 0.05.

Results

Demographics and clinical characteristics of septic shock patients

We prospectively included 20 adults ICU patients meeting the criteria for septic shock and tissue hypoxia. Demographics, underlying diseases and clinical and laboratory data referred to the current infections, severity, and septic shock episodes are in Table 1 and 2. Basal values of severity at inclusion were APACHE II (22.50 points [17.25-31.00]) and SOFA (9.50 points [8.25-12.75]). Regional oxygen saturation index was 59.50% [54.25-68.50]. Twelve patients had had major surgery (60%) previously. Most sources of infection was the intra-abdominal space (n = 16), with two respiratory tract and skin and soft tissue infections each. Etiology of infection was identified in 15 (75%) patients, and two of them had bacteremia. Six patients died during the follow up of 7 days; the overall 30-days mortality was 55%.

Demographics of healthy adult controls

Ten healthy adult volunteers were included in the study as controls to obtain reference values of non-standard determinations (pyruvate, HIF-1α, LPC, PCT, and HLA-DR on circulating monocytes). Age was 58 years [36.5-60.25] and four individuals were female (40%). Table 1 shows demographics data.

Acid-base balance, inflammatory biomarkers, and hypoxia-inducible factor-1 at inclusion and the 7-days follow up

Clinical data and data of the different biomarkers at the basal and follow up time-points are in Table 2. Patients had increased levels of leukocytes, neutrophils, CRP and lactate compared to normal physiological levels on the day of inclusion. These levels decreased during the 7 days follow up. Moreover, patients had lower basal venous pH levels, increasing over time until reach normal levels. Pyruvate levels were higher than in controls on the day of inclusion and they were decreasing during the 7 days, but they didn't reach control levels. In contrast, levels of HLA-DR on circulating monocytes in patients were 1.48 times lower than in controls on the day of inclusion and they diminished at the day 3^{rd} and increased at the day 7^{th}, but they were still lower than in controls. IL-6 and IL-10 levels in patients were much higher than in controls on the day of inclusion with marked reduction at day 3^{rd} by 22.22 and 2.59 times, respectively. TNF-α values were undetectable in 19 patients who received glucocorticoids before the blood collection; in the remaining was 2864.62 pg/ml. PCT levels were higher in patients than in controls, with high variability among patients (range 1.31-284 ng/ml). LPC levels were lower in patients than in control and they increased on the day 3^{rd}. Finally, levels of HIF-1α were higher in patients than in controls due to the tissue hypoxia they suffered and the maximum levels were reached on day 3^{rd}.

Variables differences between survivors and non-survivors

The objective of the study was to early identification of parameters predicting the patient survival. Among all studied variables, those that presented a significant difference between survivors from non-survivors were APACHE II, lactate, pyruvate, IL-6, IL-10 and LPC (Fig. 1). As we were interested in an early prediction of the outcome, we discarded IL-6 because the difference was on the day 7^{th}. The other variables did not show differences between survivors and non-survivors, including the HIF-1α levels and regional oxygen saturation.

Discriminative power of clinical, metabolic and inflammatory biomarkers to predict survival

To assess the discriminative value of clinical, hypoxia and acid-base data, and inflammatory biomarkers, we obtained the ROC curves of those variables that showed significant differences between survivors and non-survivors (Fig. 2A and 2B). Lactate at day 3^{rd} yielded the highest discriminative value, with an area under the curve (AUC) of 0.90 (95% CI 0.73 to 1.00; $p < 0.05$), followed by APACHE II at day 3^{rd} (AUC, 0.84; 95% CI, 0.65-1.00; $p < 0.05$), basal lactate (AUC, 0.82; 95% CI, 0.62-1.00; $p < 0.05$) and LPC at day 3^{rd} (AUC, 0.82; 95% CI, 0.58-1.00; $p < 0.05$) (Fig. 2A and 2B). The discriminative values of the other variables are in Table 3), including the cutoff points for all the parameters to obtain the highest possible values for sensitivity and specificity.

Taking all these data into account, it is possible to make combinations of parameters to obtain better results of sensitivity and specificity, and therefore, better positive and negative predictive values. This approach may increase the clinical usefulness of these biomarkers. Thus, we evaluated the combination of these clinical and biological variables as predictors of survival using binary logistic regression and AUC analysis. The best combinations were basal APACHE II (x_1), lactate (x_2) and pyruvate (x_3) (AUC, 0.91; 95% CI, 0.78-1.00; $p < 0.01$),

(Fig. 2C) and basal APACHE II (x_1), lactate (x_2), pyruvate (x_3) and IL-10 (x_4) (AUC, 0.90; 95% CI, 0.76-1.00; $p < 0.01$) (Fig. 2D). The figures show the equations that include the chosen parameters to obtain a coefficient and determine the patient outcome depending on the selected cutoff. The best cutoff derived from the ROC curves for the first combination was > 0.25 (sensitivity = 100%, specificity = 72.7%, PPV = 75% and NPV = 100%) and for the second combination was > 0.26 (sensitivity = 100%, specificity = 72.7%, PPV = 75% and NPV = 100%). Both combinations increase the results of sensitivity, specificity, and positive and negative predictive values.

Discussion

The results of the present study show that APACHE II score and several biological parameters, as lactate, pyruvate, IL-10 and LPC serum levels, have an early significant difference between survivors and non-survivors in patients with septic shock. Additionally, we explore if the combination of clinical data and biological variables was better in predicting the of survival of septic shock patients. Using a binary logistic regression and AUC analysis we found that the combinations of APACHE II, lactate and pyruvate and that of APACHE II, lactate, pyruvate and IL-10, with cutoffs derived from the ROC curves > 0.25 and > 0.26, respectively, have a negative predictive value for survival of 100%, with a sensitivity of 100%.

Critical care attending physicians have a variety of data that may serve as a guide in discriminating the outcome in newly admitted septic shock patients. Discrimination between infectious (sepsis) and non-infectious conditions (systemic inflammatory response syndrome, SIRS) is better stablished, with the general acceptation of PCT (cutoff of 0.5-1.1 ng/ml) and SOFA (cutoff of 2) as the best markers [13, 31, 32]. However, nowadays, there is not a

defined protocol to predict septic shock patients' outcome. The Third International Consensus Definitions for Sepsis and Septic Shock (Sepsis-3) in 2016 agreed that 3 variables (hypotension, elevated lactate level, and a sustained need for vasopressor therapy) should be test in cohort studies, exploring alternative combinations and different lactate thresholds [32]. Two different studies reported that the combination of hypotension, vasopressor use, and lactate level greater than 2 mmol/L identified patients with mortality rates of 54% at University of Pittsburgh Medical Center and 35% at Kaiser Permanente Northern California. Therefore, it is necessary to look for new better predictor variables. Some studies propose serum PCT on day 5^{th} as a biomarker to identify the clinical outcome of sepsis patients [33-35]. However, our study shows that PCT on the day of inclusion was not a good biomarker because there was a high variability between patients, and no difference between survivors and non-survivors. Moreover, our objective was to find an early biomarker due a recent study showed that the crude mortality rate of septic shock patients is 32% within the first 3 days of ICU admission [36].

The parameters that presented an early significant difference between survivors and non-survivors in our study were APACHE II score and lactate, pyruvate, IL-10 and LPC serum levels. APACHE II has shown to be a good predictor for hospital mortality in ICU patients [37], and our data confirms it. Higher APACHE II score on the 3^{rd} day indicate a worse prognostic in septic shock patients. Lactate and pyruvate are important parameters because they are associated to tissue hypoxia, as we confirmed in our results. Septic shock patients had increased HIF-1α levels, which have been shown to promote cell survival under hypoxia by switching metabolism from oxidative to glycolytic, increasing the flux of glucose to pyruvate [38], which explain why the patients had increased levels of pyruvate compared to controls. Pyruvate is transformed in lactate through anaerobic metabolic pathways causing a lactic acidosis in these patients. It is not known if lactic acid has beneficial or negative effects. A

study showed that lactic acid provoked an increase in TNF-α release in LPS-stimulated peritoneal macrophages [39]. On the other hand, other studies have shown that lactate based dialysis solutions decrease TNF-α synthesis and release [40, 41]. Experiments in LPS-stimulated RAW 264.7 murine macrophages showed that the pH of the cell culture medium alters the release of inflammatory mediators, and acid lactic had anti-inflammatory effect reducing IL-6 and IL-10 expression [42]. Therefore, acidosis may have beneficial effects, but data from clinical studies are very limited. However, our results showed that non-survivors had higher lactate levels on the day of inclusion and on the 3rd day (and higher pyruvate levels on the day of inclusion), indicating a negative outcome effect. Although septic shock patients had higher HIF-1α levels compared to control, we have demonstrated that it is not a biomarker predicting the survival prognosis.

Recent evidences indicate that increased production of pro- and anti-inflammatory cytokines may be used as a marker of poor outcome in septic patients. In fact, IL-10 levels are associated with mortality in these patients (non-survivors had higher levels of IL-10) [43-46]. It seems that patients with septic shock release more IL-10 from monocytes when TNF-α release is down-regulated, what happens in our study probably by the glucocorticoid therapy [47]. This persistent release causes an impairment of monocyte proinflammatory cytokine release and immune dysfunction [48]. Therefore, observing high levels of IL-10 in serum may reflect the immunosuppressive state in these patients and poorer outcomes. In our study, we observed higher levels of basal IL-10 in non-survivors compared to survivors, indicating the excellent prognostic value of this parameter. An important immunomodulatory molecule is LPC, which is generated by inflammatory lipases and involved in immune cell recruitment and stimulation [14, 49]. It is an inflammatory lipid mediator in the septic process because it has a pro-inflammatory effect and promotes an excessive immune response [50]. Recent reports showed that LPC levels on the 7th day [51] and on the days 4th and 11th [52] in patients

with severe sepsis or septic shock was lower in non-survivors than in survivors. Here we have demonstrated that LPC level already on day 3rd may be a useful prognostic marker for septic shock patients.

In this study we show several useful parameters to predict the survival outcome in patients with septic shock. A combination of these parameters allows to obtain a better prognostic value. Thus, the combinations of basal APACHE II score and basal lactate and pyruvate levels (related variables), with or without IL-10, have achieved the best results.

Conclusion

In summary, we have shown in this prospective and observational clinical study that basal APACHE II score, lactate, pyruvate and IL-10 levels, and APACHE II score, lactate and LPC levels on day 3rd have a good ability to discriminate between survivors and non-survivors alone. However, we propose the combination of basal APACHE II score, and serum lactate and pyruvate levels, which strongly predict the survival outcome of septic shock patients and they are parameters widespread used in the current clinical setting. Previous studies usually just focus on biomarkers to predict the outcome of septic shock. However, we propose a scoring system using a combination of biomarkers plus a clinical score which is an innovative approach. A positive correlation was also established between the values of lactate and pyruvate.

Table 1. Demographics and clinical data of Septic Shock Patients at inclusion and the 7-days follow up and Controls.

	Patients (n = 20)	Controls (n = 10)
Age (yr.)	67 [57.30-74.50]	58 [36.50-60.25]
Female sex, n (%)	7 (35%)	4 (40%)
Charlson Index	1.50 [0.00-3.00]	
Source on infection		
Intra-abdominal space	16 (80%)	
Community-acquired pneumonia	2 (10%)	
Skin and soft tissue infection	2 (10%)	
Etiology		
Enterobacteriaceae [a]	8 (40%)	
Stenotrophomonas maltophilia	1 (5%)	
Bacteroides thetaiotaomicron	1 (5%)	
Clostridium spp. [b]	2 (10%)	
Aeromonas veronnii	1 (5%)	
Enterococcus ssp. [c]	2 (10%)	
Staphylococcus aureus	1 (5%)	
Candida albicans	1 (5%)	
Mixed infections	5 (25%)	
No isolates	5 (25%)	
Bacteremia [d]	2 (10%)	
Appropriate antimicrobial therapy [e]	10/15 (66.67%)	
Mechanical ventilation [e]	20 (100%)	
Vasopressor therapy (noradrenalin) [e]	20 (100%)	
Glucocorticoid therapy [e]	19 (95%)	
Death at 7-days	6 (30%)	
Death at 30-days	9 (45%)	

All data expressed as percentage or median and interquartile range.
[a] *Escherichia coli, Enterobacter aerogenes, Klebsiella pneumoniae*; [b] *C. hathewayi, C. inocuum,* [c] *E. faecium, E. faecalis* [d] *E. coli, Clostridium tertium.* [e] In the first 24 hours

Table 2. Clinical severity data, acid-base balance, hypoxia-inducible factor-1, and inflammatory biomarkers at inclusion and the 7-days follow up.

	Control	Basal	Day 3	Day 7	p-value
SOFA (points)	-	9.50 [8.25-12.75]	7.00 [2.50-11]	2.00 [1.00-5-50]	$p < 0.05^b$ $p < 0.01^c$
APACHE II (points)	-	22.50 [17.25-31.00]	12.00 [9.50-19.50]	12.00 [5..0-15.00]	$p < 0.001^a$ $p < 0.05^b$ $p < 0.001^c$
Arterial $SatO_2$ (%)	-	96.75 [95.45-98.05]	96.28 [94.21-98.35]	-	-
$rSatO_2$ (%) [d]	-	58.55 [51.94-65.16]	66.40 [61.91-70.89]	-	$p < 0.01^a$
Lactate (mmol/l)	1.80 [1.58-2.63]	3.65 [2.25-5-23]*	1.30 [1.00-2-00]	-	$p < 0.001^a$
Pyruvate (µM)	8.11 [0.00-15.34]	125.52 [71.14-154.05]***	49.75 [30.08-83.26]***	46.39 [26.28-84.67]**	$p < 0.01^a$ $p < 0.01^c$
Venous Ph	7.33 [7.25-7.36]	7.31 [7.25-7.37]	7.38 [7.35-7.40]]**	-	$p < 0.05^a$
CRP (mg/l)	-	278.25 [186.63-376.90]	218.50 [113.35-321.00]	189.65 [127.50-259.55]	$p < 0.05^a$
Leukocytes (1000 cells/µl)	-	16.56 [5.13-20.52]	12.85 [10.65-20.93]	14.01 [10.77-16.94]	-
Neutrophils (1000 cells/µl)	-	13.10 [4.33-19.35]	10.70 [8.95-18.15]	11.70 [8.68-14.55]	-
HIF-1α (pg/ml)	115.08 [23.97-449.58]	443.18 [116.44-715.72]	448.54 [311.65-654.56]*	348.15 [158.07-534.34]	NS
IL-6 (pg/ml)	0.14 [0.00-0.39]	713.48 [28.58-1102.82]***	32.11 [1.12-125.55]**	27.63 [4.55-54.21]***	$p < 0.001^a$ $p < 0.05^b$ $p < 0.001^c$
IL-10 (pg/ml)	0.00 [0.00-1.48]	46.15 [19.31-234.38]***	17.84 [6.50-39.85]***	3.52 [0.35-11.69]*	$p < 0.05^a$ $p < 0.05^b$ $p < 0.05^c$

HLA-DR (%)	88.09 [80.19-95.99]	59.14 [47.20-71.09]**	33.64 [22.86-44.43]***	44.19 [31.29-57.10]***	$p < 0.05^{a}$
PCT (ng/ml)	0.03 [0.02-0.05]	47.09 [22.88-113.56]***	-	-	-
LPC (µM)	203.37 [158.80-240.65]	24.35 [18.24-34.95]***	54.74 [30.06-63.36]***	-	$p < 0.05^{a}$

All data expressed as percentage or median and interquartile range.
[a] Basal data *vs.* day 3 data comparison; [b] Day 3 data *vs.* day 7 data comparison; [c] Basal data *vs.* day 7 data comparison. Wilcoxon signed-rank test; [d] $rSatO_2$ regional oxygen saturation index. *p<0.05, compared with controls; **p<0.01, compared with controls; ***p<0.001, compared with controls. Mann-Whitney U Test. NS, non-significant.

Table 3. Diagnostic performance of different metabolic, severity sepsis biomarkers.

	Lactate Basal	Lactate Day 3	Pyruvate Basal	APACHE II Basal	APACHE II Day 3	IL-10 Basal	LPC Day 3
Cutoff value*	> 4 mM	> 2 mM	> 135 µM	> 21 points	> 13 points	> 61 pg/ml	< 26 µM
Sensitivity, %	77.8	75	77.8	88.9	83.3	66.7	66.7
Specificity, %	81.8	90.9	81.8	63.6	72.7	81.8	100
PPV, %	77.8	75	77.8	66.7	62.5	75	100
NPV, %	81.8	90.9	81.8	87.5	88.9	75	84.6
AUC (95% CI)	0.82 (0.62-1.00)	0.90 (0.73-1.00)	0.80 (0.58-1.00)	0.74 (0.51-0.96)	0.84 (0.65-1.00)	0.77 (0.56-0.98)	0.82 (0.58-1.00)

* Sensitivity, specificity and predictive values are referred to each cutoff, which represented the best discrimination values as derived from the ROC curves. PPV, positive predictive value; NPV, negative predictive value; AUC, area under ROC curve; ROC, Receiver Operating Characteristic; LPC, lysophosphatidylcholine.

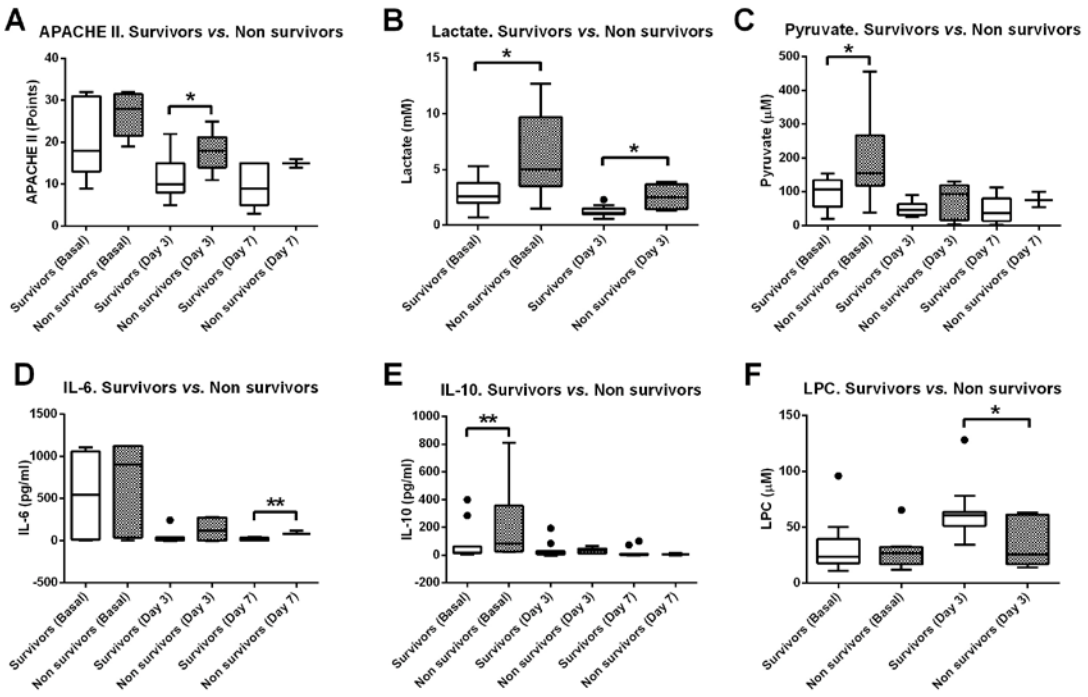

Figure 1. Variables with significant difference between survivors and non-survivors in the follow up (Wilcoxon signed-rank test. *$p < 0.05$; **$p < 0.001$).

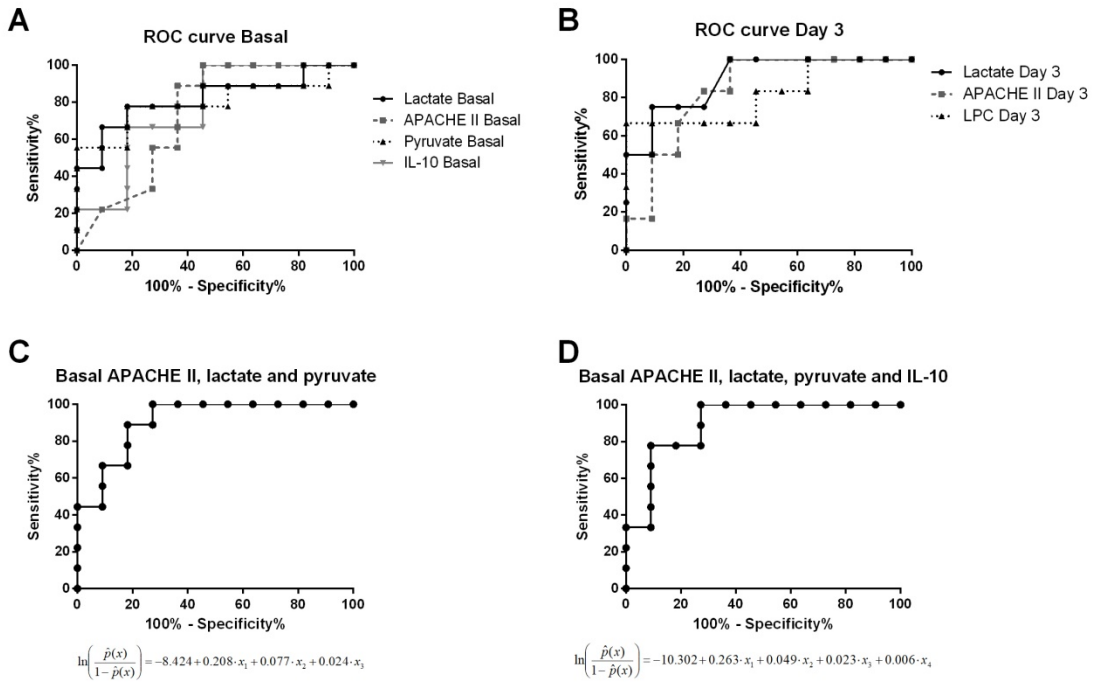

Figure 2. A. ROC curves for parameters with significant differences between survivors and non-survivors at the day of inclusion (lactate, APACHE II, pyruvate and IL-10). **B.** ROC curves for parameters with significant differences between survivors and non-survivors on the 3rd day (lactate, APACHE II and LPC). **C.** ROC curves of a combination of parameters in a binary logistic regression with the corresponding equation [basal APACHE II (x_1), lactate(x_2) and pyruvate (x_3)]. **D.** ROC curves of a combination of parameters in a binary logistic regression with the corresponding equation [basal APACHE II (x_1), lactate (x_2), pyruvate (x_3) and IL-10 (x_4)].

References

1. Fleischmann C, Scherag A, Adhikari NK, et al. Assessment of global incidence and mortality of hospital-treated sepsis – Current estimates and limitations. Am J Respir Crit Care Med 2015; 193:259-272
2. Annane D, Bellissant E, Cavaillon JM. Septic shock. Lancet 2005; 365:63-78
3. Glauser MP, Zanetti G, Baumgartner JD, et al. Septic shock: pathogenesis. Lancet 1991; 338:732-736
4. Kasper DL, Hauser SL, Jameson JL, Fauci AS, Longo DL, Loscalzo J (Eds): Harrison's principles of internal medicine. Mc Graw Hill Education, 19th Edition 2015
5. De Backer D, Orbegozo Cortes D, Donadello K, et al. Pathophysiology of microcirculatory dysfunction and the pathogenesis of septic shock. Virulence 2014; 5:73-79
6. Martin GS, Mannino DM, Eaton S, et al. The epidemiology of sepsis in the United States from 1979 through 2000. N Engl J Med 2003; 348:1546-1554
7. Walkey AJ, Lagu T, Lindenauer PK. Trends in sepsis and infection sources in the United States. A population-based study. Ann Am Thorac Soc 2015; 12:216-220
8. Rangel-Frausto MS, Pittet D, Hwang T, et al. The dynamics of disease progression in sepsis: Markov modeling describing the natural history and the likely impact of effective antisepsis agents. Clin Infect Dis 1998; 27:185-190
9. Annane D, Aegerter P, Jars-Guincestre MC, et al. Current epidemiology of septic shock: the CUB-Rea Network. Am J Respir Crit Care Med 2003; 168:165-172
10. Parrillo JE. Pathogenetic mechanism of septic shock. N Engl J Med 1993; 328:1471-1477

11. Rivers E, Nguyen B, Havstad S, et al. Early goal-directed therapy in the treatment of severe sepsis and septic shock. N Engl J Med 2001; 345:1368-1377
12. Meisner M. Biomarkers of sepsis: clinically useful? Curr Opin Crit Care 2005; 11:473-480
13. Harbarth S, Holeckova K, Froidevaux C, et al. Diagnostic value of procalcitonin, interleukin-6, and interleukin-8 in critically ill patients admitted with suspected sepsis. Am J Respir Crit Care Med 2001; 164:396-402
14. Cho WH, Park T, Park YY, et al. Clinical significance of enzymatic lysophosphatidylcholine (LPC) assay data in patients with sepsis. Eur J Clin Microbiol Infect Dis 2012; 31:1805-1810
15. Gibot S, Béné MC, Noel R, et al. Combination biomarkers to diagnose sepsis in the critically ill patient. Am J Respir Crit Care Med 2012; 186:65-71
16. Mikkelsen ME, Miltiades AN, Gaieski DF, et al. Serum lactate is associated with mortality in severe sepsis independent of organ failure and shock. Crit Care Med 2009; 37:1670-1677
17. Ugarte H, Silva E, Mercan D, et al. Procalcitonin used as a marker of infection in the intensive care unit. Crit Care Med 1999; 27:498-504
18. Tang BM, Eslick GD, Craig JC, et al. Accuracy of procalcitonin for sepsis diagnosis in critically ill patients: systematic review and meta-analysis. Lancet Infect Dis 2007; 7:210-217
19. Nguyen HB, Rivers EP, Knoblich BP, et al. Early lactate clearance is associated with improved outcome in severe sepsis and septic shock. Crit Care Med 2004; 32:1637-1642

20. Suistomaa M, Ruokonen E, Kari A, et al. Time-pattern of lactate and lactate to pyruvate ratio in the first 24 hours of intensive care emergency admissions. Shock 2000; 14:8-12
21. Levy B, Sadoune LO, Gelot AM, et al. Evolution of lactate/pyruvate and arterial ketone body ratios in the early course of catecholamine-treated septic shock. Crit Care Med 2000; 28:114-119
22. Zhou J, Song J, Gong S et al. Persistent hyperlactatemia-high central venous-arterial carbon dioxide to arterial-venous oxygen content ratio is associated with poor outcomes in early resuscitation of septic shock. Am J Emerg Med 2017; 35:1136-1141
23. Rodriguez A, Lisboa T, Martín-Loeches I, et al. Mortality and regional oxygen saturation index in septic shock patients: A Pilot Study. J Trauma 2011; 70:1145-1152
24. Bhandari T, Nizet V. Hipoxia-Inducible Factor (HIF) as a pharmacological target for prevention and treatment of infectious diseases. Infect Dis Ther 2014; 3:159-74
25. Zinkernagel AS, Johnson RS, Nizet V. Hipoxia inducible factor (HIF) function in innate immunity and infection. J Mol Med 2007; 85:1339-1346
26. Charlson ME, Pompei P, Ales KL, et al. A new method of classifying prognostic comorbidity in longitudinal studies: development and validation. J Chronic Dis 1987; 40:373-383
27. Vincent JL, Moreno R, Takala J, et al. Working group on sepsis-related problems of the European Society of intensive care medicine. The SOFA (Sepsis-related Organ Failure Assessment) score to describe organ dysfunction/failure. Intensive Care Med 1996; 22:707-710

28. Knaus WA, Draper EA, Wagner DP, et al. APACHE II: a severity of disease classification system. Crit Care Med 1985; 13:818–829
29. Giménez E, Blanco-Lobo P, Muñoz-Cobo B, Solano C, Amat P, Pérez-Romero P, Navarro D. Role of cytomegalovirus (CMV)-specific polyfunctional CD8+ T-cells and antibodies neutralizing virus epithelial infection in the control of CMV infection in an allogeneic stem-cell transplantation setting. J Gen Viro. 2015; 96:2822-2831.
30. Farr BM, Shapiro DE. Diagnostic tests: distinguishing good tests from bad and even ugly ones. Infect Control Hosp Epidemiol 2000; 21:278–284
31. Taylor R, Jones A, Kelly S, et al. A review of the value of procalcitonin as a marker of infection. Cureus 2017; 9:e1148
32. Singer M, Deutschman CS, Seymour CW, et al. the third international consensus definitions for sepsis and septic shock (Sepsis-3). JAMA 2016; 315:801-810
33. Rebello A, Thabah MM, Dutta TK, et al. Procalcitonin levels in sepsis and its association with clinical outcome in southern India. Trop Doct 2017; 47:331-336
34. Poddar B, Gurjar M, Singh S, et al. Procalcitonin kinetics as a prognostic marker in severe sepsis/septic shock. Indian J Crit Care Med 2015; 19:140-146
35. Ríos-Toro JJ, Márquez-Coello M, García-Álvarez JM, et al. Soluble membrane receptors, interleukin 6, procalcitonin and C reactive protein as prognostic markers in patients with severe sepsis and septic shock. Plos One 2017; 12:e0175254
36. Daviaud F, Grimaldi D, Dechartres A, et al. Timing and causes of death in septic shock. Ann Intensive Care 2015; 5:16
37. Godinjak A, Iglica A, Rama A, et al. Predictive value of SAPS II and APACHE II scoring systems for patient outcome in a medical intensive care unit. Acta Med Acad 2016; 45:97-103

38. Drazen JM. Physiological effects of chronic hypoxia. N Engl J Med 2017; 376:1965-1971
39. Jensen JC, Buresh C, Norton JA. Lactic acidosis increases tumor necrosis factor secretion and transcription in vivo. J Surg Res 1990; 49:350-353
40. Jörres A, Gahl GM, Frei U. In vitro studies on the effect of dialysis solutions on peritoneal leukocytes. Perit Dial Int 1995; 15:S41-S45
41. Douvdevani A, Abramson O, Tamir A, et al. Commercial dialysate inhibits TNF-α mRNA expression and NK-κβ DNA-binding activity in LPS-stimulated macrophages. Kidney Int 1995; 47:1537-1545
42. Kellum JA. Metabolic acidosis in patients with sepsis: epiphenomenon or part of the pathophysiology? Crit Care Resusc 2004; 6:197-203
43. Wu HP, Chu CM, Kao KC, et al. High interleukin-10 expression in Type 2 T Helper cells in septic patients. Immunol Invest 2017; 46:385-394
44. Leonidou L, Mouzaki A, Michalaki M, et al. Cytokine production and hospital mortality in patients with sepsis-induced stress hyperglycemia. J Infect 2007; 55:340-346
45. Hynninen M, Pettilä V, Takkunen O, et al. Predictive value of monocyte histocompatibility leukocyte antigen-DR expression and plasma interleukin-4 and -10 levels in critically ill patients with sepsis. Shock 2003; 20:1-4
46. Wu HP, Chen CK, Chung K, et al. Serial cytokine levels in patients with severe sepsis. Inflamm Res 2009; 58:385-393
47. Sfeir T, Saha DC, Astiz M, et al. Role of interleukin-10 in monocyte hyporesponsiveness associated with septic shock. Crit Care Med 2001; 29:129-133
48. Brattsand R, Linden M. Cytokine modulation by glucocorticoids: mechanisms and actions in cellular studies. Aliment Pharmacol Ther 1996; 10

49. Parra Millán R, Jiménez Mejías ME, Sánchez Encinales V, et al. Efficacy of lysophosphatidylcholine in combination with antimicrobial agents against *Acinetobacter baumannii* in experimental murine peritoneal sepsis and pneumonia models. Antimicrob Agents Chemother 2016; 60:4464-4470
50. Kabarowski JH, Xu Y, Witte ON. Lysophosphatidylcholine as a ligand for immunoregulation. Biochem Pharmacol 2002; 64:161-167
51. Park DW, Kwak DS, Park YY, et al. Impact of serial measurements of lysophosphatidylcholine on 28-day mortality prediction in patients admitted to the intensive care unit with severe sepsis or septic shock. J Crit Care 2014; 29:882.e5–882.e11
52. Drobnik W, Liebisch G, Audebert FX, et al. Plasma ceramide and lysophosphatidylcholine inversely correlate with mortality in sepsis patients. J Lipid Res 2003; 44:754-761

Final Discussion

DISCUSSION

Antimicrobial resistance in Gram-negative pathogens causing nosocomial infections is nowadays a major public health concern due to the emergence of MDR strains and the lack of active antibiotics. The increasing problem of MDR is not followed by the development of novel antimicrobials. Hence, there is an important need to develop new strategies to combat this kind of infections.

First step is to have a better understanding of microbial pathogenesis. During the course of infection, bacteria are found in different microenvironments which influence bacterial pathogenesis and virulence factors expression. The focus of infection is usually a hypoxic environment [140], so understanding bacterial behavior under hypoxia could help to discover new targets to develop antimicrobials. Moreover, studying the consequences of systemic hypoxia and bacterial infection acting together is highly relevant to some clinical situations in which both situations co-exist, such as the Adult Respiratory Distress Syndrome (ARDS) [160], or a systemic hypoxia and bacterial colonization of the airways occurs, like in chronic obstructive pulmonary disease (COPD) or CF [161, 162].

Then, our work in this doctoral thesis is focused on the study of bacterial pathogenesis under hypoxia. To increase the knowledge of impact of the hypoxia in the clinical setting, we have also studied septic shock patients which suffer from tissue hypoxia. The results obtained will be discussed below.

Chapter I. Article I. Comparative gene expression profile of *Acinetobacter baumannii* growing under microaerobiosis and normoxia.

Nowadays, identifying bacterial virulence factor is an important research line due to the high rate of MDR bacteria emergence. The determation of new antibiotic targets is increasing in importance because of the lack of new compounds and omics technologies are facilitating the elucidation of key components in multiple bacterial functions. Transcriptomic analysis, as RNA-seq, permit the quantification of RNA levels and the characterization of important bacterial factors for survival or to infect [163]. Liu et al. [164] showed the critical role of OtpR in regulating *Brucella melitensis* metabolism and virulence under acidic stress using this technique. Another study used differential RNA-seq of wild-type *Vibrio cholerae* and a locked low-cell-density QS-mutant strain to identify the VqmR small RNA as a regulator of biofilm formation and virulence [165].

In our study we identified multiple genes that were upregulated under microaerobiosis. We selected five of them (*A1S_0030*, *A1S_2532*, *A1S_0464*, *A1S_0172* and *A1S_2448*) to check out their potential role as virulence factors. First of all, we determined their growth rate in MHB and minimal medium M9 under normoxia and hypoxia, and under microaerobiosis in the case of MHB. We did not find significant differences in the growth between mutants and the wild-type strain (Fig. 3 and Fig. A1, Art.I). Secondly, we evaluated the extracellular bacterial concentration of the mutants in a A549 cells infection at 2 and 24 h under normoxia and hypoxia 1%O_2. We just found significant differences in the mutant *A1S_2448* (Fig. 4 and Fig. A2, Art. I). We showed that bacterial adherence was decreased in all the mutant strains at 2 h post-infection (Fig. 4 and Fig. A3, Art. I), but bacterial invasion was just decreased in the mutants *A1S_0030*, *A1S_2532*, *A1S_02448* at 24 post-infection (Fig. 4 and Fig A4, Art. I). However, the

mutant *A1S_02448* (*pstS*) showed the most promising results. For this reason, we continue with the analysis only with this mutant strain.

PstS is involved in phosphate uptake in different bacteria [166]. A PstS overexpression leads to a PhoB activation which regulates the expression of multiple genes [167]. Inorganic phosphate is a very essential limiting nutrient. Thus, mutations in the *pst* operon may affect metabolic and physiological processes, and the expression of some virulence genes. Many lines of evidence suggest that the Pho regulon and the bacterial stress response and virulence are connected [168]. Lamarche et al. [169] determined that the *pst* mutation affects different virulence attributes, such a reduction in the resistance to the bactericidal effect of serum, to acidity and to cationic antimicrobial peptides (polymyxin). Proteome studies of *Edwardsiella tarda* wild-type strain and its *pst* mutant revealed that the T3SS proteins as well as other virulence proteins were absent in the mutant, suggesting that *pst* mutation causes a bacterial cell surface modification [170]. This might explain why the *pstS* mutant is less adherent and invasive than the wild-type strain (Fig. 4, Art. I). However, we have not found any differences in antibiotic susceptibility or permeability between wild-type and *pstS* mutant strains (data not shown).

PstS is a phosphate transporter, but it is also a highly immunogenic protein that induces Th1 immunity [171] and antibody responses. A previous study also indicated that mice immunized with a recombinant form of the Streptococcus mutans PstS protein exhibited protective antibody response, demonstrating its potential as an immunogen in vaccine strategies [172]. Therefore, it seems that PstS is not only a bacterial virulence factor, regulating adherence, invasion, biofilm formation and motility (Fig. 4 and 5, Art. I), but also a potential vaccine.

There are multiple clinical situations that induce hypophosphatemia, as sepsis [173]. During sepsis, the high density of immune cells and bacteria increase oxygen consumption. This situation together with a decreased perfusion generate an hypoxic state [174]. Both acute and chronic hypoxia are conditions that promote hypophosphatemia [175, 176], maintaining this hypophosphatemic condition. Orihuela et al. [177] demonstrated a twofold increase of PstS expression in *S. pneumoniae* in a murine peritoneal culture model due the low concentration of phosphate present the peritoneum. This study suggests that phosphate acquisition is necessary for survival *in vivo*, and PstS might be an important *A. baumannii* virulence factor.

Chapter II. Article II. Effect of hypoxia on the pathogenesis of *Acinetobacter baumannii* and *Pseudomonas aeruginosa in vitro* and in murine experimental models of infections.

It is known that hypoxia, through HIF-1α, regulates both host cells and bacteria, influencing the outcome of infection. We observed that HIF-1α is an important cellular factor and its levels increase in cell cultures under hypoxia, reaching a maximum concentration after 6 h. Therefore, cellular response to hypoxia seems to be pretty fast. When cells are under hypoxic condition they start to produce active HIF-1α and it regulates multiple genes [178] but it looks like a negative feedback on HIF-1α expression over time does exist because HIF-1α levels decrease after 24 h. Thence, hypoxia affects the course of acute infections through HIF-1α expression and this effect can last for a long period of time during chronic inflammation due to the multiple signaling pathways that are activated [140, 179].

In this study we observed that hypoxia does not affect the *in vitro* growth of *A. baumannii* and *P. aeruginosa* (Fig. 1A, Art II). Nevertheless, several studies have shown that hypoxia decelerates the progress of infection. Thompson et al. [180] reported that acute hypoxia increased mortality in a pneumonia model by *S. pneumoniae*. However, expositions of animals to hypoxia prior infection changed bone marrow leukocytes, repressing HIF pathway and glycolysis genes, and protected against the infection. HIF-1α also seem to mediate the functional reprogramming of monocytes in sepsis, enhancing protective actions like phagocytosis, tissue re-modeling and antimicrobial activity [181]. Another study showed that HIF-1α-deficient macrophages have a hampered metabolic adaptation to hypoxia resulting in a decreased motility and reduced capacity to clear bacterial infection [122]. Moreover, VEGF secretion is

increased under hypoxia which enhance vascular permeability and allow immune cells to access to the focus of infection [182].

Hypoxia also influences adaptive immunity, e.g. hypoxia-induced signaling pathways stimulate the proliferation and differentiation of regulatory T cells [183]. In summary, hypoxia affects host response to infection because it regulates both innate and adaptive immune responses, and it also affects to the environment in the foci of infection. Therefore, hypoxia increases bactericidal activity of host cells and that is the reason why hypoxia hinders infection progress. Our study confirms these results in two different cell cultures (A549 and RAW 264.7) and using two different pathogens (*A. baumannii* and *P. aeruginosa*), proving that hypoxia effect is not restricted to a specific kind of cells or to a pathogen (Fig. 1B, 1C, Art. II). The treatment with DMOG, a HIF-1α stabilizer that mimic the hypoxia condition, also showed an increase in the bactericidal activity of epithelial and macrophage cells (Fig. 1B, 1C, Art. II). However, the increase in the bactericidal activity wasn't as higher as in the hypoxia condition. This could be due to the missing effect of hypoxia on the bacteria and to the fact that hypoxia regulates other eukaryotic genes more than HIF-1α.

Different studies have reported hypoxia effect on bacteria. Hypoxia reduces the pathogenicity of *P. aeruginosa* by decreasing the expression of virulence factors as the siderophores pyoverdine, pyochelin [154], and pyocyanin [184]. Pyocyanin induces reactive oxygen species (ROI)-mediated lysosomal dysfunction and neutrophil apoptosis [185], so under hypoxia neutrophil apoptosis is decreased and they can help to clear the infection. Another study showed that the exposure to hypoxia leads to downregulation of RNA and the protein biosynthetic machinery of *Mycobacterium tuberculosis*, impairing its growth [186]. Therefore, hypoxia manages to slow down the course of infection altering host response as well as bacterial activity.

Our study also showed that hypoxia decreased *A. baumannii* and *P. aeruginosa* adherence to host cells (A549 and RAW 264.7) and invasion, demonstrating again the global character of hypoxia influence on different host cells and pathogens (Fig. 2A, 2B, 2C, 2D, Art. II). This reduction in bacterial adherence and invasion is due hypoxia effect on bacterial and host cell gene/protein expression. The iTRAQ experiment that we performed in an infection of A549 cells by *A. baumannii* ATCC 17978 showed a total of 174 *A. baumannii* proteins identified as differentially expressed (51 proteins were subexpressed and 123 were overexpressed under hypoxia) (Table S1, A1, Art. II). This accounts for almost 5% of the *A. baumannii* ATCC 17978 genome. Some of the proteins that were subexpressed have been described to be involved in adherence to host cell, as OmpW [187], Putative ferric siderophore receptor protein *A1S_3339*, Putative ferric siderophore receptor protein *A1S_0474*, Ferric enterobactin receptor *A1S_0981*, Ferrichrome-iron receptor *A1S_1921* [188-190] and the hypothetical protein *A1S_3900* which has a SH3 domain [191]. Therefore, this subexpression under hypoxia would explain why bacterial adherence decreases under this condition. Moreover, we also found 73 A549 proteins identified as differentially expressed (33 proteins were subexpressed and 40 were overexpressed under hypoxia) (Table A2, A3, Art. II). Between the subexpressed proteins, we find proteins that are involved in the cytoskeleton structure (TSKS, GAS2L1, ACTBL2, SEPT9 and USH1G) and in the transport through the cytoskeleton (DNAH8, KIF14, MYO5A and BET3L). DNAH8 is an axonemal dynein and KIF14 is a kinesin. Dynein and kinesin are motor proteins involved in transporting cellular cargoes toward opposite ends of microtubule net [192]. In epithelial cells, microtubule accumulation is accompanied by the recruitment of both kinesin and dynein to transport vacuoles that contain *Salmonella enterica* serovar Typhimurium [193]. MYO5A is a myosin Va that can bind to both actin and

microtubules resulting in the formation of cross-linked gels of microtubules and actin [194]. Wang et al. [195] reported that the actin cytoskeleton of the T84 epithelial cells was required for *Neisseria gonorrhoeae* invasion into and traversal through the cells. Furthermore, microtubule inhibitors blocked the traversal movement of the bacteria and the inhibition of the motor activity of myosins reduced both invasion and traversal. Therefore, the subexpression of these motor proteins under hypoxia might be an explanation of why hypoxia decreases bacterial invasion.

All the results that we obtained *in vitro* were also confirmed *in vivo* in a sepsis model by *A. baumannii* and a pneumonia model by *P. aeruginosa*. Hypoxia *in vivo* diminished bacterial load in fluids and tissues (Table 1, 2, Art. II), which may be due to the increase in the bactericidal activity as well as the decrease in the bacterial adherence and invasion. However, mice survival time was shorter under hypoxia (Fig. 3A, Art. II). It is known that adaptation to hypoxia depends on co-ordinated metabolic responses that maintain ATP production and modify energy requirements. Thompson et al. [180] reported that animals infected in the setting of acute hypoxia switched towards carbohydrate utilization, increasing glycolysis pathway, in contrast to normoxia where carbohydrates and fat were consumed. Therefore, hypoxic mice displayed a loss of liver glycogen. Infection combined with acute hypoxia resulted in a negative energy state with increased serum ketone production, loss of white and brown adipose tissue, and lower circulating glucose levels. For this reason, in our study animals that were infected under acute hypoxia (from 6 h before infection until animal death) died before the ones that were under normoxia. However, hypoxic preconditioning for a longer time rescued the animals from this negative energy state and allowed a restoration of proportionate carbohydrate and fat consumption, liver glycogen reserves and fat mass, reduction in circulating ketones and a restoration of glucose levels [180]. We also showed that

maintaining the mice just 6 h under hypoxia before the infection was enough to reduce bacterial load and increased survival time, proving the effect of hypoxia on the outcome of infection.

In conclusion, hypoxia is a common feature in the site of infection and has implications in the development of bacterial infection. As multidrug resistant bacterial infections are a worldwide problem, a better understanding of the interplay host-pathogen could provide new drugs targets for the treatment of these pathogens [196] and new methods to alter the hypoxic response, boosting endogenous immunity. Thus, targeting the host response in combination with an anti-microbial strategy could improve outcomes where hypoxia and infection co-exist.

Chapter III. Article III. Predictive value of APACHE II, and serum lactate, pyruvate, IL-10 and lysophosphatidylcholine levels on survival in patients with septic shock

Despite the development of diagnostic and therapeutic methods, the mortality of sepsis and septic shock remains high [197, 198]. It is important to diagnose these patients and predict the outcome as soon as possible because early resuscitation and intensive care can increase survival rate [199, 200]. Therefore, the early detection of sepsis/septic shock and the prediction of the outcome are essential in the emergency department. Nowadays, various diagnostic tools are being used but there is no gold standard guideline to predict the outcome of these patients. Moreover, the definition of sepsis/septic shock was recently revised in the Third International Consensus Definitions for Sepsis and Septic Shock (Sepsis-3) in 2016 [201]. They proposed a combination of three variables (hypotension, elevated lactate level, and a sustained need for vasopressor therapy) to identify septic shock that should be tested. However, these variables just identified patients with mortality rates of 54% and 35% in two different studies. Therefore, there is an urgent need of new predictor tools.

Several studies have proposed serum PCT [202] or CPR [203], nevertheless their values may be elevated in clinical settings without sepsis, and they often fail to provide reliable prediction of the patient outcome. Our study confirmed that PCT was not a good biomarker because of its high variability between patients. Another study reported that serum amyloid P might be used for prediction of mortality in adults with bacterial sepsis [204]. Serum amyloid P diminish neutrophil recruitment and adhesion, activates the complement pathway, inhibits monocyte differentiation into fibrocytes, and promotes phagocytosis [205]. Serum amyloid P is secreted and catabolized by the liver, so it

could be also decreased in patients with liver insufficiency. Therefore, further studies are required.

Searching for new biomarkers is a difficult task. Nowadays, omics technologies allow high-throughput screening of biomarkers and they are being used in this field too [206]. Another study reported Secretory Phospholipase A2 Group IIA (sPLA2-IIA), which is a protein that is triggered in response to inflammation, to be a potential biomarker to distinguish sepsis from other disease entities. However, further study is warranted to identify predictive value of trends in sPLA-IIA during the course of the disease [207]. Prognostic value of secretoneurin in patients with septic shock has also been studied. Secretoneurin influences cardiomyocyte calcium handling, and serum secretoneurin levels seem to improve risk prediction in patients with myocardial dysfunction. Therefore, secretoneurin would provide early prognostic information in patients with septic shock because these patients are hemodynamically unstable [208]. Pan et al. [209] reported that peripheral perfusion index and proportion of perfusion vessel change rate from sublingual microcirculation monitoring in septic shock patients were related to lactate clearance and combining these two parameters to assess microcirculation might predict organ dysfunction and 28-day mortality in patients with septic shock. In summary, there are a lot of different studies which analyze very different kind of new biomarkers to predict the prognosis in septic shock patients, but it is still an unsolved challenge.

In our study all the patients suffered from tissue hypoxia due to the hypoperfusion they experienced. We confirmed it measuring regional oxygen saturation by NIRS (Table 1, Art. III) and serum HIF-1α levels, which were higher than in controls (Fig. 1A, Art. III). However, HIF-1α levels were not a good biomarker to predict the outcome of these patients because there were no significant differences between survivors and non-

survivors (Fig. 1B, Art. III). However, APACHE II, lactate, pyruvate, IL-6, IL-10 and LPC presented an early significant difference between survivors and non-survivors (Fig. 2A, 2B, 2C, 2D, 2E, 2F, Art. III). Lactate and pyruvate levels were also higher than in controls due to the effect of hypoxia (Table 1, Art. III), and levels were higher in non-survivor patients. The same happened to the APACHE II score.

Septic shock patients show a systemic hyperinflammatory response at the beginning that is followed by an immunosuppressive phase during which multiple organ dysfunction occur and patients are susceptible to nosocomial infection [210]. During this state of functional immunosuppression, a decreased production of both pro- and anti-inflammatory cytokines, a reduced monocyte HLA-DR expression, and a decreased immunocompetent cell count are present [211]. In our study IL-10 levels at the day of inclusion were higher in non-survivor patients, which indicated that these patients were in an advanced septic shock state and the outcome would be worse (Fig. 2E, Art. III). Finally, the levels of the immunomodulatory molecule LPC, that has a pro-inflammatory effect and promotes an exorbitant immune response [212], were also higher in non-survivors on day 3rd after inclusion (Fig. 2F, Art. III).

Having into account all the biomarkers and clinical scores that showed a significant difference between survivors and non-survivors, we proposed that the best combination was basal APACHE II score and basal lactate and pyruvate levels, which are available in the clinical setting, with cutoffs of >21 points, >4 mM and >135 μM, respectively (Table 2, Art. III).

Conclusions

CONCLUSIONS

1. Differences in gene expression were observed between normoxia and microaerobiosis in *A. baumannii* ATCC 17978, being the gene pstS overexpressed under microaerobiosis.
2. The loss of the phosphate sensor pstS produces a decrease in adherence, invasion, motility and biofilm formation in *A. baumannii* ATCC 17978, supporting its role as *A. baumannii* virulence factor.
3. Hypoxia increases HIF-1α levels and the bactericidal activity of host cells and reduces the adherence and invasion of *A. baumannii* and *P. aeruginosa*.
4. The mice survival time is significantly different between hypoxia and normoxia in murine models, being shorter under hypoxia due to the negative energy state that animals experiment.
5. Patients with septic shock have a marked and prolonged peripheral tissue hypoxia.
6. Although septic shock patients suffer from tissue hypoxia, HIF-1α level is not a sensitive biomarker to predict the outcome, with no differences between survivors and non-survivors.
7. The combination of basal APACHE II, and serum lactate and pyruvate is the best score system to predict the outcome of septic shock patients, which is an innovative approach because it includes available biomarkers in the clinical setting and a widespread used clinical score.

REFERENCES

1. Zaragoza R, Ramírez P, López-Pueyo MJ. Nosocomial infections in intensive care units. Enferm Infecc Microbiol Clin. 2014; 32:320-7.
2. European Centre for Disease Prevention and Control. Annual Epidemiological Report. Antimicrobial Resistance and Healthcare Associated Infections. 2014.
3. Chopra I, Schofield C, Everett M, O'Neill A, Miller K, Wilcox M, Frère JM, Dawson M, Czaplewski L, Urleb U, Courvalin P. Treatment of health-care-associated infections caused by Gram-negative bacteria: a consensus statement. Lancet Infect Dis. 2008; 8:133-9.
4. Peleg AY, Hooper DC. Hospital-Acquired Infections Due to Gram-Negative Bacteria. N Engl J Med. 2010; 362:1804-13.
5. Kung HC, Hoyert DL, Xu J, Murphy SL. Deaths: final data for 2005. Natl Vital Stat Rep. 2008; 56:1-120.
6. Roberts RR, Scott RD 2nd, Hota B, Kampe LM, Abbasi F, Schabowski S, Ahmad I, Ciavarella GG, Cordell R, Solomon SL, Hagtvedt R, Weinstein RA. Costs attributable to healthcare-acquired infection in hospitalized adults and a comparison of economic methods. Med Care. 2010; 48:1026-35.
7. Enne VI, Personne Y, Grgic L, Gant V, Zumla A. Aetiology of hospital-acquired pneumonia and trends in antimicrobial resistance. Current opinion in pulmonary medicine. 2014; 2:252-8.
8. Nair GB, Niederman MS. Ventilator-associated pneumonia: present understanding and ongoing debates. Intensive care medicine. 2015; 41:34-48.
9. Kaye KS, Marchaim D, Chen TY, Baures T, Anderson DJ, Choi Y, Sloane R, Schmader KE. Effect of nosocomial bloodstream infections on mortality, length of stay, and hospital costs in older adults. J Am Geriatr Soc. 2014; 62:306-11.

10. Hidron AI, Edwards JR, Patel J, Horan TC, Sievert DM, Pollock DA, Fridkin SK; National Healthcare Safety Network Team; Participating National Healthcare Safety Network Facilities. NHSN annual update: antimicrobial-resistant pathogens associated with healthcare associated infections: annual summary of data reported to the National Healthcare Safety Network at the Centers for Disease Control and Prevention, 2006-2007. Infect Control Hosp Epidemiol 2008; 29:996-1011. [Erratum: Infect Control Hosp Epidemiol 2009; 30:107.]
11. Gaynes R, Edwards JR. Overview of nosocomial infections caused by gramnegative bacilli. Clin Infect Dis 2005; 41:848-54.
12. Lõivukene K, Kermes K, Sepp E, Adamson V, Mitt P, Kallandi U, Otter K, Naaber P; European Antimicrobial Resistance Surveillance System, Estonian Study Group. Surveillance of antimicrobial resistance of invasive pathogens: the Estonian experience. Euro Surveill 2006; 11: 47-9.
13. Bonn D. Antimicrobial resistance rising in Europe. Lancet Infect Dis 2007; 7: 86.
14. Doi Y, Bonomo RA, Hooper DC, Kaye KS, Johnson JR, Clancy CJ, Thaden JT, Stryjewski ME, van Duin D; Gram-Negative Committee of the Antibacterial Resistance Leadership Group (ARLG)a. Gram-negative bacterial infections: Research priorities, accomplishments, and future directions of the antibacterial resistance leadership group. Clin Infect Dis. 2017; 64:S30-S35.
15. World Healt Organization. Antimicrobial Resistance: Global Report on Surveillance. WHOint. 2014.
16. Giamarellou H, Poulakou G. Multidrug-resistant Gram-negative infections: what are the treatment options? Drugs. 2009; 69:1879-901.
17. Fraimow H, Nahra R. Resistant gram-negative infections. Crit Care Clin. 2013; 29:895-921.

18. Magiorakos AP, Srinivasan A, Carey RB, Carmeli Y, Falagas ME, Giske CG, Harbarth S, Hindler JF, Kahlmeter G, Olsson-Liljequist B, Paterson DL, Rice LB, Stelling J, Struelens MJ, Vatopoulos A, Weber JT, Monnet DL. Multidrug-resistant, extensively drug-resistant and pandrug-resistant bacteria: an international expert proposal for interim standard definitions for acquired resistance. Clin Microbiol Infect 2012; 18:268–81.
19. Adler A, Friedman ND, Marchaim D. Multidrug-resistant gram-negative bacilli: Infection control implications. Infect Dis Clin North Am. 2016; 30:967-997.
20. Cisneros JM, Ortiz-Leyba C, Lepe JA, Obando I, Conde M, Cayuela A, et al. Prudent use of antibiotics and suggestions for improvement from hospital-based medicine. Enferm Infecc Microbiol Clin. 2010; 28 Suppl 4:28-31.
21. Vasudevan A, Mukhopadhyay A, Li J, Yuen EG, Tambyah PA. A prediction tool for nosocomial multi-drug Resistant Gram-Negative Bacilli infections in critically ill patients - prospective observational study. BMC Infect Dis. 2014; 14:615.
22. Ren Y, Ma G, Peng L, Ren Y, Zhang F. Active screening of multi-drug resistant bacteria effectively prevent and control the potential infections. Cell Biochem Biophys. 2015; 71:1235-8.
23. Kunz AN, Brook I. Emerging resistant Gram-negative aerobic bacilli in hospital-acquired infections. Chemotherapy. 2010; 56:492-500.
24. Guervil DJ, Chau T. Trends in multidrug-resistant gram-negative bacilli and the role of prolonged β-lactam infusion in the intensive care unit. Crit Care Nurs Q. 2013; 36:345-55.
25. Theuretzbacher U. Antibiotic innovation for future public health needs. Clin Microbiol Infect. 2017; 23:713-7.

26. Wright H, Bonomo RA, Paterson DL. New agents for the treatment of infections with Gram-negative bacteria: restoring the miracle or false dawn? Clin Microbiol Infect. 2017; 23:704-12.

27. Rice LB. Federal funding for the study of antimicrobial resistance in nosocomial pathogens: no ESKAPE. J Infect Dis 2008; 197:1079–81.

28. Boucher HW, Talbot GH, Bradley JS, Edwards JE, Gilbert D, Rice LB, Scheld M, Spellberg B, Bartlett J. Bad bugs, no drugs: no ESKAPE! An update from the Infectious Diseases Society of America. Clin Infect Dis 2009; 48:1–12.

29. Mehrad B, Clark NM, Zhanel GG, Lynch JP 3rd. Antimicrobial resistance in hospital-acquired gram-negative bacterial infections. Chest. 2015; 147:1413-21.

30. Tacconelli E, Carrara E, Savoldi A, Harbarth S, Mendelson M, Monnet DL, Pulcini C, Kahlmeter G, Kluytmans J, Carmeli Y, Ouellette M, Outterson K, Patel J13, Cavaleri M, Cox EM, Houchens CR, Grayson ML, Hansen P, Singh N, Theuretzbacher U, Magrini N; WHO Pathogens Priority List Working Group. Discovery, research, and development of new antibiotics: the WHO priority list of antibiotic-resistant bacteria and tuberculosis. Lancet Infect Dis. 2018; 18:318-27.

31. Howard A, O'Donoghue M, Feeney A, Sleator RD. *Acinetobacter baumannii*: an emerging opportunistic pathogen. Virulence. 2012; 3:243-50.

32. Hirai Y. Survival of bacteria under dry conditions; from a viewpoint of nosocomial infection. J Hosp Infect. 1991; 19:191-200.

33. Lin, MF, Lan, CY. Antimicrobial resistance in Acinetobacter baumannii: from bench to bedside. World J Clin Cases. 2014; 2:787-814.

34. Vincent JL, Rello J, Marshall J, Silva E, Anzueto A, Martin CD, Moreno R, Lipman J, Gomersall C, Sakr Y, Reinhart K; EPIC II Group of Investigators.

International study of the prevalence and outcomes of infection in intensive care units. JAMA. 2009; 302:2323-9.

35. Lee CR, Lee JH, Park M, Park KS, Bae IK, Kim YB, Cha CJ, Jeong BC, Lee SH. Biology of *Acinetobacter baumannii*: Pathogenesis, antibiotic resistance mechanisms, and prospective treatment options. Front Cell Infect Microbiol. 2017; 7:55.
36. Almasaudi SB. *Acinetobacter* spp. as nosocomial pathogens: Epidemiology and resistance features. Saudi J Biol Sci. 2018; 25:586-596.
37. Manchanda V, Sanchaita S, Singh N. Multidrug resistant *Acinetobacter*. J Glob Infect Dis. 2010; 2:291-304.
38. Nowak P, Paluchowska P. *Acinetobacter baumannii*: biology and drug resistance - role of carbapenemases. Folia Histochem Cytobiol. 2016; 54:61-74.
39. Giamarellou H. Multidrug-resistant Gram-negative bacteria: how to treat and for how long. Int J Antimicrob Agents. 2010; 36 Suppl 2:S50-4.
40. Peleg AY, Seifert H, Paterson DL. *Acinetobacter baumannii*: emergence of a successful pathogen. Clin Microbiol Rev. 2008; 21:538-82.
41. Wong D, Nielsen TB, Bonomo RA, Pantapalangkoor P, Luna B, Spellberg B. Clinical and pathophysiological overview of *Acinetobacter* infections: a century of challenges. Clin Microbiol Rev. 2017; 30:409-447.
42. McConnell M J, Actis L, Pachon J. Acinetobacter baumannii: human infections, factors contributing to pathogenesis and animal models. FEMS Microbiol. 2013; 37:130-55.
43. Khalid S, Berglund NA, Holdbrook DA, Leung YM1, Parkin J. The membranes of Gram-negative bacteria: progress in molecular modelling and simulation. Biochem Soc Trans. 2015; 43:162-7.

44. Rollauer SE, Sooreshjani MA, Noinaj N, Buchanan SK. Outer membrane protein biogenesis in Gram-negative bacteria. Philos Trans R Soc Lond B Biol Sci. 2015; 370(1679).

45. Fairman JW, Noinaj N, Buchanan SK. The structural biology of β-barrel membrane proteins: a summary of recent reports. Curr Opin Struct Biol. 2011; 21:523-31.

46. Smani Y, McConnell MJ, Pachón J. Role of fibronectin in the adhesion of *Acinetobacter baumannii* to host cells. PLoS One. 2012; 7:e33073.

47. Kim SW, Choi CH, Moon DC, Jin JS, Lee JH, Shin JH, Kim JM, Lee YC, Seol SY, Cho DT, Lee JC. Serum resistance of *Acinetobacter baumannii* through the binding of factor H to outer membrane proteins. FEMS Microbiol Lett. 2009; 301:224-31.

48. Sugawara E, and Nikaido H. OmpA is the principal nonspecific slow porin of Acinetobacter baumannii. J Bacteriol. 2012; 194:4089-96.

49. Smani Y, Fàbrega A, Roca I, Sánchez-Encinales V, Vila J, Pachón J. Role of OmpA in the multidrug resistance phenotype of Acinetobacter baumannii. Antimicrob Agents Chemother. 2014; 58:1806-8.

50. Gaddy JA, Tomaras AP, Actis LA. The *Acinetobacter baumannii* 19606 OmpA protein plays a role in biofilm formation on abiotic surfaces and in the interaction of this pathogen with eukaryotic cells. Infect Immun. 2009; 77:3150-60.

51. Smani Y, Dominguez-Herrera J, Pachon J. Association of the outer membrane protein Omp33 with fitness and virulence of *Acinetobacter baumannii*. J. Infect. Dis. 2013; 208:1561-70.

52. Fernández-Cuenca F, Smani Y, Gómez-Sánchez MC, Docobo-Pérez F, Caballero-Moyano FJ, Domínguez-Herrera J, Pascual A, Pachón J. Attenuated virulence of a

slow-growing pandrug-resistant *Acinetobacter baumannii* is associated with decreased expression of genes encoding the porins CarO and OprD-like. Int J Antimicrob Agents. 2011; 38:548-9.

53. Geisinger E, Isberg RR. Antibiotic modulation of capsular exopolysaccharide and virulence in *Acinetobacter baumannii*. PLoS Pathog. 2015 Feb; 11:e1004691.

54. Wang N, Ozer EA, Mandel MJ, Hauser AR. Genome-wide identification of Acinetobacter baumannii genes necessary for persistence in the lung. MBio. 2014; 5:e01163-14.

55. Liou ML, Soo PC, Ling SR, Kuo HY, Tang CY, Chang KC. The sensor kinase BfmS mediates virulence in *Acinetobacter baumannii*. J Microbiol Immunol Infect. 2014; 47:275-81.

56. Luke NR, Sauberan SL, Russo TA, Beanan JM, Olson R, Loehfelm TW, Cox AD, St Michael F, Vinogradov EV, Campagnari AA. Identification and characterization of a glycosyltransferase involved in *Acinetobacter baumannii* lipopolysaccharide core biosynthesis. Infect Immun. 2010; 78:2017-23.

57. McQueary CN, Kirkup BC, Si Y, Barlow M, Actis LA, Craft DW, Zurawski DV. Extracellular stress and lipopolysaccharide modulate *Acinetobacter baumannii* surface-associated motility. J Microbiol. 2012; 50:434-43.

58. Flores-Díaz M, Monturiol-Gross L, Naylor C, Alape-Girón A, Flieger A. Bacterial sphingomyelinases and phospholipases as virulence factors. Microbiol Mol Biol Rev. 2016; 80:597-628.

59. Songer JG. Bacterial phospholipases and their role in virulence. Trends Microbiol. 1997; 5:156-61.

60. Ellis TN, Kuehn MJ. Virulence and immunomodulatory roles of bacterial outer membrane vesicles. Microbiol Mol Biol Rev. 2010; 74:81-94.

61. Kwon SO, Gho YS, Lee JC, Kim SI. Proteome analysis of outer membrane vesicles froma clinical *Acinetobacter baumannii* isolate. FEMS Microbiol Lett. 2009; 297:150-6.

62. Rumbo C, Fernández-Moreira E, Merino M, Poza M, Mendez JA, Soares NC, Mosquera A, Chaves F, Bou G. Horizontal transfer of the OXA-24 carbapenemase gene via outer membrane vesicles: a new mechanism of dissemination of carbapenem resistance genes in *Acinetobacter baumannii*. Antimicrob Agents Chemother. 2011; 55:3084-90.

63. Gaddy JA, Arivett BA, McConnell MJ, López-Rojas R, Pachón J, Actis LA. Role of acinetobactin-mediated iron acquisition functions in the interaction of *Acinetobacter baumannii* strain ATCC 19606T with human lung epithelial cells, *Galleria mellonella* caterpillars, and mice. Infect Immun. 2012; 80:1015-24.

64. Zimbler DL, Park TM, Arivett BA, Penwell WF, Greer SM, Woodruff TM, Tierney DL, Actis LA. Stress response and virulence functions of the *Acinetobacter baumannii* NfuA Fe-S scaffold protein. J Bacteriol. 2012; 194:2884-93.

65. Corbin BD, Seeley EH, Raab A, Feldmann J, Miller MR, Torres VJ, Anderson KL, Dattilo BM, Dunman PM, Gerads R, Caprioli RM, Nacken W, Chazin WJ, Skaar EP. Metal chelation and inhibition of bacterial growth in tissue abscesses. Science. 2008; 319:962-5.

66. Hood MI, Mortensen BL, Moore JL, Zhang Y, Kehl-Fie TE, Sugitani N, Chazin WJ, Caprioli RM, Skaar EP. Identification of an *Acinetobacter baumannii* zinc acquisition system that facilitates resistance to calprotectin-mediated zinc sequestration. PLoS Pathog. 2012; 8:e1003068.

67. Korotkov KV, Sandkvist M, Hol WG. The type II secretion system: biogenesis, molecular architecture and mechanism. Nat Rev Microbiol. 2012; 10:336-51.

68. Johnson TL, Waack U, Smith S, Mobley H, Sandkvist M. *Acinetobacter baumannii* is dependent on the type II secretion system and its substrate LipA for lipid utilization and *in vivo* fitness. J Bacteriol. 2015; 198:711-9.

69. Weber BS, Kinsella RL, Harding CM, Feldman MF. The secrets of *Acinetobacter* secretion. Trends Microbiol. 2017; 25:532-545.

70. Repizo GD, Gagné S, Foucault-Grunenwald ML, Borges V, Charpentier X, Limansky AS, Gomes JP, Viale AM, Salcedo SP. Differential role of the T6SS in *Acinetobacter baumannii* virulence. PLoS One. 2015; 10:e0138265.

71. Weber BS, Ly PM, Irwin JN, Pukatzki S, Feldman MF. A multidrug resistance plasmid contains the molecular switch for type VI secretion in *Acinetobacter baumannii*. Proc Natl Acad Sci U S A. 2015; 112:9442-7.

72. Bentancor LV, Camacho-Peiro A, Bozkurt-Guzel C, Pier GB, Maira-Litrán T. Identification of Ata, a multifunctional trimeric autotransporter of *Acinetobacter baumannii*. J Bacteriol. 2012; 194:3950-60.

73. Badave GK, Kulkarni D. Biofilm Producing Multidrug Resistant Acinetobacter baumannii: An Emerging Challenge. J Clin Diagn Res. 2015; 9:DC08–DC10.

74. de Breij A, Dijkshoorn L, Lagendijk E, van der Meer J, Koster A, Bloemberg G, Wolterbeek R, van den Broek P, Nibbering P. Do biofilm formation and interactions with human cells explain the clinical success of *Acinetobacter baumannii*? PLoS One. 2010; 5:e10732.

75. Tomaras AP, Dorsey CW, Edelmann RE, Actis LA. Attachment to and biofilm formation on abiotic surfaces by *Acinetobacter baumannii*: involvement of a novel chaperone-usher pili assembly system. Microbiology. 2003; 149:3473-84.

76. Harding CM, Hennon SW, Feldman MF. Uncovering the mechanisms of *Acinetobacter baumannii* virulence. Nat Rev Microbiol. 2018; 16(2):91-102.

77. Choi AH, Slamti L, Avci FY, Pier GB, Maira-Litrán T. The pgaABCD locus of *Acinetobacter baumannii* encodes the production of poly-beta-1-6-N-acetylglucosamine, which is critical for biofilm formation. J Bacteriol. 2009; 191:5953.

78. Gellatly SL, Hancock RE. *Pseudomonas aeruginosa*: new insights into pathogenesis and host defenses. Pathog Dis. 2013; 67:159-73.

79. Hidron AI, Edwards JR, Patel J, Horan TC, Sievert DM, Pollock DA, Fridkin SK, National Healthcare Safety Network Team & Participating National Healthcare Safety Network Facilities. NHSN annual update: antimicrobial-resistant pathogens associated with healthcare-associated infections: annual summary of data reported to the National Healthcare Safety Network at the Centers for Disease Control and Prevention, 2006–2007. Infect Control Hosp Epidemiol. 2008; 29:996–1011.

80. Bodey GP, Bolivar R, Fainstein V, Jadeja L. Infections caused by *Pseudomonas aeruginosa*. Rev Infect Dis. 1983; 5:279-313.

81. Lu Q, Eggimann P, Luyt CE, Wolff M, Tamm M, François B, Mercier E, Garbino J, Laterre PF, Koch H, Gafner V, Rudolf MP, Mus E, Perez A, Lazar H, Chastre J, Rouby JJ. Pseudomonas aeruginosa serotypes in nosocomial pneumonia: prevalence and clinical outcomes. Crit Care. 2014; 18:R17.

82. Strateva T, Yordanov D. *Pseudomonas aeruginosa* – a phenomenon of bacterial resistance. J Med Microbiol. 2009; 58:1133-48.

83. Ruiz-Garbajosa P, Cantón R. Epidemiology of antibiotic resistance in *Pseudomonas aeruginosa*. Implications for empiric and definitive therapy. Rev Esp Quimioter. 2017; 30:8-12.

84. European Centre for Disease Prevention and Control. Antimicrobial resistance surveillance in Europe 2015. Annual Report of the European Antimicrobial Resistance Surveillance Network (EARSNet). Stockholm: ECDC; 2017.

85. Smith EE, Buckley DG, Wu Z, Saenphimmachak C, Hoffman LR, D'Argenio DA, Miller SI, Ramsey BW, Speert DP, Moskowitz SM, Burns JL, Kaul R, Olson MV. Genetic adaptation by *Pseudomonas aeruginosa* to the airways of cystic fibrosis patients. Proc Natl Acad Sci U S A. 2006; 103:8487-92.

86. Sadikot RT, Blackwell TS, Christman JW, Prince AS. Pathogen-host interactions in *Pseudomonas aeruginosa* pneumonia. Am J Respir Crit Care Med. 2005; 171:1209-23.

87. Schweizer HP. Efflux as a mechanism of resistance to antimicrobials in *Pseudomonas aeruginosa* and related bacteria: unanswered questions. Genet Mol Res. 2003; 2:48-62.

88. Confer AW, Ayalew S. The OmpA family of proteins: roles in bacterial pathogenesis and immunity. Vet. Microbiol. 2013; 163:207-22.

89. Chevalier S, Bouffartigues E, Bodilis J, Maillot O, Lesouhaitier O, Feuilloley MGJ, Orange N, Dufour A, Cornelis P. Structure, function and regulation of *Pseudomonas aeruginosa* porins. FEMS Microbiol Rev. 2017; 41:698-722.

90. Miao EA, Andersen-Nissen E, Warren SE, Aderem A. TLR5 and Ipaf: dual sensors of bacterial flagellin in the innate immune system. Semin Immunopathol. 2007; 29:275-288.

91. Feldman M, Bryan R, Rajan S, Scheffler L, Brunnert S, Tang H, Prince A. Role of flagella in pathogenesis of *Pseudomonas aeruginosa* pulmonary infection. Infect Immun. 1998; 66: 43–51.

92. Kipnis E, Sawa T, Wiener-Kronish J. Targeting mechanisms of *Pseudomonas aeruginosa* pathogenesis. Med Mal Infect. 2006; 36:78–91.

93. Kohler T, Curty LK, Barja F, van Delden C, Pechere J. Swarming of *Pseudomonas aeruginosa* is dependent on cell-to-cell signaling and requires flagella and pili. J Bacteriol. 2000; 182:5990-96.

94. Craig L, Pique ME, Tainer JA. Type 4 pilus structure and bacterial pathogenicity. Nat Rev Microbiol. 2004; 2:363-78.

95. Hauser AR. The type 3 secretion system of *Pseudomonas aeruginosa*: infection by injection. Nat Rev Microbiol. 2009; 7:654-65.

96. Yahr TL, Wolfgang MC. Transcriptional regulation of the *Pseudomonas aeruginosa* type 3 secretion system. Mol Microbiol. 2006; 62:631-40.

97. Deep A, Chaudhary U, Gupta V. Quorum sensing and bacterial pathogenicity: from molecules to disease. J Lab Physicians. 2011; 3:4–11.

98. Pearson JP, Feldman M, Iglewski BH, Prince A. *Pseudomonas aeruginosa* cell-to-cell signaling is required for virulence in a model of acute pulmonary infection. Infect Immun. 2000; 68:4331-34.

99. Hall-Stoodley L, Stoodley P. Evolving concepts in biofilm infections. Cell Microbiol. 2009; 11:1034-43.

100. Waite RD, Paccanaro A, Papakonstantinopoulou A, Hurst JM, Saqi M, Littler E, Curtis MA. Clustering of *Pseudomonas aeruginosa* transcriptomes from planktonic cultures, developing and mature biofilms reveals distinct expression profiles. BMC Genomics. 2006; 7:162.

101. Mah TC, O'Toole GA. Mechanisms of biofilm resistance to antimicrobial agents. Trends Microbiol. 2001; 9:34-9.

102. Moscoso JA, Mikkelsen H, Heeb S, Williams P, Filloux A. The *Pseudomonas aeruginosa* sensor RetS switches type 3 and type 6 secretion via c-di-GMP signalling. Environ Microbiol. 2012; 13:3128-38.

103. Alnour TMS, Ahmed-Abak EH. Multidrug Resistant *Pseudomonas (P) aeruginosa*: Medical impact, pathogenicity, resistance mechanisms and epidemiology. JSM Microbiol. 2017; 5:1046.

104. King JD, Kocincova D, Westman EL, Lam JS. Lipopolysaccharide biosynthesis in *Pseudomonas aeruginosa*. Innate Immun 2009; 15(5):261-312. [Erratum in: Innate Immun. 2010; 16:273.]

105. Akira S, Uematsu S, Takeuchi O. Pathogen recognition and innate immunity. Cell. 2006; 124:783-801.

106. Ernst RK, Moskowitz SM, Emerson JC, Kraig GM, Adams KN, Harvey MD, Ramsey B, Speert DP, Burns JL, Miller SI. Unique lipid A modifications in *Pseudomonas aeruginosa* isolated from the airways of patients with cystic fibrosis. J Infect Dis. 2007; 196:1088-92.

107. Schultz MJ, Speelman P, Zaat SA, Hack CE, van Deventer SJ, van der Poll T. The effect of Pseudomonas exotoxin A on cytokine production in whole blood exposed to *Pseudomonas aeruginosa*. FEMS Immunol Med Microbiol. 2000; 29:227-32.

108. Wolf P, Elsässer-Beile U. Pseudomonas exotoxin A: from virulence factor to anti-cancer agent International. J Med Microbiol. 2009; 299:161-76.

109. Miyazaki S, Matsumoto T, Tateda K, Ohno A, Yamaguchi K. Role of exotoxin A in inducing severe Pseudomonas aeruginosa infections in mice. J Med Microbiol. 1995; 43:169-75.

110. Lau GW, Hassett DJ, Ran H, Kong F. The role of pyocyanin in *Pseudomonas aeruginosa* infection. Trends Mol Med. 2004; 10:599-606.

111. Bianchi SM, Prince LR, McPhillips K et al. (2008) Impairment of apoptotic cell engulfment by pyocyanin, a toxic metabolite of *Pseudomonas aeruginosa*. AmJ Respir Crit Care Med. 177: 5-43.

112. Jimenez PN, Koch G, Thompson JA, Xavier KB, Cool RH, Quax WJ, The multiple signaling systems regulating virulence in *Pseudomonas aeruginosa*. Microbiol Mol Biol Rev. 2012; 76:46-65.

113. Schaffer K, Taylor CT. The impact of hypoxia on bacterial infection. FEBS J. 2015; 282:2260-6.

114. Eltzschig HK, Carmeliet P. Hypoxia and Inflammation. N Engl J Med. 2011; 364: 656-65.

115. Zinkernagel AS, Johnson RS, Nizet V. Hypoxia inducible factor (HIF) function in innate immunity and infection. J Mol Med. 2007; 85:1339-46.

116. Cummins EP, Taylor CT. Hypoxia-responsive transcription factors. Pflugers Arch – Eur J Physiol. 2005; 450:363-71.

117. Suzuki N, Gradin K, Poellinger L, Yamamoto M. Regulation of hypoxia-inducible gene expression after HIF activation. Exp Cell Res. 2017; 356:182-6.

118. Devraj G, Beerlage C, Brüne B, Kempf VA. Hypoxia and HIF-1 activation in bacterial infections. Microbes Infect. 2017; 19:144-56.

119. Yang SL, Wu C, Xiong ZF, Fang X. Progress on hypoxia-inducible factor-3: Its structure, gene regulation and biological function (Review). Mol Med Rep. 2015; 12:2411-6.

120. Adams JM, Difazio LT, Rolandelli RH, Luján JJ, Haskó G, Csóka B, Selmeczy Z, Németh ZH. HIF-1: a key mediator in hypoxia. Acta Physiol Hung. 2009; 96:19-28.

121. Ho TK, Rajkumar V, Ponticos M, Leoni P, Black DC, Abraham DJ, Baker DM. Increased endogenous angiogenic response and hypoxia-inducible factor-1α in human critical limb ischemia. J. Vasc. Surg. 2006; 43:125-33.

122. Cramer T, Yamanishi Y, Clausen BE, Förster I, Pawlinski R, Mackman N, Haase VH, Jaenisch R, Corr M, Nizet V, Firestein GS, Gerber HP, Ferrara N, Johnson RS. HIF-1α is essential for myeloid cell mediated inflammation. Cell. 2003; 112:645-57. [Erratum in: Cell. 2003; 113:419.]

123. Oda T, Hirota K, Nishi K, Takabuchi S, Oda S, Yamada H, Arai T, Fukuda K, Kita T, Adachi T, Semenza GL, Nohara R. Activation of hypoxia-inducible factor 1 during macrophage differentiation. Am. J. Physiol. Cell Physiol. 2006; 291:C104-13.

124. Carmeliet P, Dor Y, Herbert J, Fukumura D, Brusselmans K, Dewerchin M, Neeman M, Bono F, Abramovitch R, Maxwell P, Koch CJ, Ratcliffe P, Moons L, Jain RK, Collen D, Keshert E. Role of HIF- 1α in hypoxia-mediated apoptosis, cell proliferation and tumor angiogenesis. Nature. 1998; 394:485-90. [Erratum in Nature. 1998; 395(6701):525.]

125. Papandreou I, Cairns RA, Fontana L, Lim AL, Denko NC. HIF-1 mediates adaptation to hypoxia by actively downregulating mitochondrial oxygen consumption. Cell Metab. 2006; 3:150-55.

126. Richard DE, Berra E, Pouyssegur J. Nonhypoxic pathway mediates the induction of hypoxia-inducible factor 1α in vascular smooth muscle cells. J. Biol. Chem. 2000; 275:26765-71.

127. Zagzag D, Zhong H, Scalzitti JM, Laughner E, Simons JW, Semenza GL. Expression of hypoxiainducible factor 1α in brain tumors: association with angiogenesis, invasion, and progression. Cancer. 2000; 88:2606-18.

128. Zhang H, Gao P, Fukuda R, Kumar G, Krishnamachary B, Zeller KI, Dang CV, Semenza GL. HIF-1 inhibits mitochondrial biogenesis and cellular respiration in VHL-deficient renal cell carcinoma by repression of C-MYC activity. Cancer Cell. 2007; 11:407-20.

129. Krick S, Eul BG, Hänze J, Savai R, Grimminger F, Seeger W, Rose F. Role of hypoxia-inducible factor-1 alpha in hypoxia-induced apoptosis of primary alveolar epithelial type II cells. Am. J. Respir. Cell. Mol. Biol. 2005; 32:395-403.

130. Li L, Qu Y, Li J, Xiong Y, Mao M, Mu D. Relationship between HIF-1alpha expression and neuronal apoptosis in neonatal rats with hypoxia-ischemia brain injury. Brain Res. 2007; 1180:133-9.

131. Worlitzsch D, Tarran R, Ulrich M, Schwab U, Cekici A, Meyer KC, Birrer P, Bellon G, Berger J, Weiss T, Botzenhart K, Yankaskas JR, Randell S, Boucher RC, Döring G. Effects of reduced mucus oxygen concentration in airway *Pseudomonas infections* of cystic fibrosis patients. J Clin Invest. 2002; 109:317-25.

132. Via LE, Lin PL, Ray SM, Carrillo J, Allen SS, Eum SY, Taylor K, Klein E, Manjunatha U, Gonzales J, Lee EG, Park SK, Raleigh JA, Cho SN, McMurray DN, Flynn JL, Barry CE 3rd.Tuberculous granulomas are hypoxic in guinea pigs, rabbits, and nonhuman primates. Infect Immun. 2008; 76:2333-40.

133. Grahl N, Puttikamonkul S, Macdonald JM, Gamcsik MP, Ngo LY, Hohl TM, Cramer RA. *In vivo* hypoxia and a fungal alcohol dehydrogenase influence the pathogenesis of invasive pulmonary aspergillosis. PLoS Pathog. 2011; 7:e1002145.

134. Ebbesen P, Toth FD, Villadsen JA, Norskov-Lauritsen N. *In vitro* interferon and virus production at *in vivo* physiologic oxygen tensions. In Vivo. 1991; 5:355-8.

135. Werth N, Beerlage C, Rosenberger C, Yazdi AS, Edelmann M, Amr A, Bernhardt W, von Eiff C, Becker K, Schäfer A, Peschel A, Kempf VA. Activation of hypoxia inducible factor 1 is a general phenomenon in infections with human pathogens. PLoS One. 2010; 5:e11576.

136. Riess T, Andersson SG, Lupas A, Schaller M, Schäfer A, Kyme P, Martin J, Wälzlein JH, Ehehalt U, Lindroos H, Schirle M, Nordheim A, Autenrieth IB, Kempf VA. Bartonella adhesin a mediates a proangiogenic host cell response. J Exp Med. 2004; 200:1267-78.

137. Holden VI, Breen P, Houle S, Dozois CM, Bachman MA. *Klebsiella pneumoniae* siderophores induce inflammation, bacterial dissemination, and HIF-1α stabilization during pneumonia. MBio. 2016; 7.

138. Frede S, Stockmann C, Freitag P, Fandrey J. Bacterial lipopolysaccharide induces HIF-1 activation in human monocytes via p44/42 MAPK and NF-kappaB. Biochem J. 2006; 396:517-27.

139. Anand RJ, Gribar SC, Li J, Kohler JW, Branca MF, Dubowski T, Sodhi CP, Hackam DJ. Hypoxia causes an increase in phagocytosis by macrophages in a HIF-1alpha-dependent manner. J Leukoc Biol. 2007; 82:1257-65.

140. Nizet V, Johnson RS. Interdependence of hypoxic and innate immune responses. Nat Rev Immunol. 2009; 9:609-17.

141. Bhandari T, Olson J, Johnson RS, Nizet V.HIF-1α influences myeloid cell antigen presentation and response to subcutaneous OVA vaccination. J Mol Med (Berl). 2013; 91:1199-205.

142. Leire E, Olson J, Isaacs H, Nizet V, Hollands A. Role of hypoxia inducible factor-1 in keratinocyte inflammatory response and neutrophil recruitment. J Inflamm (Lond). 2013; 10:28.

143. Peyssonnaux C, Boutin AT, Zinkernagel AS, Datta V, Nizet V, Johnson RS. Critical role of HIF-1alpha in keratinocyte defense against bacterial infection. J Invest Dermatol. 2008; 128:1964-8.

144. Schaible B, McClean S, Selfridge A, Broquet A, Asehnoune K, Taylor CT, Schaffer K. Hypoxia modulates infection of epithelial cells by *Pseudomonas aeruginosa*. PLoS One. 2013; 8:e56491.

145. Berger EA, McClellan SA, Vistisen KS, Hazlett LD. HIF-1α is essential for effective PMN bacterial killing, antimicrobial peptide production and apoptosis in Pseudomonas aeruginosa keratitis. PLoS Pathog. 2013; 9:e1003457.

146. Okumura CY, Hollands A, Tran DN, Olson J, Dahesh S, von Köckritz-Blickwede M, Thienphrapa W, Corle C, Jeung SN, Kotsakis A, Shalwitz RA, Johnson RS, Nizet V. A new pharmacological agent (AKB-4924) stabilizes hypoxia inducible factor-1 (HIF-1) and increases skin innate defenses against bacterial infection. J Mol Med. 2012; 90:1079–1089.

147. Peyssonnaux C, Cejudo-Martin P, Doedens A, Zinkernagel AS, Johnson RS, Nizet V. Cutting edge: essential role of hypoxia inducible Factor-1 in development of lipopolysaccharide-induced sepsis. J Immunol. 2007; 178(:7516-9.

148. Enkhbaatar P, Traber L, Traber D. Methicillin-resistant *Staphylococcus aureus*-induced sepsis: role of nitric oxide. Intensive Care Med. 2000; 404-10.

149. Van der Flier M, Stockhammer G, Vonk GJ, Nikkels PG, van Diemen-Steenvoorde RA, van der Vlist GJ, et al. Vascular endothelial growth factor in bacterial meningitis: detection in cerebrospinal fluid and localization in postmortem brain. J Infect Dis. 2001; 183:149-53.

150. Yano K, Liaw PC, Mullington JM, Shih SC, Okada H, Bodyak N, Kang PM, Toltl L, Belikoff B, Buras J, Simms BT, Mizgerd JP, Carmeliet P, Karumanchi SA, Aird WC. Vascular endothelial growth factor is an important determinant of sepsis morbidity and mortality. J Exp Med. 2006; 203:1447-58.

151. Pickkers P, Sprong T, van Eijk L, van der Hoeven H, Smits P, van Deuren M. Vascular endothelial growth factor is increased during the first 48 hours of human septic shock and correlates with vascular permeability. Shock 2005; 24:508-12.

152. Santos SAD, Andrade DR Júnior. HIF-1alpha and infectious diseases: a new frontier for the development of new therapies. Rev Inst Med Trop Sao Paulo. 2017; 59:e92.

153. Hirota K. Involvement of hypoxia-inducible factors in the dysregulation of oxygen homeostasis in sepsis. Cardiovasc Hematol Disord Drug Targets. 2015; 15:29-40.

154. Schaible B, Rodriguez J, Garcia A, von Kriegsheim A, McClean S, Hickey C, Keogh CE, Brown E, Schaffer K, Broquet A, Taylor CT. Hypoxia reduces the pathogenicity of *Pseudomonas aeruginosa* by decreasing the expression of multiple virulence factors. J Infect Dis. 2017; 215:1459-67.

155. Schaible B, Taylor CT, Schaffer K. Hypoxia increases antibiotic resistance in Pseudomonas aeruginosa through altering the composition of multidrug efflux pumps. Antimicrob Agents Chemother. 2012; 56:2114-8.

156. Worlitzsch D, Tarran R, Ulrich M, Schwab U, Cekici A, Meyer KC, Birrer P, Bellon G, Berger J, Weiss T, Botzenhart K, Yankaskas JR, Randell S, Boucher RC, Döring G. Effects of reduced mucus oxygen concentration in airway Pseudomonas infections of cystic fibrosis patients. J Clin Invest. 2002; 109:317-25.

157. Rupp J, Gieffers J, Klinger M, van Zandbergen G, Wrase R, Maass M, Solbach W, Deiwick J, Hellwig-Burgel T. Chlamydia pneumoniae directly interferes with HIF-1a stabilization in human host cells. Cell Microbiol. 2007; 9:2181-91.

158. Spear W, Chan D, Coppens I, Johnson RS, Giaccia A, Blader IJ. The host cell transcription factor hypoxia-inducible factor 1 is required for *Toxoplasma gondii* growth and survival at physiological oxygen levels. Cell Microbiol. 2006; 8:339-52.

159. Staab A, Loeffler J, Said HM, Diehlmann D, Katzer A, Beyer M, Fleischer M, Schwab F, Baier K, Einsele H, Flentje M, Vordermark D. Effects of HIF-1 inhibition by chetomin on hypoxia-related transcription and radiosensitivity in HT 1080 human fibrosarcoma cells. BMC Cancer 2007; 7:213.

160. Kwizera A, Dünser MW. A Global Perspective on Acute Respiratory Distress Syndrome and the Truth about Hypoxia in Resource-limited Settings. Am J Respir Crit Care Med. 2016; 193:5-7.

161. Brusselle GG, Joos GF, Bracke KR. New insights into the immunology of chronic obstructive pulmonary disease. Lancet. 2011; 378:1015-26.

162. Cullen L, McClean S. Bacterial adaptation during chronic respiratory infections. Pathogens. 2015; 4:66-89.

163. Pulido MR, García-Quintanilla M, Gil-Marqués ML, McConnell MJ. Identifying targets for antibiotic development using omics technologies. Drug Discov Today. 2016; 21:465-72.

164. Liu W, Dong H, Li J, Ou Q, Lv Y, Wang X, Xiang Z, He Y, Wu Q. RNA-seq reveals the critical role of OtpR in regulating *Brucella melitensis* metabolism and virulence under acidic stress. Sci Rep 2015; 5:10864.

165. Papenfort K, Förstner KU, Cong JP, Sharma CM, Bassler BL. Differential RNA-seq of *Vibrio cholerae* identifies the VqmR small RNA as a regulator of biofilm formation. Proc Natl Acad Sci U S A 2015; 112:E766-75.

166. O'May G, Jacobsen SM, Longwell M, Stoodley P, Mobley HL, Shirtliff ME. The high-affinity phosphate transporter Pst in *Proteus mirabilis* HI4320 and its importance in biofilm formation. Microbiology. 2009; 155:1523-35.

167. Chekabab SM, Harel J, Dozois CM. Interplay between genetic regulation of phosphate homeostasis and bacterial virulence. Virulence. 2014; 5:786-93.

168. Schurdell MS, Woodbury GM, McCleary WR. Genetic evidence suggests that the intergenic region between pstA and pstB plays a role in the regulation of rpoS translation during phosphate limitation. J Bacteriol. 2007; 189:1150-53.

169. Lamarche MG, Dozois CM, Daigle F, Caza M, Curtiss R III, Dubreuil JD, Harel J. Inactivation of the pst system reduces the virulence of an avian pathogenic *Escherichia coli* O78 strain. Infect Immun. 2005; 73:4138-45.

170. Rao PS, Yamada Y, Tan YP, Leung KY. Use of proteomics to identify novel virulence determinants that are required for *Edwardsiella tarda* pathogenesis. Mol Microbiol. 2004; 53:573-86.

171. Palma C, Spallek R, Piccaro G, Pardini M, Jonas F et al. The *M. tuberculosis* phosphatebinding lipoproteins PstS1 and PstS3 induce Th1 and Th17 responses that are not associated with protection against *M. tuberculosis* infection. Clin Dev Immunol. 2011; 2011:690328.

172. Ferreira EL, Batista MT, Cavalcante RC, Pegos VR1, Passos HM, Silva DA, Balan A, Ferreira LC, Ferreira RC. Sublingual immunization with the phosphate-binding-protein (PstS) reduces oral colonization by *Streptococcus mutans*. Mol Oral Microbiol 2016; 31:410-22.

173. Barak V, Schwartz A, Kalickman I, Nisman B, Gurman G, Shoenfeld Y. Prevalence of hypophosphatemia in sepsis and infection: the role of cytokines. Am J Med. 1998; 104:40-47.

174. Cummins EP, Keogh CE, Crean D, Taylor CT. The role of HIF in immunity and inflammation. Mol Aspects Med. 2016; 47-48:24-34.

175. Mimura Y. Phosphate excretion during 24 h of hypoxia in conscious rats. Acta Physiol Scand. 1995; 155:283-9.

176. Mimura Y. Phosphate and cyclic AMP excretion decreases during less than 12 hours of hypoxia in conscious rats. Acta Physiol Scand. 1996; 158:317-23.

177. Orihuela CJ, Mills J, Robb CW, Wilson CJ, Watson DA, Niesel DW. *Streptococcus pneumoniae* PstS production is phosphate responsive and enhanced during growth in the murine peritoneal cavity. Infect Immun. 2001; 69:7565-71.

178. Krzywinska E, Stockmann C. Hypoxia, metabolism and immune cell function. Biomedicines. 2018; 6.

179. Cummins EP, Keogh CE, Crean D, Taylor CT. The role of HIF in immunity and inflammation. Mol Aspects Med. 2016; 47-48:24-34.

180. Thompson AA, Dickinson RS, Murphy F, Thomson JP, Marriott HM, Tavares A, Willson J, Williams L, Lewis A, Mirchandani A, Dos Santos Coelho P, Doherty C, Ryan E, Watts E, Morton NM, Forbes S, Stimson RH, Hameed AG, Arnold N, Preston JA, Lawrie A, Finisguerra V, Mazzone M, Sadiku P, Goveia J, Taverna F, Carmeliet P, Foster SJ, Chilvers ER, Cowburn AS, Dockrell DH, Johnson RS, Meehan RR, Whyte MK, Walmsley SR. Hypoxia determines survival outcomes of bacterial infection through HIF-1alpha dependent re-programming of leukocyte metabolism. Sci Immunol. 2017; 2.

181. Shalova IN, Lim JY, Chittezhath M, Zinkernagel AS, Beasley F, Hernández-Jiménez, et al. Human monocytes undergo functional re-programming during sepsis mediated by hypoxiainducible factor-1alpha. Immunity. 2015; 42:484-98.

182. Ramakrishnan S, Anand V, Roy S. Vascular endothelial growth factor signaling in hypoxia and inflammation. J Neuroimmune Pharmacol. 2014; 9:142-60.

183. Ben-Shoshan J, Maysel-Auslender S, Mor A, Keren G, George J. Hypoxia controls CD4+CD25+ regulatory T-cell homeostasis via hypoxia-inducible factor-1alpha. Eur J Immunol. 2008; 38:2412–8.

184. Dickinson RS, Murphy F, Doherty C, Williams S, Mirchandani A, Willson J, Scotti JS, Preston G, Schofield CJ, Whyte MKB, Walmsley SR. *Pseudomonas* expression of an oxygen sensing prolyl hydroxylase homologue regulates neutrophil host responses *in vitro* and *in vivo*. Wellcome Open Res. 2017; 2:104.

185. Prince LR, Bianchi SM, Vaughan KM, Bewley MA, Marriott HM, Walmsley SR, Taylor GW, Buttle DJ, Sabroe I, Dockrell DH, Whyte MK. Subversion of a lysosomal pathway regulating neutrophil apoptosis by a major bacterial toxin, pyocyanin. J Immunol. 2008; 180:3502–11.

186. Sherman DR, Voskuil M, Schnappinger D, Liao R, Harrell MI, Schoolnik GK. Regulation of the *Mycobacterium tuberculosis* hypoxic response gene encoding alpha -crystallin. Proc. Natl. Acad. Sci. U. S. A. 2001; 98:7534-9.

187. McClean S, Healy ME, Collins C, Carberry S, O'Shaughnessy L, Dennehy R, Adams Á, Kennelly H, Corbett JM, Carty F, Cahill LA, Callaghan M, English K, Mahon BP, Doyle S, Shinoy M. Linocin and OmpW are involved in attachment of the cystic fibrosis-associated pathogen Burkholderia cepacia complex to lung epithelial cells and protect mice against infection. Infect Immun. 2016; 84:1424-37.

188. Carnielli CM, Artier J, de Oliveira JC, Novo-Mansur MT. *Xanthomonas citri* subsp. *citri* surface proteome by 2D-DIGE: Ferric enterobactin receptor and other outer membrane proteins potentially involved in citric host interaction. J Proteomics. 2017; 151:251-63.

189. Russo TA, McFadden CD, Carlino-MacDonald UB, Beanan JM, Barnard TJ, Johnson JR. IroN functions as a siderophore receptor and is a urovirulence factor in an extraintestinal pathogenic isolate of *Escherichia coli*. Infect Immun. 2002; 70:7156-60.

190. Feldmann F, Sorsa LJ, Hildinger K, Schubert S. The salmochelin siderophore receptor IroN contributes to invasion of urothelial cells by extraintestinal pathogenic *Escherichia coli in vitro*. Infect Immun. 2007; 75:3183-7.

191. Kurochkina N. SH Domains. Springer International Publishing. {Structure-Function Relationship of Bacterial SH3 Domains}. 2015; 71-89.

192. Dixit R, Ross JL, Goldman YE, Holzbaur EL. Differential regulation of dynein and kinesin motor proteins by tau. Science. 2008; 319:1086-9.

193. Guignot J, Caron E, Beuzón C, Bucci C, Kagan J, Roy C, Holden DW. Microtubule motors control membrane dynamics of Salmonella-containing vacuoles. J Cell Sci. 2004; 117:1033-45.

194. Cao TT, Chang W, Masters SE, Mooseker MS. Myosin-Va binds to and mechanochemically couples microtubules to actin filaments. Mol Biol Cell. 2004; 15:151-61.

195. Wang JA, Meyer TF, Rudel T. Cytoskeleton and motor proteins are required for the transcytosis of Neisseria gonorrhoeae through polarized epithelial cells. Int J Med Microbiol. 2008; 298:209-21.

196. Schaible B, Schaffer K, Taylor CT. Hypoxia, innate immunity and infection in the lung. Respir Physiol Neurobiol. 2010; 174:235-43.

197. Kaukonen KM, Bailey M, Suzuki S, Pilcher D, Bellomo R. Mortality related to severe sepsis and septic shock among critically ill patients in Australia and New Zealand, 2000-2012. Jama. 2014; 311:1308-16.

198. Stevenson EK, Rubenstein AR, Radin GT, Wiener RS, Walkey AJ. Two decades of mortality trends among patients with severe sepsis: a comparative meta-analysis*. Crit Care Med. 2014; 42:625-31.

199. Ferrer R, Artigas A, Suarez D, Palencia E, Levy MM, Arenzana A, Pérez XL, Sirvent JM; Edusepsis Study Group. Effectiveness of treatments for severe sepsis: a prospective, multicenter, observational study. Am J Respir Crit Care Med. 2009; 180:861-6.

200. Kumar A, Roberts D, Wood KE, Light B, Parrillo JE, Sharma S, Suppes R, Feinstein D, Zanotti S, Taiberg L, Gurka D, Kumar A, Cheang M. Duration of hypotension before initiation of effective antimicrobial therapy is the critical determinant of survival in human septic shock. Crit Care Med. 2006; 34:1589-96.

201. Singer M, Deutschman CS, Seymour CW, Shankar-Hari M, Annane D, Bauer M, Bellomo R, Bernard GR, Chiche JD, Coopersmith CM, Hotchkiss RS, Levy MM, Marshall JC, Martin GS, Opal SM, Rubenfeld GD, van der Poll T, Vincent JL, Angus DC. The Third International Consensus Definitions for Sepsis and Septic Shock (Sepsis-3). JAMA. 2016; 315:801-10.

202. Kim SJ, Hwang SO, Kim YW, Lee JH, Cha KC. Procalcitonin as a diagnostic marker for sepsis/septic shock in the emergency department; a study based on Sepsis-3 definition. Am J Emerg Med. 2018; S0735-6757:30428-5.

203. Giannakopoulos K, Hoffmann U, Ansari U, Bertsch T, Borggrefe M, Akin I, Behnes M. The Use of Biomarkers in Sepsis: A Systematic Review. Curr Pharm Biotechnol. 2017; 18:499-507.

204. Kelly BJ, Lautenbach E, Nachamkin I, Coffin SE, Gerber JS, Fuchs BD, Garrigan C, Han X, Bilker WB, Wise J, Tolomeo P, Han JH; Centers for Disease Control and Prevention (CDC) Prevention Epicenters Program. Combined biomarkers predict acute mortality among critically ill patients with suspected sepsis. Crit Care Med. 2018; 46:1106-13.

205. Gerlach AT. Sepsis Biomarkers…The Long and Winding Road. Crit Care Med. 2018; 46:1194-95.

206. Liu X, Ren H, Peng D. Sepsis biomarkers: an omics perspective. Front Med. 2014; 8:58-67.

207. Berg E, Paukovits J, Axelband J, Trager J, Ryan D, Cichonski K, Kopnitsky M, Zweitzig D, Jeanmonod R. Measurement of a novel biomarker, Secretory Phospholipase A2 Group IIA as a marker of sepsis: a pilot study. J Emerg Trauma Shock. 2018; 11:135-139.

208. Røsjø H, Masson S, Caironi P, Stridsberg M, Magnoli M, Christensen G, Moise G, Urbano MC, Gattinoni L, Pesenti A, Latini R, Omland T; ALBIOS Biomarkers Study Investigators. Prognostic Value of Secretoneurin in Patients With Severe Sepsis and Septic Shock: Data From the Albumin Italian Outcome Sepsis Study. Crit Care Med. 2018; 46:e404-e410.

209. Pan P, Liu DW, Su LX, He HW, Wang XT, Yu C. Role of Combining Peripheral with Sublingual Perfusion on Evaluating Microcirculation and Predicting Prognosis in Patients with Septic Shock. Chin Med J (Engl). 2018; 131:1158-1166.

210. Faix JD. Biomarkers of sepsis. Crit Rev Clin Lab Sci. 2013; 50:23-36.

211. Prucha M, Bellingan G, Zazula R. Sepsis biomarkers. Clin Chim Acta. 2015; 440:97-103.

212. Kabarowski JH, Xu Y, Witte ON. Lysophosphatidylcholine as a ligand for immunoregulation. Biochem Pharmacol. 2002; 64:161-7.